

# ALLAHABAD UNIVERSITY STUDIES

VOL. VII—PART II (SCIENCE SECTION)

EDITED BY

The Vice-Chancellor and the Heads of Departments

---

SENATE HOUSE  
ALLAHABAD

1931

*Price Rs. Seven and As. Eight only.*

two-thirds as wide as the layer of follicle cells immediately surrounding it.

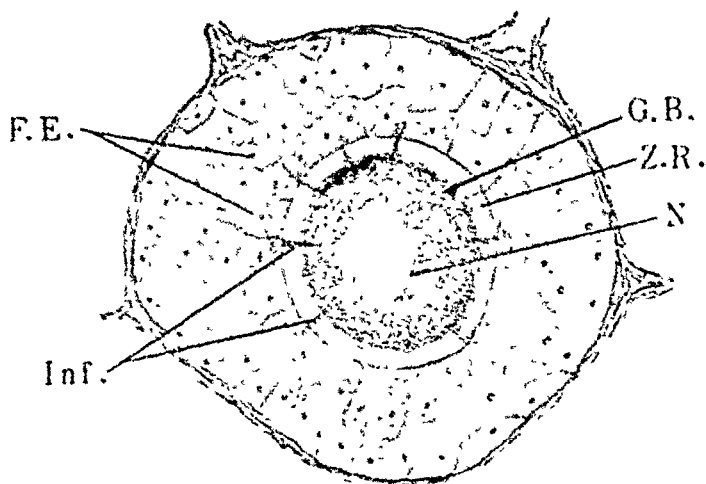


Fig. 1.

— 0.1 mm. —

Fig. 1. Graafian follicle of the squirrel showing infiltration. X 310. (Camera lucida drawing, Ludford preparation.)

Each graafian follicle consists at first of a single layer of cells surrounding the ovum. The follicle cells increase rapidly by division so that the follicle soon becomes several cells thick. When the outer layer of the cell grows more rapidly than the inner layer spaces generally crescentic in shape appear between the two layers and are filled with fluid (fig. 3 Sp.). In the rabbit and the rat the zona-radiata (figs. 4 and 5 Z.R.) are less well defined and the striations are much fainter.

*The infiltration of Golgi bodies :—*The process of infiltration of Golgi bodies has been described in detail by Bhattacharya and others in the tortoises (1, 2 and 3). According to them the follicle cells become very active at a particular stage of development and produce a large number of Golgi.

bodies which generally accumulate towards the side adjacent to the zona-radiata. This can also be well demonstrated in the squirrel (fig. 2 : G.B.).

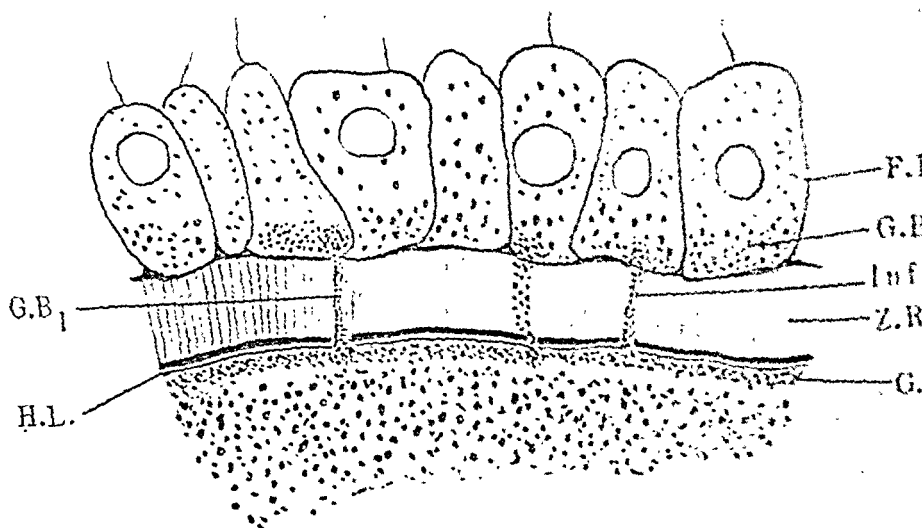


Fig. 2.

05 mm.

Fig. 2. A portion of the egg of the squirrel showing infiltration through zona-radiata. X 3100. (Ludford preparation.)

It appears that this mass accumulation is a preliminary to the Golgi elements being infiltrated or exuded from the follicle cells to the zona-radiata. The above-mentioned authors have described two kinds of infiltration of Golgi bodies, (i) where Golgi elements are extruded in comparatively big lumps as, e.g., in Calotes (4) and Fowl (5). (ii) where Golgi elements filter through canalicular passages in zona-radiata in the shape of small granules (1 and 2). In the animals examined by me the Golgi elements appear to be exuded as extremely small granules and appear to lie in the striations of the zona-radiata (fig. 2. G.B.1).

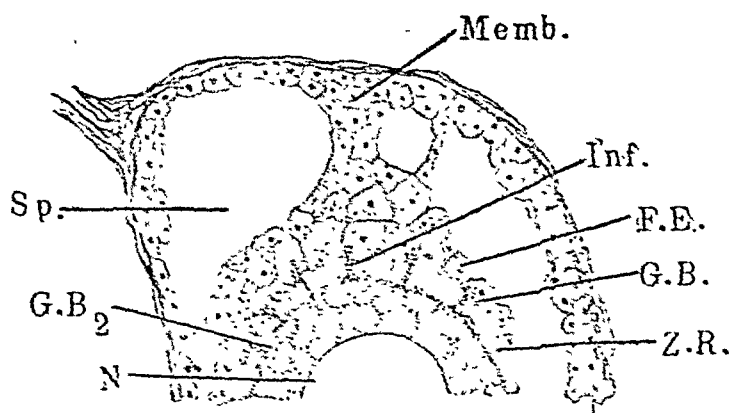


Fig. 3.

0.1 mm.

Fig. 3. A portion of the graafian follicle of squirrel showing infiltration from the epithelium to the egg. X 250. Cajal preparation (Camera Lucida.)

In the rabbit, the striations are not visible and the Golgi elements exuded from the follicle cells appear to lie

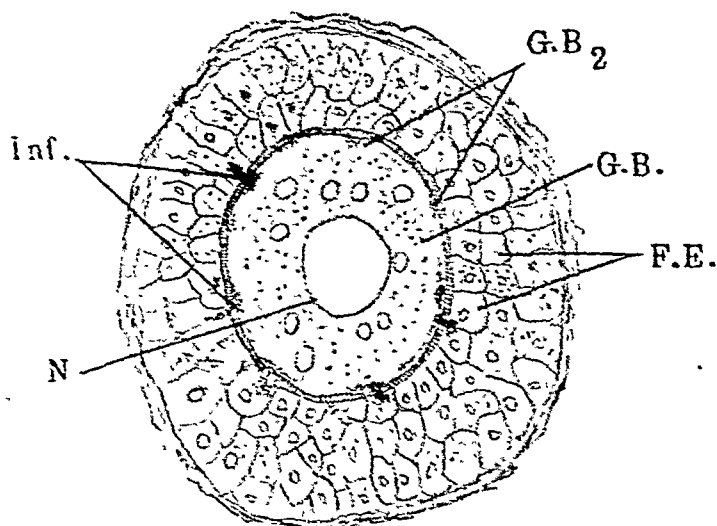


Fig. 4.

0.1 mm.

Fig. 4. A young follicle of rabbit showing infiltration (Camera. Lucida.) X 310. DaFano preparation.



scattered in the zona-radiata. After entering the egg they lie in patches just beneath the membrane of the egg (fig. 4 G.B. 2).

The rat conforms in many ways to the conditions found in rabbit. The radial striations are not visible in the zona-radiata. The process of infiltration is the same as has been described by Bhattacharya and others in fishes, amphibians and birds. Definite channel-like passages are not observable and the manner of transmission is haphazard.

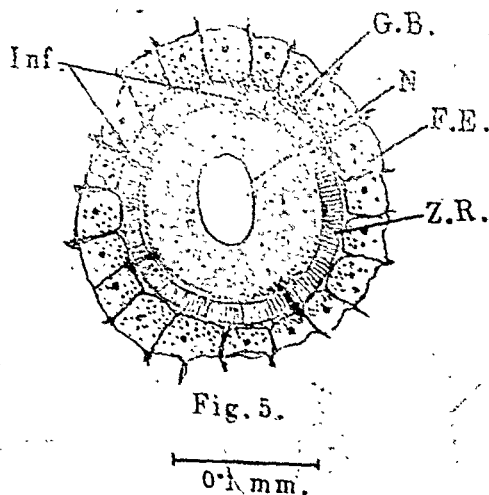


Fig. 5. A young follicle of the ovary of rat showing infiltration through the zona-radiata. The cytoplasm is much vacuolated. X 220. (Camera lucida drawing)

## DISCUSSION

The fact that granules pass from the egg membranes to the egg is not a new idea. Many previous workers have laid emphasis on this fact. These granules were generally supposed to be nutrient granules meant for the development of

the egg. That these granules could be cell organs like Golgi bodies and mitochondria is an idea which we owe mainly to the work of Professor Bhattacharya and his pupils. If slides are properly prepared and toned by methods that are specific for the demonstration of Golgi bodies there is no reason to doubt that what we see in good preparations, in the zona and fibrillar region of the egg could be anything but Golgi elements. Since all the stages beginning with accumulation of the Golgi elements at one pole of the cell and their passages through zona-radiata region are available, the fact of the transmission of the Golgi elements from the egg membranes to the egg is a phenomenon established in a large variety of Vertebrate animals. No Invertebrates have been tackled so far from this point of view.

### SUMMARY

1. In the mammals described above the Golgi elements are in the form of small granules in the follicle cells.
2. Before their transmission to the Zona-radiata they accumulate in mass formation at the side of the cell adjacent to the Zona.
3. The Zona at this stage is well established and in certain cases shows definite striations.
4. The Golgi elements from the follicle cells pass into the Zona-radiata sometimes in an orderly manner through the striated passages and sometimes in an haphazard manner.
5. From the Zona-radiata they pass into a fine homogeneous layer which lies between the egg and the Zona-radiata.
6. Before entering the eggs through the limiting membrane, the Golgi elements make a comparatively long halt in the region of the homogeneous layer.
7. After their entry into the eggs through the limiting membrane, the Golgi elements have a tendency to crowd together in the extreme cortical region of the egg.
8. Big lumps of Golgi bodies such as those described by Brambell in the fowl and by Bhattacharya in Calotes are never exuded from the follicular epithelium in the mammals examined by me.

## LETTERING

- F. E. Follicular Epithelium.  
 G. B. Golgi bodies.  
 G. B. 1. Golgi bodies lying in the striations  
                     of Zona-radiata.  
 G. B. 2. Golgi bodies lying beneath the limit-  
                     ing membrane of the egg.  
 H. L. Homogeneous layer between the Zona-  
                     radiata and the limiting membrane.  
 Inf. Infiltration.  
 N. Nucleus.  
 Memb. Membrane granulosa.  
 Sp. Crescent space in the graafian follicle.  
 Z. R. Zona-radiata.

## BIBLIOGRAPHY

1. Bhattacharya, D. R.—Les Inclusions Cytoplasmic dans l'oogenese de certains Reptiles. Thèse de Paris, 1925.
2. Bhattacharya, D. R. and K. B. Lal—The Cytoplasmic Inclusion in the Oogenesis of Certain Indian Tortoises. Allahabad University Studies, Vol. VI, 1929.
3. Bhattacharya, D. R.; Das, R. S. and Dutta, S. K.—On the Infiltration of Golgi Bodies and from the Follicular Epithelium to the Egg. Zeitschrift fur Zellforschung und Mikroskopische Anatomie, Berlin, 1929.
4. Dutta, S. K. and Asana, J. J.—On the Behaviour of the Golgi Apparatus in the Oogenesis of Calotes Versicolor (Daud). Allahabad University Studies, Vol. IV, 1928.
5. Brambell, P. W. R.—The Oogenesis of Fowl. Phil. Trans. Roy. Soc., 1925.
6. Gatenby, J. B.—Notes on the Gamitogenesis of Ornithorhynchus Paradoxus. Q.J.M. S. 66 (1922).
7. Gatenby, J. B. and Cowdry—Microtomet Vade Mecum (1928).
8. Ludford, R. J.—Some Modification of the Osmic Acid Method in Cytological Technique. Jour. Roy. Micr. Soc., 1925.
9. Ibid.—Further Modification of the Osmic Acid Method in Cytological Technique. Jour. Roy. Micr. Soc., 1926.

# VITAL STAINING EXPERIMENTS ON CLARIAS BATRACHUS

BY

P. R. BHATTACHARYA, M.Sc.

*Research Student, Zoology Department.*

AND

S. K. DUTTA, M.Sc.

*Lecturer in Zoology, Allahabad University, Allahabad.*

## INTRODUCTION

Of late a rich field for Cytological work by intra-vitam methods has been opened through the efforts of such masters of Microtechnique as Möllendorff, Parat (12—16), Bowen (2), Gatenby (7), and others. In India, Vishwanath (11) and Bhattacharya (3—5) have made substantial contributions towards the elucidation of certain cytological problems in oogenesis. The enunciation of Parat's vacuome theory, as a result of his vital staining methods brought to the forefront the importance of combining the classical methods with an intra-vitam examination of the tissues. Parat (13) laid particular stress on his neutral red and Janus green methods and came to the conclusion that the vacuome discovered by him in the animal cell was homologous with the Golgi bodies described by the classical workers. It was not long before the claim was disputed, firstly, by Avel (1) and later on, by Gatenby (7 and 8), Bowen (2), and Bhattacharya (5). As the discussion regarding the homology of the Golgi bodies and vacuome is still raging, the present work was suggested to us by Professor Bhattacharya for throwing further light on the subject.

For a successful intra-vitam examination on the female gonads several factors come into play :—

- (1) The ovary must contain a fairly large number of small eggs.
- (2) The eggs should be as free as possible from yolk.
- (3) The follicular membranes must be thin and preferably single layered to allow of a quick penetration of vital stains.
- (4) The slides, coverslips, and instruments should be thoroughly sterilised.
- (5) The physiological salt solution and the vital-stains used should be freshly made.
- (6) The sex-cells should be numerous enough so as to show various grades of development.
- (7) Early oocyte and oogonial stages should be present.
- (8) A large number of microscopes fitted with oil immersion lens and strong artificial light should be handy for examining the tissue immediately after removal from the body of the animal in various strengths of vital stains.
- (9) The right kind of vital stains should be used, because Neutral red and Janus green B of all makers do not give satisfactory results.

After examining the gonads of a number of animals we pitched upon the mud-fish *Clarias batrachus* as a very suitable material for the examination of its gonads. The eggs of this fish in the early stages are comparatively free from yolk and thus allow of an easy examination of its cell organs even without the aid of vital stains. Our results are based mostly on the action of neutral red, Janus green B and dilute osmic acid. Stock solutions of Neutral red

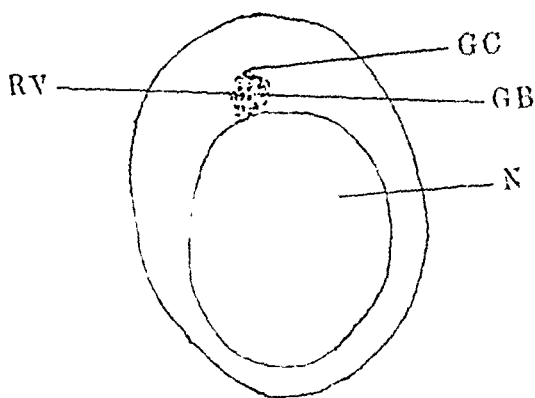


Fig.1

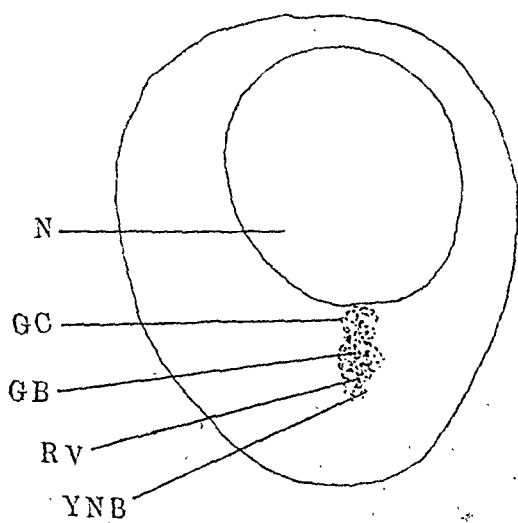


Fig 2

and Janus green B. each of the strength of 1 to 500 in physiological salt solution as recommended by Gatenby (6 and 7) were prepared. These were kept in a bath overnight at about  $35^{\circ}\text{C}$  temperature as recommended by Parat and Bhattacharya (15). Before use the stains were cooled to the room temperature and a very dilute pink solution was prepared by adding a drop of Neutral red to a watchglass full of physiological salt solution. The approximate strength of this solution would be about 1 in 30,000.

## OBSERVATIONS

The ovary immediately after its removal from the body was transferred to a sterilised pot containing a dilute solution of neutral red as referred to above. With the aid of sterilised scissors and forceps small pieces were cut and examined in the same solution under the highest powers of the microscope. According to Gatenby and others, if proper precaution is taken the tissues can safely be examined under the microscope for nearly an hour. In the case of this fish the stain penetrates very quickly and the vacuome is stained by neutral red in about 10 minutes time. Thus, this material gives ample time for proper examination and Camera lucida sketches. Our Janus green experiments were not much of a success as the stain was not of good quality. We are lucky in being able to get some early stages.

Figure 1 shows a late oogonium with a large nucleus and juxtannuclear concentration of Golgi bodies (G.B.) and Vacuome (R.V.). The number of both these cell-organs is not very large at this stage, and they are to be found only in this area and nowhere else in the cell. The Golgi crescents (G.C.) seem to lie in many cases in close approximation to each other.

Figure 2 shows in early oocyte stage where the archoplasmic area generally known as the yolk-nucleus of Balbiani (Y.N.B.) is more highly developed. The nucleus becomes comparatively smaller and the Golgi bodies (G.B.) and Vacuome (R.V.) lie mostly in the interior of this area either as isolated bodies or in contact with one another.

Figure 3 shows a later oocyte where the yolk-nucleus of Balbiani (Y.N.B.) is well established and forms a cap-like investment over the nucleus. It is a distinct crescent-shaped structure with a tendency to spread around the periphery of the nucleus. The cortical region of this area is formed mostly by Golgi elements. The red staining vacuoles or vacuome (R.V.) appear in patches in the medullary region of this area. There is a tendency now for the vacuome to become isolated.

Figure 4 shows a slightly older stage where the horns of the yolk-nucleus crescents (Y.N.B.) become extended so as to surround the nucleus (N.) entirely; the vacuome (R.V.) may be seen in patches and also as isolated; where they appear in patches, the Golgi dictyosomes (G.C.) still surround the vacuome in many cases.

Figure 5 shows a still later stage where the yolk-nucleus area is lost and the vacuome (R.V.) and Golgi bodies (G.B.) appear in patches or isolated throughout the cytoplasm. In the patches there is a greater tendency for the vacuome to loose their apparent connection with Golgi bodies.

Figure 6 shows an advanced oocyte where the red staining vacuoles (R.V.) and Golgi bodies (G.B.) spread even throughout the cytoplasm and the yolk formation is fairly well established. The nucleolar extrusions (N.L.E.X.) at this stage are a marked feature in the development of the oocyte.

In a still older oocyte yolk formation obliterates the proper examination of Golgi bodies and vacuome.



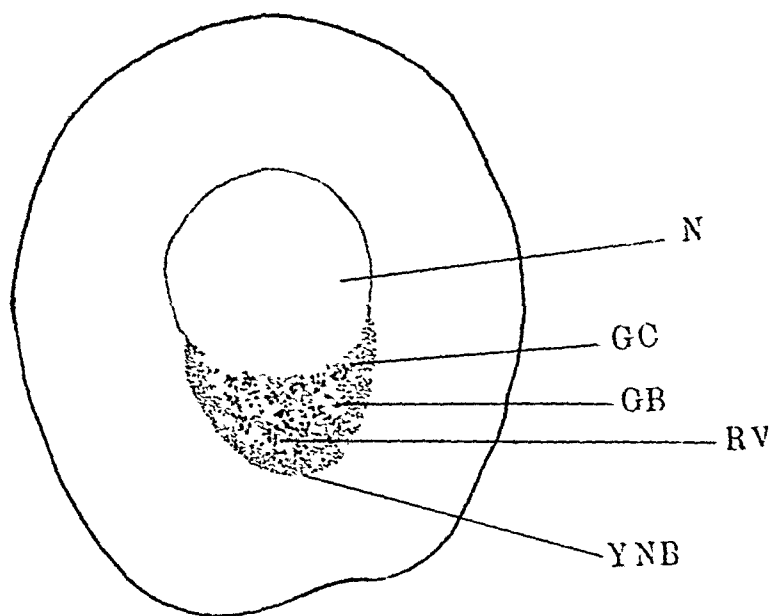


Fig. 3

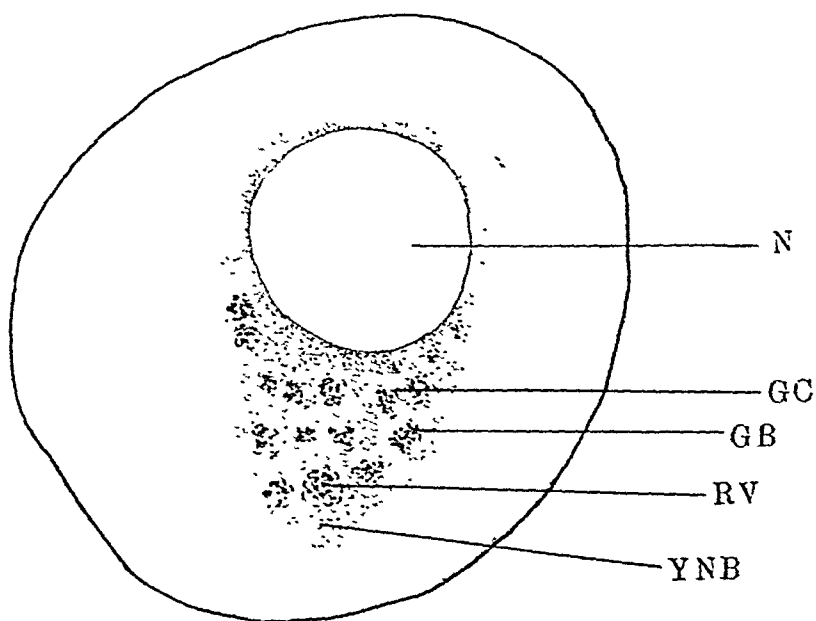


Fig. 4.

## DISCUSSION

The results of our observations described above lead us unmistakably to the conclusion that the neutral red vital staining experiments show two distinct cell organs side by side, *i.e.*, the Golgi bodies and Vacuome. What is remarkable is the fact that in the oogonial and the early oocyte stages the red staining vacuoles are either surrounded by or lie closely approximated to the Golgi elements. The Golgi bodies themselves appear in the form of crescents, spherules or granules. Of these the crescents appear more deeply stained black than the others. Even without the aid of any stain their greyish-black colour brings them prominently into view. After the addition of the neutral red stain they assume a still darker colour and afford a sharp contrast to the red staining vacuoles and the refractory yolk bodies of a lighter colour which are not stained at all. The close approximation of the vacuome to the Golgi crescent raises the question, whether in the early stages the vacuome is derived from the Golgi body. The second alternative is that the vacuome, from the very beginning, arise independently of the Golgi bodies and their topographical situation in yolk-nucleus area is due to the fact that the force which brings all the other cell organs within the yolk-nucleus area is also responsible for keeping the vacuome in close proximity to the Golgi elements. In later stages, during the development of the oocyte, the vacuome like the Golgi bodies break out from the archoplasmic area and have a tendency to spread out in the cytoplasm. It is towards the end of the process that the patches also disappear and the Golgi bodies and the vacuome become absolutely isolated. The neutral red staining experiments have been confirmed by an examination in a very dilute solution of osmic acid. Here also the Golgi crescents come prominently into view but the vacuome is invisible. If a small quantity of dilute neutral red is now added, within a very short time the

vacuoles are coloured. This conclusively proves that the vacuome and Golgi bodies could not possibly be homologous structures as claimed by Parat (12—16). Janus green B is supposed to be a specific for mitochondria. The Golgi crescent could not thus be a modified form of mitochondria as claimed by Parat (16) for they show no reaction with Janus green B whereas along with Golgi spherules and granules they come prominently into view with neutral red or with dilute osmic acid treatment. Our conclusions thus do not support Parat's Lepidosome Theory or his contention that the Golgi bodies and the vacuome are homologous. We are in agreement with the views lately expressed by Gatenby (7 and 8), Mukerji (9 and 10), Bhattacharya and Das (5) on this point.

## EXPLANATION OF FIGURES

All figures are drawn under oil immersion with the aid of a camera lucida.

Fig. 1.—A later oogonium stained with neutral red showing vacuoles (vacuome) with granular and crescentic Golgi elements situated on one side of the nucleus.

Fig. 2.—A very early oocyte treated with neutral red stains. It shows red vacuome in the medullary region, the Golgi crescents forming a cortex of the yolk nucleus of Balbiani.

Fig. 3.—A later oocyte showing the yolk-nucleus of Balbiani forming a cap over the nucleus. It contains patches of vacuoles, Golgi granules and crescents scattered in the area.

Fig. 4.—A still later stage of oocyte showing the perinuclear arrangement of the Golgi bodies and vacuome in the yolk-nucleus of Balbiani.

Fig. 5.—An advanced stage of oocyte in which the yolk nucleus of Balbiani has disappeared. Vacuoles in patches and Golgi bodies are seen scattered in the general cytoplasm.

Fig. 6.—A still older oocyte in which the vacuoles have lost the group arrangement and lie individually dissociated with Golgi crescents and smaller spherical Golgi bodies.

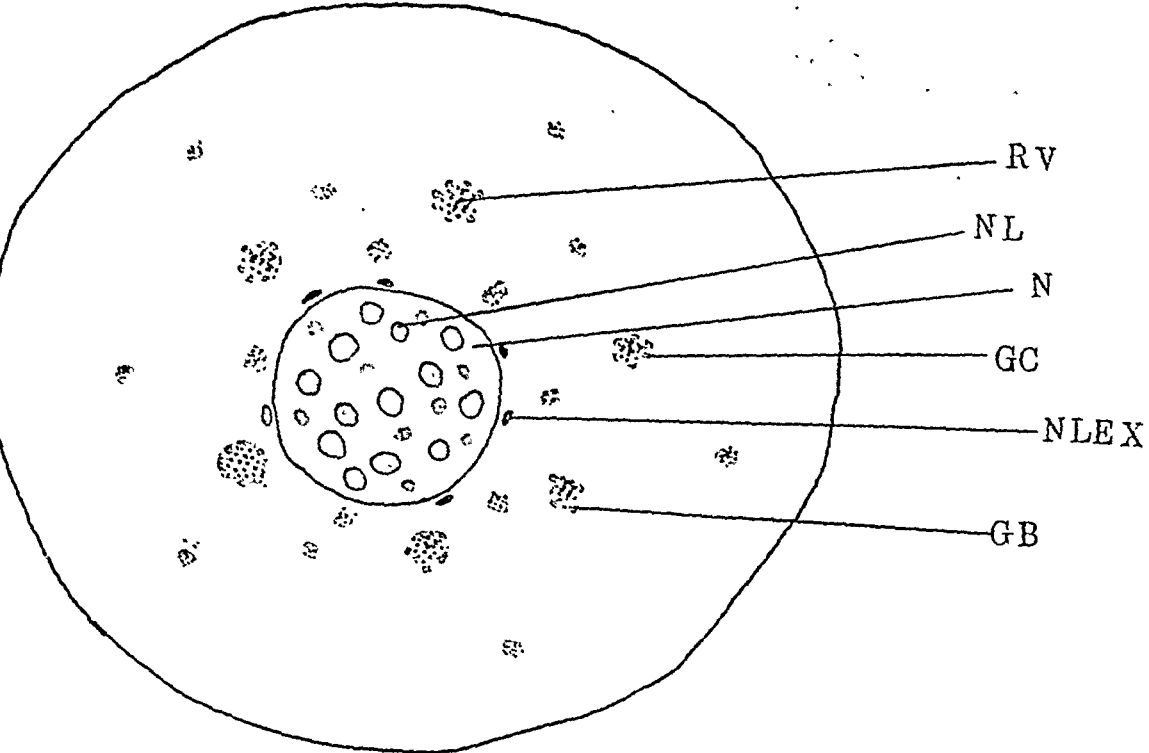


Fig. 5

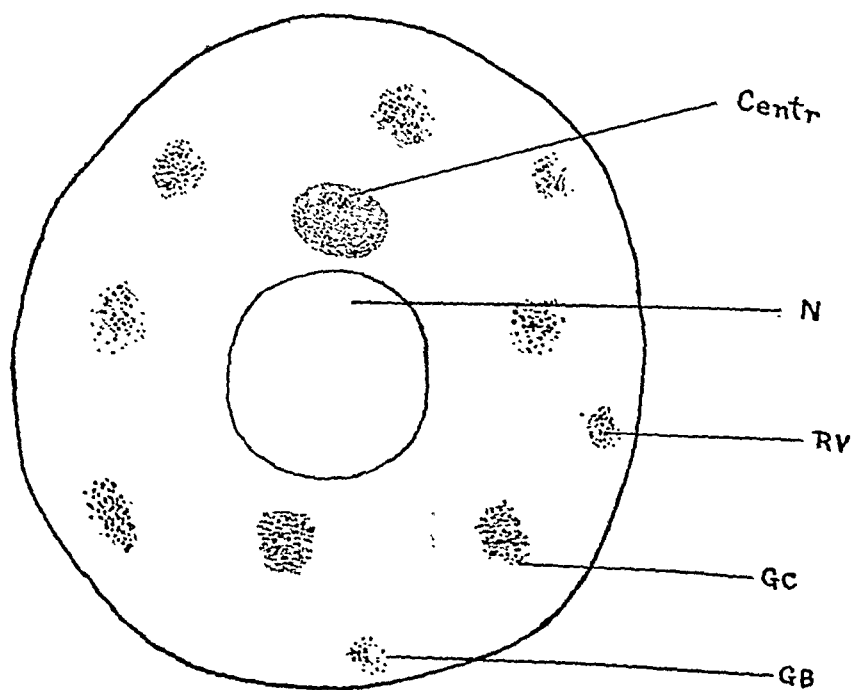


Fig. 5A

## LETTERING

- GB. Golgi body.  
GC. Golgi crescent.  
NLEX. Nucleolar extrusion.  
NL. Nucleolus.  
N. Nucleus.  
RV. Neutral red vacuome.  
Y. Refractive yolk body.  
YNB. Yolk-nucleus of Balbiani.

## LITERATURE CITED

1. Avel, Marcel—Vacuome et appareil de Golgi Chez les Vertebres. Comptes rendus de l'Acad des Sciences, Tome 180, No. 12, 1925.
2. Bowen, R. H.—Golgi Apparatus and Vacuome. Anat. Rec. V. 35, No. 4, 1925.
3. Bhattacharya, D. R.—Les Inclusions Cytoplasmiques dans l'oogenese de certains Reptiles. Thèse, Sciences de Paris. 1925.
4. Bhattacharya, D. R.—The Golgi Apparatus and Vacuome Theory. Allahabad University Studies, Vol. III, 1927.
5. Bhattacharya, D. and Das, R. S.—Golgi Body and Vacuome. Nature, November 2, 1929.
6. Gatenby, J. B. and Cowdry, E. V.—Microtomists' Vade-Mecum. 1928.
7. Gatenby, J. B.—Study of Golgi Apparatus and Vacuolar System of *Caira Helix*. Abraxas by Intra-Vital Methods. Proc. Roy. Soc. Ser. B. Vol. 104, 1929.
8. Gatenby, J. B.—Cell Nomenclatures. J. R. Micr. Soc., 1930.
9. Gatenby, J. B. and Mukerji, R. N.—The Spermatogenesis of *Lipisma Domestica*. Q. J. M. S., Vol. 73, Part 1, 1929.
10. Mukerji, R. N.—Later Stages in the Spermatogenesis of *Lepisma Domestica* with a note on its vacuolar system. Jour. Roy. Micr. Soc., Vol. XLIX, pp. 1-8, 1929.
11. Nath, V.—The Golgi Origin of Fatty Yolk in the Light of Parat's Work. Nature, 27th November, 1926.

12. Parat, M. et Painleve, J.—Appareil reticulaire interne de Golgi, Trophosponge, de Holmgren et Vacuome. C. R. Acad. Sci, t. 179, 1924.
13. Parat, M. et Painleve, J.—Techniques relatives a la demonstration du vacuome et sa comparaison avec l' appareil de Golgi, C. R. Soc. Biol., Tome XCII, 1925.
14. Parat, M.—Vacuome et appareil de Golgi, C. R. de l. Assoc des Anatomistes, 1925.
15. Parat, M. et Bhattacharya, D. R.—Les Constituants Cytoplasmiques de la cellule germinale femelle de l' ovocyte de *Ciona intestinalis*, C. R. Soc. Biol., Tome XCIV, 1926.
16. Parat M.—Sur la constitution de l' appareil de Golgi et de l' idiozome; Vrais et faux dictyosomes. C. R. Acad. Sci., T. 182., 1926.

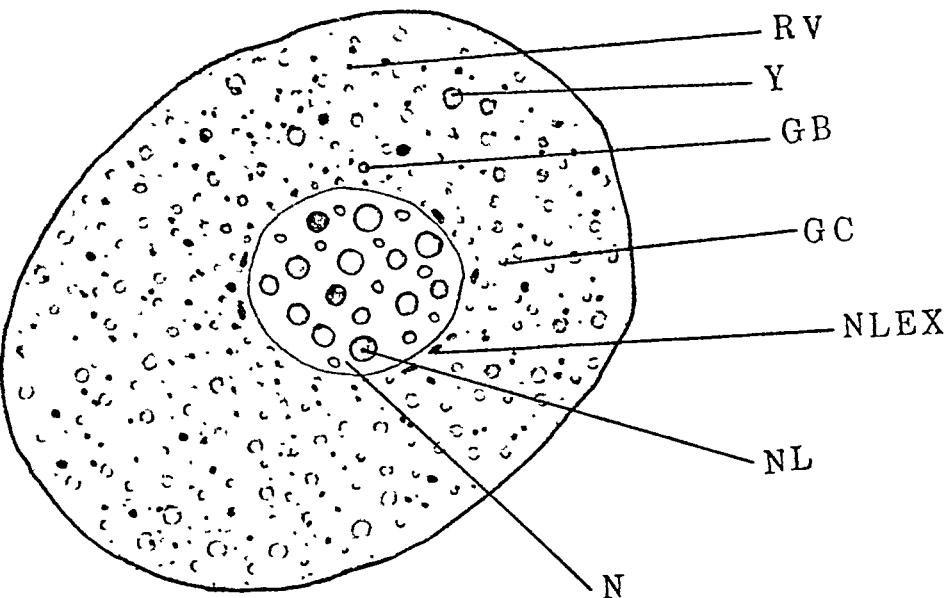


Fig. 6

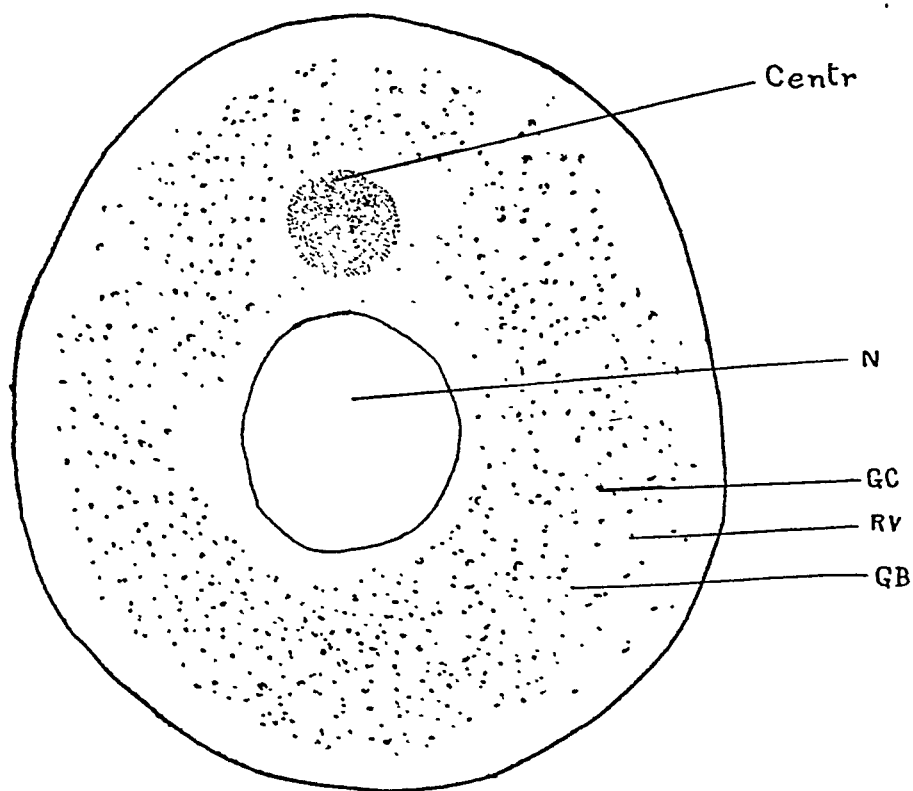


Fig. 6A

NOTES ON A PAIR OF ABNORMAL DIVERTICULA  
OF THE GIZZARD IN A PIGEON (COLUMBA  
INTERMEDIA STRICKL)

BY

S. K. DUTTA, M.Sc.,

*Lecturer in Zoology, University of Allahabad,  
Allahabad.*

This paper deals with an abnormality in the gizzard of a female pigeon observed during the course of a demonstration to the junior students of the Zoology Department of the University of Allahabad. In only one out of thirty-eight pigeons dissected on this occasion, was this abnormality in the gizzard observed. Subsequently a large number of pigeons were dissected and no other instance of this kind of abnormality was found.

The pigeon in question was fixed in 5 per cent formalin and preserved in formol-alcohol and the anatomy of the gizzard studied by careful dissection and sectioning.



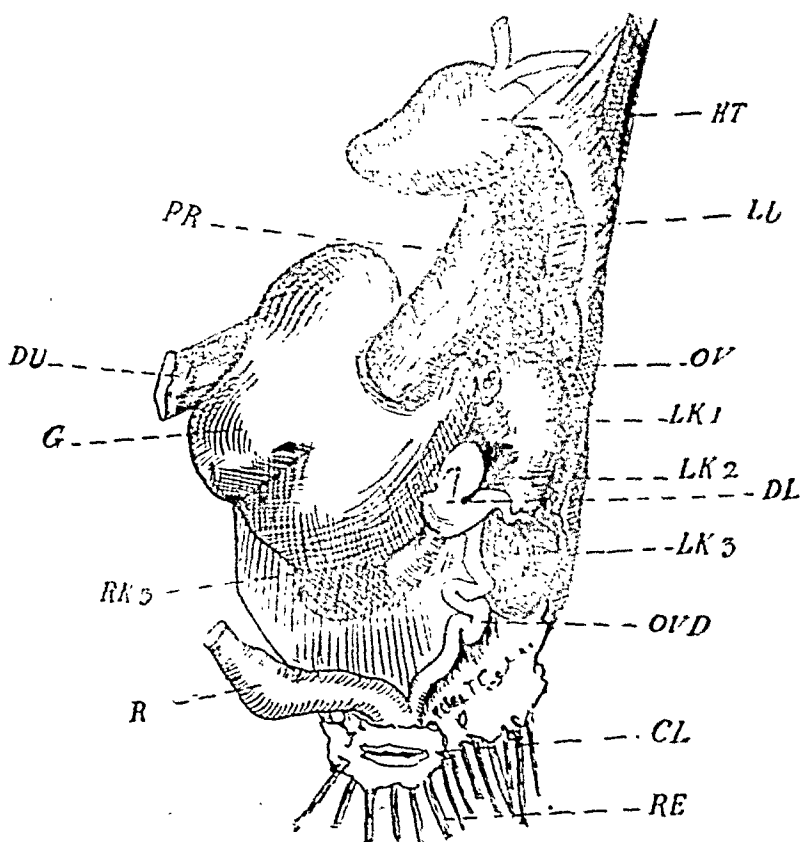


FIG 1.

Fig. 1.—The dissection of the pigeon showing the viscera in situation.

The diverticulum of the gizzard is seen to pass through the kidney.

[CL—Cloaca. DL—Left diverticulum. DU—Duodenum. G—Gizzard. Ht—Heart. LK<sub>1</sub>, LK<sub>2</sub>, LK<sub>3</sub>, First, second and third lobes of the left kidney. LU—Lung. OV—Ovary. OVD—Oviduct. PR—Proventriculus. R—Rectum. RE—Retrices. RK<sub>3</sub>—Third lobe of the right kidney.]

The abdominal viscera of this bird (Fig. 1) presents quite normal structures in its relative position except with regard

to the gizzard, (Fig. 1 G) which is slightly dilated, owing perhaps to its contents which consisted of large quantities of food grains and sand particles. Curiously enough, a brass pin about 3 cm. long was found inside the gizzard lying transversely. The gizzard like other organs of the abdomen is invested with a fold of peritoneum. The abnormality consists in the fact that from its dorso-lateral walls there arises a pair of slightly convoluted diverticula (Fig. 1 DL) measuring about 17 mm. in length and 8 mm. in its greatest width. Each diverticulum passing upward and outward penetrates the kidney of the respective side between its middle and posterior lobes and becomes attached to the ventral sur-

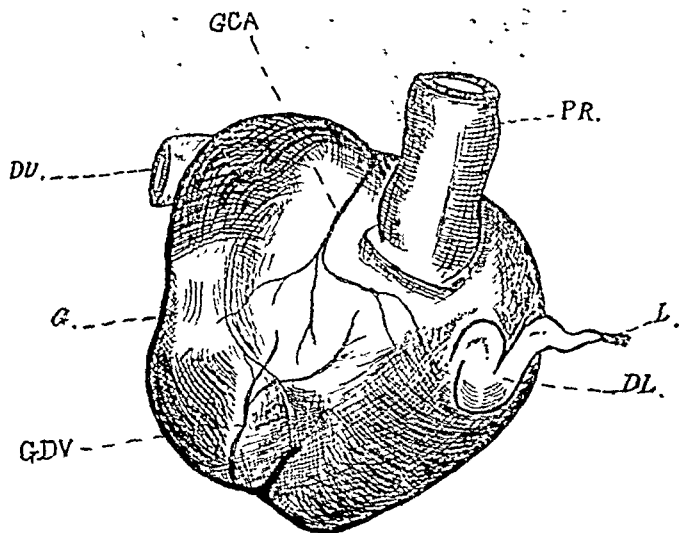


FIG 2

Fig. 2.—The gizzard showing the ligament of connective tissue at the extremity of the diverticulum for the attachment with ilium.

DU—Duodenum. DL—Left diverticulum. G—Gizzard. GCA—Gastro-intestinal branch of the coeliac artery. GDV—Gastro-duodenal vein. L—Ligament. PR—Proventriculus. The diverticula bear no organic connection with the kidney tissue which only allows it to pass through its substance.

face of the ilium of the pelvic girdle by a short connective tissue ligament which was seen by carefully removing the lobes of the kidney.

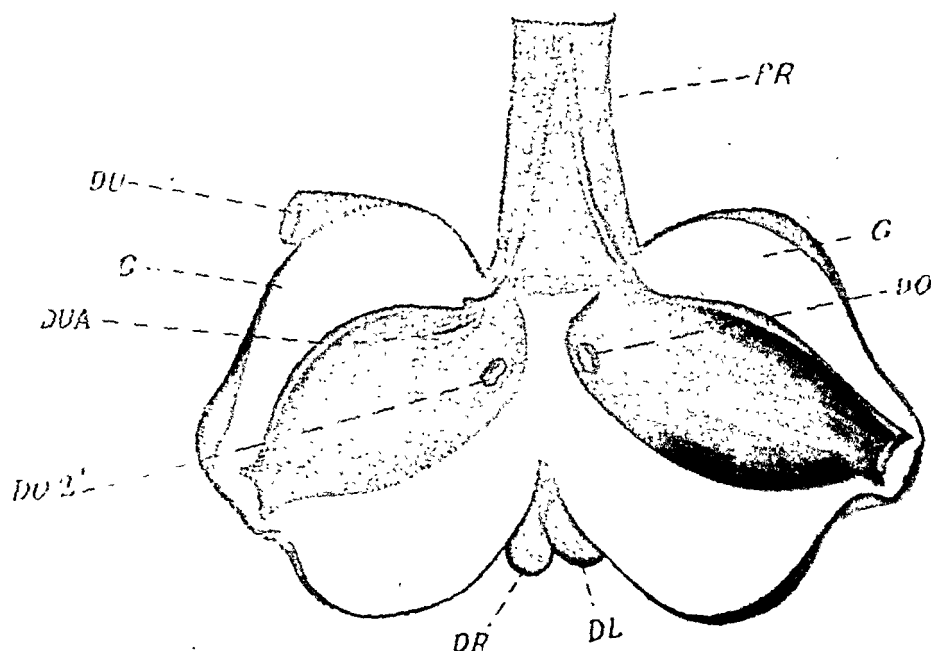


FIG 3

Fig. 3.—The gizzard bisected and laid open to show the internal orifices of the two diverticula.

[DU—Duodenum. DUA—Duodenal aperture in the gizzard. DO<sub>2</sub>—Left aperture of the diverticulum of the gizzard. DO—Right aperture of the diverticulum of the gizzard. DL—Left diverticulum. DR—Right diverticulum. G—Gizzard. PR—Proventriculus.]

The lumen of each diverticulum communicates with that of the gizzard by a small aperture (Fig. 3 DO<sub>2</sub>) which was

observed by cutting open the very thick muscular wall and washing away the contents from the cavity of the gizzard (Fig. 3 DO<sub>2</sub> & DO'<sub>2</sub>). On the two lateral walls of the gizzard there are two large and two small apertures, the larger ones (DUA & PR) open respectively into the proventriculus and the duodenum as usual, while the smaller ones (DO<sub>2</sub> & DO'<sub>2</sub>) communicate with the two diverticula. The openings of the proventriculus and that of the duodenum into the gizzard are in the normal position, while the orifices of the two diverticula are placed a little posterior to the apertures referred to above and in the middle of the side walls of the gizzard.

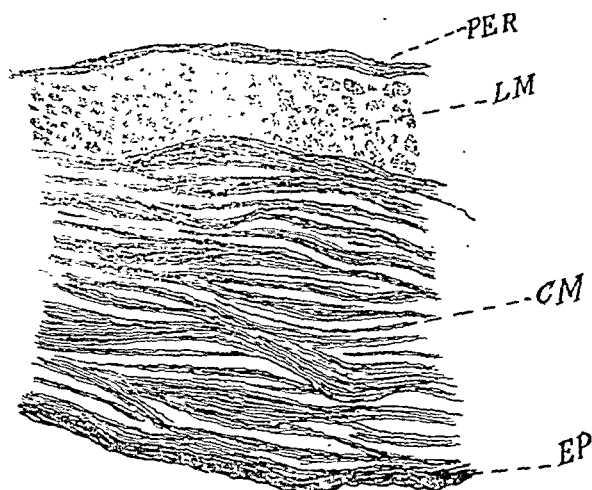
Apparently the two diverticula increase to a slight extent the internal dimensions of the cavity of the gizzard (Fig. 3 DR & DL). They evidently cause no disadvantage to the bird for it seemed to be quite normal and healthy before being killed.

It has been mentioned above that on cutting open the gizzard a small pin was found lying inside it. It lay across the cavity of the gizzard and its two ends, encrusted with lime, were lodged in the lumen of the two diverticula. It appears that the animal sometimes swallowed a pin which got fixed transversely in its gizzard. Its presence must have caused injury to the walls of the gizzard particularly when it worked as a gastric mill.

The diverticula show little peculiarity so far as their microscopic structure is concerned. A transverse section (Fig. 4.) of it shows a thick parchment like internal lining (Fig. 4 EP) composed of flat cells and superposed one above the other lie the circular (CM) and the longitudinal (LM) muscle layers. The circular muscle fibre is very thick constituting the greater part of the thickness of the wall of the diverticulum.

The blood vascular system supplying the organs in this region consists of very fine branches of the coeliac artery. The blood supply of the diverticula, however, is not very

copious as very little absorption of food takes place in this part. Each diverticulum is supplied by a very slender



## FIG 4

Fig. 4.—Transverse section of the diverticulum of the gizzard showing the thick muscular wall.

[CM—Very thick circular muscle fibre layer. EP—Internal epithelial lining of the diverticulum of the gizzard.

LM—Longitudinal muscle layer. PER—Peritoneal investment of the gizzard.]

and thin vessel from the gastro-intestinal branch of the coeliac artery (Fig. 2 GCA) and this apparently capillarises eventually to open into the gastro-duodenal vein of the Heptic portal system (Fig. 2 GDV).

The author wishes to express his sincere thanks to Professor D. R. Bhattacharya, for his advice and criticisms.

# NOTES ON THE ANATOMY OF AN ABNORMAL HEN (*GALLUS DOMESTICA*)

BY

GYANENDRANATH ROY, M.Sc.,

*Research Scholar, Zoology Department,  
University of Allahabad.*

In this communication I propose to describe the anatomy of an abnormal hen obtained locally. The abnormality lay in the structure of the cloacal sac and in the possession of a pair of supernumerary pelvic appendages not touching the ground in addition to the normal pair of hind legs. The hen was normal and was fully developed in all other respects and could walk about with ease. Its age could not be ascertained.

The work was done in the Department of Zoology of the University of Allahabad under the supervision of Prof. D. R. Bhattacharya. I have to acknowledge my sincere thanks to him for kindly allowing me to work on the specimen and for guidance and criticism.

The anatomy of the fowl was studied by careful dissection. There are two external openings (Fig. C) in the anal region situated on either side of the base of the abnormal limbs. The right abnormal leg (Figs. A, B and C) is small and is bent upon itself. It measures 2.1 inches from the base to the tip of the toe. Its proximal end is fused with the left abnormal hind leg which has all the parts well represented. The femur of the left abnormal leg is 3.2" long and to this is articulated the tibio-tarsus at right angles to its long axis. The tibio-tarsus measures 2.9", tarso-metatarsus 2.5", and the

digits which are four in number measure .4", 1.5", 2.1" and 1.5". The measurement of the normal legs is as follows:—

Tibio-tarsus 4.5", tarso-metatarsus 3.5" and the digits .5", 2.0", 2.8" and 1.8" respectively. Apparently it seems that the hanging part of these abnormal limbs has no skeletal support of its own and the femur of the right abnormal hind leg is partly fused with the femur of the left abnormal hind leg. This pair of peculiar hind legs used to hang downwards and was not functional.

**Body Cavity.**—Nothing very singular can be found in the body cavity except for the fact that there is a thick layer of fat enclosing almost all the organs contained within it.

**Digestive System.**—The anterior portion of the digestive system presents no peculiarities. The cloaca is a dilated sac (Fig. 1) which superficially appears to possess two distinct openings—one being the normal anus situated on the right side and the other the cloacal orifice on the left side. Careful dissection, however, revealed the fact (Fig. 2) that though the rectum lies in close approximation to this dilated chamber (cloaca), it has no communication with it. It passes by it and opens into the right anus. The oviduct, on the other hand, runs along and opens into this dilated chamber which in its turn opens on the left side of the body by the cloacal aperture. The ureters from the kidneys descend in the usual way and open into this dilated sac near the base of the oviduct. It appears probable that the urodeum in this case has lost its connection with the gut and has become enlarged into an extremely large sac-like chamber opening separately outside by the cloacal aperture on the left side of the abnormal pair of hind limbs.

**Vascular System.**—So far as the vascular system of the bird in question is concerned, only the vessels in connection with the pelvis and the abnormal limbs present certain peculiarities.

With regard to the venous system (Fig. 3), the posterior mesenteric vein arising at the point of bifurcation of the caudals runs posteriorly and divides into two branches: the left branch (n) goes to supply the cloaca while the right branch (m) supplies the mesenterial folds and the posterior region of the rectum. The left internal iliac vein supplies the abnormal limbs. It first gives out two branches (a & b), one to the rectum and the other to the cloaca. It then divides into three branches: one of these (d) supplies the right abnormal hind limb while the other two enter the long (left) abnormal hind leg. The corresponding right internal iliac vein possesses no such ramifications. Thus the entire abnormal structures—limbs, rectum and cloaca are supplied by branches of the left internal iliac vein.

The left sciatic vein before entering the kidney gives out a branch (Q—Fig. 3) which ramifies over the whole of the left side of the pelvic region. The right sciatic vein does not possess a similar corresponding branch and the right side of the pelvis is supplied by branches of the right internal iliac vein.

The arterial supply of the pelvic region is somewhat remarkable (Fig. 4). The iliacs divide into two branches, one of which (h) supplies the pelvic region while the other (j) supplies either the rectum or the cloaca as the case may be. The abnormal limbs are supplied by the posterior mesenteric artery which courses alongside the posterior mesenteric vein. It divides into two branches, one of which goes to supply the right abnormal leg while the other supplies the left abnormal one. During its course inside the left abnormal leg it further subdivides into two branches.

The sciatic artery after emerging from the kidney gives off a branch which divides into two: one of these (g) supplies the ovary and the oviduct while the other (f) runs obliquely downwards under the biceps to supply the muscles lying in the pelvis. The third and the main branch gives off many branches to the thigh.



The femoral artery during its course gives off a long branch (a) which runs posteriorly over the whole length of the pelvis supplying arteries to the abdominal muscles and a few branches to the rectum and the cloaca. This branch also appears to supply the oviduct and the ovary. In this case, as in a normal fowl, the hind limbs are supplied by the femoral and the sciatic arteries, but the abnormal pair of hind limbs, curiously enough, is supplied by the branches of the posterior mesenteric artery which under ordinary circumstances only supplies the mesenterial folds and the anal region.

**Reproductive System.**—In most birds the left ovary persists throughout life. But in this case both the right and the left ovaries are present in a well developed form. Only the left oviduct is well developed and functional, the right being represented by a small vestige lying close to the rectum. The left oviduct opens into the left side of the cloacal chamber. This chamber in which the oviducal opening is situated is entirely separated from the rectum, and opens to the exterior by the cloacal opening situated on the left side of the abnormal limbs. Into this chamber also open the urinary ducts which arising from the kidneys run downwards and open separately into it.

**Skeletal System.**—The most interesting feature in this bird is the skeletal system of the abnormal limbs and also of the pelvic girdle. The abnormal pair of hind limbs hang downwards and seem to be attached only by a cartilaginous plate. On dissection, however, it was found that the head of the femurs of the abnormal pair of hind limbs is peculiarly modified into a cup-shaped structure articulating with the pygostyle. This cup-shaped structure has a notch at the upper end (as shown at K in Figs. 5 and 6) into which fits the pygostyle. This cup-shaped process is in continuation with a cartilaginous plate which covers the lower abdominal region.

The tibio-tarsus of the right abnormal leg (Fig. 5) is small and bent and there is no trace of the fibula. Its two ends are not spherical to form articulating knobs but are fused respectively with the femur and the tarso-metatarsus. The latter turns over the tibio-tarsus and the two phalanges are fused with it. The tibio-tarsus of the left abnormal hind leg (Fig. 5) is fused with the femur. Both in the right and the left abnormal limbs there is no cnemial process and no patella. The fibula in this leg is quite well developed. The tarso-metatarsus is fused with the tibio-tarsus. There are four well-developed phalanges articulating with the tarso-metatarsus.

The pelvic girdle is large and very wide. The ventral view (Figs. 7 & 8) shows that the width of the girdle is greater than that in a normal bird. Had it not been so wide, the abnormal pair of hind limbs would not have so easily articulated with the pygostyle. Moreover the synsacrum is bent and the pygostyle is fused to form a compact smooth knob with which the cup-shaped head of the femurs of the abnormal limbs is easily articulated. Thus we see that the width of the girdle is more of the nature of an adaptation for assisting the articulation of the peculiar hind limbs.

Dr. Bhattacharya\* described a case of a fowl with two heads and necks but the rest of the body joined together.

The duplicity of the orifices in the posterior region has recently been observed and its morphological significance described by Pires De Lima.† He has recorded two cases. The first one was a male child four years old. This child possessed two anal orifices, one alongside the other. The

---

\* Bhattacharya, D. R.—Notes on the Anatomy of a Double Monstrosity in the Chick.

† Pires De Lima.—La Duplicite De L'Anus et sa Signification Morphologique. (Comptes Rendus de l'Association de Anatomistes, Vols. 11—13, 1927.)

right one only functioned as the normal anus while the left one, which was of approximately the same calibre as the right, was a cul-de-sac. Only a thin cutaneous bridge separated the two. This child was physically well developed. In the second case which was a fowl the animal presented an identical anomaly. It possessed two anal openings, one larger than the other. The one which was situated on the left of the median line being of larger calibre than the one on the right. Both of these apertures possessed sphincter muscles which contracted simultaneously in a rhythmic fashion. The faeces could be eliminated by the left aperture only. The right one led into a blind canal and did not open into the cloaca situated on the left side. Into this cloaca the rectum and the oviduct open. Pires De Lima quotes other cases of such deformities in animals other than birds from the works of previous authors.

In conclusion, it may be said, that the animal I have described is peculiar (1) in the possession of an additional pair of hind limbs, and (2) in the possession of two external orifices in the anal region. It differs from those described by Pires De Lima and others in possessing a big cloacal chamber into which the oviduct opens but not the anus, the anal aperture being separate and distinct from the cloacal aperture.



PLATE II



Fig. C

## EXPLANATION OF PLATES

- Fig. A.—A side view of the animal in the live condition.
- Fig. B.—Ventral view of the bird with feathers and skin intact.
- Fig. C.—Posterior view of the bird with feathers removed.
- Fig. 1.—Entire view of the cloacal chamber and the rectum.
- Fig. 2.—Horizontal section of the cloacal chamber and the rectum.
- Fig. 3.—Venous supply of the posterior region.
- Fig. 4.—Arterial supply of the posterior region.
- Fig. 5.—Skeleton of the abnormal limbs. fe=femur; fi=fibula;  
ti. ts=tibio-tarsus; ts. mtts=tarso-metatarsus; ph=  
phalanges.
- Fig. 6.—Enlarged head of the fused Femurs of the Abnormal  
Limbs.
- Fig. 7.—Ventral view of the pelvic girdle. il=ilium; isc=ischium;  
pu=pubis; ac=acetabulum; is. for.=ischiatic foramen;  
obt. ntc.=obturator notch; pyg. st.=pygostyle;  
syn. scr.=syn-sacrum.
- Fig. 8.—Side view of the Pelvic Girdle.
-

# TWO DISTOMATE TREMATODES FROM INDIAN REPTILES

BY

H. R. MEHRA, M.Sc., Ph.D. (Cantab.),  
Reader of Zoology, University of Allahabad.

## INTRODUCTION

In this paper I describe *Ommatobrephus lobatum* Mehra, 1928 (syn. *Om. folium* Thapar and Farzand Ali, 1929) and *Encyclometra caudata* (Polonio, 1924). The former is a common parasite of the rectum of snakes and lizards of the genus *Varanus* in northern India. The fact that the only other species of the genus *Ommatobrephus* Nicoll was obtained from a North African lizard *Uromastix acanthinurus* shows that in its distribution this genus is restricted to the lizards and snakes of North Africa and South Asia. *Encyclometra caudata* extends from the heart of the Mediterranean region to the extreme Orient. It has been found by Bhalerao in Burma and Joyeux and Houdemer in Indo-China.

*Ommatobrephus lobatum* was described by me in a paper read before the Zoology Section of the Indian Science Congress, Calcutta 1928, and an abstract thereof appeared in the proceedings of that body for that year. The publication of the full account has been, however, delayed till now. Thapar and Farzand Ali in December 1929, published an account of this very species under the name of *Om. folium*. This raises an important question of nomenclature, which on the basis of priority should be decided in favour of the name given by me. As will be seen from the following description, the account given by the joint authors is incomplete. The name *Om. lobatum* is also appropriate on account of the lobed appearance of the testes.

Thapar and Farzand Ali are silent about the systematic position of the genus *Ommatobrephus*, which following Nicoll they probably assign to the family Lepodermatidae Odhner. They seem to be unaware of the more recent work of Poche in 1925, in which he has created the family Ommatobrephidae to receive this genus. This is clear from the omission of the latter author's work from their list of references.

I am not sure whether *Encyclometra* belongs to the family Lepodermatidae, in which I have tentatively included it, as it shows closer affinities with the genus *Ommatobrephus* than with any genus of that family. It may be considered possible later on to remove the Encyclometriinae Mehra from the Lepodermatidae and include it in the family Ommatobrephidae Poche, which in that case should consist of two sub-families Ommatobrephinae and Encyclometriinae.

OMMATOBREPHUS LOBATUM MEHRA (SYN. OM. FOLIUM  
THAPAR AND FARZAND ALI)

The distomes were obtained in large numbers from the rectum of six *Zamenis mucosus* at Allahabad in July 1926. In all I examined eight snakes, out of which six harboured these parasites. Subsequently more snakes have been examined and it appears that one out of every three snakes is infected with it. The number of parasites in a host varies considerably; it is usually large 50-80 or even more but sometimes 6-10 only. A large number of immature specimens, entirely devoid of ova were obtained from the rectum of two *Varanus bengalensis* and kept alive for twelve days in normal salt solution at the laboratory temperature from December 17-27 1929. Apparently this species is tenacious of life and can live outside the body of its host in normal salt solution for a long time. The parasites are firmly attached to the walls of the rectum by the large stout ventral sucker and do not get easily detached when the rectum is opened. When fixed without being flattened under pressure they become



so contracted that the dorsal side is arched or convex and the ventral side depressed. The same appearance is presented when they are fixed attached to the walls. The size is small, 2·4-4 mm. in length and 0·9-1·3 mm. in maximum breadth in the region of the ventral sucker. The shape is conical with a bluntly pointed anterior end and a broad rounded posterior end. The body has considerable power of extension and contraction specially in the immature specimens, on account of which it may assume various forms. In front of the ventral sucker it is capable of being stretched out as a long narrow neck. The œsophagus in the extended condition is long and narrow; in the contracted specimen it is short with somewhat folded walls and a broad lumen. The body-wall is smooth and entirely devoid of spines. The oral sucker measures 0·25-0·3 mm. in diameter. The ventral sucker is stouter and much larger, a little more than double the size of the oral sucker measuring 0·5-0·7 mm. in diameter. It is situated a little behind one-third body length from the anterior end. The ratio in the size of the oral and ventral suckers is 1: 2·3.

A small prepharynx easily perceptible in life and entire mounts of extended specimens is present. The pharynx is nearly spherical, measuring 0·14-0·2 mm. in diameter; it is somewhat elongated in the extended specimens. The œsophagus is long having 0·27-0·4 mm. length. It is broadest immediately behind the pharynx, the greatest breadth attained being 0·14-0·16 mm. The intestinal bifurcation lies a little in front of the ventral sucker at 0·7-0·85 mm. distance from the anterior end. The intestinal caeca are long reaching a little distance in front of the posterior end of the body and terminating at about the anterior margin or in much flattened specimens the middle of the testes with their blind ends converging towards the latter.

The excretory opening is situated ventrally near the posterior end. It leads into a small transversely oval or somewhat triangular contractile vesicle, which at about the

centre of the testes passes by a very short stem into two long, fairly broad and somewhat winding diverticula extending forwards one on each side as far as the pharynx, where they form a loop to continue backwards as the common collecting ducts. The latter divide at the level of the ventral sucker into anterior and posterior collecting ducts as shown in text-fig. 1. The vesicle represents the main short stem and the long more or less coiled limbs, the arms of the V-shaped excretory bladder. The excretory system closely resembles that of certain Echinostome cercariae and may therefore be considered as larval in its pattern. In *Om. lobatum* the main stem of the excretory bladder is smaller than that in *Om. singularis* in which according to Nicoll it bifurcates in front of the testes.

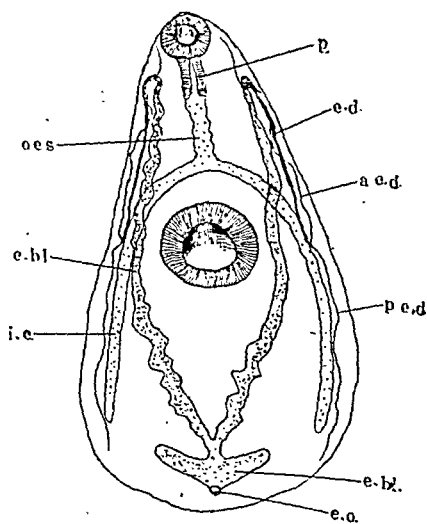


Fig. 1

Diagrammatic view of the excretory system in *Ommatobrephus lobatum*. For explanation of letters see text to text.

The genital opening is median, situated close behind the intestinal bifurcation and a little in front of the ventral sucker. The testes occupy a lateral position at the posterior end of the body close behind and within the blind ends of the caeca. They are longer than broad and lobed with their posterior parts converging towards each other near the median plane; they lie ventrally with their ventral border approaching the ventral body-wall. This species is characterised by the irregular lobulations of the testes, on account of which it is named *Om. lobatum*. The testes, separated from each other, by the mesially situated receptaculum seminis and a fold of the uterus lie at the same level and not as in *Om. singularis*, in which the left testis lies slightly in advance of the other. They are unequal in size measuring 0·37-0·57 mm. in length and 0·16-0·35 mm. in maximum breadth. The vasa efferentia arise from their anterior margin near the inner side as long thin tubes, which just before entering the cirrus sac unite to form the inconspicuous vas deferens. The cirrus sac, 0·14-0·25 mm. in length and 0·1-0·12 mm. in breadth is small, and ovoid or oval in shape having convex anterior and concave posterior sides. It lies median in front of the ventral sucker in the space between it and the intestinal bifurcation with its broad basal part near the margin of the sucker inside the left intestinal caecum. Its walls are very thin, composed of the fibres of the adjacent parenchyma and are entirely devoid of muscle fibres (Fig. 4). The vesicula seminalis is large and saccular occupying almost the entire space within the cirrus sac except a small terminal part, which contains the pars prostatica and ductus ejaculatorius. It is deeply constricted so as to be divided into two parts, subspherical in outline of which the proximal part, in which the vas deferens opens is larger measuring 0·089-0·1 × 0·1-0·13 mm. in size; the distal part measures 0·05-0·08 × 0·06-0·08 mm. It appears doubtful whether the vesicula seminalis is highly convoluted in *Om. singularis* as Nicoll describes. The pars prostatica and ductus ejaculatorius

are tubular and very small, both measuring together 0.08-0.09 mm. in length. The prostate gland cells are small and less numerous than usual surrounding the terminal part of the vesicula seminalis, pars prostatica and ductus ejaculatorius. A protrusible cirrus is absent.

The ovary of a nearly spherical shape with entire margins lies median or slightly towards the left, a little distance in front of the testes. It is much smaller than the latter measuring 0.089-0.16 mm. in diameter and is covered with a thin fibrillar wall formed of the fibres of the surrounding parenchyma. The ova contained within the ovary are relatively large, largest among them measuring 0.01-0.014 mm. in diameter. As usual in distomes only one ovum is passed into the oviduct at a time. The oviduct arises from the anterior border of the ovary near its inner margin measuring 0.017-0.02 mm. in diameter at the point of origin. After running a short distance it is joined by a small narrow duct of the receptaculum seminis of 0.027 mm. length and immediately after on the dorsal side by the Laurer's canal. Then surrounded by the shell gland cells it bends backwards to receive the yolk reservoir. The shell gland complex lies mesially near the posterior margin of the ovary. The receptaculum seminis is large, tubular and usually looped in a U-shaped manner with one limb lying over the other in its hinder part (Fig. 1). It reaches distally the hinder end of the body close in front of the excretory opening occupying a median position in the space between the testes. It has a thin wall of parenchymatous fibres and is always filled with sperms. The proximal part of its duct is lined with an epithelium of columnar cells with prominent nuclei, but the cells gradually decrease in height towards the distal end of the duct, where it passes into the receptacle. The Laurer's canal of 0.008-0.01 mm. breadth is narrow, fairly long and convoluted. It lies dorsally to the proximal part of the receptaculum seminis close to the dorsal body-wall and opens to the exterior by a minute pore situated

near the mid-dorsal line in the region of the shell gland complex. The uterine convolutions are intracaecal and transversely arranged close to one another occupying almost the entire space behind the ventral sucker to the hinder end of the body between the testes. Near the posterior margin of the ventral sucker the ascending uterus passes into the thick-walled metraterm, which extends forwards overlapping or dorsally to the right or left margin of the ventral sucker to open into the genital atrium. The metraterm has muscular walls composed of a thin layer of longitudinal muscle fibres surrounded by a layer of circular muscle fibres. The genital atrium is small, the metraterm opening lying close to that of the ductus ejaculatorius. The genital opening is hardly seen in entire mounts as it lies covered by the terminal part of the cirrus sac.

In the early sexual condition the ductus ejaculatorius does not open directly to the exterior, but it opens into the metraterm so that the sperms pass straight from the male duct into the female duct of the same worm ensuring self-fertilization. At this stage the ovary is developed but it is smaller in size, while the uterus consists of a few small convolutions entirely free from ova. There seems to be no doubt that the sperms reach the uterus and ootype before the ova are discharged from the ovary and that self-fertilization is the usual mode of fertilization in this distome.

The ova are operculate and oval, and have a thin shell measuring 0.085 mm. in length and 0.037 mm. in breadth. The ova in the ascending uterus in front of the ovary contain well-developed miracidia having black eye spots and cilia. The miracidia lying near the ovary are not so well developed and active as those lying in the upper convolutions. When the distome is allowed to die on a slide by gradual evaporation of water, larvae come out of the eggs and can be properly studied. The miracidium is uniformly ciliated except the anterior protrusible papilla and possesses a prominent X-shaped eye, which

is really composed of two eyes apposed to each other on their convex sides. It is capable of considerable degree of contraction and extension and hence assuming various forms, while it is forcing its way to make its escape through the uterus or tissues of its parent subjected to a microscopic examination under a cover glass. The anterior part of the miracidium containing the eyes lies within the opercular part of the ovum.

The vitellaria are restricted to the extreme edges of the body closely outside the intestinal caeca, sometimes overlapping the latter dorsally and ventrally. They commence immediately behind the ventral sucker and terminate a little behind the blind ends of the caeca usually extending to the anterior one-third of the testes in well-flattened specimens. The follicles are not arranged in groups but they lie near one another, sometimes joined at places. The transverse vitelline ducts arise at level with or slightly in front of the ovary and join to form the yolk reservoir near its posterior margin somewhat to the right side. The transverse ducts and yolk reservoir are composed of fairly large cells with a central nucleus and vacuolar cytoplasm filled with small yolk particles.

#### ONMATOBREPHUS LOBATUM VAR. NAJII, N. VAR.

One specimen was obtained from the rectum of an Indian cobra *Naja tripudians*. The distome has a flat conical form under slight pressure measuring 4 mm. in length and 1.3 mm. in breadth in the region of ventral sucker. The body gradually broadens behind the ventral sucker till it attains the maximum breadth about half way between the ventral sucker and posterior end. In front of the ventral sucker it gradually narrows ending in a bluntly pointed anterior end. The oral sucker measures 0.3 and the ventral sucker 0.7 mm. in diameter. A prepharynx of  $0.39 \times 0.17$  mm. size is present. The pharynx is spherical measuring 0.21 mm. in diameter. The oesophagus is long, 0.46 mm. in length; its anterior half is broader and more

muscular with the greatest breadth of 0·13 mm. near the pharynx. The intestinal caeca end a little in front of the hinder end reaching the anterior end of the testes and are situated laterally near the body-wall.

The genital opening is median close behind the intestinal bifurcation. The cirrus sac is nearly spherical measuring 0·18 mm. in length and 0·14 mm. in breadth. It is thin-walled and occupies a median position in front of the ventral sucker. The vesicula seminalis is almost bilobed with the anterior lobe rounded in outline. The prostategland cells surround the vesicula seminalis and ductus ejaculatorius. The latter is short and slightly twisted before it opens to the exterior at the genital opening. The testes are restricted to the extreme edges near the body-wall at the hinder end close behind the vitellaria and blind ends of the caeca. They are slightly lobed, elongated and much narrower than in the type specimens measuring 0·62 mm. in length and 0·46 mm. in greatest breadth.

The ovary lies a little in front of the testes and is much smaller than the latter measuring 0·12 mm. in length and 0·18 mm. in breadth. The uterus and receptaculum seminis have the same form and position as in the type specimens. The muscular metraterm measures 0·037 mm. in diameter and runs forwards dorsally to the left side of the ventral sucker slightly overlapping its margin. The ova are thin walled, transparent and contain well-developed miracidia measuring 0·0714-0·098 mm. in length and 0·047-0·051 mm. in breadth. The vitellaria are confined to the extreme edges of the body outside the intestinal caeca commencing slightly behind the ventral sucker and terminating close in front of the testes.

This distome certainly belongs to *Om. lobatum*, but it differs in some points such as the size and shape of the testes, cirrus sac and ovary and the size of the ova. As this description is based on the examination of only one specimen, it is difficult to say with certainty whether it should be included in a new variety.

REMARKS ON THE GENUS *OMMATOBREPHUS* NICOLL AND  
THE FAMILY OMMATOBREPHIDAE POCHE

Nicoll in 1914 assigned *Ommatobrephus* to the family Lepodermatidae as a somewhat aberrant genus. Baer in 1924 excluded it from that family saying that its excretory system was too aberrant. Poché in 1925 created a new family Ommatobrephidae for it. Thapar and Farzand Ali do not discuss its systematic position, but they appear to follow Nicoll taking no notice of Poché's work of which they were probably unaware. I accept the family Ommatobrephidae Poché to receive this genus, the account of which as given by previous authors differs in certain points from that by me as noted below.

(1) Nicoll and Thapar and Farzand Ali deny the presence of the prepharynx. My examination of a large number of living and mounted specimens has convinced me of its presence in *Om. lobatum*. It is easily seen in living specimens, but in entire mounts it may not be visible on account of contraction in the worm due to fixation. I believe that it is also present in *Om. singularis* and as Nicoll's study was based only on one specimen, it probably escaped his notice.

(2) Nicoll describes the excretory bladder as Y-shaped with a small winding stem bifurcating a little in front of the testes. As will be clear from the foregoing description, it is V-shaped and essentially larval in its form resembling that of the Echinostome larvae. The excretory system is very different from that of the Lepodermatidae and Thapar and Farzand Ali's remark that the bladder exhibits, together with its branches, a characteristic feature of the family Lepodermatidae is misleading.

(3) According to Thapar and Farzand Ali the terminal part of the ductus ejaculatorius is muscular and forms a narrow cirrus. I feel sure that a protrusible cirrus is absent. The account of the connection of the Laurer's canal with the receptaculum seminis given by these authors differs from mine.



(4) The cirrus sac does not possess thick muscular walls as the joint authors describe, on the other hand, it is thin-walled as Nicoll pointed out. My description and Fig. 4 will show that its thin walls are composed of a fine layer of adjacent parenchymatous fibres.

The two species of this genus are sharply separated by the following well-defined characters :

In *Om. lobatum* the genital pore lies a little behind the intestinal bifurcation; in *Om. singularis* it lies on the intestinal bifurcation. The former species is also distinguished by the greater length of its intestinal caeca, the vitellaria ending more posteriorly and the lobed appearance of its testes.

In view of these facts the definition of the family Ommatobrephidae Poche based only on Nicoll's account of *Om. singularis* needs modification. I therefore give the following altered definition of this family :

Body-wall without spines, oral sucker small, ventral sucker much larger. Prepharynx and pharynx present; œsophagus long; intestinal bifurcation a little in front of the ventral sucker; intestinal caeca of varying length. Excretory bladder larval in form resembling somewhat that of the Echinostome larvae and consisting of a contractile vesicle and long more or less winding arms, which extend as far as pharynx, where they form a loop to continue backwards as common collecting ducts. Genital opening median, situated a little behind or on the intestinal bifurcation. Testes elongated oval, entire or lobed, laterally situated at hinder end. Cirrus sac (pseudo-cirrus sac) thin-walled, composed of parenchymatous fibres and situated in the space between ventral sucker and intestinal bifurcation. Vesicula seminalis large, globular and bilobed; pars prostatica and ductus ejaculatorius small; protrusible

cirrus absent. Ovary somewhat rounded with entire margins, median or somewhat to the right in front of testes. Receptaculum seminis large and tubular; Laurer's canal present. Vitellaria of restricted extent confined to margins of the body commencing behind ventral sucker and terminating some distance in front of hinder end. Uterus intracaecal, filling entire space behind ventral sucker to the hinder end between testes. Eggs large, thin-walled and less numerous than in the Lepodermatidae; miracidia developed in the eggs in utero. Habitat rectum and intestine of lizards and snakes.

The family Ommatobrephidae is of peculiar interest. Not only does it resemble the sub-family Encyclometriinae in certain features of its anatomy as will be discussed later (see p. 48), but it is also closely related to the family Echinostomidae. It resembles the latter family in the size of its ventral sucker, which is much larger and stouter than the oral sucker. The oesophagus bifurcates a little in front of the ventral sucker in both the families, which also resemble each other in the position of the genital pore and the cirrus sac in the space between the intestinal bifurcation and the ventral sucker. The vesicula seminalis in the Echinostomidae is large and bilobed as in *Ommatobrephus*. The ovary is small and lies in front of the testes, some distance behind the ventral sucker in both these families. The excretory bladder of the Echinostomidae is no doubt Y-shaped, but the main stem is short and bifurcates behind the testes into two long cornua, which extend as far as the anterior end. In the Ommatobrephidae the main stem is shorter and vesicular giving the bladder more or less V-shaped appearance, otherwise the resemblance is fairly close. It, however, does not give off lateral anastomosing branches like that of the Echinostomidae. In the excretory system *Ommatobrephus* resembles more closely the larvae of the Echinostomidae

than the adult forms. Finally the ova of the two families are large, thin-shelled and oval measuring 0·065-0·12 mm. in length. In the genus *Pelmatostomum* Dietz and *Ech. croaticum* Stoss the miracidia have been found in the eggs in utero as in *Ommatobrephus*.

### ENCYCLOMETRA CAUDATA (POLONIO, 1859)

Six specimens were obtained from the œsophagus of *Tropidonotus piscator* and one from the stomach of *Zamenis mucosus* at Allahabad. They were yellowish grey in colour on account of the colour of the ova and firmly attached to the walls of the œsophagus. All the measurements are taken from mounted specimens slightly flattened before fixation. The length varies from 7-11 mm. and the breadth in the widest part, i.e., in the region of the ventral sucker from 2·4-3 mm. The anterior end is rounded and the posterior end tapers to a blunt point. The cuticle is thick and entirely devoid of spines. The oral sucker is subterminal facing ventrally and is slightly smaller than the ventral sucker measuring 0·73-0·9 mm. in diameter. The ventral sucker measures 1·03-1·28 mm. in diameter and is situated at about the end of one-third body length. A prepharynx of 0·1 mm. length and 0·44 mm. breadth is present. The pharynx is cup-shaped and notched in front, measuring 0·4-0·6 mm. in length and 0·4-0·5 mm. in breadth. The œsophagus is very small measuring 0·05-0·09 mm. in length. The œsophageal glands are present. The intestinal bifurcation lies 0·9 mm. distance in front of the ventral sucker. The intestinal caeca occupy a lateral position near the body-wall reaching the hinder end but not ending at the same level, the left one being a little longer.

The testes are subspherical in shape situated close behind each other in the median line in the posterior half of the

body. The anterior testis lies 2.8-3.7 mm. in front of the hinder end and 4 mm. behind the anterior end, and measures 0.38-0.53 mm. in diameter. The posterior testis, 0.4-0.53 mm. in diameter lies 0.14-0.5 mm. distance behind the anterior testis dorsally to the main stem of the excretory bladder. The vasa efferentia are long thin tubes, which unite at the base of the cirrus sac to form a short, rather inconspicuous vas deferens. The cirrus sac of 0.83-1.14 mm. length and 0.23-0.28 mm. maximum breadth occupies a transverse position entirely in front of the ventral sucker, a little behind half the distance between the latter and the intestinal bifurcation. It extends from the genital pore situated considerably to the left side to the median line of the body, where it usually touches by its basal end the anterior margin of the ventral sucker. It is crescent-shaped with the convex side directed forwards and is broader terminally than at the basal end except in contracted specimens. It has thick muscular walls composed of an inner circular and outer longitudinal layers of muscle fibres. The genital pore is situated far towards the left side at about half way between the ventral sucker and left body margin close inside the left intestinal caecum at level with or a little behind the anterior margin of the ventral sucker. The vesicula seminalis, broader at the base, is coiled on itself. The pars prostatica is long and tubular; the prostate gland cells are well developed occupying all the available space within the cirrus sac. The ductus ejaculatorius is long and coiled on itself before it opens at the genital pore.

The ovary is spherical or subspherical, 0.28-0.39 mm. in diameter, and is situated in the median line or a little to the right or left side close behind the posterior margin of the ventral sucker between it and the bifurcation of the excretory bladder. The gonads usually lie in the same median line one behind the other. The distance between the ovary and anterior testis is nearly twice of that between the anterior

and posterior testis. The shell gland complex lies mesially inwards to and at the same level with the ovary. The oviduct originates from the inner margin of the ovary near the middle of its length and after running for a short distance it is joined by the receptaculum seminis and soon after by the yolk reservoir. The receptaculum seminis is tubular, and at the end opposite to that by which it joins the oviduct it passes into a long, narrow and coiled Laurer's canal, which opens to the exterior by a minute pore situated near the mid-dorsal line slightly in front of the posterior border of the ventral sucker.

The uterus is intracaecal and is much convoluted filling nearly the entire space behind the ovary with the convolutions more or less symmetrically arranged laterally to the testes, the descending to the right and ascending to the left side. Immediately in front of the ovary the ascending uterus passes into the metraterm, which runs dorsally to the left side of the ventral sucker, sometimes overlapping its left-side margin. The eggs have a yellowish brown shell measuring 0.07-0.08 mm. in length and 0.034-0.04 mm. in maximum breadth. Most of the eggs in the uterine coils contain well-developed miracidia.

The vitellaria are of restricted extent confined to the extreme edges of the body near the body-wall lying mainly outside the intestinal caeca; a few follicles, however, extend inwards overlapping the ventral surface of the latter. They commence a little behind the ventral sucker close to the point of bifurcation of the excretory bladder and terminate at the hinder end of the body. The follicles have a fairly large size and are more or less widely separated, but they are never arranged in groups. In a contracted specimen they may lie close together near the hinder end. The transverse vitelline ducts arise from the anterior end of the vitellaria and unite in the median line or slightly to the left to form the yolk reservoir. Both the transverse ducts and yolk reservoir appear solid

being composed of rounded cells containing yolk granules as in *Ommatobrephus*.

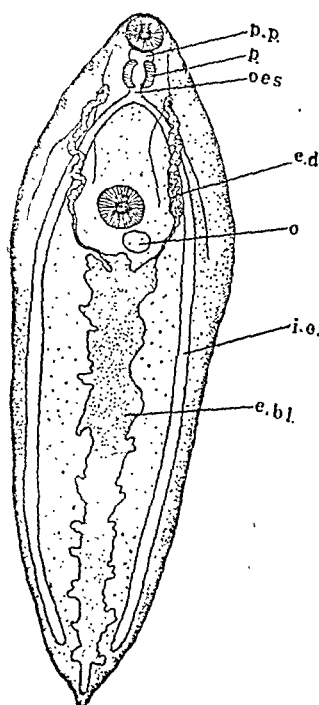


Fig. 2

Diagrammatic view of the excretory system in *Encyclometra caudata* obtained from *Zamenis mucosus*. For explanation of letters see key to lettering of plates.

I have described the excretory system in a previous paper (in press). The main stem of the Y-shaped excretory bladder bifurcates close behind the ovary into two short but prominent cornua, which extend as far as the outer border of the ventral sucker. In the specimen obtained from *Zamenis mucosus* the main stem gave off small lateral diverticula on each side. A long bladder like common collecting duct arises from each limb near its outer end, and winds its way forwards as far as

the anterior level of the pharynx, where it bends to form a loop to be continued backwards more or less in a straight course to the region behind the ventral sucker. It is wider a little distance beyond its origin and takes a wavy course presenting nearly the same appearance as the common collecting duct in certain Echinostome larvae. The bladder with these ducts shows a great resemblance to the excretory bladder with its long limbs in *Ommatobrephus* if we consider the cornua of the latter to approach each other posteriorly and unite to form the main stem giving the Y-shaped excretory bladder as described above.

DIMENSIONS OF MOUNTED SPECIMENS OF *ENCYCLOMETRA*  
CAUDATA (MM.)

Length	Breadth		Oral sucker diameter	Ventral sucker diameter
	In region of ventral sucker	Behind ventral sucker		
1. 11	2.8	2.7	0.9	1.28
2. 7	2.4	2.6	0.76	1.05
3. 8.8	2.6	2.5	0.87	1.15
4. 10.4	2.9	2.88	0.83	1.21
5. 8	2.5	2.5	0.74	1.1

Size of pharynx	Size of cirrus sac	Ovary diameter	Anterior testis diameter	Posterior testis diameter	Ova
0.48 × 0.62	1.13 × 0.28	0.35	0.4	0.48	0.078 × 0.034
0.44 × 0.51	0.83 × 0.23	0.33	0.46	0.51	0.0816 × 0.0408
0.55 × 0.6	0.87 × 0.26	0.39	0.46	0.53	0.078 × 0.034
0.5 × 0.6	1.14 × 0.28	0.33	0.53	0.53	0.0714 × 0.0408
0.4 × 0.56	0.89 × 0.25	0.28	0.39	0.46	0.0748 × 0.037

SYSTEMATIC POSITION OF THE GENUS *ENCYCLOMETRA*  
BAYLIS AND CANNON

Baer (1924) trying to throw some light on the affinities of this genus remarked that it presented several peculiarities which render its systematic position most uncertain. After showing its resemblance with *Haplometra*, *Cymatocarpus* and *Leptophallus* in certain features of its anatomy he concluded that it is unique in the Lepodermatidae, because it is distinguished from all the genera of that family in the precocious development of the eggs, miracidia being seen in the eggs in utero, a feature which is also shown by the genus *Ommatobrephus*, but no relationship whatever exists between these two genera belonging to two distinct families. Travassos (1928-29), in his sketchy classification of the Lepodermatidae assigns it to the sub-family Reniferinae Pratt without giving any reason. It is extremely difficult to discuss his classification in this as well as in many other points, because he does not mention the features on which it is based. As discussed by me previously in a paper, which is under publication, it shows no close relationship with the Reniferinae nor with any other sub-family so as to be included in it. I therefore created for this genus a new sub-family Encyclometrinae in the Lepodermatidae, which I defined.

I am inclined to the view that *Encyclometra* shows closer relationship with the genus *Ommatobrephus* than with any genus of the Lepodermatidae. The general similarity in the excretory system of the two genera has been already pointed out. The other points of resemblance are the absence of spines in the cuticle, larger size of the ventral sucker than that of the oral sucker, position of the cirrus sac entirely in front of the ventral sucker in the space between it and the intestinal bifurcation and the restricted extent of the vitellaria, which are confined to the extreme edges of the



body between the ventral sucker and the posterior end or some distance in front of it. The receptaculum seminis is tubular and a protrusible cirrus is absent in both the genera. If the ovary and shell gland complex of *Ommatobrephus* are shifted forwards so as to occupy a position close behind the ventral sucker and the testes also to move forward and lie one behind the other, we should get nearly the same topography of organs as in *Encyclometra*. Finally they show a striking resemblance in the large size and precocious development of the ova, miracidia being seen in the eggs in utero.

I do not think that the forward position of the gonads one in front of the other is by itself of such importance as to prevent us from including *Encyclometra* in the Ommatobrephidae, specially when we know that the position of the testes is very variable in some families and sub-families as for instance in the Pleurogenitinae Lss. In the Telorchiniinae Lss., which Fuhrmann and I have included in the Lepodermatidae the testes are at the hinder end—a position entirely different from that typical of the family. What offers the greatest difficulty in including *Encyclometra* in the Ommatobrephidae is the structure of the cirrus sac and the vas efferent apparatus contained within it. In *Encyclometra* the cirrus sac is thick and strongly muscular, but it is thin and parenchymatous in *Ommatobrephus*. The vesicula seminalis is large, straight and bilobed occupying a great part of the cirrus sac in the latter genus, but it is coiled and confined to the basal part of the cirrus sac in *Encyclometra* in which the pars prostatica and ductus ejaculatorius are long and well developed, reverse being the case in *Ommatobrephus*. It is well known that in the Pleurogenitinae the genus *Ganeo* Klein lacks a cirrus sac or possesses a thin parenchymatous pseudo-cirrus sac, whereas its closely allied genera *Pleurogenes* and *Prosotocus* possess a well-developed muscular cirrus sac. The difference in the structure of the vas efferent apparatus in *Encyclometra* and *Ommatobrephus* is, however, so profound

that we cannot by any stretch of imagination establish such a close relationship between these genera as will lead us to their inclusion in the same family. The cirrus sac with its contained parts in *Encyclometra* is no doubt built on the same structural plan as in the Lepodermatidae. Therefore we do not consider it advisable at present to assign this genus to the Ommatobrephidae. It must be, however, clear from the foregoing that *Encyclometra* occupies the unique position of a connecting link, which combines in itself the essential characters of two different families and that the future work may reveal the necessity of including it in the Ommatobrephidae, which then should consist of two sub-families Ommatobrephinae and Encyclometriinae.

## REFERENCES

- Baer, J. G. (1924)—Description of a New Genus of Lepodermatidae with a Systematic Essay on the Family. *Parasitology*, 16, 23—31.
- Baylis, H. A. and Cannon, H. G. (1924)—A New Trematode from the Grass-Snake. *Ann. Mag. Nat. Hist.*, 13, 194—196.
- Baylis, H. A. and Cannon, H. G. (1924)—Further Note on a New Trematode from the Grass-Snake. *Ibid.*, 13, 558—559.
- Bhalerao, G. D. (1926)—On the Trematode Parasites of a Water-Snake *Tropidonotus piscator*. *Parasitology*, 8, 1, 4-5.
- Joyeux, Ch. et Houdemer, E. (1928)—Recherches sur la Faune Helminthologique de L' Indochine (Cestodes and Trematodes). *Ann. de. Parasit.*, 6.
- Mehra, H. R. (1928)—On the Bionomics and Structure of a New Trematode *Ommatobrephus lobatum* n. sp. from *Zamenis mucosus*. *Proc. Fifteenth Ind. Sci. Con.* 199.
- Mehra, H. R. (1931)—A New Genus of the Family Lepodermatidae Odhner from a Tortoise with a Systematic Discussion and Classification of the Family. Under publication in *Parasitology*.
- Nicoll, W. (1914)—Trematode Parasites from the Animals Dying in the Zoological Society Gardens during 1911, 1912. *Proc. Zool. Soc., Lond.*, 139—154.
- Poche, F. (1925)—Das System der Platyodaria. *Arch. Natur.*, 91 A, 2, 138-139.
- Thapar, G. S. and Farzand Ali (1929)—On the Trematodes of the Digestive Tract of *Tropidonotus piscator* from Lucknow. *Journ. Helminth.*, 7, 4, 247—252.
- Travassós, L. (1928-9)—Fauna Helminthologica de Matto Grosso. Trematodes, Pt. 1. *Mem. Inst. Oswaldo Cruz*, 21, 2, 353—355.

## EXPLANATION OF PLATES 1—3

## KEY TO LETTERING USED IN FIGURES

a. c. d., anterior collecting duct; a. t., anterior testis; b. w., body wall; c. bl., cernu of excretory bladder; c. d., common collecting duct; c. s., cirrus sac; e. bl., excretory bladder; e. o., excretory opening; g. p., genital pore; i. c., intestinal caecum; L. c., Laurer's canal; m., metraterm; o., ovary; o. d., oviduct; œs., œsophagus; p., pharynx; p. c. d., posterior collecting duct; p. p., prepharynx; p. t., posterior testis; r. s., receptaculum seminis; t., testis; t. v. d., transverse vitelline duct; ut., uterus; v. e., vasa efferentia; v. s., ventral sucker; v. se., vesicula seminalis; vit., vitellaria.

FIGS. 1-5. *Ommatobrephus lobatum* Mehra

## PLATE 1

1. Dorsal view of an extended specimen.

## PLATE 2

2. Microphotograph of balsam mount.

## PLATE 3

3. Body region between intestinal bifurcation and ventral sucker showing cirrus sac, metraterm and genital pore.

## PLATE 4

4. Transverse section through cirrus sac and genital pore.

## PLATE 5

5. Part of transverse section through ovary, oviduct and Laurer's canal.

## PLATE 6

6. Ventral view of *Encyclometra caudata* (Polonio, 1859.)

# PLATE I

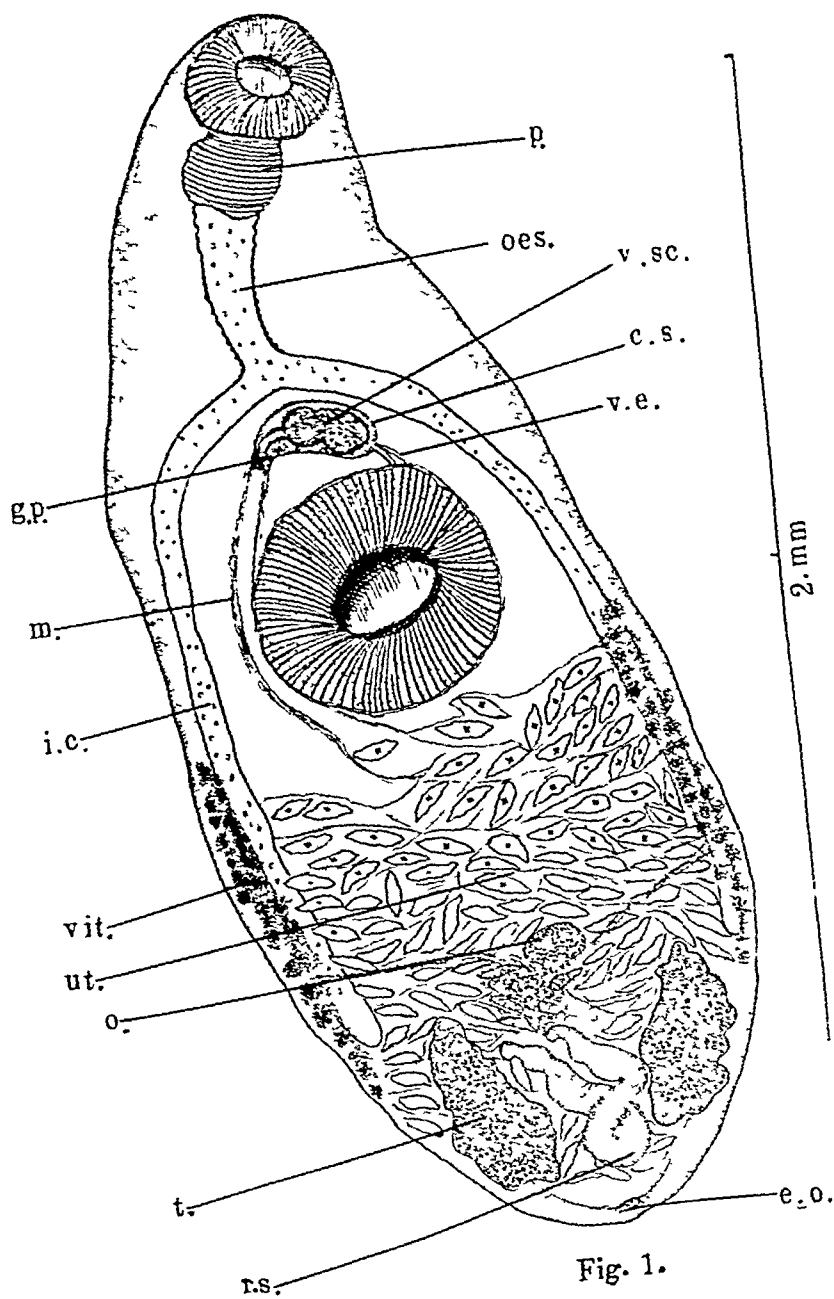


Fig. 1.

# PLATE II

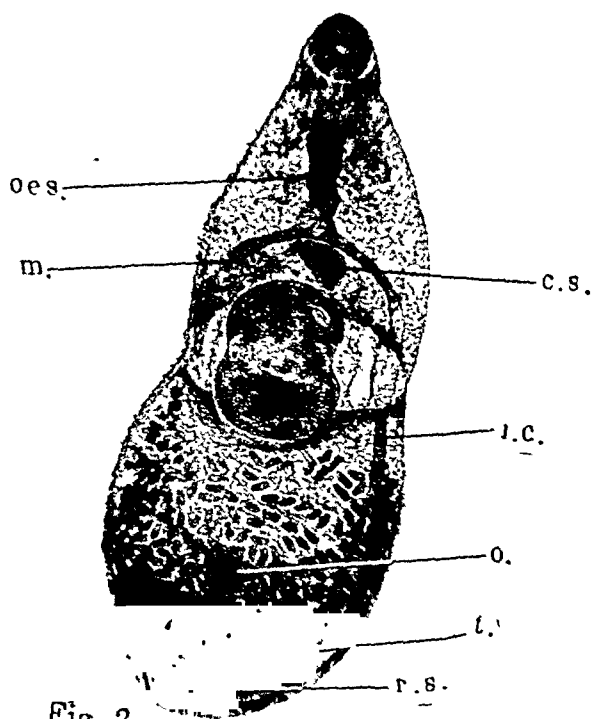


Fig. 2.

# PLATE III

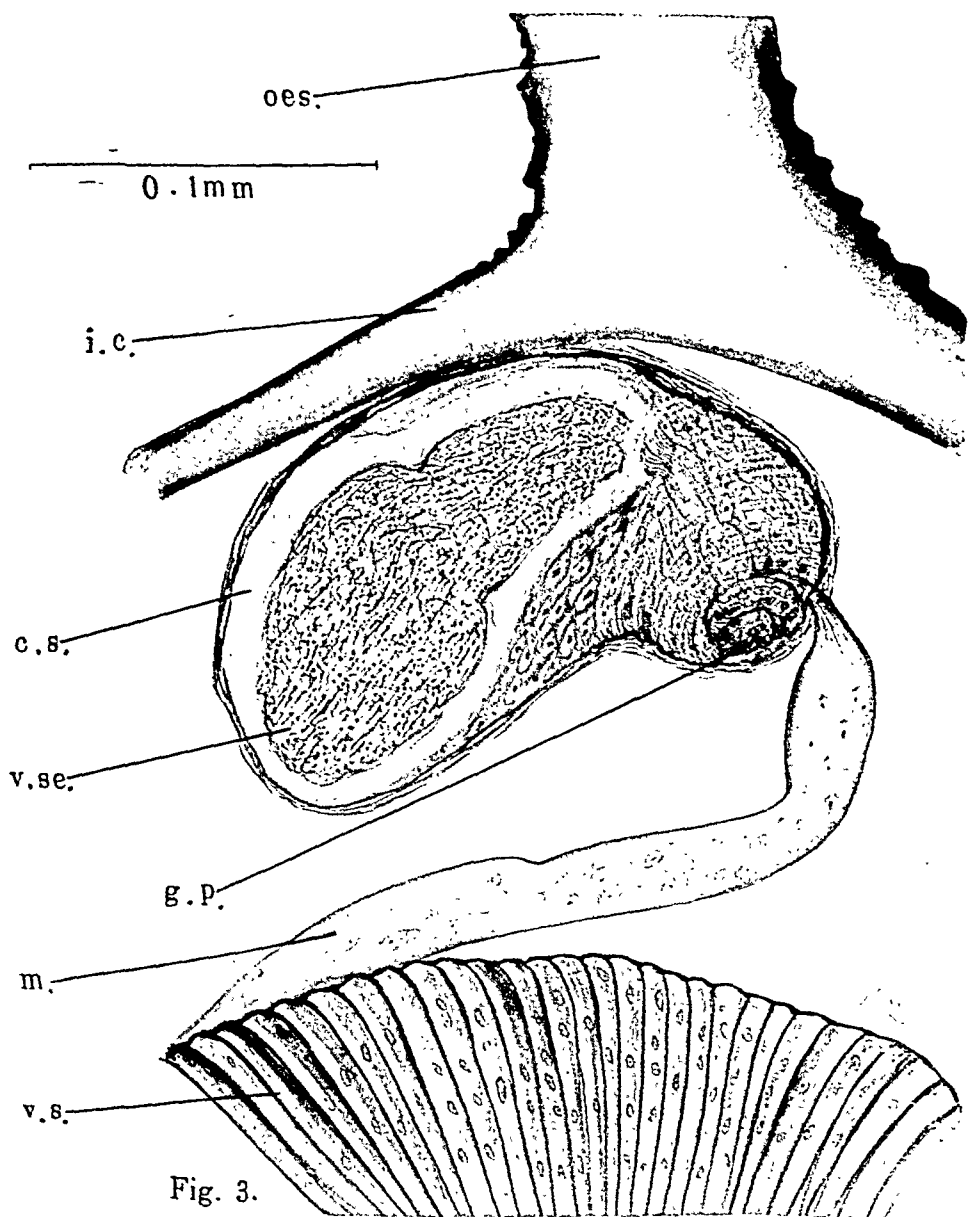


PLATE IV

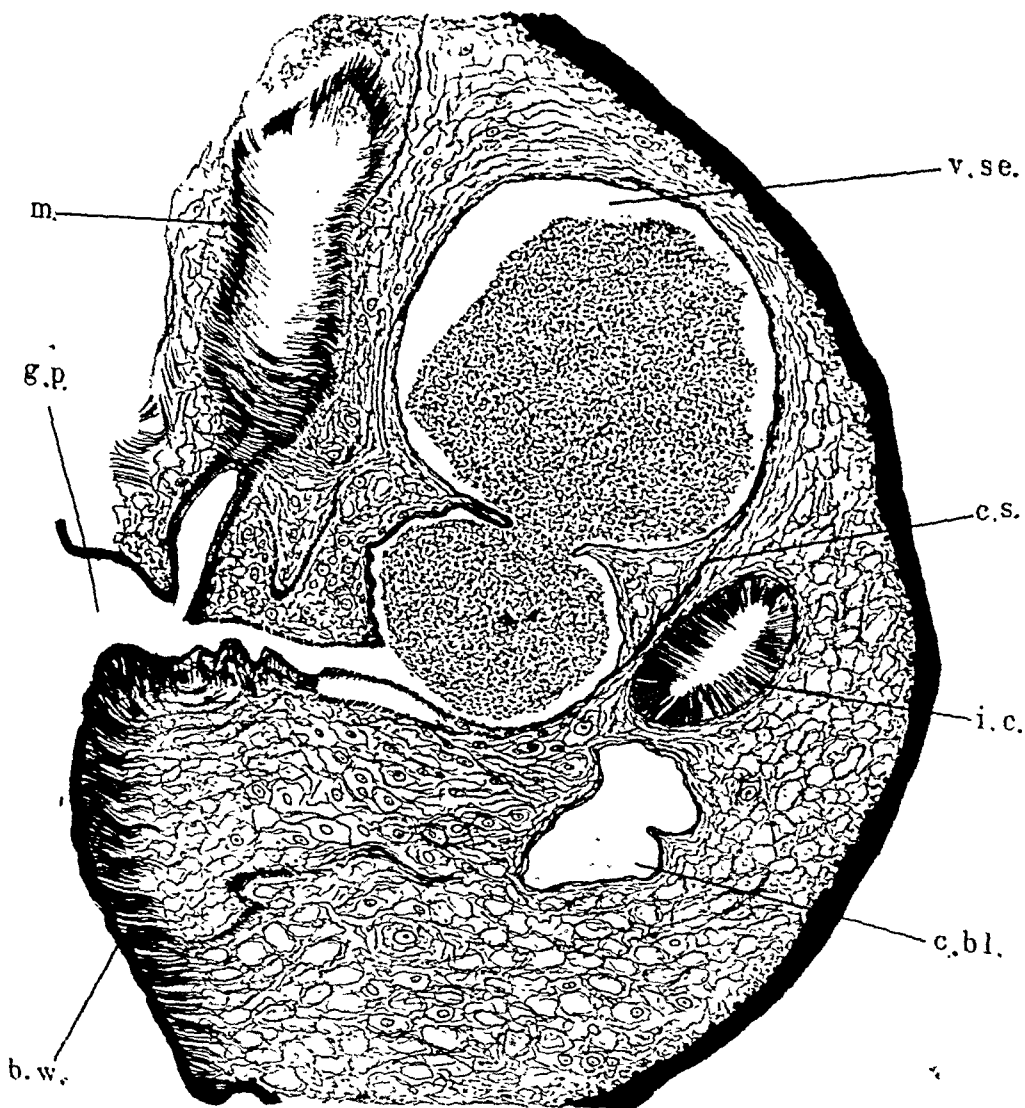


Fig. 4.

0.1mm



# PLATE V

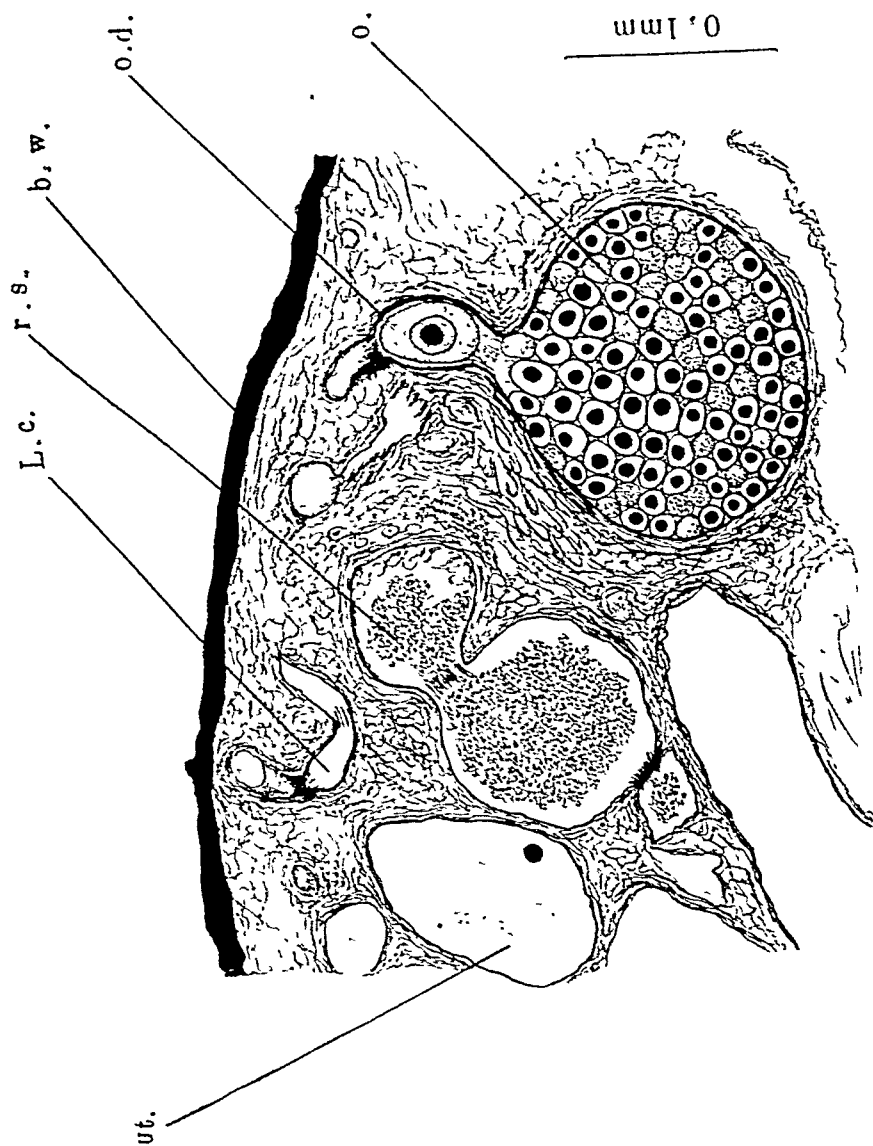


Fig. 5.

# NOTES ON THE CYCLOPIAN EYE AND OTHER DEFORMITIES OF THE HEAD IN A PIG (*SUS CRISTATUS WAGN*)

BY

S. K. DUTTA, M.Sc.,

*Lecturer in Zoology, University of Allahabad, Allahabad.*

## CONTENTS

	Page
1. Introduction ... ..	53
2. The external characters of the head ... ..	56
3. The musculature of the head ... ..	58
4. The orbit; the eye muscles; and the lens ... ..	65
5. The morphology of the skull ... ..	69
6. The cranial cavity and the brain ... ..	75
7. The cranial nerves, 1st to 8th ... ..	79
8. Summary ... ..	82
9. Explanation of Plate ... ..	83
10. Literature ... ..	83
11. Appendix—A comparative tabular statement ... ..	92

## 1. INTRODUCTION

On looking up literature it will be found that investigations concerning abnormality both in man and other animals have been carried on by a large number of distinguished workers with a view to determining the nature and if possible the cause of monstrosity. The earlier workers sought to explain the phenomenon by propounding two theories: (i) the "Amniotic theory," and (ii) the "Inherent theory." The amniotic theory maintains that the monstrosity appears owing to the amnion adhering too closely to the embryo or constricting it to bring about the variety of malformations;

while the Inherent theory holds that the abnormality is due to extraordinary behaviour of the oosperm and that the conditions are inherited by the fertilised germ cell. These theories, however, in the light of recent researches in experimental embryology and teratology are of nothing more than historical interest. In the line of experimental embryology and teratology the most noteworthy works are those of Dareste, '91 (10-11), Laeb, '93, '15 (46-48), Roux, '95, (65), Kopsch, '99 (38-39), Hertwig, '96 (30), Morgan, '02 (53-54), Newman '14, '21 (58-59), Lewis, '04 (43-44), Stockard, '06, '07, '09, '10, '13, '15, '21 (73-77), Windle, '07 (90-91), Kastner, '98 (42), Huber, '24 (33), Whitehead, '09 (88), McClendon, '12 (52), Werber, '15 (83-87), Riddle, '23 (64), Spemann, '19 (70-72). They had studied the results of changes in the egg and embryos by altering the environment physically or chemically or by certain other mechanical means and thus reared many stages of monstrous vertebrate embryos particularly of fishes. Rauber, '90 (66), Kopsch, '99 (39), Stockard, '07 (76), Spemann, '04 (70) and Werber, '15 (83), succeeded in getting experimentally many monstrous embryos of the fish, *Salmo salar*, *S. salvelinus*, *Fundulus heteroclitus* and other teleosts.

At the same time other workers tried to elucidate the problem of the origin of monstrosity by studying the comparative morbid anatomy of different organs notably of vertebrates. In this line, the most interesting works are those of Dareste, '77 (12), Le Double, '06 (14), Emery, '93 (16), Windle, '95 (90), Gemmill, '06 (24), Chidester, '14 (8-9), Newman, '14 (58), Bhattacharya, '18 (5), Spemann, '19 (72), Merrill, '19 (55), Keil, '11 (41), Lyssenkow, '26 (45), Swett, '21 (80), Fischel, '21 (18), Tsuda, '24 (81), Politzer, '26 (60), Ikeda, '28 (35), and several others.

On the other hand, many careful observations on the development of the brain and spinal cord of monsters have been recorded by a large number of renowned workers

with the aim of explaining the causation of monsters. The investigations of O. Naegeli, '97 (56), Humphrey, '24 (34), D. D. Black, '13 (6), F. P. Mall, '08 (50-51), C. Winkler, '17 (94), Zingerle and Schauenstein, '07 (96) and others in the case of cyclopia in man, V. Hanke, '03 (31) in a new-born child of anophthalmia, Keil, '11 & 12 (41), in a goat and a cat, Bien, '05 (2) in a goat, B. Gertrud, '05 in a goat of double malformation and the same author, '09, in a pig and guinea pig, M. Bishop, '21 (4) in a two-headed pig, L. V. Frankl-Hochwart, '02 (19) in blind mouse (*Spalax typhlus*), Glaisner, '24 (25) in *Chelone mydas*, Suzuki, '28 (79) in fishes all sought to explain the malformation as due to the developmental disturbances of the central nervous system of the monsters. Stockard, '21 (77) claims "that all types of monsters not of hereditary origin are to be interpreted simply as developmental arrests."

"Effective treatment (physical, chemical, and mechanical) tends to lower the rate of development. Slowing the rate at one moment will produce double monster or identical twins, and at another moment slowing, by the same method, will give rise to the cyclopiian defect."

"Insufficient oxygen decidedly slows the rate or may completely interrupt development and thereby induces various structural deformities."

Patterson, '07 (61) has found the developmental interruption to exist in armadillos (*Tatusia novecineta*).

Since the present work is not of an experimental nature the writer cannot afford to be dogmatic on the theory explaining the causation of monsters, but the observations on the structural deformities in the pig in question will go to substantiate the conclusion that cyclopia and other deformities of the mouth are correlated and depend largely upon the arrest or slowing down of the rate of development. A comprehensive survey and analysis of all the recorded monstrosities with special attention to ophthalmic defects

will be found in the works of Werber, '15 (83), Stockard, '21 (77) and Goldschmidt (26). So far as the anatomy of the pig monstrosity is concerned the following works are most interesting: M. Bishop, '20 (4) on the nervous system of a two-headed pig embryo, F. E. Chidester, '14 (8) on cyclopia in mammals (pig), J. M. Thuringer, '19 (82) on the anatomy of dicephalus pig (*monosomus diprostopus*), B. Gertrud, '05 in a double malformation of a pig, and S. R. Williams and R. M. Ruch, '17 (92) on the anatomy of a double pig (*syncephalus thoracopagus*), and the works given at the end of the list of literature from Nos. 97—108.

The material which forms the subject of this paper was a new-born one-eyed female pig which died immediately after birth. It differs in many respects from the above-mentioned recorded abnormalities and therefore I feel justified in giving an account of its anatomy.

The pig was presented to the laboratory by Mr. N. Mukerji, to whom the writer feels greatly indebted.

The work has been carried out in the department of Zoology, University of Allahabad, under the supervision of Prof. D. R. Bhattacharya, to whom the author wishes to acknowledge his sincere thanks.

## 2. EXTERNAL CHARACTERS OF THE HEAD

The body of the pig is covered with very fine bristles of hair and shows fairly normal structures with the well-developed limbs and the tail. (Plate 1, Figures 1 and 2.) The neck is short and supports an extremely remarkable head. The muzzle of the face is curiously small and is bent upwards. The jaws are therefore unusually shortened and so is the mouth opening. The external nares which are so conspicuous structures in the normal pig are altogether absent. There is only one cyclopic eye which is apparently the product of fusion of the original two

PLATE I



eye-balls (Synophthalmia). It is a median structure situated at the base of the forehead. The dome of the cranium is perfectly round almost like that of the skull of a monkey. The two external ears are quite normal except that the right pinna is slightly shorter than the left. There is a distinct eyebrow of stiff hairs arching above the cyclopiian eye and the vibressæ are present on the chin and the snout.

The measurements of the different parts of the body of the animal are as follows :

1.	Length measured along the crooked back from the crown of the head to the rump ...	29.5	cm.
2.	The tail ... ..	7.5	cm.
3.	Length of the back bone from the anterior end of the neck as far as the anus ...	21	cm.
4.	The circumference of the head ...	23	cm.
5.	Circumference measured along the eyebrow and from the base of the pinna ...	19	cm.
6.	Diameter of the head :		
	Mento-occipital diameter ...	8.5	cm.
	Fronto-occipital " " ...	6	cm.
	Biparietaler " " ...	5.5	cm.
	Bitemporaler " " ...	5	cm.
	Suboccipital " " ...	3.5	cm.
7.	Width between two shoulders ...	5	cm.
8.	Breadth of the hip ...	5	cm.
9.	Length of the hind limb measured over the posterior extremities from the median line of the rump to the tip of the toe ...	19	cm.
10.	Length of the hind limb measured from the anterior superior Iliac spine to the tip of the toe ...	17	cm.
11.	Fore limb from the shoulder to the finger tip ...	16.5	cm.
12.	Distance between the two ears dorsally ...	4	cm.
13.	" " " " " along the cyclopiian eye ...	12	cm.
14.	Length of the pinna of the left ear ...	3.5	cm.
15.	" " " " right ear ...	3.2	cm.
16.	Breadth, " " " left ear ...	2.9	cm.

17.	Breadth of the piana of the right ear	...	25	cm.
18.	Length of the eye	...	22	cm.
19.	Breadth of the eye	...	14	cm.
20.	Length of the snout from the base of the eye to the tip measured along the folds of the skin	...	3	cm.
21.	Circumference of the snout at the base	...	10.5	cm.
22.	Width of the mouth	...	4	cm.

### 3. MUSCULATURE OF THE HEAD

The muscles of the head region may be divided into the following groups according as they are situated :

1. Muscles of the Cranium.
2. Muscles associated with the sense organs :

(a) Auricular.

(b) Nasal.

(c) Palpebral.

(d) Orbital.

3. Muscles in connection with the jaws :

(a) Maxillary.

(b) Intermaxillary.

(c) Mandibular.

(d) Temporo-mandibular.

(e) Pterygo-mandibular.

The head muscles of the pig in question are greatly malformed and they will be described as far as possible in the above order. Only the muscles of the eye-ball in the orbit will be described in a separate section in connection with the eye.

#### MUSCLES OF THE CRANIAL REGION

**Occipito-frontalis (m. epicranius).**—It covers the dome of the skull from the occipital region to the eyebrow. (Figs. 1, 2, 3, OFA). It consists of two muscles—one frontal portion (F) and the other occipital portion (OC)—connected

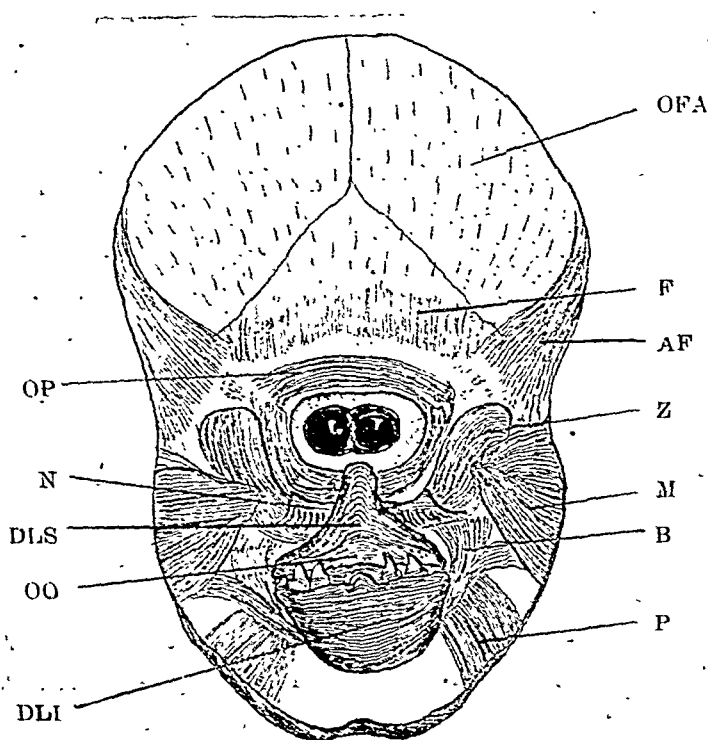


## PLATE II



Lateral aspect of the abnormal pig.

by a broad thin sheet of muscle which stretches over the dome of the cranium and is closely attached to the integument by fibrous connective tissue, while with the cranium it is connected by loose connective tissue fibres which allow of the movement of the skin on the cranium. (Fig. 1 OFA.) In the normal pig this sheet of muscle is altogether absent, obviously, owing to the small size of cranium.



Text Fig. 1.—Dissection showing the disposition of the muscles of the face front view.

AF—Auriculo frontalis m. B.—Buccinator m. DLI—Depressor and Levator Labi inferioris m. DLS—Depressor and Levator Labi superioris m. F—Frontalis m. M—Masseter m. N—Nasalis (fused) m. OFA—Occipito frontalis (Aponeurosis). OO—Orbicularis oris m. OP—Orbicularis palpebrarum m. P—Platysma m. Z—Zygomaticus m.

The occipital portion (Fig. 2, OC) (M. occipitalis) is thin and slightly broad and attached to the supra occipital, the mastoid portion of the periotic, and the exoccipitals.

The frontal portion (Fig. 2, F) (M. Frontalis) is adherent to the Frontal bone just above the eyebrow.

### MUSCLES ASSOCIATED WITH THE SENSE ORGANS

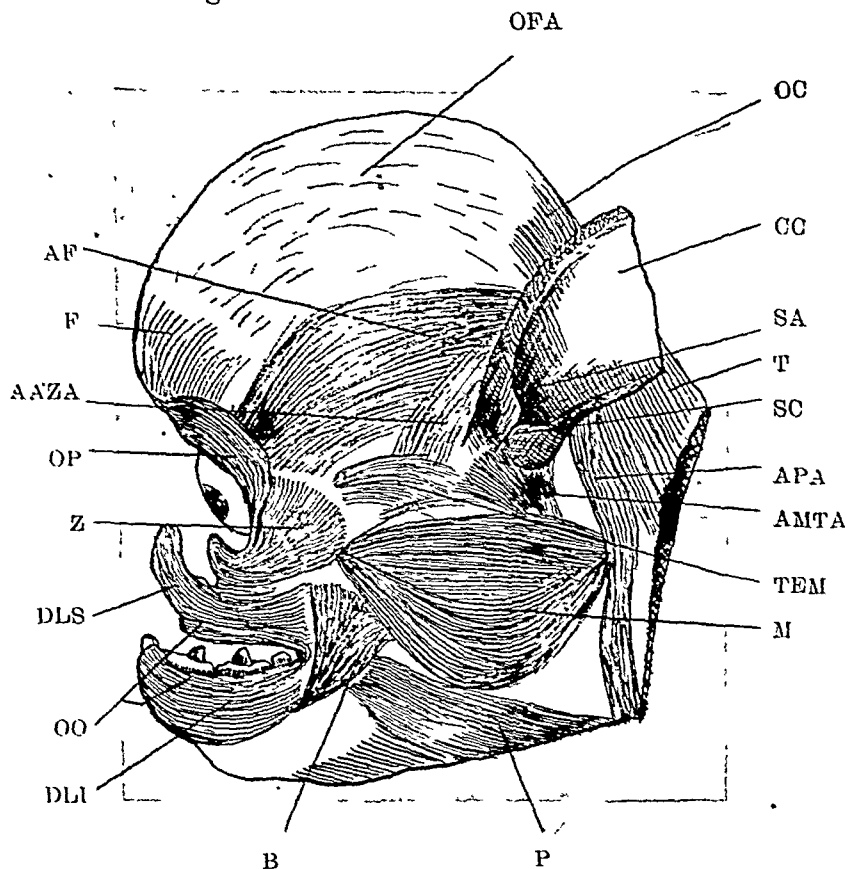
*Auricular region.*—The muscles of the pinna and those governing its movement are perfectly normal. The former, two in number, are the intrinsic and the latter eight in number are the extrinsic group.

The intrinsic muscles of the ear are the Scuto-auricularis externus and internus. The externus arises from the outer surface of the scutiform cartilage and lies on the inner side of the conchal cartilage. The internus originates from the under surface of the scutiform cartilage and is inserted at the base of the conchal. The eight extrinsic muscles controlling the movements of the pinna are the same as in the normal pig.

*The Nasal muscles.*—In most of the ungulates there are found six muscles in connection with the olfactory organs—(1) the Nasalis longus, (2) the Dilatator naris lateralis, (3) the Dilatator naris inferioris, (4) the Dilatator naris superioris, (5) the Dilatator naris transversus, (6) the Levator labi superioris alaeque nasi. In the normal pig, however, the last two, viz., the Dilatator naris transversus and the Levator labi superioris alaeque nasi are altogether wanting. There are thus only four muscles actually present in the normal pig, but in the abnormal specimen, described herein, all these four nasal muscles are indistinguishably blended together to form a small flap lying transversely below the cyclopiian eye (Fig. 1, N.)

*Palpebral region.*—The muscles of the eyelid consist of the orbicularis palpebrarum (Figs. 1 and 2, OP)—a large oval and fairly broad sphincter muscle common to the upper

and lower eyelids of the cyclopiian eye. The eyelid does not close the eye. There is a slight depression at the median dorsal portion of the oval sphincter indicating the fusion of the right and left muscles.



Text Fig. 2.—Dissection showing the disposition of the muscles of the face, lateral view.

AAZA—Zygomaticus auricularis m. (Attollens anticus). AF—Auriculo Frontalis m. AMTA—Temporo auricularis m. (Attollens maxmuis). APA—Parotido auricularis m. (Abducens). B—Buccinator m. CC—Conchal cartilage. DLI—Depressor and Levator labi inferioris m. DLS—Depressor and Levator labi superioris m. F—Frontalis m. M—Massetor m. OFA—Occipito Frontalis (Aponurosis). OC—Occipitalis m. OO—Orbicularis oris. OP—Orbicularis palpebrarum. P—Platysma m. SA—Scuto-auricularis m. SC—Scutiform cartilage. T—Trapizius m. TEM—Temporalis m. Z—Zygomaticus m.

*Orbital muscles.*—The muscles of the eyeball will be described in connection with the morphology of the cyclopiian eye.

## MUSCLES IN CONNECTION WITH THE JAWS AND PALATE

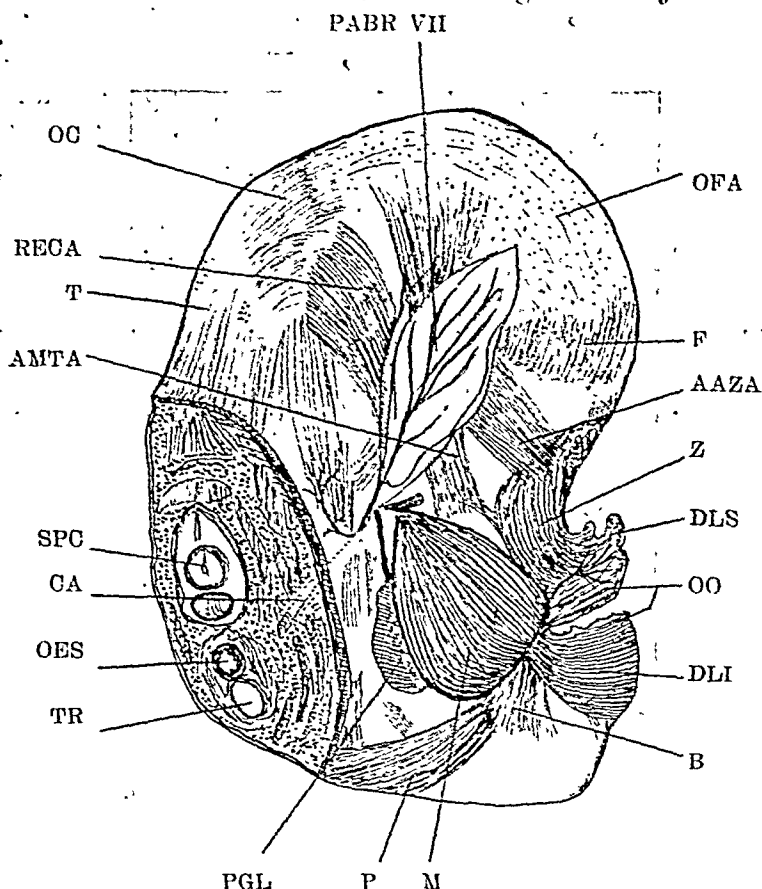
*Maxillary group.*—The Levator labi superioris (Figs. 1 & 2, DLS) together with a part of the sphincter muscle round the mouth (the orbicularis oris OO) is lumped into a fleshy mass lying medially above the upper lip. The fibres are not defined and the whole muscular mass is bent upwards hiding from view the rudimentary nasal muscle flap (Fig. 1, N) and the Zygomaticus (Fig. 1, Z).

The Zygomaticus (Zygomatico-labialis) is a broad thick ribbon-shaped muscle (Figs. 1 & 2, Z) which arises from the zygomatic process of the squamosal and instead of its being inserted near the angle of the mouth as usual, courses its way horizontally across owing to the distortion of the face, to meet with its fellow of the other side in the middle line. The muscle fibres of the two thus become blended together and run across in a straight line from the two sides beneath the cyclopiian eye and behind the mass of the Levator labi superioris muscle mentioned above.

*Intermaxillary and mandibular groups.*—The sphincter muscle of the mouth opening—the orbicularis oris (Figs. 1 & 2, OO)—of the normal pig receives the insertions of the elevator and depressor muscles of the upper and lower jaws. In this abnormal pig, however, the elevator and depressor muscles of both the maxilla and the mandible are wholly fused with the orbicularis oris, thus making the latter curiously bulky, specially the portion attached to the lower jaw. The Depressor labi superioris which normally arises from the premaxilla and passes obliquely to be inserted on the nasal bone is indistinguishable from the

sphincter of the orbicularis oris. Likewise, in the lower jaw, a similar fusion of the Levator labi inferioris (Levator manti) and the Depressor labi inferioris with the orbicularis oris has occurred owing to the malformation of the face (Figs. 1 & 2, DLS & DLI).

The Buccinator muscle (Figs. 1, 2, 3, B) is situated on the side of the face under the masseter and blends with the orbicularis oris a little below the angle of the jaws.



Text Fig. 3.—Dissection of the head showing the posterior and the lateral muscles of the face and ear.

AAZA—Zygomaticus auricularis m. (Attollens anticus). AMTA—Temporo-Auricularis (Attollens maximus). B—Buccinator m. CA—Carotid Artery. DLI—Depressor and Levator labi inferioris m. DLS—Depressor and Levator labi superioris m. F—Frontalis.

## (3) Monophthalmia asymmetrica—

(in which only one eye remains placed asymmetrically on the lateral side).

The defective eye of this pig possesses two distinct lenses which can be seen through the fused paired cornea, and in accordance with the classification, the eye presents, the type synophthalmia bilentica.

With regard to the ophthalmic defects many theories have been advanced. Spemann '04 (70), Lewis, '09 (44), Stockard, '10 (74), Werber, '15 (16)(83—85) and others have obtained experimentally fish abnormalities with cyclopiian eye or completely blind or anophthalmia. In the case of anophthalmic fish embryo their investigations show that the germ of the eye (optic anlage) is very deep-seated and rudimentary. Hanke's (31) and Frankl Hockwart's (19) researches in a blind new-born child and blind mouse (*spalax typhlus*) elucidated the fact that it was due to secondary degeneration. Stockard, '10—'21 (74 and 77) advocated that the cyclopia arise because of the non-separation of what he considered the originally single optic germ, during the process of development. Meckel opposed this view and was of opinion that the cyclopiian deformity is formed by the fusion of the two optic vesicles. Spemann and Lewis, Werber and most other investigators of the subject maintained and substantiated the fusion theory originally advanced by Meckel. Their investigations show that in the case of anophthalmia, the optic nerve and the optic chiasma are altogether lacking. In the case of cyclopia perfecta and synophthalmia unilentica the defects are the same. But in the case of synophthalmia bilentica the optic tract directly connects the brain and the optic cup without the formation of the optic chiasma. This is exactly the condition in the present cyclopiian pig and it affords another evidence in support of the view that cyclopia (synophthalmia bilentica) is the outcome of the

fusion of the two optic vesicles in the embryo : the theory upheld by Spemann, Lewis, Werber and others.

Winkler, '17 (94) has shown that the defective formation of the eye brings about malformation of the olfactory capsule and the mouth. C. J. Herrick, '21 (29) in a paper on the origin of the cerebral hemispheres says : "In response of the peripheral differentiations of the eye and nose, two pairs of lateral evaginations of the wall of the neural tube probably took place early in vertebrates ; namely, the optic vesicles and the olfactory bulbs ; the first from the midbrain or the diencephalon and the second from the forebrain or the telencephalon. The embryological evidence suggests that the optic evagination occurred earlier in phylogeny than the olfactory, at any rate it always preceded in ontogeny. Therefore the disturbance in the process of development of optical vesicles should always be accompanied by defective development of the forebrain vesicles which begin to give out the olfactory bulbs." This explanation appears plausible for it will be seen that in the present abnormal pig, the defective growth of the rudiment of the optic vesicles is mainly responsible for the suppression of the olfactory capsules and the external nares.

*The structure of the eye.*—The two eyeballs are conjoined and therefore the muscles and nerves are more or less fused together (Figs. 4—6).

The lachrymal apparatus, the lachrymal glands, ducts, etc., are all lacking in this specimen.

The eyelids are immovable—the lower being merely a fold of skin.

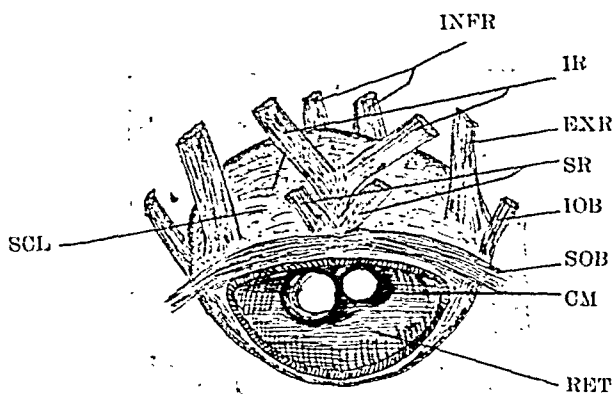
The optic foramen is single for the exit of a common optic nerve.

The tunics of the eyeball are as usual consisting of the sclerotic choroid and retina. The sclerotic (Fig. 4, SCL) is globular and there is no external mark or depression or



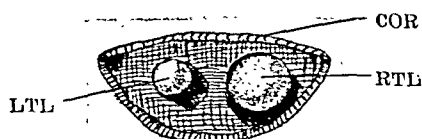
groove showing the fusion of the eyeballs. Neither there is any partition in the interior of the globe of the eye. The cornea (Fig. 4, COR) is bi-elliptical—the only sign indicating the fusion of eyeballs. The choroid is beneath the sclerotic and the Iris is degenerate. The retina (Fig. 6, RET) is pigmented deep black.

Histologically the retinal cells—rods and cones do not present any unusual structure. The Iris is almost vestigial. It is a very thin transverse elliptical diaphragm suspended in front of the crystalline lenses.



Text Fig. 6—The dissection of the eyeball.

CM—Ciliary muscle. EXR—External rectus muscle m. IR—Internal rectus m. INFR—Inferior rectus m. IOB—Inferior oblique m. RET—Retina. SCL—Sclerotic. SOB—Superior oblique m. SR—Superior rectus m.



Text Fig. 7—A portion of the cornea with two unequal lenses.

COR—Cornea. LTL—Left lens. RTL—Right lens.

*The lenses.*—There are two lenses. They are of unequal size; the left one (Fig. 7, LTL) is bigger than the right (RTL) measuring 6 mm. and 4 mm. in diameter. The suspensory ligaments of the lenses are prolongations of the ciliary muscles (Fig. 6, CM) which connect the two coats—the sclerotic and choroid.

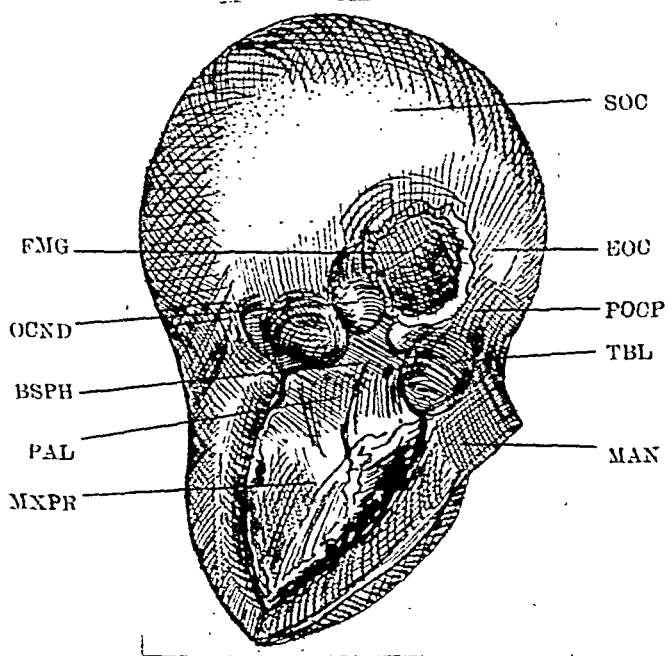
*The eye muscle.*—The motor muscles (Figs. 5 and 6) of the eye are all quite discrete excepting the superior and inferior obliques. These are fused at their distal ends with their fellows of the other side of the globe of the eye. There are thus ten eye muscles—8 recti, 4 of each half and the common superior and inferior oblique muscles. The recti muscles arise mostly from the margin of the optic foramen. The single superior oblique muscle (Fig. 5, SOB) runs across the upper part of the eyeball and the inferior oblique (Fig. 5, IOB) is situated along the lower margin. They are respectively innervated by a pair of trochlear (fourth cranial) nerve and two branches of the oculo-motor (third cranial nerve). The recti muscles of one-half of the eyeball are disposed more or less separately from those of the corresponding other half. The superior recti muscles (Fig. 5, SR) are very small lying close to each other below the superior oblique. The two internal recti muscles (Fig 5, IR) are united at their proximal ends. Distally they expand and become attached to the globe quite separately. The inferior recti (Fig. 5, INFR) are situated on the lower border of the eyeball. These recti muscles are supplied by the branches of the paired oculomotor nerve as shown in figure 5.

The two external recti (Fig. 5, EXR) are placed at the two extremities of the eyeball each supplied by the abducent (sixth cranial) nerve (Fig. 5, VI).

## 5. THE MORPHOLOGY OF THE SKULL

The cartilage has not been replaced by bone at many places such as frontal, parietal, supraoccipital and

squamosal of the skull and hence the sutures are not well-defined.



Text Fig. 8.—The skull (ventral view).

BSPH—Basisphenoid EOC—Exoccipital. FMG—Foramen Magnum. MAN—Mandible. MXPR—Maxillo Palatine process. OCND—Occipital Condyle. PAL—Palatine. POCP—Paroccipital process of exoccipital. SOC—Supraoccipital. TBL—Tympanic bulla.

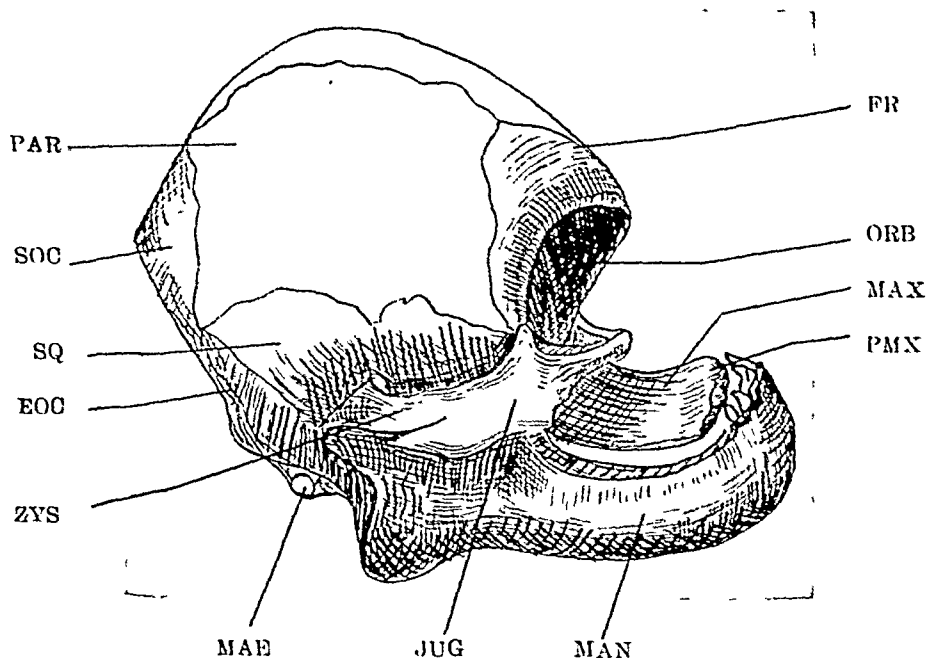
The occipital region occupies the posterior part of the skull and is made up, as usual, of supra-occipital (Fig. 8, SOC) on the roof of the cranium, the two ex-occipitals (Fig. 8, EOC) on the sides with their paroccipital process (Fig. 8, POCP) applied to the sides of the tympanic bulla (Fig. 8, TBL). The basioccipital—a flat piece of bone in conjunction with the basisphenoid (Fig. 8, BSPH) forms the floor of the posterior portion of the cranium. The occipital crest, tuberosity and ridge are wanting owing to the excessive dilatation or swelling up of the brain box. The dorsal portion of

the skull is perfectly round and much swollen. The condyles (Fig. 8, OCND) are on the exoccipital bones.

The parietal segment contains the two parietals (Fig. 9, PAR) on the roof of the skull anterior to the supra-occipital (Fig. 9, SOC). The basisphenoid (Fig. 8, BSPH) is a median bone forming a portion of the floor of the cranial cavity in the parietal region.

The sphenoidal bones, *viz.*, the Alisphenoids, the orbitosphenoids and the presphenoids are fused to form a thick stout piece of bone in front of the basisphenoid forming a basicranial plate.

The Frontals (Fig. 9, FR) are a pair of large thin bones arching over the roof and sides of the anterior part of the

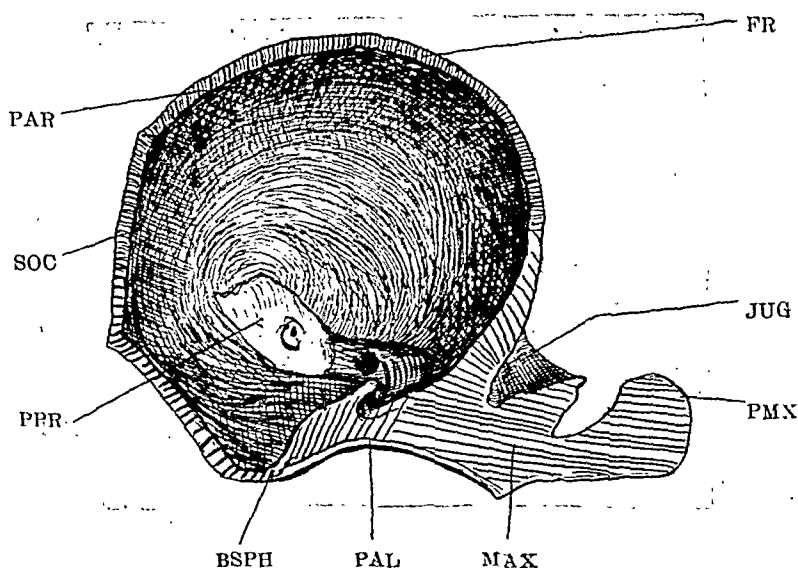


Text Fig. 9.—The skull (lateral view).

EOC—Exoccipital. FR—Frontal. JUG—Jugal. MAE—Meatus auditorius externus. MAN—Mandible. MAX—Maxilla. ORB—Orbit. PAR—Parietal. PMX.—Premaxilla. SOC—Supra-occipital. SQ—Squamosal. ZYS—Zygomatic process of Squamosal.

cranium. The lateral walls of the brain box in the parietal, and frontal region are made up of the two squamosal bones (Fig. 9, SQ) which are situated above and in front of the periotics. The squamosal is articulated with the parietal and frontals on the top and the two sides, and with the basisphenoids at its base. It sends out the zygomatic process to meet jugal bones (Fig. 9, JUG).

All the bones in relation to the olfactory capsules, namely, the nasals, the ethmoids, the vomers and turbinals are entirely wanting; the lachrymal bones are also lacking.



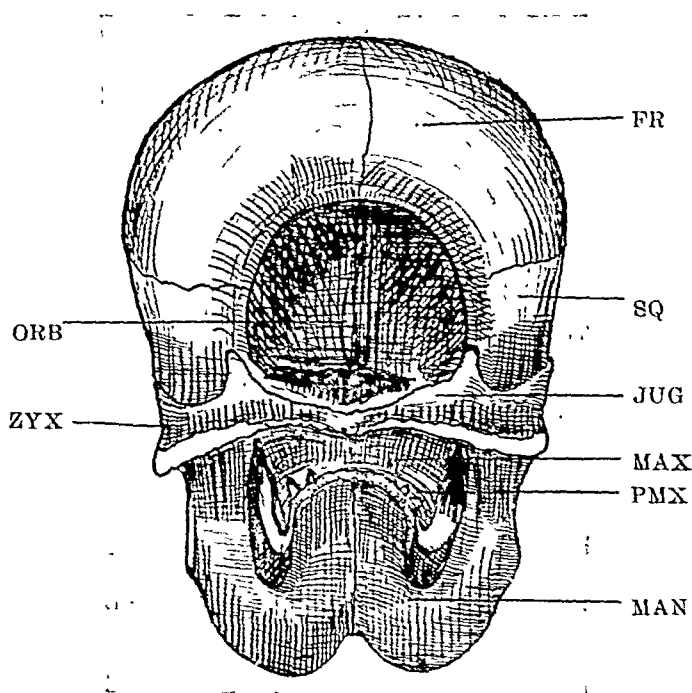
Text Fig. 10.—Median vertical section of the skull of the abnormal pig, showing the dilatation of the cranium.

BSPH—Basisphenoid. FR—Frontal. JUG—Jugal. MAX—Maxilla. PAL—Palatine. PAR—Parietal. PMX—Premaxilla. PPR—Petrus portion of the periotic bone. SOC—Supra-occipital.

The bones in connection with otic capsules are perfectly normal. The periotic is distinguishable into petrous portion, in the interior (Fig. 10, PPR) and mastoid portion on the

outside. The periotics are quite bony and very hard to cut. The tympanic bulla is well developed and lies attached to the mastoid portion of the periotic.

The jaws are much bent and shortened. The premaxilla and the maxilla are very much attenuated. On the ventral side of the skull maxilla sends out the broad palatine processes.



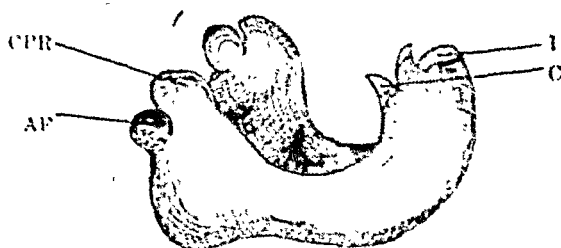
Text Fig. 11.—The skull of the abnormal pig (front view). The two jugular bones are united with each other forming a horizontal bar below the orbit. The supra-temporal vacuities of either side are united medially.

FR—Frontal bone. JUG—Jugular bone. MAN—Mandible. MAX—Maxilla. ORB—Orbit of the cyclopian eye. PMX—Premaxilla. SQ—Squamosal. ZYS—Zygomatic process of squamosal.

Since the internal narial opening is absent, the maxillo-palatine process (Fig. 8, MXPR) are on the same  
F. 10

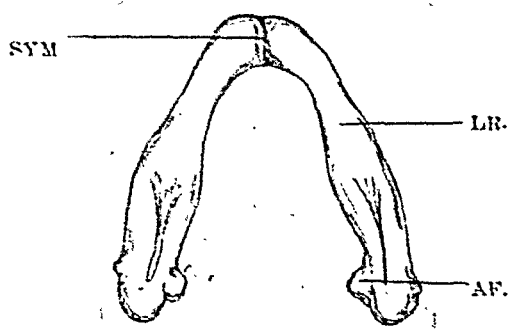
level and fused with the basisphenoid (Fig. 8, BSPH). The palatines and pterygoids are indistinguishable.

The jugals (Fig. 11, JUG) are a pair of broad bones attached to the zygomatic processes of the squamosal at one end, but distally instead of being articulated with the maxilla they meet with each other forming a horizontal bar lying across the face just beneath the orbit.



Text Fig. 12.—The lower jaw (lateral view)

AF—Articular facet of the lower jaw. CPR—Coronoid process. C—Canine tooth of the lower jaw. I—Incisor pad.

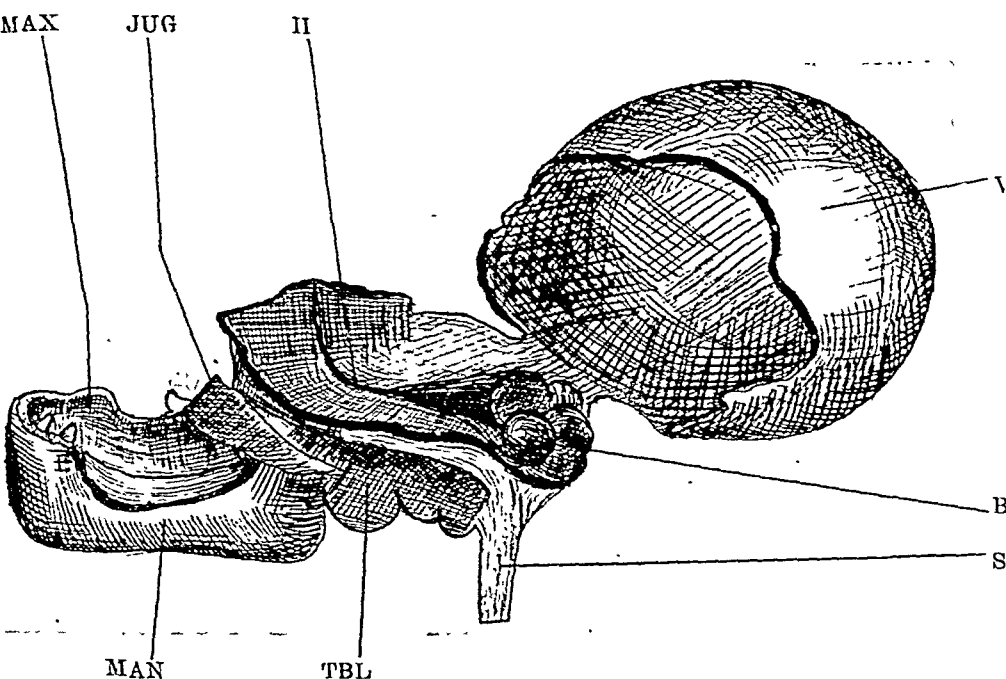


Text Fig. 13.—The lower jaw (ventral view).

AF—Articular facet. LR—Left Rami. SYM—Symphysis.

The lower jaw (Fig. 12) is also comparatively much shorter and bent upward. The rami of the mandible are as usual articulated with the zygomatic process of the squamo-

sal. The symphysis (Fig. 13; SYM) is cartilaginous. The coronoid process (Fig. 12, CPR) is slightly inflected. An anterior incisor tooth pad, a pair of incisor teeth, and a pair of rudimentary canine (Fig. 11, C and I) are present in the lower jaw. The upper jaw is totally devoid of any tooth. A comparison between the normal pig and this pig will be found in the appended table.



Text Fig. 14.—Diagram showing the brain in situ within the much swollen cranium.

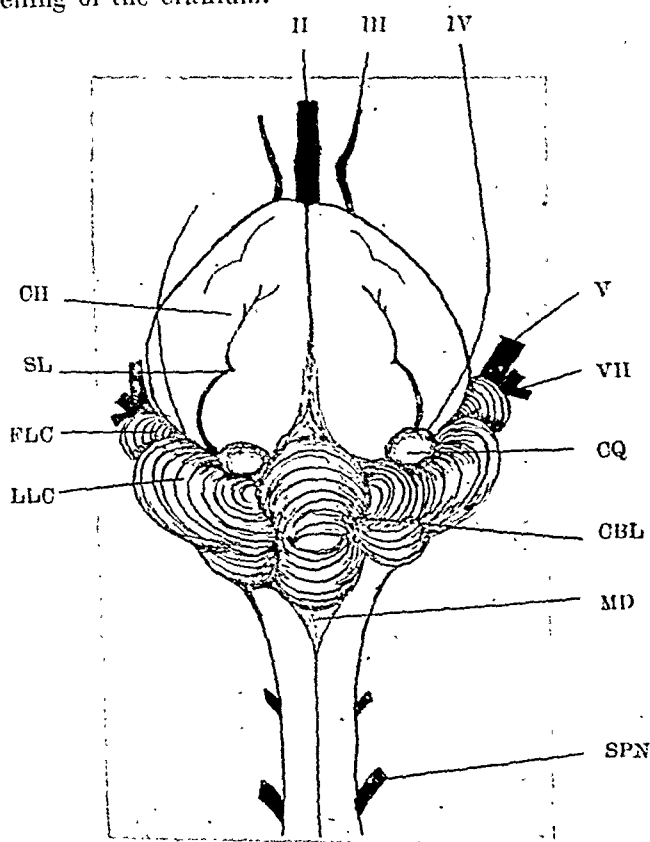
BR—Brain. JUG—Jugulars. MAX—Maxilla. MAN—Mandible. SPC—Spinal cord. TBL—Tympanic bulla. VSK—Vortex of the skull. II—Optic nerve.

## 6. THE CRANIAL CAVITY AND THE BRAIN

*The cranial cavity.*—The cavity of the much swollen cranium is lined by the dura mater. On the surface of the brain the branches of the arteries can be traced. The three membranous processes of the dura mater, *viz.*, the



falx cerebri, between the hemispheres of the cerebrum ; the Tentorium,—the transverse partition between the cerebellum and the cerebral hemispheres and the falx cerebelli ; process between the lobes of the cerebellum are all absent owing to swelling of the cranium.



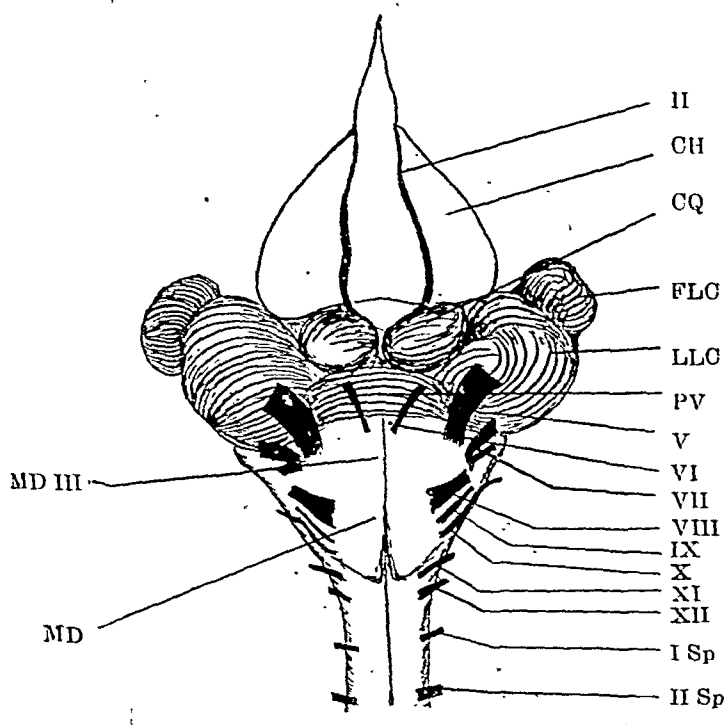
Text Fig. 15.—The dorsal aspect of the brain.

CBL—Cerebellum. CH—Cerebral hemispheres. CQ—Corpora quadrigemina. FLC—Floccular lobe of the cerebellum. LLC—lateral lobes of the cerebellum. MD—Medulla oblongata. SL—Sulci in the hemisphere. SPN—Spinal cord. II, III, IV, V and VII—Cranial nerves.

*The brain.*—The brain occupies a very small portion of the interior of the cranial cavity. The greater part of it

lined by dura mater is thus left as a simple space filled with a colourless fluid. The dimensions of the brain are as follows:—length 5 cm., and the breadth measured across the floccular lobes is 3 cm., the cerebral hemispheres 20 mm., corpora quadrigemina 6 mm., cerebellum 15 mm., and medulla oblongata 6 mm., in length.

*The fore brain*—(Prosencephalon or Telencephalon) on the dorsal surface of the brain the two cerebral hemispheres

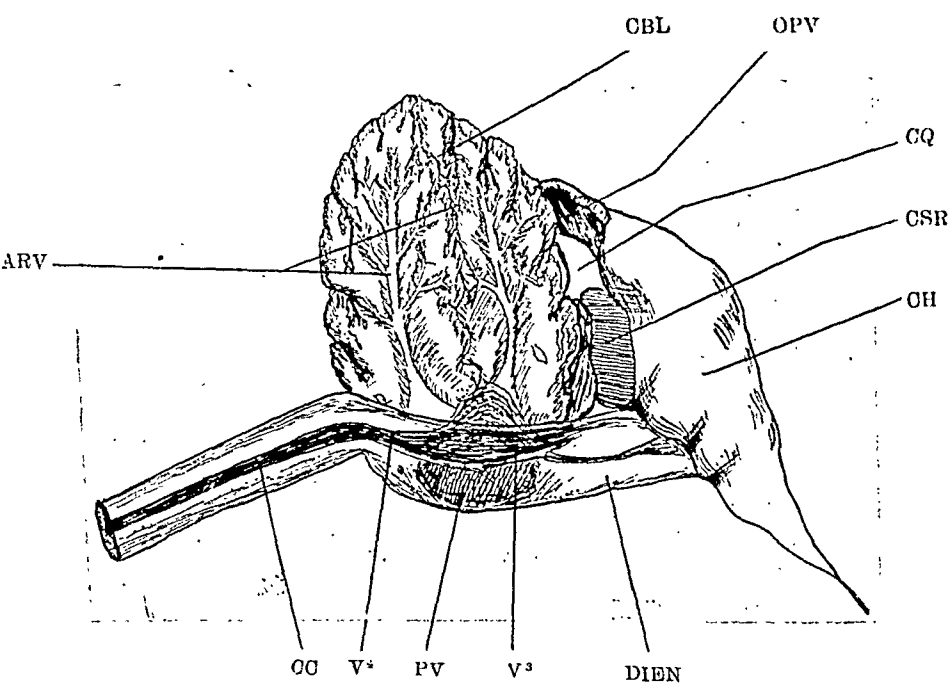


Text Fig. 16.—The ventral aspect of the brain showing the absence of the olfactory lobes and nerves, the optic chiasma, the hypophysis cerebri and the Infundibulum.

CH—Cerebral hemispheres. CQ—Corpora quadrigemina. FLC—Floccular lobes of the cerebellum. LLC—Lateral lobes of the cerebellum. MD—Medulla oblongata. PV—Pons varolli. II, III, V, VI, VII, VIII, IX, X, XI, XII—Cranial nerves. I sp, and II sp—spinal nerves.

(Fig. 15, CH) are much reduced in size marked by two sulci (Fig. 15, SL). The hemispheres are connected by the broad transverse commissure as in the normal pig by the corpus callosum (Fig. 17, CSR.). The olfactory lobes are entirely wanting hence there are no olfactory nerves.

The diencephalon is very small and the optic thalami are degenerate. Ventrally (Fig. 16) the descending optic tracts never cross to form a chiasma. The epiphysis, the infundibulum and the pituitary body are all absent.



Text Fig. 17.—A median vertical section of the brain showing internal structure and the ventricles.

ARV—Arbor vitae. CBL—Cerebellum. CC—Canalis centralis. CH—Cerebral hemisphere. CQ—Corpora quadrigemina. CSR—Corpus callosum. DIEN—Diencephalon. OPV—Optic vesicle. PV—Pons varolii. V<sup>3</sup> and V<sup>4</sup>—3rd and 4th ventricles.

*The Mid-brain*—(Metencephalon).—The corpora quadrigemina or optic lobes (Fig. 16, CQ) lie covered by the posterior extension of the cerebral hemispheres.

*The Hind-brain*—(Metencephalon)—is moderately reduced. The cerebellum (Fig. 15, CBL) apparently is the only part of the brain that has attained a normal development. The median lobe, the lateral lobes (Figs. 15 and 16, LLC), and the floccular lobes (FLC) are quite large and very well developed.

The Medulla (Figs. 15 and 16, MD) is slightly flattened. Across the ventral surface of the medulla the pons varolli (Fig. 16, PV) connects the lateral lobes of the cerebellum and in front of the pons lie the crura cerebri ventral to the mid-brain, connecting the medulla with the cerebral hemisphere.

The fourth ventricle (Fig. 17, V<sup>4</sup>), the Aqueductus Sylvii and the third ventricle (Fig. 17, V<sup>3</sup>) are very narrow. The third ventricle is slightly spacious on the dorsal aspect otherwise all the cavities are more or less of uniform nature.

## 7. CRANIAL NERVES

Only the first seven cranial nerves present some peculiarities, the others, namely eighth to twelfth, are perfectly normal in their distribution.

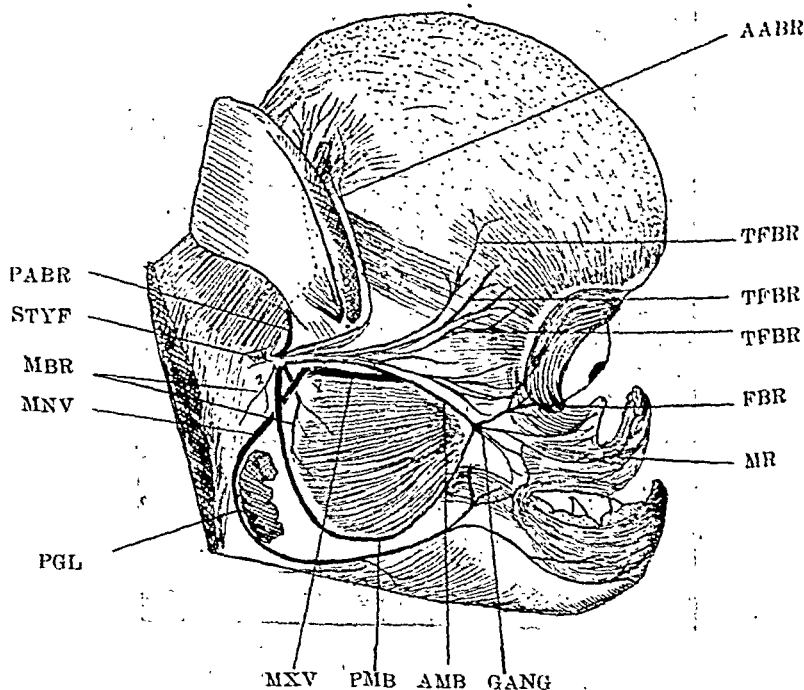
First cranial nerves the olfactory nerves are absent as are the olfactory lobes.

Second cranial nerves—the optic tracts do not cross to form a chiasma. They directly become continuous as a pair of optic nerves and run a long way in front of the brain in the interior of the cranial cavity (Fig. 14, II). At a certain distance they become joined together by a common sheath and then each makes its way out through a median optic foramen to supply the retina of the cyclopiian eye.

Third cranial nerve the oculo-motor nervē (Fig. 16, III) arises from the crura cerebri and supplies the interior oblique and all the recti muscles except the external rectus.

Fourth cranial nerve—the trochlear (Pathetic) nerve (Fig. 15, IV) arises in the usual manner from the dorsal surface near the valve of Vieussens and supplies the superior oblique muscles of the eye.

Fifth cranial nerve—The Trigeminal nerve (Fig. 16, V) originates near the pons and divides into three branches—the ophthalmic breaks up into the snout; the maxillary,



Text Fig. 18.—Dissection of the branches of the trigeminal and facial nerves.

AABR—Anterior auricular branch of the facial nerves (VII). AMB—Anterior masseter branch (VII). FBR—Facial branch (VII). GANG—Ganglion (VII). MBR—Masseter branch (VII). MNV—Mandibular branch of the trigeminal (V). MR—Branches of the upper lip (VII). MXV—Maxillary branch of the trigeminal (V). PABR—Posterior auricular branch (VII). PGL—Parotid gland. PMB—Posterior masseter branch (VII). STYF—Stylomastoid Foramen. TFBR—Temporo facial branch (VII).

supplying the upper jaw, and the mandibular, the lower jaw. The ophthalmic branch further divides into numerous finer ramifications which terminate in the anterior tip of the deformed snout.

*Sixth cranial nerve—the abducent* (Fig. 16, VI) is the most ventral and arises just in front of the pons. It supplies the external rectus of the eye.

*Seventh cranial nerve—the facial nerve* (Fig. 18) arises very near the fifth and emerges from the cranium by the stylomastoid foramen near the ear. It divides into—

- ( i ) A posterior auricular branch (Fig. 18, PABR).
- ( ii ) An anterior auricular branch (Fig. 18, AABR).
- ( iii ) Temporo facial branch (Fig. 18, TFBR).
- ( iv ) A branch supplying the masseter (Fig. 18, MBR).
- ( v ) A fairly long branch running along the outer border of the masseter, converges and meets with another coursing along the inner border of the same muscle to end in a ganglion (Fig. 18, GANG), whence numerous delicate nerves originate and distribute over the narial muscular flap, the zygomaticus, and the muscles of the upper jaw.

*Eighth cranial nerve—the auditory nerve* (Fig. 16, VIII) arises from the base of the medulla oblongata to supply the internal ear.

The 9th, 10th, 11th, and 12th cranial nerves are quite normal in their origin and distribution.

## 8. SUMMARY

1. The mouth is bent upwards and much deformed.
2. The eye is a cycloplan eye (*Synophthalmia bilentica*).
3. The lenses of the eye are of unequal size and situated side by side. The left is larger than the right measuring 6 mm. and 4 mm. respectively.
4. The lachrymal gland and ducts are lacking.
5. The muscles of the eye are fused in so far as the oblique muscles are concerned. The recti muscles are all quite discrete.
6. The auditory apparatus is practically free from deformity.
7. The muscles of the nasal capsules are wanting; they are fused to form a muscular flap.
8. The jugal bones are united at their distal ends with each other forming a horizontal bar across the face.
9. All the bones in connection with the nasal capsules are fused with the palatine process of the maxilla forming a very thick basal bone of the cranium and forming the roof of the mouth—there being no posterior narial aperture.
10. The maxillo palatine processes are united posteriorly with the basisphenoid.
11. The Palatines and Pterygoids are indistinguishable from the maxillo palatine process.
12. The fore-brain is much reduced in size.
13. The ventricles of the brain are reduced and all the cavities are more or less of uniform nature.
14. The olfactory capsule is absent. The olfactory tracts and nerves are altogether wanting.
15. The tractus opticus does not cross to form a chiasma but becomes continuous with the optic nerve.
16. The two optic nerves get ensheathed distally to form a single nerve supplying the retina.
17. There are no epiphysial or hypophysial structures.
18. The facial nerve has some branches which converge and anastomose to form a ganglion which gives rise to a large number of delicate ramifications distributing over the snout.

## 9. EXPLANATION OF PLATES

Plate 1 : Fig. 1.—Photograph of the abnormal pig showing the front view of the face. The cyclopiian eye is at the centre of the face the swollen head is extremely remarkable.

Plate 1: Fig. 2.—Photograph of the same pig showing the lateral view of the head. The mouth is bent upwards. No external nasal opening is visible.

## 10. LITERATURE

1. Adelmann, H.B.... The Development of the Eye Muscle of the Chick. Jour. of Morph and Physiol., Vol. 44, No. 1, 1927.
2. Bien, G. ... Zur Anatomie des Zentralnervensystems einer Doppelmissbildung bei der Ziege. Arb. a. d. Wiener Neurol Inst., Bd. XII, 1905.
3. Ibid. ... Doppelmissbildungen (cephalothoracopagus) Arb. a. d. Wiener Neurol Inst., Bd. XVIII, H 1, 1909. S. 188.
4. Bishop, M. ... The Nervous System of a Two-headed Pig-embryo. Jour. of Comp. Neurol., Vol. 32. 1920-21, p. 379.
5. Bhattacharya, ... Notes on the Anatomy of a Double Monstrosity in the Chick. Jour. and Proc. of Asiatic Soc. of Bengal. Vol. XIV, 1918.
6. Black, D. D. .. The Central Nervous System in a Case of Cyclopia in Homo. Jour. of Comp. Neurol., Vol. 23, 1913, p. 193.
7. Bischoff, T.L.W. Entwicklungsgeschichte des Rehes Giessen, 1854.
8. Chidester, F. E.... Cylopia in mammals (pig). Anat. Rec., Vol. 8, 1914. pp. 355—366.
9. Ibid. ... Twins in Fish. One with a Cyclopic Deformity. Anat. Rec., Vol. 8, 1914.
10. Dareste, C. ... Mode de formation de la cyclopie. Annales d'oculists, Vol. 106, 1891.
11. Dareste, C. ... Recherches sur la production artificielle des monstroses, 2nd edition. Paris, 1891.



12. Ibid. ... Mode de formation des monstres simples  
autosites. Arch. de Zool. experim., T. V.  
Ref. von Manz in Jahresber ub Fortschr  
Ophthalm., Bd. 8, 1877.
13. Dougel, D. and... A Case of Cyclopia. Brit. Med. Journ., No.  
Bride, T. M. 2792. 1914.
14. Le Double, A. ... *Traite des variations des os de la face de  
l'homme.* Paris, 1906.
15. Ibid. ... *Traite des variations du systeme musculaire  
de l'homme.* 1897.
16. Emery, C. ... Zur Morphologie der Zyklopischen Missbil-  
dungen. Anat. Anz., Bd. 8, 1893.
17. Ibid. ... Beitrage Zur Vergleichenden Entwickl-  
ungsgeschichte der Facial Musculatur.  
Anat. Hefte. H 98 (Bd. 32, H3), 1907.
18. Fischel, A. ... Über normale und abnormale Entwicklung  
des Auges. Arch. f. Entw. Mech. d Org.  
Bd. 49. 1921.
19. Frankl-Hoch- Zur Kenntnis der Anatomie des Gehirns  
wart, L. V. der Blindmaus (*Spalax typhlus*) Arb. a. d.  
Wiener Neurol Inst. Bd. VIII, 1902.
20. Gladstone, R. J....Defective Development of the Mandibular  
& Wakeley, Arch and Etiology of arrested Develop-  
C. P. G. ment and an Inquiry into the Question  
of the Inheritance of Congenital Defects.  
Jour. Anat. London, 57, 1923, pp. 149—167.
21. Gladstone, R. J....1. A Cyclopia and *Agathus Lamb.*  
2. An Anencephalic foetus with a Menin-  
gocæle and Facial Defect. Brit. Med.  
Jour., 15. No. 9, 1910.
22. Gemmill, J. F. ... *Teratology of Fishes,* Glasgow, 1912.
23. Ibid. ... A Contribution to the Study of Double  
Monstrosities in Fishes. Proc. Zool. Soc.,  
Lond., 1903.
24. Ibid. ... (a) On Cyclopia in Osseous Fishes. (b)  
Notes on Supernumerary Eyes and Local  
Deficiency and Reduplication of Notochord  
in Trout Embryos. Proc. Zool. Soc.,  
London, 1903.
25. Glaisner, L. H.... Über drei Doppelbildungen von *chelone*  
*mydas.* Zool. Anz., Bd. 60. H. 7/8, 1924.

26. Goldschmidt, R....Ein Beitrag zur Analyse der Doppelmissbildungen. Arch. f. Entw. Mech. d. Org., Bd. 47, S. 654.
27. Guinard ... *Precis de teratologie*. Paris, 1893.
28. Hayashi, M. ... Beitrage zur kenntnis der pathologischen Anatomie und Pathogenese der Zyklopie. Arch. f. Ophthalmol., Bd. 80. H 1., 1912.
29. Herrick, C. J. ... A Sketch of the Origin of the Cerebral Hemispheres. Jour. of Comp. Neurol., Vol. 32, 1921.
30. Hertwig, O. ... Beitrage zur experimentellen Morphologie und Entwicklungsgeschichte. Arch. f. Mikr. Anat., Bd. XLIV, 1895-96.
31. Hanke, V. ... Das Gehirn eines congenitalen, bilateralen Anophthalmus. Arb. a. d. Wiener. Neurol Inst., Bd. X, 1903.
32. Huber, E. ... Über das Muskelgebiet des N. facialis beim Hund, nebst allg. Betrachtungen über die facialis Muskulatur. Morphol. Jahrb., Bd. 52, 1 U, 2 T.
33. Ibid ... Über die Bedeutung der experimentellen Methode in der Facialisforschung, nebst Betrachtungen über die phylogenetische Entwicklung der Faacialismuskulatur in der Vertebraten-Reihe. Anat. Anz., Bd. 58, Nr. 8., 1924.
34. Humphrey, R.R....A Case of Cyclopia in Homo. Anat. Rec., Vol. 28, No. 3, 1924.
35. Ikeda, K. ... Beitrage zur Anatomischen Kenntnis der menschlichen Zyklopie mit besonderer Berueck sichtigung. der Kopfmuskelen. Arb. a. d. Anat. Inst. der Kaiser., Jap. Univer., z. Sendai. H. XIII, 1928.
36. Josephy, H. ... Über Russelbildung bei Zyklopie. Virchow's Arch., Bd. 206.
37. Ibid. ... Über Anophthalmie beim Huhnchen (Mit Bemerkungen über Anencephalie und Zyklopie) Sitzungsber. u. Abhandl. d. naturforsch. Gesel zu Rostock, neue Folge., Bd. 5, 1913. S 25.

38. Kopsch, Fr. ... Entwicklung der ausseren Form des Forellen-embryo. Arch. f. Mikr. Anat., Bd. LI, 1898. S. 181.
39. Kopsch, Fr. ... Die organisation der Hemididymi und Anadidymi der Knochenfische und ihre Bedeutung fur die Theorien uber Bildung und Wachstum des Knochenfischembryos Internat. Monatschr. f. Anat. u. Physiol., Bd. 16, 1899.
40. Kalbanowsky- ... Beitrag zur Kenntniss congenitalen Defekte  
Korotkina, am Schadel. Inaug. Diss., 1912.  
F. J.
41. Keil, R. ... Zyklopie bei einer Ziege. Arch. f. Vergl. Ophthalmol Jharg. Bd. 2, 1911. Zyklopie bei einer Katze Idem., Bd. 3, 1912.
42. Kastner, S. ... Doppelbildungen bei Wirbeltieren. Ein Beitrag zur Kasuistik. Arch. f. Anat. u. Physiol., 1898, S. 81.
43. Lewis, W. H. ... Experimental Studies on the Development of the Eye in Amphibia, I. On the Origin of the Lens. Amer. Jour. of Anat., Vol. 3, 1904.
44. Lewis, W. H. ... The Experimental Production of Cyclopia in the Fish Embryo (*Fundulus heteroclitus*). Anat. Rec., Vol. 3. 1909.
45. Lyssenkow, N.K....Ein Fall von Zyklopie beim Pferd. Arch. f. und Filatow, W.B. Augenheilk. Bd. 97, H 3. 1926.
46. Loeb, J. ... Beitrage zur Entwicklungsmechanik der aus einem Ei entstehenden Doppelbildungen. Arch. f. Entw. Mech. d. Org., Bd. 1.
47. Loeb, J. ... Uber die Entwicklung der Fischembryonen ohne Kreislauf. Arch. f. ges. Physiol., Bd. 54, 1893.
48. Ibid. ... The Blindness of the Cave Fauna and the Artificial Production of the Blind Fish Embryos by Heterogeneous Hybridization and by Low Temperature. Biol. Bull., Vol. 29, 1915, p. 50.
49. Mojeyko, B. E.... Zur morphologie und systematik der Doppelmissbildungen. St. Petersburg. Trav. Soc. nat., 38, 1, 1907.

50. Mall, F. P. ... A Study of the Causes underlying the Origin of Human Monsters. Jour. of Morph. Vol. 19, 1908, pp. 1—361.
51. Ibid. ... Cyclopia in the Human Embryo. Publication 226 of Carnegie Inst. of Washington, 1917.
52. McClendon, J. F. ... An Attempt Towards the Physical Chemistry of the Production of One-Eyed Monstrosities. Amer. Jour. of Physiol., Vol. 29, 1912.
53. Morgan, T. H. ... The Relation between Normal and Abnormal Development of the Embryo of Frog. I, II, (1902), Bd. 16. V, (1905), Bd. 17. VI, Bd., 19 H.3. VII—X, Bd. 19 H 4. Arch. f. Entw. Mech. d. Org.
54. Ibid. ... Experimental Zoology. 1912.
55. Morrill, C. V. ... Symmetry Reversal and Mirror Imaging in Monstrous Trout and a Comparison with Similar Conditions in Human Double Monsters. Anat. Rec., Vol. 16. No. 4, 1919.
56. Naegeli, O. ... Über eine neue mit Zyklopie verknüpfte Missbildung des Zentralnervensystems. Arch. f. Entw. Mech. d. Org., Bd. 5, 1897.
57. Nussbaum, M. ... Zur Anatomie der Orbita. Verhandl. Anat. Gesell. 16. Vers Halle, a. s.
58. Newman, H. ... Modes of Inheritance in Teleost Hybrids. Jour. of Exp. Zool., Vol. 16, 1914.
59. Ibid. ... The Experimental Production of Twins, and Double Monsters in the Larvae of the Starfish (*Patiria minata*). Jour. of Exp. Zool., Vol. 33. 1921.
60. Politzer, G. ... Die Doppelbildungen der Urodelen 1. Mitteilung. Arch. f. Entw. Mech. d. Org., Bd. 108, H2 1926, 11. Mitteilung. Idem., Bd. 108 H, 1926.
61. Patterson, J. T. Polyembryonic Development in *Tatusia novemcincta*. Jour. Morph., Vol. 24. 1907, p. 559.
62. Reesè, A. M. ... The Anatomy of a Double Cat. Anat. Rec., Vol. V, 1911, p. 383.
63. Ibid. ... The Anatomy of a Two-headed Lamb. Anat. Rec., Vol. 13, 1917, p. 179.

64. Riddle, O. ... On the Cause of Twinling and Abnormal Development in Birds. *Amer. Jour. of Anat.*, Vol. 32, 1923.
65. Roux, W. ... Einleitung zum Archiv. für Entwicklungsmechanik. *Arch. f. Entw. Mech.*, Bd. 1. 1895.
66. Rauber, A. ... Formbildung und Formstörung in der Entwicklung von Wirbeltieren. *Morph. Jahrb.*, Bd. 5. UG., 1879—90.
67. Schwalbe, E. ... Die Morphologie der Missbildungen des Menschen und der Tiere. 1, 2, und 3, T. 1906, 1907, 1913.
68. Ibid. ... Allgemeine Missbildungslehre. 1906.
69. Saint Hilaire, G. Histoire general et particuliere des anomalies de l'organisation III. Paris, 1838.
70. Spemann, H. ... Über experimentell erzeugte Doppelbildungen mit zyklischen Defekt. *Zool. Jahrb. Suppl.*, Bd. 7, und *Arch. f. Entw. Mech.*, Bd. 15. 1904.
71. Ibid. ... Entwicklungsphysiologische Studien am Triton—Ei. 1. *Arch. f. Entw. Mech.*, Bd. 14, 1903, und 2. ibidem, Bd. 15, 1904.
72. Spemann, H. und Falkenberg, H. Über asymmetrische Entwicklung und situs inversus viscerum bei Zwillingen und Doppelbildungen. *Arch. F. Entw. Mech. d. Org.*, Bd. 45 H, 1919.
73. Stockard, C. R. The Artificial Production of One-eyed Monsters and Other Defects which occur in Nature by the Use of Chemicals. *Anat. Rec.*, Vol. 3, 1907.
74. Ibid. ... The Experimental Production of Various Eye Abnormalities and an Analysis of the Development of the Primary Parts of the Eye. *Arch. f. Vergl Ophthalmol*, Bd. 1, 1910.
75. Ibid. ... The Question of Cyclopia. *Science N. S.*, XXVIII, 1908.
76. Ibid. ... The Artificial Production of a Single Median Cyclopic Eye in the Fish Embryo by means of Sea-water Solution of Magnesium chloride. *Arch. f. Entw. Mech. d. Org.*, Bd. 23, 1907.

77. Stockard, C. R.... Developmental Rate and Structural Expression : An Experimental Study of Twins, Double Monsters and Single Deformities and the Interaction among Embryonic Organs, during their Origin and Development. Amer. Jour. of Anat., Vol. 28. p. 115, 1921.
78. Stone, R. ... The Central Nervous System of a Human Cyclop. Tr. R. Canad. Inst., 14, 1923.
79. Suzuki, N. ... Contribution to the Theory of Teratogeny based on the Microscopic Investigation of the Central Nervous System of Single and Double Monsters of Dog-Salmon Embryos (*Oncorhynchus keta* Walbaum). Arb. a. d. Anat. Inst. der Kaiser. Jap. Uni., z. Sendai, H. 13, 1928.
80. Swett, F. H. ... Situs Inversus Viscerum in Double Trout. Jour. of Exp. Zool., Vol. 21, 1921.
81. Tsuda, S. ... Über die Zyklopische Fehlbildung bei *Salamandra maculosa*. Folia. Anat., Japan., Bd. 2, H<sub>2</sub>, 1924.
82. Thuringer, J. M. Anatomy of a Dicephalus Pig Monosomus Diprostopus. Anat. Rec., Vol. 1919.
83. Werber, E. L. ... Experimental Studies aiming at the Control of Defective and Monstrous Development, a Survey of recorded Monstrosities with Special Attention to the Ophthalmic Defects. Anat. Rec., Vol. 9, 1915.
84. Werber, E. L. ... On Defective and Monstrous Development due to the Ophthalmic Defect. Anat. Rec., Vol. 9, 1915 (a).
85. Ibid. ... Experimental Studies on the Origin of Monsters. 1. An Etiology and an Analysis of the Morphogenesis of Monsters. Jour. of Exp. Zool., Vol. 21, 1916.
86. Ibid. ... On the Blastolytic Origin of the Independent Lens of some Terato-ophthalmic Embryos and its Significance for the Normal Development of the Lens in Vertebrates. Jour. of Exp. Zool., Vol. 21.

87. Ibid. ... Blastolysis as a Morphogenetic Factor in the Development of Monsters. *Anat. Rec.*, Vol. 10, 1916.
88. Whitehead, R. H. A Case of Cyclopia. *Anat. Rec.*, 3, 1909.
89. Wilder, H. H. ... The Morphology of Cosmodia. Speculations Concerning the Significance of Certain Types of Monsters. *Amer. Jour. of Anat.*, Vol. 8, 1908.
90. Windle, B. C. A. On Double Malformations Amongst Fishes. *Proc. Zool. Soc., London*, Pt. 3, 1895.
91. Ibid. ... Duplicatas, Twins, and Double Monsters. *Amer. Jour. of Anat.*, Vol. 3, 1904.
92. Williams, S. R. & Ruch, R. M. The Anatomy of a Double Pig (*Syncephalus thoracopagus*). *Anat. Rec.*, Vol. 13, p. 273, 1917.
93. Woolhard, H. ... Anophthalmus Congenitus in Puppy. *Brit. Jour. of Ophthalmol.*, Vol. 10, 1926.
94. Winkler, C. ... The Brain in a Case of Cycloplan Incomplita *Folia Neuro-Biol.*, Bd. 10, Nr. 2—9, 1917.
95. Yudkin, A.M. ... Congenital Anophthalmus in Albino Rats. *Amer. Jour. of Ophthalmol.*, Vol. 10, No. 5, 1927.
96. Zingerle, H. und Schaunstein Untersuchung einer menschlichen Doppelmissbildung (*Cephalothoracopagus monosymmetros*) mit besonderer Berücksichtigung des Zentralnervensystems. *Arch. f. Entw. Mech. d. Org.*, Bd. 24.
97. Alverdes, F. ... Über die Variabilität der Monstrositäten unter besonderer Berücksichtigung eigener Untersuchungen an Schwein. *Anat. Anz. Jena.*, 57, 1923, pp. 1—17. 14 figs
98. Baumgartner, W. J. A Double Monster Pig—*Cephalothoracopagus monosymmetros*. *Anat. Rec.*, Philadelphia, 37, pp. 303—316, 1928.
99. Chidester, F. E. The Origin of Cycloplan Monsters. *Amer. Nat. New York*, 57, 1923, pp. 496—518.
100. Duckworth, W. L. H. ... Description of a Monocephalous new-born Pig, Cambridge. *Proc. Phil. Soc.*, 14, 1903 (447—56) pls. XV-XVI.

101. D'Alfonso, C. ... Una deformita faciale congenita in un suino.  
Ann. R. Scoul Super Agric Portici (2) 16,  
No. 7, 1920, pp. 1—8, 4 figs.
  102. Forsius, R. ... Dubbel embryo af *Sus scrofa domestica*.  
Helsing fors Medd. Soc. Fauna et Fl.  
Fenn. 35, 1909 (137-38).
  103. Higgins, G. M. The Anatomy of a Double Monster Pig.  
Trans. Illinois. State. Acad. Sci. Spring-  
field, 16, 1923, pp. 111—121, 10 figs.
  104. Jordan, H. E. The Operation of a Factor of Special Relation-  
and others ship in Mammalian Development as Illus-  
trated by a case of Quadruplex Larynx  
and Triplicate Mandible in a Duplicate  
Pig monster. Anat. Rec., Philadelphia, 26,  
1923, pp. 311—318.
  105. Kalujin, J. J. ... Sketches of Pigs with Three and many Toes  
Studied in White Russia. Pts. II-III, pp.  
1—30, Pt. IV, pp. 1—65; Pt. V, pp. 1—53.  
47 pls. Minsk 1925, 8vo. (Russian with  
English and German).
  106. Monterosso, B.... Su di un Monstro doppio (Sicefalo-Sinoto)  
di Maiale Note anatomiche Atti. Acc.  
Gioenia. Catania (5) 12, 1920. Mem No.  
16, pp. 1—24, pl. 1, text figs.
  107. Polara, G. et ... Spora un monstro doppio di *Sus scrofa*  
Comeo, S. (Sicefalo-sinoto) Catania Atti. Acc. Gioenia.  
Ser 4, 19, 1906, Mem XII (1—16) figs.
  108. Sumulong, M. D. Congenital Absence of Both Hind Legs in an  
Adult Pig. Philippine J. Sci. Manila,  
P. I. 31, 1926, pp. 147—159. 2 pls.
-



## APPENDIX

### A COMPARATIVE TABULAR STATEMENT

Organs.	Typical condition in a normal pig.	The condition found in the abnormal pig described.
The snout and the external character of the head.	The snout is elongated, the Nasal openings lie at the anterior end. There are two eyes and ears.	The snout is bent upwards and much deformed. There are no external nares. There is a single cyclopiian eye. The vault of the cranium is round and much swollen.
Musculature of the head. <i>Cranial region</i> Occipital muscle Frontal muscle.	The occipital frontalis is a muscle expanding over the roof of the cranium.	The occipital and frontal muscle are united with each other by the muscular sheet stretching along the swollen crown of the head.
Muscles of the sense organs. Ear	The pinna of the ear has the large conchal cartilage and the scutiform cartilage. The former is big and fan-like and the latter is an irregular triangular plate attached by muscles to the skull and the base of the ear.  The Retrahens externus has two tendinous insertions, one attached to the conchal cartilage and the other to the scutiform cartilage.	Almost like the normal except for the dimensions of the two pinna.          As in the normal state.

Organs.	Typical condition in a normal pig.	The condition found in the abnormal pig described.
Nasal muscles	<p>The Ligamentum nuchae is represented by a fibrous cord from the dorsal neural spine to the occipital region.</p> <p>The Levator labi superioris aequae nasi, the dilatator naris transversus and the lachrymalis are wanting. The nasalis longus is well developed.</p>	<p>As in the normal.</p> <p>All the nasal muscles are wanting, they are fused together to form a thin sheet of muscles lying in juxta-position across the cyclopiian eye.</p>
Palpabral region.	<p>The orbicularis palpebrarum is the sphincter muscle of the eyelids.</p>	<p>The sphincter muscles of the eyelids of either side are united together forming a broad sphincter around the cyclopiian eye.</p>
Orbital region	<p>There are usually six eye muscles in each eye; they lie quite separate from one another all originating from the margin of the optic foramen and become attached to the eyeball.</p>	<p>The eye is a synophthalmic cyclopia. The motor muscles of the eye are comparatively broader and fleshy owing to the partial fusion. The superior and inferior oblique muscles are united distally and appear to be single and continuous running obliquely over and below the globe of the eye. They are buried in a quantity of fatty tissue. The intrinsic muscles comprise Ciliary muscles suspending the two lenses.</p>

Organs.	Typical condition in a normal pig.	The condition found in the abnormal pig described.
The Jaw muscles.	The jaw muscles and the masticatory muscles are the following:—The Zygomaticus, the Buccinator, the Masseter, the Temporalis and the Pterygoideus.	In the abnormal pig these are greatly modified and much deformed. The Zygomaticus are united with each other. The Buccinator, Masseter and Temporalis are distorted owing to the bending of the mouth. The Pterygoideus both externus and internus are not distinguishable.
The Cranium	<p>The Supra-Occipital bone forms a very prominent crest.</p> <p>The condyles and the foramen magnum are small.</p> <p>The Paroccipital processes are very long and slightly bent forward.</p> <p>The Parietals and Frontals are short.</p> <p>The Petrous portion of the periotic is small, the mastoid protuberance is very large and the external auditory meatus is situated comparatively high up.</p>	<p>The Cranium is much swollen and rounded, there is no occipital crest.</p> <p>The condyles are a little ventrally situated owing perhaps to the swelling of the head, the foramen magnum is of normal size</p> <p>The Paroccipital processes are short and very little bent forward. They are closely attached to the mastoid bones.</p> <p>They are very large arching over the roof of the cranium.</p> <p>The periotic bones and the tympanic bulla are quite normal except for the auditory meatus which is lateral and not very high up.</p>

Organs.	Typical condition in a normal pig,	The condition found in the abnormal pig described.
	<p>The nasals are long straight bones articulated with the Frontal and the Maxilla. The anterior end projects forward. A part of the septum of the nose becomes ossified forming the prenasal or snout bone. The Turbinals are large and less fragile.</p>	<p>All the bones of the olfactory capsules, <i>e. g.</i>, the nasals, the ethmoids, the turbinals, etc., are wanting.</p>
	<p>The Lachrymals are small with a canal.</p>	<p>They are absent.</p>
	<p>The Jugal bone is very stout and articulates with the zygomatic process of the Squamosal and with the Maxilla.</p>	<p>The Jugals are united together in the median line to form a broad horizontal bone lying across and below the orbit.</p>
	<p>The Maxilla sends out a large protuberance whence springs the tusk.</p>	<p>The Maxilla is short and bent up, the maxillary protuberance and the tusk do not exist.</p>
	<p>The palatine plates of the Maxilla articulate with the Palatine and possess the palatine foramen.</p>	<p>The palatine plate of the Maxilla is short and slightly bent upward anteriorly. Posteriorly it is flat and evenly fused with the basisphenoid.</p>
	<p>The Premaxilla is fairly large and articulates with the Nasal and the Maxilla.</p>	<p>It lies in front of Maxilla. There is no nasal bone for its attachment.</p>

Organs.	Typical condition in a normal pig.	The condition found in the abnormal pig described.
Cranial cavity	The Palatine forms the large part of the bony palate.	As there is no internal narial opening, the palatine is difficult to distinguish from the basisphenoid and the Maxillo-palatine process which are fused to form a bony roof of the buccal cavity.
	The Basisphenoid is short with large flat pterygoid processes which are almost perpendicular.	Owing to lack of the internal narial opening the Pterygoid processes are blended with the Maxillo-palatine process and the Basisphenoid.
	The Mandible is strong, the coronoid process is short and the articulating facets are laterally compressed.	The Mandible is short and attenuated. The coronoid process is also small in size. Only 4 teeth and a pad are borne on the anterior end of the Mandible.
	The internal surface of the cranium is lined by the Dura mater which is inflected over the membranous processes, viz., the falx cerebri between the cerebral hemispheres the tentorium between the cerebellum and the hemispheres and the falx cerebelli between the lobes of the cerebellum.	On account of the much swollen condition of the skull and the small size of the brain there is a large space in the interior of the cranium. The tentorium, falx, etc., are entirely wanting.

Organs.	Typical condition in a normal pig.	The condition found in the abnormal pig described.
Brain ...	<p>The brain occupies the entire cranial cavity.</p> <p>The olfactory bulbs consist of the most anterior portions of the brain, the interior of which contains cavities communicating with the lateral ventricles.</p> <p>The cerebral hemispheres are separated by the longitudinal fissure. They are united together by the great commissure—the Corpus Callosum.</p> <p>The cerebral convolutions or sulci are very few, fewer than other Ungulates.</p> <p>The lateral ventricles or the cavities of the hemispheres lie beneath the corpus callosum. They communicate with the third ventricle by the foramen Munro.</p> <p>The third ventricle is the cavity of the Diencephalon. Its lateral walls are formed by the Optic thalami—two large thick bodies embracing the anterior portion of the crura cerebri and placed in front of the corpora quadrigemina.</p>	<p>The brain is small as compared with the normal pig.</p> <p>The olfactory bulbs are absent.</p> <p>The hemispheres are small in size. They are united by the Corpus Callosum as in the normal.</p> <p>Only two sulci are visible one on each hemisphere.</p> <p>As in the normal but very much degenerate in condition. The hippocampus, the corpus striatum, and the fornix are rudimentary.</p> <p>The optic thalami are very thick, the rest is almost the same as in the normal.</p>

Organs.	Typical condition in a normal pig.	The condition found in the abnormal pig described.
	The three commissures—the anterior, middle and the posterior run across the third ventricle.	The commissures are feeble.
	The stalk of the Pineal gland lies above the third ventricle, and the Pineal gland itself is placed between the corpora quadrigemina.	No epiphysial structure is visible.
	In the centre of the floor of the third ventricle a deep pit leads into the Infundibulum to which the Pituitary body is attached.	The Hypophysis cerebri or Pituitary body is also wanting.
	The corpora quadrigemina or optic lobes are four rounded bodies situated behind the Diencephalon and forming the roof of the Iter.	As in the normal.
	The cerebellum consists of a body, two lateral lobes and two floccular lobes. The surface presents large numbers of grooves and fissures.	The cerebellum is well developed with all its lobes which show almost the same amount of development as in the normal.
	Internally the organ shows a ramification of white fibres giving an arborescent appearance—the arborvitae.	The arbor vitae is elaborate and much branched.

Organs.	Typical condition in a normal pig.	The condition found in the abnormal pig described.
	<p>The Valve of Vieussens—the membrane extending from the posterior optic lobes covering the roof of the fourth ventricle.</p> <p>The Pons Varolli stretches transversely from one side of the cerebellum to another.</p> <p>The Crura cerebri at the base of the medulla lie in front of the Pons and run forward diverging from each other joining the medulla with the hemispheres.</p>	<p>As in the normal.</p> <p>The pons is well developed as in the normal.</p> <p>The Crura forms the floor of the mid-brain and lies anterior to the pons as in the normal.</p>
The cranial nerves.	<p>The Olfactory nerve arises from the olfactory lobes and supplies the epithelium of the olfactory organ.</p> <p>The optic nerve is a stout nerve. It arises from the optic chiasma, which is formed by the crossing of the optic tracts. The two optic tracts can be traced to the optic Thalami. They proceed forward and inward and decussate in the median ventral line ultimately supplying the retina of the eye.</p>	<p>The Olfactory nerve does not exist.</p> <p>The Optic Chiasma is absent. The optic tracts originate from the thalami and do not decussate ventrally but become continuous with the optic nerve. The inter-cranial course of this nerve is very long. The two nerves become united by a common sheath and supply the single median cyclopiian eye.</p>



Organs.	Typical condition in a normal pig.	The condition found in the abnormal pig described.
	<p>The oculo-motor originates ventrally near the Infundibulum and supplies all the muscles of the eye except the Superior Oblique and the External Rectus.</p> <p>The Pathetic arises dorsally from near the Valve of Vieussens and supplies the superior oblique.</p> <p>The trigeminal is a very stout nerve. It originates from the side of the posterior border of the pons by two roots. It divides into three branches supplying the snout, the upper and the lower jaw.</p> <p>The abducent is an extremely delicate nerve originating ventrally close behind the pons and supplying the external rectus of the eye.</p> <p>The facial originates just behind the trigeminal from the side of the brain and supplies the facial muscles.</p>	<p>The same as in the normal supplying of the cyclopian eye, the muscles on the respective side.</p> <p>The same origin and distribution as in the normal.</p> <p>The fifth cranial nerve possesses the three divisions and their distribution is almost normal except for the ophthalmic branch which is extremely short and gets distributed over the malformed snout.</p> <p>As in the normal pig.</p> <p>The facial nerve gives off numerous branches after making its exit through the stylomastoid foramen. It gives off :—</p> <p>(1) a Cervical branch supplying the skin of the neck.</p>

Organs.	Typical condition in a normal pig.	The condition found in the abnormal pig described.
	<p data-bbox="284 1049 569 1197">The auditory is a large and strong nerve arising behind the facial supplying the ear.</p> <p data-bbox="284 1239 569 1544">The Glossopharyngeal, pneumogastric, spinal accessory and the hypoglossal originate from the ventral surface of the medulla supplying the tongue, larynx, maxillary glands, viscera and neck muscle, etc.</p>	<p data-bbox="621 289 932 1032">           (2) an anterior auricular ascends in front of the ear.            (3) a posterior auricular nerve supplying the posterior muscles of the ear.            (4) a middle auricular nerve enters the concha.            (5) the temporo facials are in two sets. One passes over the external surface of the masseter and the other downwards to the lower border of the same muscle. They communicate with the maxillary division of the fifth and form a ganglion from where a large number of small nerves supply the snout and form a plexus.         </p> <p data-bbox="606 1049 906 1082">Same as in the normal.</p> <p data-bbox="606 1230 906 1263">Same as in the normal.</p>

Organs.	Typical condition in a normal pig.	The condition found in the abnormal pig described.
The Orbit and the Eye.	<p data-bbox="264 396 574 502">Two eyes are paired lying in two separate orbits or sockets.</p> <p data-bbox="264 520 574 1120">The eyeball as usual consists of (i) the sclerotic and cornea, (ii) Choroid and iris, (iii) the retina. The sclerotic is the outer coat and opaque to which the transparent cornea is firmly attached. The Choroid is a thin vascular membrane containing the ciliary muscles and nerves. It is continuous with the iris diaphragm. The ciliary muscle is continuous with the circumference of the iris.</p> <p data-bbox="264 1137 574 1384">The crystalline lens lies immediately behind the iris. It is spherical in shape and is supported by the ciliary muscles in its proper position.</p> <p data-bbox="264 1428 574 1684">The retina is supplied by the optic nerve which pierces the two outer coats. The microscopical structure of the retina shows that it is composed of nerve fibre, ganglion, rods and cone cells.</p>	<p data-bbox="626 396 958 502">The eye is a cyclopia (synophthalmia bilentica).</p> <p data-bbox="626 520 958 626">The tunics of the eyeball are three in number as in the normal.</p> <p data-bbox="626 1137 958 1420">The lenses are two in number supported by the ciliary muscles. They are globular and are of unequal diameter. The right is bigger than the left measuring 6mm. and 4mm. respectively.</p> <p data-bbox="626 1428 958 1666">The retina as in the normal pig is deeply pigmented. The united optic nerve supplies the retina. The histological structure of the retina is as in the normal.</p>

Organs.	Typical condition in a normal pig.	The condition found in the abnormal pig described.
The accessory organs of the eye.	<p data-bbox="291 303 578 386">Eyebrows are insignificant and almost absent.</p> <p data-bbox="291 419 578 535">Eyelids.—The eyelids are very prominent and both are moveable.</p> <p data-bbox="291 568 578 733">Conjunctiva.—A transparent membrane lines the under surface of the eyelids adhering very firmly to the cornea.</p> <p data-bbox="291 766 578 882">Lachrymal apparatus —consists of lachrymal glands, sac, ducts, and canals.</p>	<p data-bbox="622 303 946 386">A single eyebrow is present arching over the cyclopiian eye.</p> <p data-bbox="622 419 946 477">The lids are very small and non-functional.</p> <p data-bbox="622 568 946 626">It is firmly fixed to the conjoined cornea.</p> <p data-bbox="622 766 946 849">Lachrymal apparatus and its accessory structures are wanting.</p>

*SECTION II*  
CHEMISTRY

# THE PHOTOCHEMICAL REACTION BETWEEN SODIUM NITRITE AND IODINE

BY

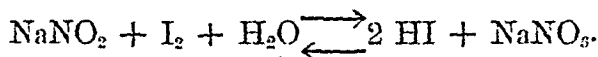
A. K. BHATTACHARYA,

*Chemistry Department, Allahabad University.*

This reaction is very sensitive to light and has been investigated in detail in these laboratories [Zeit. Anorg. V. Allg. Chem., 134, 172 (1924) ; J. Phys. Chem., 33, 850 (1929)]. The velocity of the reaction has been followed by measuring the changes in the concentration of iodine against thiosulphate solution. Recently Berthoud and Berger [J. Chem. Phys., 25, 562 (1928)] have shown that nitrite and iodine react more readily in presence of sodium thiosulphate solution and consequently the estimation of iodine by thiosulphate leads to erroneous results.

In this communication we are submitting the results obtained in the determination of the order, temperature coefficient and quantum efficiency of this reaction in light of different wavelengths. We have determined the changes in the concentration of iodine by a Nutting's Spectrophotometer.

The reaction can be represented by the equation—



The influence of the variation of intensity of the incident radiation has been investigated in different radiations and using different amounts of potassium iodide, which is a marked retarder. Both sodium acetate and borax solutions have been used as buffer solutions.

## KINETICS AND QUANTUM EFFICIENCY

The source of light and the experimental arrangement are the same as described in a previous paper [Z. Anorg. V. Allg. Chem., 176, 372 (1928)].

The following are the experimental results:—

2/3 N sodium nitrite ; N/32 iodine in N/8.2 KI

5 c. c.

10 c. c.

in presence of N/6.25 sodium acetate (5 c.c.)

Condition	Temperature in °C	K <sub>1</sub> Mono-mole- cular	K <sub>2</sub> after deducting the dark reaction	Temp. coeff.	Temperature coefficient after deduct- ing the dark reaction	Quantum efficiency
Dark ...	30	0.00319 K <sub>1</sub> 0.0090	..	2.7		
	40	0.00866 K <sub>1</sub> 0.0241	..	2.61		
	50	0.02260 K <sub>1</sub> 0.0537				
N/3 NaNO <sub>2</sub>	30	0.00162				
	40	0.00419	...	2.59		
	50	0.0104	...	2.49		

Hence the order of the reaction is bimolecular in the dark

$\lambda=4725 \text{ \AA}^\circ$	30	K <sub>2</sub> 0.0251	0.0161		2.07	5.15 × 10
	40	0.0575	0.0334		2.0	8.6 ..
	50	0.1207	0.0670		...	11.9 ..
$\lambda=5650 \text{ \AA}^\circ$	30	0.0212	0.0122		2.2	3.94 ..
	40	0.0510	0.0269		2.1	6.8 ..
	50	0.111	0.0563		...	10.2 ..
$\lambda=7504 \text{ \AA}^\circ$	30	0.0186	0.0096		2.29	3.8 ..
	40	0.0461	0.0220		2.15	6.2 ..
	50	0.101	0.0473		...	8.1 ..
$\lambda=8500 \text{ \AA}^\circ$	30	0.0147	0.0057		2.35	3.6 ..
	40	0.0375	0.0134		2.20	5.2 ..
	50	0.0835	0.0298		...	7.3 ..

From the foregoing results it will be observed that Einstein's law of photochemical equivalence is not exactly applicable to this reaction. The quantum efficiency increases with temperature and the frequency of the incident radiation. Similar results have been obtained with numerous other reactions.

The experimental results show that the temperature coefficients of the photochemical changes are less than those of the corresponding thermal reaction. The greater the acceleration in light of different wavelengths, the less the temperature coefficient. Another interesting fact is that the temperature coefficient of the purely light reaction is much greater than unity. Similar results have been obtained with several other reactions so far investigated in these laboratories. Hence we are in a position to uphold our view that the temperature coefficient of photochemical reactions need not be unity.

Many people believe that the photochemical reactions are brought about by violet and ultra-violet radiations only. Our experimental results, however, prove that this and several other reactions can be accelerated by radiations of wavelength  $7304 \text{ \AA}$  and  $8500 \text{ \AA}$  which lie in the infra-red region of the spectrum.

### Relation between Absorption of Light and Velocity

The experimental arrangements are the same as described in a previous paper [*Zeit. Anorg. V. Allg. Chem.*, 175, 357 (1928)].

The corresponding dark reaction was always subtracted from the light reaction before calculating the effect of intensity of light on the velocity of this reaction.

The following are the experimental results :—

5 c. c.— $2/3 \text{ N}$  sodium nitrite and 10 c.c.  $\text{N}/32$  iodine in presence of 5 c. c.— $\text{N}/6.25$  sodium acetate.



Temperature  $40^{\circ}\text{C}$ .

Diameter of the aperture	$K_2$ Semi-molecular	$K_3$ Semi-molecular reaction in light after deducting the dark reaction
--------------------------	-------------------------	---

A. Source—*Sunlight*.  $K_2$  dark = 0.0247

2 cms.	0.256	0.2319 (I)
0.8 cm.	0.169	0.1449 (II)
0.4 "	0.143	0.119 (III)

B. Source—*1000-watt lamp*

2 cms.	0.0885	0.0645 (I)
0.8 cm.	0.0556	0.0315 (II)
0.4 "	0.0416	0.0175 (III)

C. Region— $\lambda = 5650\text{\AA}$

2 cms.	0.0464	0.0219 (I)
0.8 cm.	0.0296	0.0055 (II)
0.4 "	0.0249	0.0018 (III)

D. Region— $\lambda = 7304\text{\AA}$

2 cms.	0.0420	0.0179 (I)
0.8 cm.	0.0377	0.0036 (II)
0.4 "	0.0251	0.0010 (III)

E. Region— $\lambda = 7304\text{\AA}$

N/32 Iodine dissolved in 0.75 gm. KI in presence of  
N/105 borax solution.

$K_2$  dark = 0.0450

2 cms.	0.0592	0.0142
0.8 cm.	0.0471	0.0021

The following results show that the absorption of radiation is approximately proportional to the intensity of the incident radiation.

*Temperature 40°C.*

Diameter of the aperture	Substance	Deflection in cms.	Difference in deflection
2 cms.	(i) Distilled water (ii) Reacting mixture	38.6 35.0	3.6 cms.
0.8 cm.	(i) Distilled water (ii) Reacting mixture	21.2 20.6	0.6 cm.
0.4 cm.	(i) Distilled water (ii) Reacting mixture	12.65 12.5	0.15 cm.

Ratio of Intensity	Ratio of absorption
$\frac{3.14}{0.5024} = 6.25$	$\frac{3.6}{0.6} = 6$
$\frac{0.5024}{0.1256} = 4$	$\frac{0.6}{0.15} = 4$
$\frac{3.14}{0.1256} = 25$	$\frac{3.16}{0.15} = 24$

A

Ratio of velocities	If directly proportional to the absorption of incident radiation	If proportional to the square root of the absorption of incident radiation
$\frac{I}{II} = \frac{0.2319}{0.1449} = 1.6$	6	$\sqrt{6} = 2.45$
$\frac{II}{III} = \frac{0.1449}{0.119} = 1.22$	4	$\sqrt{4} = 2$
$\frac{I}{III} = \frac{0.2319}{0.119} = 2.68$	24	$\sqrt{24} = 4.9$

## B

Ratio of velocities	If directly proportional to the absorption of incident radiation	If proportional to the square root of the absorption of incident radiation
$\frac{I}{II} = \frac{0.0645}{0.0315} = 2.05$	6	2.45
$\frac{II}{III} = \frac{0.0515}{0.0175} = 1.8$	4	2
$\frac{I}{III} = \frac{0.0645}{0.0175} = 3.7$	24	4.9

## C

$\frac{I}{II} = \frac{0.0219}{0.0055} = 4$	6	2.45
$\frac{II}{III} = \frac{0.0035}{0.0018} = 2$	4	2
$\frac{I}{III} = \frac{0.0219}{0.0018} = 12$	24	4.9

## D

$\frac{I}{II} = \frac{0.0179}{0.0036} = 5$	6	2.45
$\frac{II}{III} = \frac{0.0036}{0.0010} = 3.6$	4	2
$\frac{I}{III} = \frac{0.0179}{0.0010} = 17.9$	24	4.9

## E

$\frac{I}{II} = \frac{0.0142}{0.0021} = 6.76$	6	2.45
---	---	------

## DISCUSSION

The experimental results show that the relation between the absorption or intensity and the velocity of the reaction varies from a less than  $\frac{1}{3}$  to more than proportional. From this it is clear that the relation between light absorption or intensity and velocity of one and the same reaction can be varied. It depends entirely on the ratio of the velocities of the light and dark reactions.

When the velocity of the thermal reaction is less and the reaction mixture is exposed to sunlight, the relation between light absorption or intensity and the velocity tends to be less than  $\frac{1}{3}$ . This relation goes on increasing as the acceleration of light reaction over the corresponding thermal reaction is decreased. It increases so much as to show a relation approximately  $\frac{5}{2}$  in the region  $\lambda = 7304\text{\AA}^\circ$  using N/105 borax solution as a buffer solution which markedly accelerates the dark reaction. The source of light is not intense in this case. The total result is that the acceleration due to light is not marked in comparison with the dark reaction and the ratio between light absorption or intensity and velocity rises to approximately  $\frac{5}{2}$ .

These results are in entire agreement with our conclusions that the relation between light absorption or intensity and velocity of a reaction is controlled by the ratio of the light and dark reactions.

### The Influence of Sodium Nitrite on the Amount of Sodium Thiosulphate Necessary to React with Iodine

The following are the experimental results:—

N/5  $\text{NaNO}_2$ , Iodine—N/10 (approximately)

Sodium Thiosulphate—N/10

Volume of iodine solution	Volume of nitrite solution	Volume of the thiosulphate solution
10 c.c.	Nil	9.65 c.c.
10 "	10 c.c.	8.55 "
10 "	20 "	6.90 "
10 "	30 "	6.50 "

## B

Ratio of velocities	If directly proportional to the absorption of incident radiation	If proportional to the square root of the absorption of incident radiation
$\frac{I}{II} = \frac{0.0345}{0.0315} = 2.05$	6	2.45
$\frac{II}{III} = \frac{0.0315}{0.0175} = 1.8$	4	2
$\frac{I}{III} = \frac{0.0345}{0.0175} = 3.7$	24	4.9

## C

$\frac{I}{II} = \frac{0.0219}{0.0055} = 4$	6	2.45
$\frac{II}{III} = \frac{0.0055}{0.0018} = 3$	4	2
$\frac{I}{III} = \frac{0.0219}{0.0018} = 12$	24	4.9

## D

$\frac{I}{II} = \frac{0.0179}{0.0036} = 5$	6	2.45
$\frac{II}{III} = \frac{0.0036}{0.0010} = 3.6$	4	2
$\frac{I}{III} = \frac{0.0179}{0.0010} = 17.9$	24	4.9

## E

$\frac{I}{II} = \frac{0.0142}{0.0021} = 6.76$	6	2.45
---	---	------

## DISCUSSION

The experimental results show that the relation between the absorption or intensity and the velocity of the reaction varies from a less than  $\frac{1}{3}$  to more than proportional. From this it is clear that the relation between light absorption or intensity and velocity of one and the same reaction can be varied. It depends entirely on the ratio of the velocities of the light and dark reactions.

When the velocity of the thermal reaction is less and the reaction mixture is exposed to sunlight, the relation between light absorption or intensity and the velocity tends to be less than  $\frac{1}{3}$ . This relation goes on increasing as the acceleration of light reaction over the corresponding thermal reaction is decreased. It increases so much as to show a relation approximately  $\frac{5}{2}$  in the region  $\lambda = 7304\text{\AA}$  using N/105 borax solution as a buffer solution which markedly accelerates the dark reaction. The source of light is not intense in this case. The total result is that the acceleration due to light is not marked in comparison with the dark reaction and the ratio between light absorption or intensity and velocity rises to approximately  $\frac{5}{2}$ .

These results are in entire agreement with our conclusions that the relation between light absorption or intensity and velocity of a reaction is controlled by the ratio of the light and dark reactions.

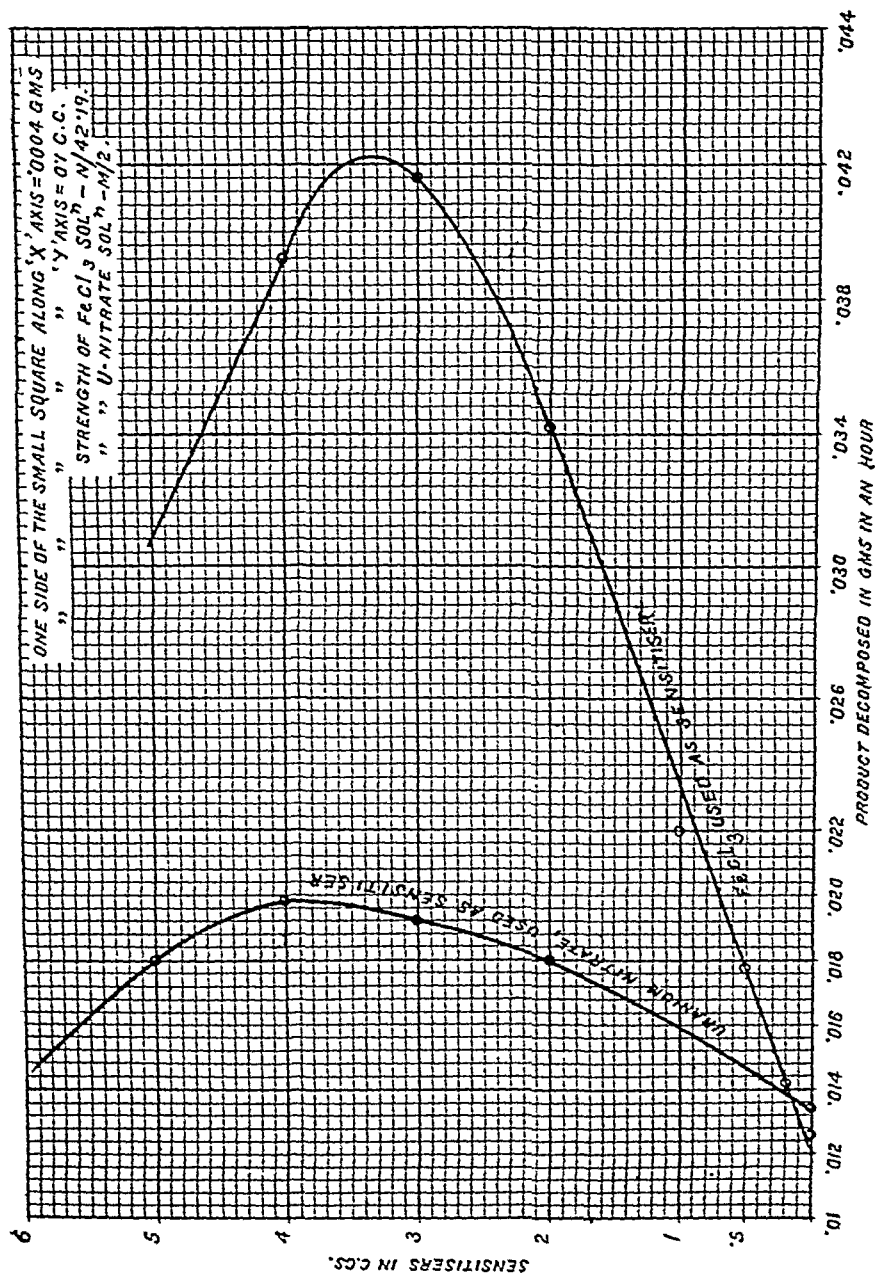
#### The Influence of Sodium Nitrite on the Amount of Sodium Thiosulphate Necessary to React with Iodine

The following are the experimental results:—

N/5  $\text{NaNO}_2$ , Iodine—N/10 (approximately)

Sodium Thiosulphate—N/10

Volume of iodine solution	Volume of nitrite solution	Volume of the thiosulphate solution
10 c.c.	Nil	9.65 c.c.
10 „	10 c.c.	8.55 „
10 „	20 „	6.90 „
10 „	30 „	6.50 „



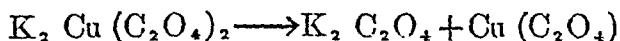
# PHOTOLYSIS OF POTASSIUM-CUPRI-OXALATE

BY

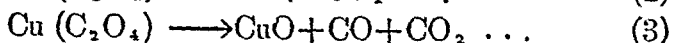
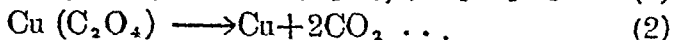
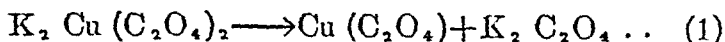
HIRA LAL DUBE, M.Sc.

In a previous paper (J. Chem. Soc. 111, 694 (1917), Z. anorg Chem. 128, 212 (1918), we observed that a solution of potassium-cupri-oxalate is decomposed in light and the velocity of this photochemical reaction is greatly accelerated by ferric and uranyl salts. No quantitative investigation of this reaction has been hitherto carried out, although corresponding photolyses of potassium-cobalti-oxalate (Vranek. Z. Elektrochem. 23, 236 (1917), of potassium-mangani-oxalate (Ghosh and Kappanna, J. Indian Chem. Soc. 3, 127, (1926), have received attention. More recently Allmand and Webb, (J. Chem. Soc. 1518, July 1929) have carried on the work on the photolysis of potassium-ferrioxalate. In this paper the results obtained in the photolysis of potassium-cupri-oxalate are studied.

The decomposition of potassium-cupri-oxalate can probably be represented thus—



No cupric oxalate is however actually observed but an admixture of copper and cuprous oxide is obtained on the decomposition of the photolyte. It therefore appears that anyhow cupric oxalate is instantaneously decomposed and the decomposition can be represented by the following equations:—



However our experiments show that cupric oxalate either by itself or in presence of a sensitiser is not decomposed



by light. Cupric oxalate was exposed as a freshly precipitated solid as it scarcely dissolves in water. It is just possible that cupric oxalate which is formed by the decomposition of potassium-cupri-oxalate is so active at the moment of its formation that it is instantaneously decomposed by the absorption of light energy into the products shown above and this may be the reason of our failure in not getting the photolysis of solid cupric oxalate. The photo-decomposition of potassium cupric oxalate continues even when light source is cut off but the velocity of the reaction is decreased. It is observed that the reaction is very slow without a sensitiser and hence a sensitiser such as ferric chloride is always used.

### Experimental

Pure copper sulphate and potassium oxalate were used in preparing the solutions of copper sulphate and potassium oxalate of  $N/5$  and normal strength respectively. In studying the photolysis of potassium-cupri-oxalate the volume exposed was always kept constant (100 c. c.) whatever may be the concentration of  $K_2Cu(C_2O_4)_2$  solution. It is found that any solution of higher concentration than the above gives precipitate which does not dissolve when the volume is made up to 100 c. c. Hence always lower concentrations than  $N/5$  for copper sulphate and  $N$  for potassium oxalate are taken. To obtain potassium-cupri-oxalate solution copper sulphate solution was taken and potassium oxalate solution was added till the precipitate of cupric oxalate first formed just redissolves. In this way a solution of potassium-cupri-oxalate of known strength is obtained.

### Velocity of the Reaction in Sunlight

Velocity of photolysis of potassium-cupri-oxalate was determined by exposing the solution directly to sunlight in presence of ferric chloride used as sensitiser. The potassium-cupri-oxalate solution was obtained by adding normal

potassium oxalate solution to N/5 copper sulphate solution till the precipitate of cupri-oxalate first formed just redissolves. The volume is always made up to 100 c. c. by adding distilled water. Following is the composition of potassium-cupri-oxalate used for the photolysis.

40 c.c. of N/5  $\text{CuSO}_4 \cdot 5 \text{H}_2\text{O}$

20 c.c. of N  $\text{K}_2 \text{C}_2\text{O}_4 \cdot \text{H}_2\text{O}$

1 c.c. of N/203  $\text{FeCl}_3$  solution used as sensitiser and

39 c.c. of distilled water

100 c.c. total volume

The velocity of the reaction is determined by weighing (Cu, CuO and  $\text{Cu}_2\text{O}$ ) the decomposed products as CuO. Following are the results obtained.

The solution of same concentration of  $\text{K}_2 \text{Cu} (\text{C}_2\text{O}_4)_2$  was exposed to sunlight every day but the light intensity was not constant.

TABLE I

Time	Amount of CuO formed in gms.	K. Zero molecular $k=x/t$
60 min.	0.0768	.00128
120 "	0.1530	.00127
180 "	0.2290	.00127

TABLE II

60 min.	0.0776	.00129
120 "	0.1546	.00128
180 "	0.2318	.00128

TABLE III

60 min.	0.0648	.00108
120 "	0.1292	.00107
180 "	0.1938	.00107

TABLE IV

Time	Amount of CuO formed in gms.	K. Zero molecular $k=x/t$
60 min.	0.0620	.00103
120 "	0.1240	.00103
180 "	0.1852	.00102

TABLE V

60 min.	0.0462	.000770
120 "	0.0928	.000773

The above tables show that the amount of decomposition in a definite time is definite provided the intensity of light is kept constant. In other words the photolysis of potassium-cupri-oxalate is independent of the concentration of the photolyte. This result is identical with that obtained by Allmand and Webb in the photolysis of potassium-ferri-oxalate and by Vranek in the photolysis of potassium-cobalti-oxalate.

The above solutions were exposed on different days but the same amount of decomposition is obtained for the same interval of time for the same day. Hence the reaction is independent of the concentration of the photolyte and therefore the reaction is zero molecular.

### Effect of Oxygen on the Reaction

It is stated that the photolysis of Eder's solution (Iodlbauer and Tappeiner, Ber., 1905, 38, 2602), of ferric-oxalate (Iodlbauer, Z. physikal. Chem. 1907, 59, 573), and of other ferric salts of organic acids (Winther and Oxholt-Howe, Z. Wiss, Phot., 1914, 14, 196) is stated to be retarded by oxygen. To test the effect of oxygen in the present reaction, two solutions of potassium-cupri-oxalate of identical concentrations were exposed to sunlight simultaneously and a current of air was passed through one solution only. The time of

exposure was same in both the cases. The following are the results obtained :—

TABLE VI

Time of exposure	Decomposition without a current of air in gms.	Decomposition in a current of air in gms.
3 hrs.	0·1398	0·0722
"	0·1594	0·0636

It is observed that the velocity of the reaction is highly retarded and is practically halved. The retardation in the case of carbon-dioxide is much less than in the case of oxygen. This inhibition is probably due to the oxidation of the ferrous salt formed by insolation of the ferric chloride used as sensitiser. Ferric chloride is first reduced to the ferrous condition and then acts as a sensitiser. So the oxygen retards the above reaction and in this way weakens the property of ferric chloride as sensitiser and therefore the photolysis of potassium-cupri-oxalate is retarded.

#### Effect of Carbon-dioxide on the Reaction

The effect of carbon-dioxide on the photolysis of potassium-cupri-oxalate was also investigated by taking two solutions of the same concentrations and exposed to sunlight for the same time. Through one solution a current of carbon-dioxide gas was passed throughout the experiment. The following results were obtained :—

TABLE VII

Time of exposure	Decomposition in air	Decomposition in CO <sub>2</sub> .
3 hrs.	0·1506	0·1492
"	0·1656	0·1470
"	0·1674	0·1498
"	0·1374	0·1348
"	0·1227	0·0936
"	0·1360	0·1155

The above results clearly show that the reaction is retarded in carbon dioxide gas.

### Effect of Excess of Potassium Oxalate Solution

A slight excess of potassium oxalate solution has practically no effect on the velocity of the reaction, while a large excess accelerates the photo decomposition of potassium-cupri-oxalate. In the case of potassium ferri oxalate (Allmand and Webb) and potassium cobalti oxalate (Vranck) found that the reactions are retarded by an excess of potassium oxalate, while in the case of potassium-mangani oxalate (Ghosh and Kappanua) it has no effect. In the present reaction we have got the following results which clearly show that the reaction is accelerated by an excess of potassium oxalate solution :—

TABLE VIII.

Time of exposure	Excess of $\text{NK}_2\text{C}_2\text{O}_4$ solution.	Amount decomposed I	Amount decomposed II	Amount decomposed III	Amount decomposed IV
1 hr.	0 c.c.	0.0654 gms.	0.0662 gms.	0.0582 gms.	0.0620 gms.
"	10 c.c.	0.0756 "	0.0698 "	0.0708 "	0.0780 "
"	20 c.c.	0.0804 "	0.0854 "	0.0802 "	...

### Temperature Coefficient of the Reaction

Temperature coefficient of the photolysis of potassium-cupri-oxalate has been determined at three different temperatures,  $27^\circ$ ,  $37^\circ$  and  $47^\circ$  in sunlight. The experiments were carried out on different days and as the intensity of sunlight did not remain constant, the values of 'K' are not same in the following tables.

TABLE IX

In each experiment time of exposure was one hour.

No. of Experiments	Amount of decomposition in gms. in an hr. at 27°C	$K_{27}^{\circ}$	Amount of decomposition in gm. in an hr. at 27°C	$K_{37}^{\circ}$	$K_{37}^{\circ}/K_{27}^{\circ}$
1	0.0424	.000706	0.0524	.000873	$\frac{.000873}{.000706} = 1.23$
2	0.0354	.00059	0.0432	.00072	$\frac{.00072}{.00059} = 1.22$
3	0.0620	.00103	0.0764	.00127	$\frac{.00127}{.00103} = 1.23$

TABLE X

Time of exposure one hour.

No. of Experiments	Amount of decomposition in gms. in an hr. at 27°C	$K_{27}^{\circ}$	Amount of decomposition in gms. in an hr. at 47°C	$K_{47}^{\circ}$	$K_{47}^{\circ}/K_{27}^{\circ}$
1	0.0778	.00129	0.0862	.00143	$\frac{.00143}{.00129} = 1.10$
2	0.0686	.00114	0.0760	.00126	$\frac{.00126}{.00114} = 1.10$
3	0.0516	.00086	0.0570	.00095	$\frac{.00095}{.00086} = 1.10$

### Effect of Different Concentrations of the Sensitisers on the Reaction

In the case of Eder's solution the effect of ferric chloride solution of different concentrations used as sensitizer has been studied. It is found that the reaction is accelerated at low concentrations of the sensitizer and as the concentration of the sensitizer is increased after a certain limit it begins to inhibit the reaction and at very high concentrations there is practically no reaction. We investigated this phenomena in the case of

photolysis of potassium-cupri-oxalate. With very dilute solutions of ferric chloride there is acceleration in the reaction. Even 0.05 c.c. of N/1015 solution of ferric chloride will show a marked acceleration in the photolysis. As the concentration of the ferric chloride solution is increased there is more and more acceleration to a certain limit. After this limit the increase in the concentration of the sensitiser will show fall in the velocity of the reaction and at high concentrations there is practically no reaction. This retardation of the reaction by strong solutions of ferric chloride is probably due to the formation of ferric oxalate.

In our experiments we prepared potassium-cupri-oxalate by taking 40 c.c. of N/5  $\text{CuSO}_4 \cdot 5\text{H}_2\text{O}$  and 20 c.c. of  $\text{NK}_2\text{C}_2\text{O}_4 \cdot \text{H}_2\text{O}$  and adding the ferric chloride solution and making the volume to 100 c.c. In the case of strong solutions of ferric chloride, there was a precipitate which dissolved on adding more of potassium oxalate solution. In all the experiments the volume was made up to 100 c.c.

By adding 10 c.c. of 2.37 N solution of ferric chloride there is practically no photolysis.

We tried uranium nitrate also as a sensitiser. It behaves similar to ferric chloride. The following tables and the accompanying graph will make the matter clear.

TABLE XI  
Strength of  $\text{FeCl}_3 = \text{N}/42.19$ .

Time of exposure	$\text{FeCl}_3$ added	Amount of decomposition in gms.
3 hrs.	0.0 c.c.	0.0126
"	0.2 "	0.0142
"	0.5 "	0.0178
"	1.0 "	0.0220
"	2 "	0.0342
"	3 "	0.0416
"	4 "	0.0392

TABLE XII

Strength of uranium nitrate =  $N/2$ .

Time of exposure	C.c. of uranium nitrate added	Amount of decomposition in gms.
3 hrs.	0 c.c.	0.0134
"	2 "	0.0180
"	3 "	0.0192
"	4 "	0.0198
"	5 "	0.0180

**Absorption Experiments with Potassium-cupri-oxalate Solution**

Nutting's photo-spectrometer was used to determine the extinction coefficients of potassium-cupri-oxalate solution and also of solutions with different concentrations of ferric chloride and uranium nitrate solutions used as sensitisers. The solution was prepared by taking—

40 c.c. of  $N/5 \text{CuSO}_4 \cdot 5 \text{H}_2\text{O}$ 20 c.c. of  $\text{NK}_2\text{C}_2\text{O}_4 \cdot \text{H}_2\text{O}$ 

and adding the sensitisers and making the volume to 100 c.c. The following results were obtained:—

Normal solution of potassium oxalate showed no absorption in the visible region.

TABLE XIII

 $N/5 \text{CuSO}_4 \cdot 5 \text{H}_2\text{O}$  solution.

Wavelengths of light	Density scale reading	Extinction coefficients
6700 Å	.25	.25
6300 Å	.13	.13
6000 Å	.06	.06
5600 Å	...	...
5000 Å	...	...
4400 Å	...	...



TABLE XIV

Potassium-cupri-oxalate solution.

40 c.c. N/5  $\text{CuSO}_4 \cdot 5 \text{H}_2\text{O}$  } made to 100 c.c.s.  
 20 c.c. N  $\text{K}_2 \text{C}_2\text{O}_4 \cdot \text{H}_2\text{O}$

Wavelengths of light	Density scale Reading	Extinction coefficients
6700 Å	'88	'88
6300 Å	'62	'62
6000 Å	'42	'42

No absorption in the rest wavelengths.

TABLE XV

Potassium-cupri-oxalate solution with 0.2 c. c.  
 of .0237 N  $\text{FeCl}_3$  solution.

6700 Å	'87	'87
6300 Å	'54	'54
6000 Å	'32	'32

No absorption in the rest wavelengths.

TABLE XVI

Potassium-cupri-oxalate solution with 0.5 c.c.  
 of .0237 N  $\text{FeCl}_3$  solution.

6700 Å	'87	'87
6300 Å	'54	'54
6000 Å	'34	'34

No absorption in the rest wavelengths.

TABLE XVII

Potassium-cupri-oxalate solution with 1 c.c.  
 of .0237 N  $\text{FeCl}_3$  solution.

6700 Å	'87	'87
6300 Å	'55	'55
6000 Å	'35	'35

No absorption in the rest wavelengths.

TABLE XVIII

Potassium-cupri-oxalate solution with 2 c.c.  
of .0237 N  $\text{FeCl}_3$  solution.

Wavelengths of light	Density scale Reading	Extinction co-efficients
6700 Å	.87	.87
6300 Å	.55	.55
6000 Å	.35	.35

No absorption in the rest wavelengths.

The following are the results got by using uranium nitrate solution as sensitiser.

TABLE XIX

$\text{K}_2 \text{Cu} (\text{C}_2\text{O}_4)_2$  with 0.4 c.c. of M/200  
uranium nitrate solution.

Wavelengths of light	Density scale reading	Extinction co-efficients
6700 Å	.88	.88
6300 Å	.59	.59
6000 Å	.38	.38
5600 Å	...	...
5000 Å	...	...
4400 Å	...	...

TABLE XIX

$\text{K}_2 \text{Cu} (\text{C}_2\text{O}_4)_2$  with 1 c.c. of M/200  
uranium nitrate solution.

6700 Å	.88	.88
6300 Å	.60	.60
6000 Å	.39	.39

No absorption in the rest wavelengths.

TABLE XXI

$K_2 Cu (C_2O_4)_2$  with 2 c.c.s. of M/200  
uranium nitrate solution.

Wavelengths of light	Density scale reading	Extinction coefficients
6700 Å	·88	·88
6300 Å	·59	·59
6000 Å	·39	·39

No absorption in the rest wavelengths.

TABLE XXII

$K_2 Cu (C_2O_4)_2$  with 3 c.c.s. of M/200  
uranium nitrate solution.

6700 Å	·89	·89
6300 Å	·59	·59
6000 Å	·39	·39

No absorption in the rest wavelengths.

The above tables clearly show that there is no increase in the absorption as the concentration of the sensitisers is increased. This led us to believe that the increase in the velocity of the reaction in sunlight as the concentration (not high) of the sensitisers is increased is probably due to the absorption of ultra-violet rays.

We also tried artificial light on the reaction. Potassium-cupri-oxalate solution with ferric chloride as sensitiser was exposed to the light of 1000 watt gas filled tungsten filament lamp for six hours in quartz cell. There was practically no reaction after six hours insolation. By this result we were convinced of the fact that the reaction is due to the absorption of ultra-violet rays only. To be sure of the fact we photographed the absorption spectra of the potassium-cupri-oxalate solution without any sensitiser and with ferric chloride and uranium nitrate solutions as sensitisers. Quartz spectrograph and copper arc were used for the purpose. The spectrum showed complete absorption in the ultra-violet region in all the three cases.

### Quantum Efficiency

The Quantum efficiency of the photochemical decomposition of potassium-cupri-oxalate was determined by means of thermopile and a sensitive galvanometer at three temperatures. The thermopile was standardised by means of Haffner's lamp. The source of light was Sun. A heliostat was used to throw the sunlight on the thermopile. The deflections of the galvanometer were noted on a scale. The solutions were insolated in a quartz cell. Decompositions of the potassium-cupri-oxalate solution at the three temperatures were also determined by exposing the solutions for an hour in the sunlight and weighing the products as cupric oxide. The sensitisers were also used. The following results were obtained.

TABLE XXIII

$K_2 Cu (C_2O_4)_2$  with no sensitiser.

Temp.	Time of Exposure	Amounts of the decomposed products in gms	Reading with distilled water	Reading with the solution	Absorption in Solution	Moles. decomposed per quanta
27°	1 hour	0·0064	33	14	19	·49
37°	"	0·0100	"	13	20	·73
47°	"	0·0092	"	12·5	20·5	·66

TABLE XXIV

$K_2 Cu (C_2O_4)_2$  with 1c.c. of 0·0237 N-FeCl<sub>3</sub> solution

27°	1 hour	0·0086	33	9·7	23·3	·54
37°	"	0·0144	"	9	24	·88
47°	"	0·0136	"	8·5	24·5	·81

TABLE XXV

$K_2 Cu (C_2 O_4)_2$  with 1c.c. of M/200 uranium nitrate solution.

27°	1 hour	0·0074	33	12·5	20·5	·53
37°	"	0·0110	"	12	21	·77
47°	"	0·0106	"	11·5	21·5	·72

It is clear from the above tables that the quantum efficiency is less than one. The quantum efficiency is increased by adding sensitisers. It increases at 37°C but decreases at 47°C in all the three cases.

### DISCUSSIONS

Einstein's Law of photochemical equivalence does not hold in this case. The quantum efficiency is less than one. This shows that one quanta of light has not got enough energy to decompose one molecule of potassium-cupri-oxalate.

The tables IX and X show the temperature coefficients of the reaction. At lower temperatures the temperature coefficient is higher than at higher temperatures. This supports the view that at lower temperatures there are more molecules which can be activated than at higher temperatures and hence the temperature coefficient at lower temperatures is greater.

## SUMMARY

1. The velocity of the photolysis of potassium-cupri-oxalate solution is independent of the concentration of the photolyte, therefore the reaction is zero-molecular.

2. In presence of oxygen and carbondioxide gases, the photolysis of potassium-cupri-oxalate solution is retarded.

3. A large excess of potassium oxlate solution accelerates the photolysis of potassium-cupri-oxalate solution, while it retards the photo-decomposition of potassium ferrioxalate and potassium cobaltioxalate and has no effect on potassium manganioxalate.

4. The temperature coefficient of the reaction at  $K\ 37^{\circ}/K\ 27^{\circ}$  is 1.23 and 1.10 at  $K\ 47^{\circ}/K\ 37^{\circ}$ . This shows that temperature coefficient is greater at lower temperatures than at higher.

5. With very dilute solutions of ferric chloride and uranium nitrate, used as sensitisers, the photolysis of potassium-cupri-oxalate solution is accelerated and as the concentration is increased after a certain limit it begins to inhibit the reaction and at very high concentration there is practically no reaction.

6. The solution of potassium-cupri-oxalate absorbs only ultra-violet rays and the photolysis is due to the ultra-violet region.

7. The quantum efficiency of the reaction is less than one and therefore Einstein's law of photochemical equivalence fails in this case.

# STUDIES IN LIESEGANG RING FORMATION

BY

MISS S. ROY.

*Allahabad University.*

The object of this communication is to study the formation of periodic precipitation in inorganic and other jellies and the effect of light on the same.

So far silicic acid is the only inorganic jelly which has been utilised for obtaining periodic precipitates. I have used jellies of vanadium pentoxide, ceric hydroxide, zinc and manganese arsenates and silicic acid as media for Liesegang rings.

The experiments and the conclusions therefrom are recorded below:—

## 1. Experiments with Vanadium Pentoxide Gel as Medium.

A sol of vanadium pentoxide containing 16.345 gms. of vanadium pentoxide per litre was prepared by the interaction of ammonium vanadate and hydrochloric acid. The sol obtained was purified by dialysis.

5 c.c.s. of the sol were taken in jena glass test tubes to which 1 c.c. of normal potassium iodide was added and a jelly was obtained. To each of these tubes 5 c.c.s. each of mercuric chloride and lead nitrate of varying concentrations were allowed to diffuse from the top. Only in the case of mercuric iodide, formation of precipitates consisting of bands of shiny brown crystals followed by red bands of mercuric iodide was observed.

With jellies of vanadium pentoxide as medium I have not been able to obtain periodic precipitates of chromates of silver, lead, barium and thallium, and, iodides of lead and copper (cuprous).

## 2. Experiments with Ceric Hydroxide Gel as Medium.

25.014 gms. of ceric-ammonium nitrate were dissolved in 250 c.cs. of water and allowed to dialyse for seven days.

5 c.cs. of the sol thus prepared were taken in several jena glass test tubes and were set to a gel by adding 1 c.c. of N/2 potassium chromate or N potassium iodide. From the top 5 c.cs. each of silver nitrate, barium chloride, lead nitrate, thallium acetate, mercuric chloride and cupric chloride were allowed to diffuse.

In the case of *mercuric iodide* spirals of red mercuric iodide followed by clear space were obtained. *Silver chromate* showed bands of green mass followed by a brown layer in the tubes kept in the dark and brown mass with spots of green silver chromate in the tubes exposed to light.

No other periodic structure was observed with ceric hydroxide as gel, the latter being completely precipitated by the addition of electrolytes.

## 3. Experiments with Zinc Arsenate Gel as Medium.

1 c.c. of N potassium iodide was added to 10 c.cs. of N/2 potassium hydrogen arsenate ( $K_2HAsO_4$ ) and 5 c.cs. of N/2 zinc sulphate ( $ZnSO_4 \cdot 6H_2O$ ) giving rise to a gel of zinc arsenate, 5 c.cs. of cupric chloride, mercuric chloride, lead nitrate and thallous acetate were allowed to diffuse from the top of jena glass test tubes in which the gel was set. *Thallous iodide* has a tendency for developing band of yellow dotted crystals which in course of time become pink in the tube kept in the dark.

*Mercuric iodide*.—Broad bands of red flakes of mercuric iodide followed by narrow clear spaces were observed.

## 4. Experiments with Manganese Arsenate Gel as Medium.

A gel of manganese arsenate ( $MnHAsO_4$ ) was prepared by adding 1 c.c. of N potassium iodide to 10 c.cs. of N/2 potassium hydrogen arsenate ( $K_2HAsO_4$ ) and 5 c.cs. of



N/2 manganese sulphate ( $\text{MnSO}_4, 5\text{H}_2\text{O}$ ), solutions of mercuric chloride, thallium acetate, lead nitrate and cupric chloride were allowed to diffuse from the top.

*Mercuric iodide* shows bands of red and white needle-shaped shiny crystals which later on form bands of red flakes followed by clear space.

*Thallous iodide* shows tendency towards band formation. The bands are yellow and orange in colour and appear to develop better with dilute solutions of thallium acetate.

## 5. Experiments with Silicic Acid Gel as Medium.

The silicic acid sol was prepared by the action of silicon tetrachloride on cold water and the hydrochloric acid formed was removed by dialysis. The sol contained 15.42 grms. of silicon dioxide ( $\text{Si O}_2$ ) per litre.

10 c.c.s. of the sol was set to a gel by adding 1 c.c. of either N/2 potassium chromate or N potassium iodide; solutions of lead nitrate, barium chloride, thallium acetate, silver nitrate, mercuric chloride of varying concentrations were allowed to diffuse from the top.

In the case of *silver chromate* dark brown bands developed in light. In the dark on the top of the tube there were rings of silver chromate followed by clear spaces which were followed by a broad dark brown band of silver chromate.

*Mercuric iodide*.—In the dark there were red and yellow bands which on exposure to light formed themselves into red crystals of mercuric iodide followed by clear spaces.

*Silver iodide* forms bands of dark and lighter shades of whitish yellow colour developed only in light.

*Silver chloride* gave bluish white bands of dark and lighter shade. In light a dark brown band containing two black rings were developed.

*Thallous chromate* formed light green and orange bands.

*Barium chromate* showed yellowish white band in the beginning which developed into a broad light green band followed by an orange one.

*Lead chromate* showed broad orange band in the bottom followed by yellow and orange rings on top.

#### 6. Starch Gel as Medium.

Chatterji and Dhar (Koll. Zeit., 1926, 40, 97) were the first to obtain Liesegang rings with starch gel as medium. I have attempted to obtain rings of lead iodide, cuprous iodide, mercuric iodide, thallous iodide and silver iodide in starch gel.

20 gms. of starch and 5 gms. of potassium iodide were dissolved in 400 ccs. of water and then 10 ccs. of the mixture were allowed to set in several tubes. Solutions of lead nitrate, cupric chloride, mercuric chloride, thallium acetate and silver nitrate of different concentrations were allowed to diffuse from the top.

*Silver iodide* developed bands both in the dark and light with 10 per cent silver nitrate solution. The bands were of brown and blue shade on top followed by a dark brown band which in its turn was followed by light blue and yellowish white band. The bands in light were more pronounced than those in the dark.

*Thallous iodide* gave an uniform band of yellow colour. No rings were obtained with cuprous iodide.

*Lead iodide* formed rings of scattered yellow crystals both in the dark and in light. The lead iodide in the exposed condition turned black.

*Mercuric iodide*.—Bands of red and yellow colour were developed in the dark only.

#### 7. Experiments with Agar as Medium.

2 gms. of Agar and 5 gms. of potassium iodide were dissolved in 200 ccs. and 400 ccs. of water respectively. 5 ccs. of 2N, N, N/2 cupric chloride and lead nitrate and N, N/2 of thallium acetate were allowed to diffuse in jena glass

test tubes containing 5 c.cs. of agar and potassium iodide set to a gel.

*Cuprous iodide* rings developed in the dark with the more concentrated agar and N cupric chloride. With other concentrations of cupric chloride and agar rings of white and black colour are developed only in the dark.

*Thallous iodide* developed bands of red and green shades in the light. There is very little difference between the exposed and unexposed conditions, excepting the formation of a broad red band relieved by a spot of yellow colour in the dark. The green turns yellow after a time. Red and yellow bands developed in the concentrated agar in tubes kept both in the dark and in light.

*Lead iodide* rings developed both in the dark and in the light—better in light and dilute solution of agar.

*Mercuric iodide* in dilute agar developed red and yellow bands both in the dark and light. The bands formed in the light undergo a change giving rise to red bands and clear spaces with concentrated solutions of mercuric chloride.

From the foregoing results it will be seen that light facilitates the formation of periodic precipitates separated by clear spaces in several cases; thus with mercuric iodide at first we get alternate layers of red and yellow bands. In presence of light, these red and yellow bands are replaced by red layers of mercuric iodide separated by clear space. Dhar and Chatterji [J. Phys. Chem., 1924, 41 (1924)] have shown that in agar the yellow layer of mercuric iodide consists of the same substance in the colloidal state and the red layer forms crystals of  $\text{HgI}_2$ . On exposure to light the yellow sol of mercuric iodide gets coagulated to red crystals. It is well known that light coagulates many sols.

Similarly with thallous iodide in agar, the green bands probably consist of thallous iodide in the colloidal state which on exposure to light become yellow, finally turning red. Light accelerates the coagulation of the colloidal thallous iodide, so

that there is a change from green to yellow and finally to red crystals which are the precipitated form of thallous iodide.

With silver iodide too it was found that in starch the effect of light was to make the bands of silver iodide more pronounced. In silicic acid gel bands of silver iodide were developed only in the light.

In silicic acid medium silver chloride showed a marked difference in band formation. Bands were darker and lighter shades of bluish white, in the unexposed tubes, but when exposed the dark blue white turned to distinct black rings of silver chloride. This can be explained from the fact that all the silver salts are very light sensitive so that the suspended silver chloride not only coagulates, but also turns black.

Silver chromate in silicic acid showed dark brown rings of silver chromate followed by a clear space and bands of silver chromate in the dark. Whilst in the light there were broad bands of dark brown silver chromate, the colour was more deep.

There were some instances where the ring formation was more pronounced in the dark than in light.

For example in starch medium, mercuric iodide rings were developed only in the dark as contrary to the ring formation of the same being more pronounced in the light in other media.

Cuprous iodide in agar developed rings only in the dark—there was not even the slightest tendency towards ring formation in light. Thallous iodide in zinc arsenate gel showed yellow bands in the light and in the dark, but the yellow bands in the dark were turning pink which finally turned to red crystals of thallous iodide.

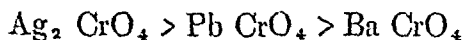
According to the theory of Dhar and Chatterji (J. Phys. Chem., 1924, 28, 41) peptisation plays an important part in Liesegang ring formation, hence it was thought advisable to study the peptising influence of agar, gelatin, starch and silicic acid on different sparingly soluble substances. The following conclusions have been arrived at:

*Peptising Influence of Agar.*—Agar peptises iodides of lead and mercury and it was found that mercuric iodide is more readily peptised in this media.

*Peptisation by Starch.*—Starch peptises chromates of silver and lead readily but barium chromate is very slightly peptised. Iodides are easily peptised by starch. Mercuric iodide is more easily peptised.

Peptising power of starch is of the following order:—lead chloride > lead chromate > silver chromate > silver iodide > silver chloride > mercuric iodide > lead iodide > barium chromate. Thallium bromide is also peptised by starch.

*Peptising Power of Gelatin.*—Gelatin peptises iodides of lead and mercury but not of thallium. Barium sulphate is very slightly peptised. The peptising influence of gelatin on the chromates in general is quite prominent and the degree of peptisation varies in the following manner:—



*Peptising Influence of Silicic Acid.*—Silicic acid peptises the iodides of lead and mercury—peptisation more marked in the case of mercuric iodide.

The peptising influence of silicic acid is more developed in the case of chromates. The peptising power of silicic acid is almost the same towards lead chromate and silver chromate and best towards barium chromate.

## SUMMARY

1. Liesegang rings of mercuric iodide have been obtained for the first time in vanadium pentoxide, cerium hydroxide, zinc and manganese arsenates as gel.

2. Periodic precipitates of the following substances were obtained for the first time :

Thallous iodide	...	in starch, agar, zinc and manganese arsenate gels.
Cuprous iodide	...	in agar.
Silver iodide	...	in starch.
Silver chromate	...	in cerium hydroxide.
Barium and thallous chromate, and silver iodide	...	in silicic acid medium.

3. Influence of light on periodic precipitates of the following substances have also been investigated :

Lead iodide	...	in agar, starch,
Mercuric iodide	...	in agar, starch, zinc and manganese arsenates, silicic acid, cerium hydroxide and vanadium pentoxide gels.
Thallous iodide	...	in starch, agar, zinc and manganese arsenate.
Chromates of barium, thallium, lead	...	in silicic acid.
Silver iodide	...	in starch and silicic acid gels.
Silver chromate	...	in silicic acid and cerium hydroxide.

4. Generally in presence of light the Liesegang rings are more prominent than in the dark. In the dark mercuric iodide forms alternate layers of yellow colloidal mercuric iodide followed by red crystals of mercuric iodide. When exposed to light this is changed to red crystals of mercuric iodide followed by clear spaces. This is due to the fact that light accelerates the coagulation of a sol.

5. The peptising influences of agar, starch, gelatin and silicic acid have also been studied and it has been found that these substances exert different peptising influence on different sparingly soluble substances.

# ANALYSIS OF INSOLUBLE SUBSTANCES

BY

DR. I. K. TAIMNI,

*Chemical Laboratory, University of Allahabad.*

One of the most difficult problems that a student has to face in qualitative analysis is the identification of compounds left in the insoluble residue after a mixture has been treated with water and various acids. Yet no problem is treated less satisfactorily than the identification of compounds that may form part of the "insoluble" portion of a mixture given for analysis. What one finds in most books on qualitative analysis is a list of compounds which are termed "insoluble substances" and a certain number of general tests which should be applied one after the other to detect the presence of these substances in the insoluble residue.

When one considers how thoroughly the various methods of identifying the acids and the bases in solution have been systematized, it is really surprising how little attention has been paid to the elaboration of a definite clear-cut scheme by following which a student may be able to detect the presence of these so-called insoluble substances in the easiest and quickest manner. It is generally assumed that the student has the necessary knowledge of the chemical properties of these compounds to enable him to adopt the most suitable methods for their identification. Since, however, the identification of these "insoluble" substances is one of the most difficult and important problems that a student has to tackle in qualitative analysis, there does not appear any valid reason why he should be left mainly to his own resources in solving this difficult problem, when in solving much easier problems it is considered necessary to provide him with systematic and detailed methods of procedure. If, in carrying out the separation of various groups and identification of substances in solution it is thought essential to provide him with definite

clear-cut schemes, surely the necessity of such a scheme is all the greater in the treatment and identification of the "insoluble" substances.

When we turn to the literature on the subject we not only find no definite schemes for the identification of "insoluble" substances but we also find an utter want of agreement among the various authors with regard to the inclusion of different compounds in the list of "insoluble" substances. The degree of confusion that prevails in the existing literature with regard to this matter may be judged by a comparison of the following four lists of "insoluble" substances given by different authors on this subject :

#### CAVEN

CaF<sub>2</sub>, SrSO<sub>4</sub>, BaSO<sub>4</sub>, PbSO<sub>4</sub>  
 Fe<sub>4</sub> {Fe (CN)<sub>6</sub>}<sub>3</sub>, Cu<sub>2</sub>Fe (CN)<sub>6</sub>, Zn<sub>2</sub>Fe (CN)<sub>6</sub>  
 AgCl, AgBr, AgI  
 SnO<sub>2</sub>, SnS<sub>2</sub> (mosaic gold), Sb<sub>2</sub>O<sub>4</sub>, Sb<sub>2</sub>O<sub>5</sub>  
 PbCrO<sub>4</sub> (ignited), FeCr<sub>2</sub>O<sub>4</sub> (chrome iron stone)  
 Fe<sub>2</sub>O<sub>3</sub> (ignited), Al<sub>2</sub>O<sub>3</sub> (ignited), Cr<sub>2</sub>O<sub>3</sub> (ignited)  
 SiO<sub>2</sub>, various silicates.

#### STEIGLITZ

CaF<sub>2</sub>, other fluorides  
 SrSO<sub>4</sub>, BaSO<sub>4</sub>, CaSO<sub>4</sub>, PbSO<sub>4</sub>  
 A number of ferrocyanides and ferricyanides  
 AgCl, AgBr, AgI, AgCN  
 FeCr<sub>2</sub>O<sub>4</sub> (chrome iron ore), CrCl<sub>3</sub> (anhydrous),  
     Cr<sub>2</sub> (SO<sub>4</sub>)<sub>3</sub> (anhydrous)  
 Al<sub>2</sub>O<sub>3</sub> (ignited), Cr<sub>2</sub>O<sub>3</sub> (ignited), SnO<sub>2</sub>  
 SiO<sub>2</sub>, silicates, aluminates

#### MOLLWO PERKIN

CaF<sub>2</sub>, SrSO<sub>4</sub>, BaSO<sub>4</sub>, PbSO<sub>4</sub>  
 AgCl, AgBr, AgI  
 Al<sub>2</sub>O<sub>3</sub> (ignited), Cr<sub>2</sub>O<sub>3</sub> (ignited), SnO<sub>2</sub>, PbCrO<sub>4</sub> (fused)  
 SiO<sub>2</sub>, silicates



## TREADWELL

$\text{CaF}_2$ ,  $\text{SrSO}_4$ ,  $\text{BaSO}_4$ ,  $\text{PbSO}_4$

$\text{AgCl}$ ,  $\text{AgBr}$ ,  $\text{AgI}$ ,  $\text{AgCN}$

$\text{Al}_2\text{O}_3$  (ignited),  $\text{Cr}_2\text{O}_3$  (ignited),  $\text{SnO}_2$ ,  $\text{PbCrO}_4$  (fused)

$\text{SiO}_2$ , silicates

An inspection of the four lists given above will show at once that there are many compounds which have been classed as insoluble substances by some authors and not by others. This must be very confusing to the ordinary student who has not only no definite scheme to guide him in the analysis of the insoluble residue, but who does not even know clearly which substances to look for in such a residue. It is obvious that if the analysis of the insoluble residue is to be undertaken in a systematic manner, the chemical properties of such compounds as may occur in such a residue should be thoroughly studied especially with reference to their solution in various acidic or basic solvents. This will not only enable us to classify them with greater precision but will also pave the way for the elaboration of a satisfactory scheme for their analysis.

The author is carrying on a systematic and thorough investigation of the analytical properties of all such compounds as have been classed by different authors under the heading of "insoluble substances" with the following objects :

- (1) To determine how far their properties justify their being classed with the "insoluble substances."
- (2) To determine the best method of their identification by bringing them into solution or otherwise.
- (3) To evolve a systematic method for the identification of all compounds in an insoluble residue which will be convenient, quick, and reliable.

In the present paper an effort is made to devise a scheme for the identification of insoluble substances based on the already known properties of the compounds. Only the insoluble compounds derived from the common elements and

native substances like fluorspar and tinstone will be included in the scheme, as the scheme is devised for the common student and is not meant for the use of the professional analyst.

Before discussing the scheme for the identification of insoluble substances, it is necessary to have a clear idea as to what we mean by the term "insoluble substances," for much of the confusion prevailing on the subject is due to the fact that different authors attach different meanings to the phrase. In the present paper "insoluble substances" will stand for all those substances that do not dissolve at all, or dissolve in an inordinately long time on heating with water, HCl or HNO<sub>3</sub>, dilute or concentrated. Some of the authors also include aqua regia as one of the acid solvents but since it dissolves a comparatively small number of substances and its use is inconvenient, it is better to omit it as one of the general solvents. It may be used as one of the solvents in the treatment of the insoluble residue when the colour of the latter indicates the presence of compounds like HgS, etc.

The substances that are generally treated as insoluble in water, HCl, HNO<sub>3</sub>, are the following :

AgCl, AgBr, AgI, CrCl<sub>3</sub>, CaF<sub>2</sub> (Halides)  
 BaSO<sub>4</sub>, SrSO<sub>4</sub>, (CaSO<sub>4</sub>), (PbSO<sub>4</sub>), (Cr<sub>2</sub>SO<sub>4</sub>),  
 (Sulphates)  
 (Fe<sub>2</sub>O<sub>3</sub>), Cr<sub>2</sub>O<sub>3</sub>, Al<sub>2</sub>O<sub>3</sub>, SnO<sub>2</sub>, Sb<sub>2</sub>O<sub>4</sub>, Sb<sub>2</sub>O<sub>3</sub>,  
 SiO<sub>2</sub> (Ignited oxides)  
 SnS<sub>2</sub>, HgS (Sulphides)  
 AgCN, Fe<sub>4</sub>[Fe(CN)<sub>6</sub>]<sub>3</sub>, Cu<sub>2</sub>Fe(CN)<sub>6</sub>, Zn<sub>2</sub>Fe(CN)<sub>6</sub>  
 (Cyanides and ferrocyanides)  
 (PbCrO<sub>4</sub>), FeCr<sub>2</sub>O<sub>4</sub> (Chromites and chromates)  
 Some silicates and aluminates.

Before dealing with the general scheme of analysis it will be advisable to discuss briefly those properties of the insoluble compounds upon which the scheme for their identification is based. In the list given above, all the compounds

which have been classed with the "insoluble substances" by different authors are included, but as far as the author is aware there seems no justification for including  $\text{CaSO}_4$ ,  $\text{PbSO}_4$ , ignited  $\text{Fe}_2\text{O}_3$ , and fused  $\text{PbCrO}_4$  in this list.  $\text{CaSO}_4$  dissolves in concentrated  $\text{HCl}$  without much difficulty.  $\text{PbSO}_4$  also dissolves on boiling with concentrated  $\text{HCl}$ , and though  $\text{PbCl}_2$  crystallizes out on cooling this can be removed by washing with hot water. If  $\text{PbSO}_4$  is to be included in the list of insoluble substances, there is no reason why  $\text{PbCl}_2$  should also not be included. Ignited ferric oxide dissolves gradually on boiling with concentrated  $\text{HCl}$  and it is quite unjustifiable to include it in the list. Fused lead chromate, in spite of the fact that so many authors have classed it with the insoluble substances, dissolves so easily in boiling concentrated  $\text{HCl}$  (with formation of  $\text{CrCl}_3$ ) that it should not be considered as an insoluble substance. All the four substances mentioned above which do not really belong to the class of "insoluble substances" have been put within brackets and need not be considered in the scheme of analysis.

The properties of the insoluble compounds which are utilized in the scheme for their identification are given in the following paragraphs :

*AgCl, AgBr, AgI, AgCN.*—All these compounds of silver are insoluble in  $\text{HCl}$  or  $\text{HNO}_3$  except  $\text{AgCN}$  which is converted into  $\text{AgCl}$  by heating with concentrated  $\text{HCl}$ . Aqua regia converts  $\text{AgBr}$ ,  $\text{AgI}$ , and  $\text{AgCN}$  into  $\text{AgCl}$  which can then be dissolved out by  $\text{NH}_4\text{OH}$  solution.

*BaSO<sub>4</sub>, SrSO<sub>4</sub>* are changed completely into the corresponding carbonates by fusion with  $\text{Na}_2\text{CO}_3 + \text{K}_2\text{CO}_3$  (fusion mixture).

*SnS<sub>2</sub> (sublimed), HgS* are changed to chlorides by heating with aqua regia.

*Ferrocyanides of Cu, Fe, and Zn, etc.*—All these ferrocyanides are partly dissolved by aqua regia. Zinc ferrocyanide dissolves completely but on diluting the solution, a part is

again precipitated. Some other ferrocyanides and ferricyanides besides the three mentioned above (Ag, Ni, CO) may be found in the insoluble residue. All ferrocyanides and ferricyanides are decomposed by boiling with NaOH solution into the corresponding hydroxide and  $\text{Na}_4\text{FeCN}_6$ . If the hydroxide [e.g.,  $\text{Zn}(\text{OH})_2$ ] is insoluble in excess of alkali, the ferrocyanide dissolves completely, otherwise the hydroxide remains precipitated.

$\text{Cr}_2\text{O}_3$ ,  $\text{CrCl}_3$ ,  $\text{Cr}_2(\text{SO}_4)_3$ ,  $\text{FeCr}_2\text{O}_4$ .—All compounds containing chromium are decomposed on fusion with  $\text{Na}_2\text{CO}_3 + \text{KNO}_3$ , the chromium being converted into soluble sodium chromate. In the case of ferrous chromite (chrome iron stone), a residue of  $\text{Fe}_2\text{O}_3$  remains.

$\text{SiO}_2$ , *silicates*.—Silica forms soluble sodium silicate on fusion with  $\text{Na}_2\text{CO}_3$ . Most of the silicates are completely decomposed on fusion with  $\text{Na}_2\text{CO}_3$ , forming soluble sodium silicates and insoluble carbonate or oxide of the metal.

$\text{SnO}_2$ ,  $\text{Sb}_2\text{O}_3$ ,  $\text{Sb}_2\text{O}_5$ ,  $\text{CaF}_2$ ,  $\text{Al}_2\text{O}_3$ .—All these compounds are at least partly decomposed on fusion with sodium carbonate forming sodium stannate, sodium antimonate, sodium fluoride and sodium aluminate, so that the melt obtained by fusing the insoluble residue with  $\text{Na}_2\text{CO}_3$  must contain at least a part of tin, antimony, aluminium, and fluoride in the soluble form. If it is necessary only to detect the presence of these elements, then the insoluble portion obtained after fusion with  $\text{Na}_2\text{CO}_3 + \text{KNO}_3$  and extraction with dilute HCl can be safely neglected. If, on the other hand, it is necessary to get an approximate idea of the quantity of each of these substances ( $\text{SnO}_2$ ,  $\text{CaF}_2$ , etc.), then each of these substances must be brought into solution by appropriate means. The oxides of tin and antimony can be best brought into solution by fusion with  $\text{Na}_2\text{CO}_3 + \text{S}$ , when soluble thiosalts are formed.  $\text{Al}_2\text{O}_3$  (ignited) is best brought into solution by fusion with  $\text{K}_2\text{S}_2\text{O}_7$ , when soluble aluminium sulphate is formed.  $\text{CaF}_2$  is best brought into solution by

evaporating to dryness with concentrated sulphuric acid (Pt. dish) when  $\text{CaSO}_4$  is formed.

The systematic scheme for the identification of "insoluble substances" is based on their properties that have been given above. The residue left after the mixture given for analysis has been extracted with  $\text{HCl}$  or  $\text{HNO}_3$ , is treated successively with the following three reagents:

- (1) boiling  $\text{NaOH}$ ,
- (2) aqua regia,
- (3) fused  $\text{Na}_2\text{CO}_3$  (+  $\text{K}_2\text{CO}_3$  +  $\text{KNO}_3$ ).

On treating the insoluble residue with each of these reagents (a) some of the substances that may be present in the residue dissolve completely, (b) some are changed into different compounds which can be brought into solution by means of appropriate solvents, (c) some are partly decomposed, and (d) some are quite unaffected by the treatment.

The undecomposed portion of substances belonging to section (c) and substances belonging to section (d) which are not at all affected are then together treated with the next reagent in the order given above.

(1) *Treatment with boiling NaOH solution.*—On boiling the residue with  $\text{NaOH}$  solution  $\text{Zn}_2\text{Fe}(\text{CN})_6$  dissolves completely.  $\text{Al}_2\text{O}_3$  and  $\text{SiO}_2$  may dissolve completely or in part. Filter off the residue and test the filtrate for zinc, aluminium silicate and ferrocyanide. If ferrocyanide is found in the filtrate, the residue obtained after treatment with  $\text{NaOH}$  solution should be extracted with  $\text{HCl}$  to dissolve out the metallic hydroxide formed by the decomposition of the insoluble ferrocyanides ( $\text{Fe}$ ,  $\text{Cu}$ , etc.), and the  $\text{HCl}$  extract tested for  $\text{Fe}$ ,  $\text{Cu}$ , etc. Boiling with  $\text{NaOH}$  solution may be omitted in case ferrocyanides are known to be absent.

(2) *Treatment with Aqua regia.*—The insoluble residue obtained after boiling with  $\text{NaOH}$  solution is treated with aqua regia. This completely dissolves  $\text{HgS}$ ,  $\text{SnS}_2$  and changes  $\text{AgBr}$ ,  $\text{AgI}$ , and  $\text{AgCN}$  into  $\text{AgCl}$ . Small quantities of  $\text{CaF}_2$ ,

$\text{Sb}_2\text{O}_3$ , may also go into solution. After filtering off the residue that does not dissolve in aqua regia, the filtrate is tested for Hg and Sn. If Hg or Sn is found, a portion of the original insoluble residue is tested for sulphide by means of tin and hydrochloric acid. The filtrate may also be tested for antimony but it is not necessary to test it for Ca as very little  $\text{CaF}_2$  is dissolved by boiling with aqua regia. The insoluble portion that does not dissolve in aqua regia is shaken with  $\text{NH}_4\text{OH}$  solution and the ammoniacal extract treated with excess of  $\text{HNO}_3$ . If a precipitate of  $\text{AgCl}$  is obtained a portion of the original insoluble residue is treated with zinc and sulphuric acid to test for bromide, iodide, and cyanide. Since all the substances (except  $\text{AgCN}$ ) that are affected by treatment with aqua regia are coloured ( $\text{SnS}_2$ ,  $\text{HgS}$ ,  $\text{AgBr}$ ,  $\text{AgI}$ ) it is obviously unnecessary to treat the insoluble residue with aqua regia if it is white. In case this step is omitted, the residue should be shaken with  $\text{NH}_4\text{OH}$  solution to dissolve out  $\text{AgCN}$  and  $\text{AgCl}$  (white) and if a white precipitate is obtained on adding excess of  $\text{HNO}_3$  the original insoluble residue tested for Cl and CN as already indicated.

(3) *Fusion with  $\text{Na}_2\text{CO}_3$ ,  $\text{K}_2\text{CO}_3$ ,  $\text{KNO}_3$ .*—The residue left undissolved after treatment with  $\text{NaOH}$  solution and aqua regia is thoroughly mixed with about 10 times its weight of fusion mixture ( $\text{K}_2\text{CO}_3 + \text{Na}_2\text{CO}_3$ ) and a little  $\text{KNO}_3$  and fused in a porcelain crucible. This completely changes silica into soluble sodium silicate, all chromium compounds into soluble sodium chromate,  $\text{BaSO}_4$ , and  $\text{SrSO}_4$ , into the corresponding carbonates. Any insoluble silicates that may be present form the corresponding carbonates and soluble sodium silicate.  $\text{Al}_2\text{O}_3$ ,  $\text{CaF}_2$ ,  $\text{SnO}_2$ ,  $\text{Sb}_2\text{O}_3$  ( $\text{Sb}_2\text{O}_5$ ) are converted at least in part into sodium aluminate, sodium fluoride, sodium stannate, and sodium antimonate respectively.

The fused mass after boiling with water is filtered and the filtrate tested for silicate (from  $\text{SiO}_2$  or insoluble silicates), chromate (from chromium compounds), sulphate [from  $\text{Cr}_2(\text{SO}_4)_3$ ,  $\text{BaSO}_4$  etc.], chloride (from  $\text{CrCl}_3$ ), aluminium

(from  $\text{Al}_2\text{O}_3$ ), tin (from  $\text{SnO}_2$ ), antimony (from  $\text{Sb}_2\text{O}_3$ ,  $\text{Sb}_2\text{O}_5$ ), and fluoride (from  $\text{CaF}_2$ ).

The residue that does not dissolve in water is washed thoroughly with water to remove sulphate, etc., and then treated with dilute  $\text{HCl}$  to dissolve out  $\text{BaCO}_3$ ,  $\text{SrCO}_3$ ,  $\text{CaCO}_3$  and other carbonates derived from insoluble silicates. The dilute  $\text{HCl}$  also dissolves the ferric oxide derived from  $\text{FeCr}_2\text{O}_4$ . The extract obtained with dilute  $\text{HCl}$  is tested for Ba, Sr, Ca, Fe, and other metals (if insoluble silicates are likely to be present).

The insoluble portion obtained after extraction with dilute  $\text{HCl}$  may contain some undecomposed  $\text{SnO}_2$ ,  $\text{Sb}_2\text{O}_3$ ,  $\text{Sb}_2\text{O}_5$ ,  $\text{Al}_2\text{O}_3$ , and  $\text{CaF}_2$ . This may be neglected under ordinary circumstances, but should it be necessary to obtain an approximate idea of the relative quantities of the different constituents, it should be successively fused (1) with  $\text{Na}_2\text{CO}_3 + \text{S}$  to bring into solution  $\text{SnO}_2$ ,  $\text{Sb}_2\text{O}_3$ ,  $\text{Sb}_2\text{O}_5$ , (2) with  $\text{K}_2\text{S}_2\text{O}_7$  to bring into solution  $\text{Al}_2\text{O}_3$ .  $\text{CaF}_2$  is best brought into solution by evaporating it to dryness with concentrated sulphuric acid and boiling the residue with water.

The scheme for the analysis of insoluble substances may be summarized as shown below :

The "insoluble residue" may contain the following compounds—

$\text{AgCl}$ ,  $\text{AgBr}$ ,  $\text{AgI}$ ,  $\text{AgCN}$ ,  $\text{CrCl}_3$

$\text{BaSO}_4$ ,  $\text{SrSO}_4$ ,  $\text{Cr}_2(\text{SO}_4)_3$

$\text{Al}_2\text{O}_3$ ,  $\text{Cr}_2\text{O}_3$ ,  $\text{FeCr}_2\text{O}_4$

$\text{SnO}_2$ ,  $\text{Sb}_2\text{O}_3$ ,  $\text{Sb}_2\text{O}_5$ ,  $\text{SnS}_2$ ,

$\text{HgS}$

Ferrocyanides of Fe, Zn, Cu, etc.

$\text{CaF}_2$ ,  $\text{SiO}_2$ , insoluble silicates

*Boil with NaOH solution—*

(a)  $\text{Zn}_2\text{Fe}(\text{CN})_6$  dissolves completely.

(b)  $\text{Al}_2\text{O}_3$ ,  $\text{SiO}_2$  may dissolve partly.

(c)  $\text{Fe}_4\{\text{Fe}(\text{CN})_6\}_3$  and  $\text{Cu}_2\text{Fe}(\text{CN})_6$  decomposed forming corresponding hydroxides and soluble  $\text{Na}_4\text{Fe}(\text{CN})_6$ .

The residue obtained after boiling with NaOH solution and extracting with dilute HCl may contain the following substances:

AgCl, AgBr, AgI, AgCN,  
 CrCl<sub>3</sub>,  
 BaSO<sub>4</sub>, SrSO<sub>4</sub>, Cr<sub>2</sub>(SO<sub>4</sub>)<sub>3</sub>,  
 Al<sub>2</sub>O<sub>3</sub>, Cr<sub>2</sub>O<sub>3</sub>, FeCr<sub>2</sub>O<sub>4</sub>,  
 SnO<sub>2</sub>, Sb<sub>2</sub>O<sub>4</sub>, Sb<sub>2</sub>O<sub>3</sub>, SnS<sub>2</sub>,  
 HgS  
 CaF<sub>2</sub>, SiO<sub>2</sub>, insoluble silicates

*Treat with aqua regia—*

- (a) HgS, SnS<sub>2</sub> dissolve completely
- (b) CaF<sub>2</sub>, Sb<sub>2</sub>O<sub>4</sub> may dissolve partly.
- (c) AgBr, AgI, AgCN changed into AgCl.

The residue obtained after treatment with aqua regia and extraction with NH<sub>4</sub>OH may contain the following substances:

BaSO<sub>4</sub>, SrSO<sub>4</sub>, Cr<sub>2</sub>(SO<sub>4</sub>)<sub>3</sub>,  
 Al<sub>2</sub>O<sub>3</sub>, Cr<sub>2</sub>O<sub>3</sub>, SnO<sub>2</sub>, Sb<sub>2</sub>O<sub>4</sub>,  
 Sb<sub>2</sub>O<sub>3</sub>,  
 CrCl<sub>3</sub>, FeCr<sub>2</sub>O<sub>4</sub>, CaF<sub>2</sub>, SiO<sub>2</sub>  
 Insoluble silicates

*Fuse with Na<sub>2</sub>CO<sub>3</sub>, K<sub>2</sub>CO<sub>3</sub>,  
 KNO<sub>3</sub>—*

- (a) Cr<sub>2</sub>O<sub>3</sub>, CrCl<sub>3</sub>, Cr<sub>2</sub>(SO<sub>4</sub>)<sub>3</sub>,  
 SiO<sub>2</sub> are converted into soluble compounds.
- (b) CaF<sub>2</sub>, SnO<sub>2</sub>, Sb<sub>2</sub>O<sub>4</sub>,  
 Sb<sub>2</sub>O<sub>3</sub>, Al<sub>2</sub>O<sub>3</sub> changed partly into soluble compounds.
- (c) BaSO<sub>4</sub>, SrSO<sub>4</sub> changed into the corresponding carbonates. Insoluble silicates give the corresponding carbonates. FeCr<sub>2</sub>O<sub>4</sub> gives Fe<sub>2</sub>O<sub>3</sub>.

The residue obtained after fusion with Na<sub>2</sub>CO<sub>3</sub> + K<sub>2</sub>CO<sub>3</sub> may contain

<u>CaF<sub>2</sub></u>	<u>SnO<sub>2</sub>, Sb<sub>2</sub>O<sub>4</sub>, Sb<sub>2</sub>O<sub>3</sub></u>	<u>Al<sub>2</sub>O<sub>3</sub></u>
Evaporate with con- centrated sulphuric acid	Fuse with Na <sub>2</sub> CO <sub>3</sub> + S	Fuse with K <sub>2</sub> S <sub>2</sub> O <sub>7</sub>



# THE EFFECT OF THE FUSED BENZENE CHROMOPHORES ON THE PYRONINE DYESTUFFS


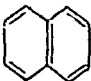

BY

JAMUNA DATTA TEWARI,

*Chemical Laboratory, University of Allahabad.*

As a general rule the multiplication of the benzene rings in a given compound increases its unstability, and consequently the internal strain of the molecule. This fact is clearly noticed when the properties of benzene and naphthalene, the two simple aromatic hydrocarbons, are considered. The difference between the structure of the two is only of one benzene nucleus, naphthalene being the compound formed by the fusion of the two benzene nuclei. It is seen that naphthalene and its derivatives take up hydrogen and the halogens more readily than benzene and its derivatives. Only strong oxidisers are capable of oxidising benzene, and oxidation completely disintegrates the benzene nucleus. Naphthalene on the other hand is oxidised by potassium permanganate to phthalic acid, a derivative of benzene. Benzene does not form any picrate, while naphthalene forms a well-defined picrate. These properties clearly indicate that the molecule of naphthalene is much more strained than that of benzene. The molecular strain goes on increasing to anthracene. In anthracene there are three condensed benzene nuclei with the para linkage between the two carbon atoms of the middle nucleus. After anthracene is much more strained than naphthalene, is quite apparent from its transference to more stable para-anthracene on exposure to sunlight. Moreover, by roughly calculating the molecular strain in these three compounds on the basis of the strain produced by various double bonds

which are present in these molecules (Dutt, J.C.S., 1926, 129, 171, and J.I.C.S., Vol. IV, No. 2, 99) it is found that as the number of the benzene rings increases, the strain also increases. On examining the absorption maxima of these compounds the same conclusion is confirmed:

Name	Structure	Molecular strain (in terms of angular distortion)	Abs. Max.
Benzene		$(109.5 \times 3)$	2500
Naphthalene		$(109.5 \times 5)$	2760
Anthracene		$(109.5 \times 6)$	2950

Considering all the above facts, it is but natural to expect that the dyestuffs containing fused benzene nuclei in the chromophore must be more coloured than those which contain only one benzene nucleus (Dutt, J., 1926, 129, 1171, and J.I.C.S., IV, 2, 99). While preparing dyestuffs from 1, 2, 3, Quinoline tricarboxylic acid, in order to study the effect of heterocyclic nitrogen atom on colour, it was thought that it would be much interesting to study the effect of fused benzene nuclei also on the dyestuffs. In order to study this point dyestuffs were obtained, from phthalic, naphthalic, quinolinic, 1, 2, 3, Quinolinic tricarboxylic acids, by condensing these with resorcinol, phloroglucinol, and m-diethylamidophenol, in a pure state and their absorption spectra taken. On making a study of the absorption spectra, quite contrary to the above-mentioned facts, it was found that dyes containing fused benzene nuclei as chromophores are invariably less coloured than those containing only one benzene nucleus in the chromophore. Thus it will be apparent from

the following table which gives the absorption maxima of these dyestuffs in approximate wavelengths, that dyes containing fused benzene nuclei as chromophores are less absorptive. These observations seem to go against the established fact that whenever there is a more strained system, there is a greater development of colour (Dutt, J.C.S., 1926, 129, 1171, and J.I.C.S., IV, 2, 99).

Compound obtained from	Phthalic acid	Naphthalic Acid
(1) Resorcinol	4940 (Absorption Maxima)	4430 (Absorption Maxima)
Phloroglucinol	4950     "     "	4480     "     "
m-diethylamidophenol	5540     "     "	5140     "     "
	Quinolinic acid	1, 2, 3. quinoline tricarboxylic acid
(2) Resorcinol	4950 (Absorption Maxima)	4900 Absorption Maxima
Phloroglucinol	4990     "     "	4930     "     "
m-diethylamidophenol	5540     "     "	5340     "     "

The only explanation that can be advanced to explain this apparent anomaly is that when dyes are prepared by condensing aromatic hydroxy and amino-compounds with chromophores containing fused benzene nuclei, the entrance of the auxichrome in such a strained chromophore so orientates the whole molecule internally that the more strained chromophore loses its strain and becomes more stable and consequently less strained even in comparison to single benzene ring chromophore, where there is no such possibility of internal orientation of the molecule. The result of this orientation becomes manifested when the dyestuffs so obtained are dissolved in alkali. The transference of the dye-molecule into the quinonoid structure, which more or less measures the intensity of the colour, is much restricted in case of fused benzene nuclei chromophores, while in the case of the single benzene nucleus it is not so. From the above table of the absorption spectra the effect of heterocyclic nitrogen atom is quite clear in the fused benzene ring also. It is clear that nitrogen-carbon double-bond structure is

much more absorptive than carbon-carbon double bond. For comparison, 1. 2. 3-quinoline tricarboxylic acid is taken in the above table, for studying the effect of the nitrogen atom and also the fused benzene nucleus. It contains one carboxyl group more than naphthalic and quinolinic acids, over and above the heterocyclic nitrogen atom. The question may arise that this extra carboxyl group may produce some effect in the dyestuff. It has been shown in a paper (Tewari and Dutt, J.I.C.S., Vol. 1, 59) that the carboxyl group in the chromophore does not in any way affect the intensity of colour.

My thanks are due to Dr. S. Dutt for the interest he has taken in the discussion.

# PHOTOCHEMICAL AND INDUCED OXIDATION OF GLYCEROL BY AIR

BY

DR. C. G. PALIT, D.Sc.,

*Chemistry Department.*

In previous papers we have shown that in presence of light or inductors like  $\text{Fe}(\text{OH})_2$ ,  $\text{Ce}(\text{OH})_3$ ,  $\text{Mn}(\text{OH})_2$ ,  $\text{Na}_2\text{SO}_3$ , etc., several carbohydrates, glycogen, lecithin, cholesterol, butter, egg white, egg yellow, nitrogenous substances, potassium palmitate, stearate, oleate, tartrate, formate, citrate, etc., can be oxidised by simply passing air at the ordinary temperature through aqueous solutions or suspensions of the above oxidizable substances.

Our experimental results on the estimation of carbon-dioxide prove that these slow oxidations lead to the formation of carbon dioxide and not to any intermediate product. The interest which centres round these slow oxidations is greatly increased by the fact of the generation of carbon dioxide and hence it appears that we have been successful in imitating the physiological processes of metabolism on which animal life depends.

In this paper, we are recording our results on the slow oxidation of glycerol by air in sunlight and in presence of inductors like  $\text{Fe}(\text{OH})_2$ ,  $\text{Ce}(\text{OH})_3$ , and sodium sulphite.

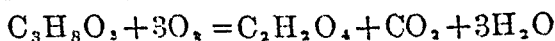
## PHOTOCHEMICAL OXIDATION

Glass bottles containing aqueous solution of glycerol were exposed to sunlight and a known volume of air was passed through them for a definite length of time. In each case 10 c.c. of the solution of glycerol (1 per cent concentration) were taken and the volume was made up to 100 c.c. The amount of unoxidised glycerol was then estimated after the

experiment by the well-known method of R. Benedikt and R. Zsigmondy which is noted below :

### METHOD OF ESTIMATION

The estimation depends upon the complete oxidation of the glycerol in cold, strongly alkaline solution to oxalic acid according to the equation



For the test 0.2-0.3 gm. of glycerol or the corresponding quantity of dilute glycerol is placed in a capacious flask and diluted to about 250 c.c. with water. To this 10 grms. of solid caustic potash are added and then finely powdered potassium permanganate is added little by little at the ordinary temperature until the solution is no longer green but blue or blackish. On heating to boiling, hydrated manganese dioxide separates out and the liquid becomes red. A solution of sulphurous acid or sodium sulphite is then added until the liquid is just decolourised. The solution is then filtered at once and the precipitate is carefully washed with hot water and the filtrate is acidified with acetic acid. The solution is heated to boiling and the oxalic acid is then precipitated by the addition of requisite amount of calcium chloride solution (10 per cent concentration). The precipitate of calcium oxalate is dissolved in hot dilute sulphuric acid and then titrated in the usual way by standard permanganate. The oxalic acid is then calculated to glycerol according to the above equation (Chem. Zeit., 1885, 9, 975 and J. Soc. Chem. Ind., 1885, 4, 610). The following are the results of some blank experiments :

Weighed out exactly 2.5 grms. of pure anhydrous glycerol and made up the solution to 250 c.c. For the experiment 25 c.c. of this solution were taken which therefore contain 0.25 gm. of glycerol. The estimations were done twice and in both cases the precipitate of calcium oxalate when treated with hot and dilute sulphuric acid required 54.1 c.c. of N/10  $\text{KMnO}_4$  from which after calculation the amount of

glycerol was found to be 0.2490 gm., a result which is within an experimental error of 0.4 per cent.

In each case the colorimetric determinations were made for the  $p_H$ -values before and after the experiment. It will be found from the results that the  $p_H$ -value after the experiment decreased in every case. The following are the experimental results :

TABLE I

Substance used in the experiment.			Time of exposure in hrs.	Vol. of air passed in litre.	Vol. of N/10 permanganate reqd. for the ppt. of Cal oxalate obtained from 10 c.c. of glycerol taken (Blank).	Vol. of N/10 permanganate for the ppt. of Cal. oxalate obtained from glycerol left after the experiment.	Amt. of glycerol oxidised in terms of N/10 permanganate.	Percentage of glycerol oxidised
1.	Glycerol	...	6	40	21.7 c.c.	20.4 c.c.	1.3	6.0
2.	"	...	15	100	"	18.8	3.9	18.0

TABLE II

*Estimation of Carbon dioxide*

Experiments on the oxidation of glycerol in sunlight and the estimation of carbon dioxide. The volume of air passed was 60 litres in 12 hours and the amount of glycerol taken was 10 c.c. (=0.125 gm.) in each case. The value for  $p_H$  before the experiment = 7.5 and that after the experiment = 7.3

Vol. of N/10 KMnO <sub>4</sub> reqd. for the ppt. of Cal. oxalate obtained from 10 c.c. of glycerol taken (Blank).	Amt. of CO <sub>2</sub> formed as found by direct weighing in potash bulbs in grms.	Amt. of glycerol oxidised as calculated from the value of CO <sub>2</sub> in grms.	Percentage amount of glycerol oxidised.	Vol. of N/10 KMnO <sub>4</sub> reqd. for the ppt. of Cal oxalate obtained for glycerol left after the exp. in c.c. as found by direct estimation.	Amt. of glycerol oxidised as found by direct estimation in terms of N/10 KMnO <sub>4</sub> in c.c.	Percentage of glycerol oxidised.
27.1 c.c. (0.125 gm.)	0.0148	0.01036	8.3	24.9	2.2	8.1
"	0.0156	0.0192	8.7	24.75	2.35	8.6

## EXPERIMENTS ON INDUCED OXIDATION

In these experiments, a slow current of air was passed through glass bottles containing solution of glycerol in presence of inductors such as freshly precipitated ferrous hydroxide or cerous hydroxide or sodium sulphite. The hydroxides of the metals were precipitated from the salt solutions by the addition of exact equivalent amount of caustic soda so as to render the whole mixture quite neutral. In each case 10 c.c. of glycerol were taken and the total volume was made up to 100 c.c. After the experiments the contents of the bottles were treated with potassium chloride so as to completely coagulate the precipitates of the hydroxides which were then filtered and washed thoroughly with hot water. The amount of glycerol left in the filtrate was then estimated in the usual way as already described. The following are the experimental results:

TABLE III

Experiment on the oxidation of glycerol in presence of (i) freshly precipitated and neutral ferrous hydroxide, (ii) freshly precipitated and neutral cerous hydroxide, and (iii) sodium sulphite as inductors. The volume of air passed was 112.5 litres in 17 hours and the amount of glycerol taken was 10 c.c. of 1 per cent concentration in each case.

Substance used as inductors.	Amt. of inductor used in grm.	Vol. of N/10 $\text{KMnO}_4$ reqd. for the ppt. of Cal. oxalate obtained from 10 c.c. of glycerol taken in c.c. (Blank).	Vol. of N/10 $\text{KMnO}_4$ reqd. for the ppt. of Cal. oxalate obtained from glycerol left after the expt. in c.c.	Amt. of glycerol oxidised in terms of N/10 $\text{KMnO}_4$ in c.c.	Percentage amount of glycerol oxidised.
Freshly precipitated ferrous hydroxide in neutral soln.	0.06476	21.7	17.6	4.1	18.9
Freshly precipitated cerous hydroxide in neutral soln.	0.1069	21.7	19.7	3.0	9.2
Sodium sulphite.	0.20	21.7	20.3	1.4	6.5



TABLE IV

*Estimation of Carbon dioxide*

Experiments on the oxidation of glycerol in presence of  
 (i) freshly precipitated and neutral ferrous hydroxide,  
 (ii) freshly precipitated and neutral cerous hydroxide and  
 (iii) sodium sulphite as inductors. The volume of air passed was 66.5 litres in 10 hours and the amount of glycerol taken was 10 c.c. (=0.125 gm.) in each case. The value for  $p_H$  before the experiment = 7.5.

Substance used as inductor.	Amount of inductor used in gm.	Vol. of N/10 KMnO <sub>4</sub> reqd. for the ppt. of Cal. oxalate obtained from 10 c.c. of glycerol taken before the expt. in c.c. (Blank).	Amt. of carbon dioxide formed as found by direct weighing in potash bulbs in grms.	Percentage amount of glycerol oxidised.	Vol. of N/10 KMnO <sub>4</sub> reqd. for the ppt. of Cal. oxalate obtained from glycerol left after the experiment in c.c. as found by direct estimation.	Percentage amount of glycerol oxidised.
Ferrous hydroxide in neutral solution.	0.06476	27.1 (0.125 gm.)	0.0212	11.8	23.95	11.6
Cerous hydroxide in neutral solution.	0.1069	"	0.0120	6.7	25.3	6.6
Sodium sulphite.	0.20	"	0.0072	4.03*	25.8	4.8

\* In the case of sodium sulphite, the amount of oxidation as obtained by experiment from the estimation of carbon dioxide, was a little lower than the value obtained by direct experiment and this low value may be due to the absorption of carbon dioxide, by the alkali set free by the hydrolysis of sodium sulphite. Exactly similar results have also been obtained in other cases in presence of sodium sulphite as inductor.

The following  $p_H$  values have been obtained in presence of inductors after the experiment:

- |     |                     |  |       |
|-----|---------------------|--|-------|
| (1) | The value for $p_H$ | before the experiment                                    | = 7.5 |
| (2) | do.                 | after the experiment in presence<br>of ferrous hydroxide | = 6.8 |
| (3) | do.                 | in presence of cerous hydroxide                          | = 7.0 |
| (4) | do.                 | in presence of sodium sulphite                           | = 7.3 |

The foregoing results show that aqueous solution of glycerol can be oxidised to carbon dioxide by passing air at the ordinary temperature in presence of sunlight or in presence of inductors like ferrous hydroxide, cerous hydroxide, and sodium sulphite, which undergo oxidation simultaneously. Moreover the amount of oxidation in sunlight increases with the time of exposure. The experimental results on the estimation of carbon dioxide show that in the slow photochemical or induced oxidation of glycerol, the oxidation is complete and carbon dioxide is the main end product.

## SUMMARY

1. Aqueous solution of glycerol has been oxidised by passing air at the ordinary temperature in presence of sunlight.

2. Experimental results on the estimation of carbon dioxide prove that glycerol is oxidised by air in presence of sunlight chiefly to carbon dioxide and not to any intermediate product.

3. Aqueous solution of glycerol has been oxidised by air at 25°C. in presence of inductors such as freshly precipitated ferrous or cerous hydroxide and sodium sulphite and the order in which it is oxidised is as follows :

Ferrous hydroxide > cerous hydroxide > sodium sulphite.

4. Experimental results on the estimation of carbon dioxide prove that glycerol is oxidised by air at 25°C. in presence of inductors chiefly to carbon dioxide and not to any intermediate product.

5. The colorimetric determinations of the  $p_H$ -value show that it decreases in every case in presence of sunlight as well as inductors.

6. These results on slow and induced oxidation of substances by air at the ordinary temperature are important, because these oxidations are of the same type as that taking place in the animal body.

---

# REVERSAL OF CHARGE OF SERUM AND ITS COAGULATION AND GELATINISATION WITH ACIDS

BY

SATYA PRAKASH, M.Sc.,

*Empress Victoria Research Scholar, Chemistry Department.*

In a previous communication (J. Indian Chem. Soc., 1928, 5, 313) from these laboratories, we have studied the coagulation of serum with various salts and acids, and have shown that polyvalent cations and acids possess high coagulating powers towards serum. The stability of a diluted serum towards its coagulation by univalent ions from salts like sodium acetate, potassium fluoride, oxalate, etc., is far greater than that of the concentrated serum. While the normal dilution effect has been observed when serum is coagulated by acids and polyvalent cations, we have observed that marked ionic antagonism is developed when it is coagulated by the cations of varying valencies or an acid and a salt. The phenomenon of positive acclimatisation is more marked for the diluted serum than the concentrated one when coagulated by salts, while with acids, the phenomenon is less developed with dilute serum. We have shown that like the sols of gamboge, mastic, arsenious sulphide, etc., serum is also capable of adsorbing similarly charged ions when coagulated with electrolytes.

In the present communication, we are recording further results on the coagulation of serum by acids, and have found that there are two distinct points of coagulation, one when

serum is coagulated by dilute acids and the other when coagulated by concentrated acids. We have also studied the influence of hydrogen ion concentrations on coagulation of serum and the gelatinisation of serum by acids.

Goat-blood was collected in a glass vessel in which it clotted within a few minutes and the clear straw-coloured serum was squeezed out due to syneresis and this serum was used for the coagulation experiments.

Two c.c. of original serum were mixed with different concentrations of dilute and concentrated acids and the total volume was made up to 10 c.c. in every case by adding the requisite amount of water, and the coagulation was observed after an hour.

TABLE I

Acids.	Concentration necessary for coagulation	
	by dilute acids	concentrated acids
Hydrochloric ...	0.0029 N	0.2275 N
Nitric ...	0.0034 N	0.0889 N
Sulphuric ...	0.0024 N	0.1161 N
Monochloracetic ...	0.0024 N	0.6854 N
Trichloracetic ...	0.0034 N	0.0348 N
Formic ...	0.0036 N	5.9454 N
Acetic ...	0.0038 N	2.8458 N
Hypophosphorous ...	0.0033 N	0.6304 N

The effect of dilution of serum on coagulation with concentrated acids has also been investigated.

A serum = 2 c.c. of serum.

A/2 serum = 1 c.c. of serum.

2A serum = 4 c.c. of serum.

Total volume = 10 c.c.      Time = 1 hour.

TABLE II

Acids.			Amount necessary for coagulation.		
			A/2	A	2A
1.75 N	Hydrochloric	...	1.6 c.c.	1.3 c.c.	1.0 c.c.
0.741 N	Nitric	...	1.5 "	1.2 "	0.8 "
1.452 N	Sulphuric	...	1.4 "	0.8 "	0.55 "
4.896 N	Monochloracetic	...	2.3 "	1.4 "	0.6 "
0.174 N	Trichloracetic	...	2.4 "	2.0 "	1.4 "
22.02 N	Formic	...	3.6 "	2.7 "	1.3 "
15.81 N	Acetic	...	3.2 "	1.8 "	1.0 "
7.88 N	Hypophosphorous	...	1.3 "	0.8 "	0.45 "

From the results recorded in the above tables, it will be seen that for the second point of coagulation, much higher concentrations of acids are necessary than for the first point; and when the serum is coagulated by concentrated acids, it behaves abnormally towards dilution, due to its high tendency of adsorbing similarly charged ions from the acids. It has been found (*loc. cit.*) that for the first point of coagulation by dilute acids, the serum behaves normally towards dilution, and smaller amounts of acids are necessary to coagulate the dilute serum than the concentrated one.

Serum is not coagulated even by molar solutions of ammonium sulphate and its globulin content is only precipitated out when it is half saturated by the salt. The results recorded in the following table show that in presence of small quantities of acids, serum is sensitised and is easily coagulated by ammonium sulphate. When the amount of hydrochloric acid added to the serum is small, the serum becomes unstable towards ammonium sulphate. This behaviour has been explained from the view-point that in presence of small amount of acid, the hydrolysis of serum is checked and thus

it is made unstable. Similar results have been obtained with the sols of Prussian blue, copper ferrocyanide, arsenious sulphide, gamboge, mastic and gum dammar. (Compare J. Phys. Chem., 1926, 30, 830; Kolloid Z., 1926, 29, 346.)

Amount of serum = 2 c.c.

Total volume = 10 c.c.

Time = 1 hour.

TABLE III

Amount of 1.75N hydrochloric acid added.	Amount of M/10 ammonium sulphate necessary to coagulate.
1.3 c.c.	0
0	more than 5 c.c. of 2M
0.2	0.8
0.3	1.7
0.4	2.6
0.5	1.6

From these results, it appears that as the concentration of hydrochloric acid is increased, the serum becomes more and more stabilised by the adsorption of hydrogen ions, and evidently there is a reversal of charge on the serum, which becomes positive on account of the adsorption of hydrogen ions. With higher concentrations of acids, both cations and anions influence the coagulation points and the positively-charged serum is coagulated by anions. The marked tendency of adsorbing similarly charged hydrogen ions by the positively-reversed serum is shown from the fact that dilute serum is more stable towards coagulation by concentrated acids than a concentrated one.

Serum contains, besides other substances, two proteins—serum albumin and serum globulin, and it has long been known that serum globulin is precipitated from the serum when it is half-saturated with ammonium sulphate, but serum albumin is only obtained when the filtrate after removing

globulins is saturated with ammonium sulphate and acidified with 10 per cent acetic acid (resulting solution containing 1 per cent acetic acid) and allowed to stand for two or more hours. The addition of acetic acid for the precipitation of albumin by ammonium sulphate is in accord to the view just described, and it appears that on the addition of sufficient quantity of acids, a reversal in the charge of serum takes place, which helps its coagulation by multivalent anions.

It appears that in these coagulating experiments on serum, the whole of the colloidal phase is never completely precipitated. When serum is coagulated by dilute acids, or by sodium acetate, tartrate, citrate, etc., it is mainly the globulin portion which is thrown down as is the case when it is half-saturated with ammonium sulphate. But serum albumin is also precipitated when coagulation is carried by either concentrated acids, or salts with polyvalent cations. Two distinct points of coagulation as with acids are also obtained when serum is coagulated by such electrolytes as aluminium nitrate, cerous nitrate, thorium nitrate, copper sulphate, etc.

The coagulation of serum by acids appears to be mainly controlled by hydrogen ion concentrations. In the following table, we are recording the variation in  $p_{\pi}$ -values with different amounts of acids.  $P_{\pi}$ -values were determined by indicator method, using nitrophenols as indicators. Original serum has a  $p_{\pi}$ -7.8. When water is mixed with serum, an opalescent solution is obtained and on the addition of dilute acids, turbidity at first increases corresponding to the first coagulation point, but after a certain concentration, the turbidity begins to disappear indicating the beginning of the reversal of charge of serum and on further increase of the concentration of the electrolytes, quite transparent serum is obtained when the charge reversal is complete.



Original serum =  $p_H$ -7.8:

2 c.c. of serum + 8 c.c. water =  $p_H$ -7.6

2 c.c. of serum were mixed with different concentrations of N/10 acids and the total volume was made up to 10 c.c. The hydrogen ion concentrations are recorded in the following table :

TABLE IV

Amount of N/10 acid in c.c.		HCl	Nitric acid	Sulphuric acid	Monochlor-acetic acid	Trichlor-acetic acid	Formic acid
		$p_H$	$p_H$	$p_H$	$p_H$	$p_H$	$p_H$
0.1 c.c.	...	7.3	7.3	7.3	7.5	7.5	7.3
0.3 "	...	6.8A	6.9A	7.0A	7.15A	6.9A	6.9A
0.5 "	...	6.0	6.2	6.3	6.6	6.2	6.4
0.6 "	...	...	...	6.1	...	...	...
0.7 "	...	5.6B	5.6B	5.7	6.1	5.7	6.0
0.9 "	...	...	...	5.6	...	...	...
1.0 "	...	5.4	5.5	5.4	5.4	5.3	5.4
1.1 "	...	5.3	...	...	...	4.9B	...
1.2 "	...	5.2C	5.3C	5.3B	5.3B	4.7	5.3B
1.4 "	...	...	4.9	4.9	5.2	4.4C	5.3
1.5 "	...	4.9	...	...	...	...	...
1.6 "	...	...	...	4.6	5.0C	4.4	5.3
1.8 "	...	...	...	4.3 C	4.7	...	5.3C
2.0 "	...	...	...	4.0	...	...	5.1

In the above table, the region from A to B is the region of the first coagulation point, while at B, the

opalescence begins to disappear, and the reversal of charge on serum takes place. At C the charge reversal is complete. From the above, it will be seen that the charge reversal takes place in almost the same region for different acids.

TABLE V

Acids.	Charge reversal region.
Hydrochloric ...	$p_n$ 5·5-5·3
Nitric ...	5·6-5·3
Sulphuric ...	5·3-4·3
Monochloracetic ...	5·3-5·0
Trichloracetic ...	4·9-4·4
Formic ...	5·3

From this it will be seen that the conditions most favourable for the charge reversal of serum are near the  $p_n$  5·3-5·0. As has already been stated that the dissolution of the turbid phase was taken as an indication of the reversal of charge, some allowance has to be made in the measurements where the anion effects are more marked as in the case of sulphuric acid, where due to the coagulating influence of  $SO_4^{2-}$  ions on the positively-charged serum, the turbidity did not disappear till it has reached the  $p_n$  4·3. Thus it appears that the coagulation of serum by dilute acids is mainly a function of hydrogen ions, and anions exert only a secondary influence.

The coagulating power of concentrated acids for the second point, as is seen from the Table I, is in the following order:

Trichloracetic > nitric > sulphuric > hydrochloric > hypophosphorous > monochloracetic > acetic > formic.

From this it appears that the degree of dissociation of the acids influences the coagulation of serum markedly so far as the second coagulation point is concerned.

The two coagulation points of serum also differ much in the development of hydration tendency of particles in the two cases. From the nature of the coagulated mass it appears that serum coagulated by dilute acids is more flocculent than gelatinous. After the reversal of charge, further coagulation is accompanied by the marked adsorption of the solvent medium, and the viscosity of the system also gradually increases, and finally under suitable concentrations, stable jellies of the serum are obtained. It appears that serum albumin which has a greater probability of being precipitated near the second coagulation point, is more capable of undergoing hydration than the serum globulin which is exclusively precipitated by dilute acids.

In the following tables, we are recording our observations regarding the gelatinisation of serum by different acids. Serum has been mixed and well-shaken with different amount of acids and the total volume was kept constant in every case, and their time of setting to jellies was noted.

TABLE VI  
*Gelatinisation by hydrochloric acid.*

Serum.	1.75 N HCl	Total volume.	Observation.
3 c.c.	1.0 c.c.	5 c.c.	No jelly in 2 days.
3 "	1.2 "	5 "	No jelly in 2 days.
3 "	1.4 "	5 "	Opaque jelly in 22 hours.
3 "	1.6 "	5 "	Opaque jelly within 22 hours.
3 "	1.8 "	5 "	Opaque jelly in 3 hours.
3 "	2.0 "	5 "	Flocculent precipitate setting to loose jelly within 22 hours.

TABLE VII

*Gelatinisation by nitric acid.*

Serum.	2·65N Nitric acid.	Total volume.	Observation.
3 c.c.	0·1 c.c.	5 c.c.	No jelly in 1 day.
3 "	0·2 "	5 "	No jelly in 1 day.
3 "	0·4 "	5 "	Opaque jelly in 3 hours.
3 "	0·6 "	5 "	Opaque loose jelly in 3 mins. soon breaking.
4 "	0·2 "	5 "	No jelly in 1 day.
4 "	0·3 "	5 "	Opaque jelly in 3½ hours.
4 "	0·4 "	5 "	Opaque jelly in 2½ hours.
4 "	0·5 "	5 "	Opaque jelly in 30 mins.
4·5 "	0·2 "	5 "	Translucent jelly in 1 day.
4·5 "	0·3 "	5 "	Opaque jelly in 3½ hours.
4·5 "	0·4 "	5 "	Opaque jelly in 25 mins.
4·5 "	0·5 "	5 "	Opaque jelly in 25 mins.

TABLE VIII

*Gelatinisation by sulphuric acid.*

Serum.	7·26N H <sub>2</sub> SO <sub>4</sub>	Total volume.	Observation.
3 c.c.	0·5 c.c.	5 c.c.	Opaque jelly in 1 day.
3 "	0·8 "	5 "	Opaque jelly in 1 day.
3 "	1·1 "	5 "	Opaque jelly in 7 hours.
3 "	1·4 "	5 "	Opaque jelly in 4 hours.
4 "	0·4 "	5 "	Opaque jelly in 1 day.
4 "	0·6 "	5 "	Opaque jelly in 1 day.
4 "	0·8 "	5 "	Opaque jelly in 6 hours.
4 "	1·0 "	5 "	Opaque jelly in 4 hours.
4·5 "	0·2 "	5 "	Opaque jelly in 1 day.
4·5 "	0·3 "	5 "	Opaque jelly in 1 day.
4·5 "	0·4 "	5 "	Opaque jelly in 1 day.
4·5 "	0·5 "	5 "	Opaque jelly in 1 day.

TABLE IX

*Gelatinisation by acetic acid.*

Serum.	15.81 N acetic acid (glacial).	Total volume.	Observation.
3 c.c.	0.5 c.c.	5 c.c.	No jelly in 1 day.
3 "	1.0 "	5 "	Translucent jelly in 40 mins.
3 "	1.5 "	5 "	Opaque jelly in 3 mins.
3 "	2.0 "	5 "	Opaque jelly in 2 mins.
4 "	0.1 "	5 "	No jelly in 1 day.
4 "	0.4 "	5 "	Translucent jelly in 3 days.
4 "	0.7 "	5 "	Translucent jelly in 45 mins.
4 "	1.0 "	5 "	Translucent jelly in 3 mins.
4.5 "	0.1 "	5 "	No jelly in 1 day.
4.5 "	0.3 "	5 "	No jelly in 1 day.
4.5 "	0.5 "	5 "	Translucent jelly in 1 day.

TABLE X

*Gelatinisation by monochloroacetic acid.*

Serum.	4.896N Cl. CH <sub>2</sub> COOH.	Total volume.	Observation.
3 c.c.	0.3 c.c.	5 c.c.	No jelly.
3 "	0.6 "	5 "	Translucent jelly in 1 day.
3 "	0.9 "	5 "	Translucent jelly in 1 hr.
3 "	1.2 "	5 "	Opaque jelly in 25 mins.
4 "	0.4 "	5 "	Translucent jelly in 1 day.
4 "	0.6 "	5 "	Translucent jelly in 2½ hrs.
4 "	0.8 "	5 "	Translucent jelly in 25 mins.
4 "	1.0 "	5 "	Loose translucent jelly in 1 day.
4.5 "	0.3 "	5 "	Translucent jelly in 1 day.
4.5 "	0.4 "	5 "	Translucent jelly in 1 day.
4.5 "	0.5 "	5 "	Translucent jelly in 3 hrs.

TABLE XI

*Gelatinisation by trichloroacetic acid.*

Serum.	0·879N Cl <sub>3</sub> C. COOH.	Total volume.	Observation.
3 c.c.	0·2 c.c.	5 c.c.	No jelly obtained.
3 "	0·4 "	5 "	Opaque jelly in 3 hrs.
3 "	0·5 "	5 "	Loose opaque jelly in 10 mins.
3 "	0·6 "	5 "	Loose opaque jelly in 5 mins.
4 "	0·3 "	5 "	No jelly.
4 "	0·4 "	5 "	No jelly.
4 "	0·5 "	5 "	Opaque jelly in 1 hr.
4 "	0·6 "	5 "	Opaque jelly in 5 mins.
4·5 "	0·4 "	5 "	No jelly.
4·5 "	0·5 "	5 "	No jelly.

TABLE XII

*Gelatinisation by formic acid*

Serum.	22·02N formic acid.	Total volume.	Observation.
3 c.c.	0·4 c.c.	5 c.c.	No jelly in 1 day.
3 "	0·6 "	5 "	No jelly in 1 day.
3 "	0·8 "	5 "	Translucent jelly in 1 day.
4 "	0·4 "	5 "	No jelly in 1 day.
4 "	0·6 "	5 "	Translucent jelly in 3½ hrs.
4 "	0·8 "	5 "	Translucent jelly in 20 mins.
4 "	1·0 "	5 "	Translucent jelly in 3 mins.
4·5 "	0·1 "	5 "	No jelly in 1 day.
4·5 "	0·3 "	5 "	No jelly in 1 day.
4·5 "	0·5 "	5 "	Translucent jelly in 2¼ hrs.

TABLE XIII

*Gelatinisation by oxalic acid.*

No jelly could be obtained by using even saturated solution of oxalic acid. However, jellies could be prepared by shaking serum with solid oxalic acid, and allowing it to set.

Serum.	Solid oxalic acid.	Total volume	Observation.
3 c.c.	0.9 gm.	5 c.c.	No jelly in even 3 days.
3 "	1.1 "	5 "	No jelly in even 3 days.
3 "	1.3 "	5 "	Translucent jelly in 3 days.
4 "	0.7 "	5 "	Loose translucent jelly in 1 day.
4 "	0.9 "	5 "	Loose translucent jelly in 1 day.
4 "	1.1 "	5 "	Firm translucent jelly in 1 day.
4 "	1.3 "	5 "	Firm translucent jelly in 1 day.
4.5 "	0.5 "	5 "	Opaque jelly in 1 day.
4.5 "	0.7 "	5 "	Opaque jelly in 1 day.
4.5 "	0.9 "	5 "	Opaque loose jelly in 1 day.

TABLE XIV

*Gelatinisation by hypophosphorous acid.*

Serum.	7.888 N hypophosphorous acid.	Total volume.	Observation.
3 c.c.	0.5 c.c.	5 c.c.	No jelly in 1 day.
3 "	0.8 "	5 "	No jelly in 1 day.
3 "	1.1 "	5 "	Translucent jelly in 1 day.
3 "	1.4 "	5 "	Opaque jelly in 1 day.
4 "	0.4 "	5 "	No jelly in 1 day.
4 "	0.6 "	5 "	No jelly in 1 day.
4 "	0.8 "	5 "	Translucent jelly in 1 day.
4 "	1.0 "	5 "	Translucent jelly in 4½ hours.
4.5 "	0.3 "	5 "	No jelly in 1 day.
4.5 "	0.4 "	5 "	No jelly in 1 day.
4.5 "	0.5 "	5 "	Translucent jelly in 1 day.

TABLE XV  
*Gelatinisation by aluminium nitrate.*

Serum.	M/1·27 aluminium nitrate.	Total volume.	Observation.
3 c.c.	0·5 c.c.	5 c. c.	No jelly.
3 "	1·0 "	5 "	Opaque jelly in 1 day.
3 "	1·5 "	5 "	Opaque jelly in 1 hour.
3 "	2·0 "	5 "	Opaque loose jelly immediately.
4 "	0·8 "	5 "	No jelly.
4 "	1·0 "	5 "	Opaque jelly in 1 day.
4·5 "	0·3 "	5 "	Opaque jelly in 1 day.

It will be seen from these tables that the jellies of the best texture are those which have been obtained by the use of weak acids. Glacial acetic, formic, monochloracetic, hypophosphorous, and oxalic acids yield almost transparent jellies, while opaque jellies are obtained when serum is gelatinised by strong acids such as hydrochloric, sulphuric, nitric or trichloracetic acids. Salts containing polyvalent cations, like aluminium nitrate also give opaque jellies. These jellies are very stable and do not undergo any marked syneresis, though putrefaction begins after a couple of days. An attempt to gelatinise serum by very weak acids like citric, tartaric and also by phosphoric acids has been so far unsuccessful. It appears that it is partly due to the weak nature of these acids and partly due to the fact that their solutions cannot be obtained in such concentrations as that of formic and acetic acids. The gelatinisation of serum appears to be a function of hydrogen ion concentration. The concentrations of the acids used for this purpose are in the following order :

Trichloracetic < nitric < sulphuric < hydrochloric <  
monochloracetic < hypophosphorous < acetic < formic.

This order is generally the same as was obtained when serum was coagulated by concentrated acids.



## SUMMARY

1. It has been observed that there are two distinct points of coagulation when serum is coagulated by acids or salts of polyvalent cations. The first point is obtained with the use of dilute acids, and the second by concentrated acids.

2. The coagulating power of concentrated acids for the second point is in the following order :

Trichloroacetic > nitric > sulphuric > hydrochloric > hypophosphorous > monochloroacetic > acetic > formic.

3. When serum is coagulated by concentrated acids, it behaves abnormally towards dilution, as it has a high tendency of adsorbing similarly charged ions from the acids.

4. It has been shown that in the presence of small quantities of acids, serum is sensitised, and is easily coagulated by ammonium sulphate. This is partly due to the fact that the hydrolysis of serum is checked by acids, and partly because the charge on serum is reversed by the adsorption of hydrogen ions.

5. It has been shown that charge reversal of serum takes place near  $p_{\pi}$  -5.3-5.0, when serum is coagulated by acids. It is the globulin portion of serum which is exclusively precipitated by dilute acids near the first coagulation point, while at the second coagulation point, serum albumin is also thrown down.

6. When serum is coagulated by dilute acids, the precipitated mass is flocculent, while with concentrated acids, a gelatinous mass is obtained. Under suitable concentrations of acids, jellies of serum can also be obtained.

7. Very stable translucent jellies of serum undergoing no marked syneresis are obtained when serum is coagulated by concentrated solutions of acetic, monochloroacetic, formic and hypophosphorous acids, and solid oxalic acid. Hydrochloric, nitric, sulphuric and trichloroacetic acids yield opaque stable jellies of serum.

8. The concentrations of acids necessary for the preparation of jellies are in the following order :

Trichloroacetic < nitric < sulphuric < hydrochloric < monochloroacetic < hypophosphorous < acetic < formic.

# INFLUENCE OF ELECTROLYTES ON THE SYNERESIS AND CLOTTING OF BLOOD

BY

SATYA PRAKASH, M.Sc.,

*Empress Victoria Research Scholar, Chemistry Department.*

In a previous communication,<sup>1</sup> we have advanced the view that clotting of blood and jelly formation are essentially similar processes. Blood may be regarded as an unstable colloidal system which remains fluid in the body partly due to its motion and partly to the capillary action of the blood vessels.

We<sup>2</sup> have investigated the influence of various electrolytes on the time of setting of jellies as well as on the extent of syneresis with numerous inorganic and some organic jellies. Moreover, we have shown that a sol is stabilised by the adsorption of similarly charged ions and is sensitised by the oppositely-charged ions, and under similar conditions, the uncharged particles are more hydrated than the charged ones. By the adsorption of similarly charged ions, the charge on the particles increases and the system becomes more stable, less viscous, and less hydrated.

Blood is regarded as a negatively-charged fibrin sol, which exists in the liquid condition, in some mysterious way. When it is collected in a glass vessel, it spontaneously forms a solid clot within a few minutes, but it is well-known that if it is received in solutions of sodium, or ammonium oxalate, fluoride or citrate, it can indefinitely remain liquid, and further, if calcium chloride is added in excess to the oxalated or citrated blood, the clotting occurs normally. As the normal blood also contains calcium, this behaviour was ascribed to the formation of insoluble or undissociated calcium salts of citrated and oxalated blood and thus to the

<sup>1</sup> J. Phys. Chem., 33, 459 (1929).

<sup>2</sup> J. Indian Chem., Soc., 7, 417 (1930).

removal of calcium ions. We have shown in the previous communication that blood has a great tendency of adsorbing similarly charged ions from such electrolytes as sodium acetate, tartrate and citrate, and also potassium fluoride and oxalate, and the stabilising influence of the salt is due to this fact and not to the removal of calcium ions.

In the present communication we have investigated the influence of the concentration of electrolytes on the extent of syneresis and have shown that blood is markedly stabilised by the addition of calcium chloride.

For these experiments on the syneresis of blood-clot, goat's blood was received in 250 c.c. glass bottles containing different amounts of electrolytes and made up to a definite volume. A blank experiment was always performed with the same blood, as the blood from different animals behaves slightly differently. After definite intervals, the synerised serum was carefully collected in a graduated measuring cylinder and the volume was measured. The experiments were carried at the room temperature ( $27^{\circ}$ – $29^{\circ}$ ). The results are recorded in the following tables :—

TABLE I  
*Influence of dilution on syneresis.*

Time			Amount of syneresis	
			250 c.c. blood.	230 c.c. blood + 20 c.c. water
30 min.	...	...	9 c.c.	28 c.c.
1 hr.	...	...	30	58
1 hr. 30 min.	...	...	47	77
2 hr. 30 min.	...	...	67	99
3 hr. 30 min.	...	...	83	112
4 hr. 30 min.	...	...	93	118
5 hr. 30 min.	...	...	98	122
17 hr.	...	...	127	141
22 hr.	...	...	129	141

The serum when no water was mixed was straw-coloured, but in the presence of water, blood was hemolysed and the serum was dark red.

TABLE II

*Influence of potassium chloride on syneresis*

5 c.c., 10 c.c., and 15 c.c. of 3N potassium chloride made up to 20 c.c. were taken into bottles in which 230 c.c. of blood were received. In the blank bottle, 20 c.c. of water and 230 c.c. of blood were taken.

Time	KCl	Amount of syneresis			
		0	5 c.c.	10 c.c.	15 c.c.
30 min.	...	10 c.c.	16 c.c.	2 c.c.	0.5 c.c.
1 hr.	...	38	30	5	1.0
1 hr 30 min.	...	50	48	5	3
2 hr. 30 min.	...	67	63	7	4
3 hr. 30 min.	...	83	74	7.5	4.5
4 hr. 30 min.	...	93	81	8	5
5 hr. 30 min.	...	98	83	8	7
21 hr.	...	128	127	8	8

Hemolysis was checked in the presence of potassium chloride and the serum was straw-coloured.

TABLE III

*Influence of calcium chloride on syneresis*

Concentration of calcium chloride = 1.76 M.

Blood = 230 c.c. Total volume = 250 c.c.

Time	CaCl <sub>2</sub>	Amount of syneresis				
		0	5 c.c.	6 c.c.	7 c.c.	8 c.c.
30 min.	...	2 c.c.	0.2 c.c.	0	not set	not set
1 hr.	...	21	0.2	0	just set	not set
1 hr. 30 min.	...	51	0.2	0.1	0	not set
2 hr. 30 min.	...	73	0.2	0.1	0	not set
3 hr. 30 min.	...	86	0.2	0.1	0	not set
4 hr. 30 min.	...	92	0.7	0.1	0	not set
5 hr. 30 min.	...	92	1.0	0.1	0	not set
13 hr. 30 min.	...	108	2.0	1.0	0.5	...
21 hr. 30 min.	...	110	7.0	...	...	just set
48 hr.	...	...	...	...	...	3 c.c.

TABLE IV

*Influence of ammonium sulphate on syneresis*

Concentration of ammonium sulphate = 2M.

Blood = 230 c.c. Total volume = 250 c.c.

Time	Am <sub>2</sub> SO <sub>4</sub>	Amount of syneresis			
		0	5 c.c.	8 c.c.	11 c.c.
30 min.	...	28 c.c.	29 c.c.	2 c.c.	not set
1 hr.	...	59	56	15	just set
1 hr. 30 min.	...	70	71	17	2
2 hr.	...	81	82	64	8
3 hr. 30 min.	...	102	103	84	27
4 hr. 30 min.	...	102	108	92	36
5 hr. 30 min.	...	108	113	94	41
13 hr.	...	119	128	117	52
17 hr.	...	122	128	118	55

(VIDE TABLE IV)

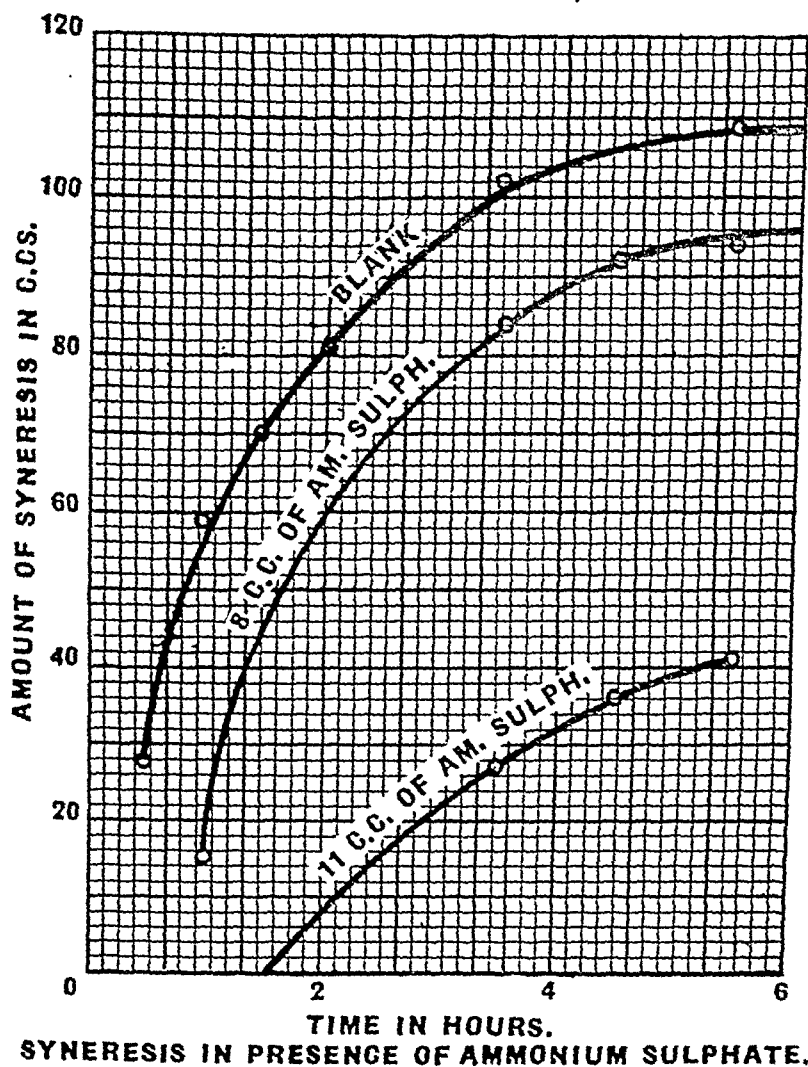


TABLE V

*Influence of potassium oxalate on syneresis*

Concentration of potassium oxalate = N

Blood = 230 c.c. Total volume = 250 c.c.

Time Potassium oxalate	Amount of syneresis			
	0	2 c.c.	3 c.c.	4 c.c.
30 min. ...	10 c.c.	10 c.c.	not set	not set
1 hr. ...	57	57	2 c.c.	half set
1 hr. 30 min. ...	85	68	4	half set
2 hr. ...	96	70	5	just set
3 hr. 30 min. ...	115	75	8	2 c.c.
4 hr. 30 min. ...	118	78	12	4
5 hr. 30 min. ...	121	78.5	13	5

TABLE VI

*Influence of sodium acetate on syneresis*

Concentration of sodium acetate = N

Blood = 230 c.c. Total volume = 250 c.c.

Time Sodium acetate	Amount of syneresis			
	0	2 c.c.	4 c.c.	6 c.c.
30 min. ...	20 c.c.	30 c.c.	32 c.c.	39 c.c.
1 hr. ...	31	56	66	62
1 hr. 30 min. ...	66	75	84	78
3 hr. 30 min. ...	100	105	115	112
4 hr. 30 min. ...	108	108	118	117
5 hr. 30 min. ...	115	111	122	121
20 hr. ...	130	111	135	135

TABLE VII

*Influence of sodium tartrate on syneresis*

Concentration of sodium tartrate = N

Blood = 230 c.c. Total volume = 250 c.c.

Time			Amount of syneresis			
Sodium tartrate			0	2 c.c.	4 c.c.	6 c.c.
30 min.	...	...	6 c.c.	34 c.c.	42 c.c.	32 c.c.
1 hr.	...	...	64	62	67	52
1 hr. 30 min.	...	...	77	77	80	66
2 hr.	...	...	82	84	86	74
2 hr. 30 min.	...	...	92	93	94	80
3 hr. 30 min.	...	...	106	102	107	91
4 hr. 30 min.	...	...	111	105	113	93
16 hr.	...	...	120	120	125	113

TABLE VIII

*Influence of sodium citrate on syneresis*

Concentration of sodium citrate = N

Blood = 230 c.c. Total volume = 250 c.c.

Time			Amount of syneresis			
Sodium citrate			0	2 c. c.	4 c. c.	6 c. c.
30 min.	...	...	26 c. c.	31 c.c.	half set	not set
1 hr.	...	...	61	62	half set	not set
1 hr. 30 min.	...	...	86	70	half set	not set
2 hr. 30 min.	...	...	109	94	half set	not set
3 hr. 30 min.	...	...	120	113	just set	not set
4 hr. 30 min.	...	...	121	116	0	not set
14 hr.	...	...	...	...	10 c.c.	loose dis-
					...	turbed clot



TABLE IX

*Influence of potassium fluoride on syneresis*  
 Concentration of potassium fluoride = 4.08 N  
 Blood = 230 c.c.      Total volume = 250 c.c.

Time		Amount of syneresis			
K <sub>2</sub> F <sub>2</sub>		0	1 c.c.	3 c.c.	5 c.c.
1 hr.	30 min. ...	21 c.c.	7 c.c.	not set	not set
	...	56	14	setting begins	not set
1 hr.	30 min. ...	80	22	loose clot	not set
2 hr.	30 min. ...	97	30	0	not set
3 hr.	30 min. ...	104	39	0	not set
4 hr.	30 min. ..	111	44	0	setting begins
14 hr.	...	122	50	7	0

TABLE X

*Influence of sodium hydroxide on syneresis*  
 Concentration of sodium hydroxide = 2.47 N  
 Blood = 230 c.c.      Total volume = 250 c.c.

Time		Amount of syneresis			
NaOH		0	2 c.c.	5 c.c.	8 c.c.
1 hr.	30 min. ...	19 c.c.	6 c.c.	not set	not set
	...	53	17	not set	not set
1 hr.	30 min. ...	71	25	not set	not set
2 hr.	...	84	30	not set	not set
3 hr.	...	98	42	not set	not set
4 hr.	...	104	47	not set	not set
4 hr.	30 min. ...	...	...	setting begins	not set
5 hr.	...	110	54	sets	not set
17 hr.	...	122	65	firm clot no syn. in 2 days.	not set

Our results on the syneresis of blood recorded in the above tables show that as the concentration of electrolytes is increased, the amount of syneresis gradually decreases and in some cases the syneresis of blood-clot is totally stopped. Even in two days, no marked syneresis is observed. In some cases, with the increase in the concentration of electrolytes, the blood becomes so stable that it either sets after a long time or does not set at all.

In a previous communication,<sup>1</sup> we have investigated the influence of the concentration of electrolytes on the syneresis of various inorganic jellies. We have shown that as the concentration of the coagulating electrolytes, *i.e.*, those electrolytes from which ions containing charge opposite to that of the sol are mostly adsorbed, is increased, the amount of syneresis is also increased. From our results we have also shown, that by increasing the concentration of coagulating electrolytes, the time of setting of jellies is much decreased.

The behaviour of blood is quite contrary to that of the jelly-forming inorganic sols. It possesses a high tendency to adsorb similarly charged ions, *i.e.*, anions; and does not appear to adsorb cations to a marked extent. For this reason, the addition of electrolytes invariably stabilises blood. The function of stabilising ions in the case of jellies is to increase the original time of setting and decrease the extent of syneresis. Thus on increasing the concentration of the stabilising electrolytes, the following may happen:

- (i) upto a certain limit—no marked influence on the extent of syneresis of the original clot;
- (ii) upto the second limit—gradual decrease in the amount of syneresis;
- (iii) within the next limited range—total inhibition of syneresis;

<sup>1</sup> Loc. cit.

(iv) above this limit—blood not clotting at all, but remaining fluid indefinitely.

Hence the function of stabilising electrolytes is just opposite to that of the coagulating electrolytes. From our observations, it will be seen that blood has a high tendency of adsorbing chloride, sulphate, oxalate, citrate, fluoride and hydroxyl ions, and in presence of these, the amount of syneresis is markedly decreased. Acetate and tartrate ions do not possess much stabilising influence. In the following table, the comparative influence of acetate, tartrate, citrate, and oxalate has been recorded.

TABLE XI

*Concentration of salts = N*

Blood = 230 c.c. Total volume = 250 c. c.

4 c.c. of N salts have been mixed with blood.

Time	Amount of syneresis			
	Sodium acetate	Sodium tartrate	Sodium citrate	Potassium oxalate
30 min. ...	32 c.c.	42 c.c.	half set	not set
1 hr. ...	66	67	half set	half set
1 hr. 30 min. ...	84	80	half set	half set
3 hr. 30 min. ...	115	107	just set	2 c.c.
4 hr. 30 min. ...	118	113	set, no syneresis	4 c.c.
5 hr. 30 min. ...	122	...	0	5 c.c.

From this, it will be seen that the stabilising influence of these ions is in the following decreasing order :

citrate > oxalate > tartrate > acetate.

Our results on the influence of calcium chloride on the syneresis of blood-clot show that even in presence of calcium

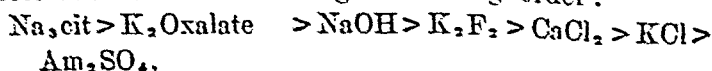
chloride ions are preferentially adsorbed, and the view that the stabilising influence of citrate, oxalate, fluoride and other anions is due to the removal of calcium ions appears to be incorrect. We have shown that by increasing the concentration of calcium chloride also, blood is much stabilised, and the amount of syneresis is markedly decreased, and at higher concentrations, blood does not set at all. This is due to the high tendency for the adsorption of chloride ions, as has been observed in the case of potassium chloride also.

In the following table we are indicating the approximate concentrations of various salts necessary to stabilise the blood to such an extent that no marked syneresis may occur after the formation of clot within 12 hours.

TABLE XII

Electrolyte	Concentration to give clot undergoing no marked syneresis
Potassium chloride ...	0.12 N
Calcium chloride ...	0.0845 N
Ammonium sulphate ...	0.176 N
Potassium oxalate ...	0.016 N
Sodium citrate ...	0.016 N
Potassium fluoride ...	0.049 N
Sodium hydroxide ...	0.039 N

From the table it will be seen that the stabilising influence of these salts is in the following decreasing order :



From this order it appears that the stabilising influence depends both on the valency of the ions and alkalinity of the medium.

The clotting of blood has generally been regarded as the conversion of soluble fibrinogen to insoluble fibrin under the action of an enzyme known as thrombin. We are of the opinion that thrombin may assist the process of clotting

but it is not essentially the cause of the phenomenon. The clotting of blood is guided by the same forces which bring out the gelation of other organic and inorganic jellies. Fibrin has a high hydration tendency and yields an unstable colloidal suspension. The clotting of blood is guided by the characteristic unstable nature of fibrin, its concentration, and the nature and concentration of electrolytes present in blood, and all this has been so regulated in blood, that as soon as the capillary action of blood-vessels and circulatory motion are stopped, jelly-forming forces begin to react and finally a solid clot is obtained in a few minutes. The presence of an excessive amount of coagulating electrolytes causes the agglomeration of particles, and the contraction of the clot and the synerised serum is squeezed out of the network. Such syneresis has been observed with various inorganic jellies, such as those of vanadium pentoxide, silicic acid, ferric arsenate, borate and various zirconium jellies. These jellies on ageing, lose markedly the hydration capacity, and on account of the agglomeration of particles give out the solvent.

In previous communications<sup>1</sup> from these laboratories, we have mentioned that the process of jelly-formation is guided by the agglomeration and hydration tendencies of the particles. In presence of coagulating electrolytes, the charge on the jelly-forming sol decreases and the amount of hydration increases up to a limiting value. When the concentration of the electrolyte is increased, agglomeration of the particles begins, with the result that the jelly contracts and undergoes syneresis. The same is applicable to the blood-clot also. Under the action of coagulating ions, blood forms a clot, and due to the presence of an excess of the same ions, its particles agglomerate and undergo contraction, and finally the serum is squeezed out.

<sup>1</sup> J. Indian Chem. Soc., 6, 391 (1929).

Waele<sup>1</sup> has shown that the blood-fibrinogen exists in a highly buffered system, of which the  $p_H$  however is subject to variations. He has also observed that fibrinogen is precipitated at  $p_H$ -5-6, forms a gel at  $p_H$  7-9, and remains dissolved at  $p_H$ -10. This dissolution of fibrinogen can be explained on the view that it is stabilised by the adsorption of similarly charged  $OH'$  ions from the alkaline medium. The observations of Herzfeld and Klinger<sup>2</sup> that acids accelerate the precipitation of fibrin and alkalis exert an inhibitory action can also be explained on the same basis. As we have mentioned in a previous paper,<sup>3</sup> the clotting tendency of blood is most marked near the neutral point. On the acid side and alkaline side, the charge on the blood is increased and hence the hydration tendency is less. Stuber and Heim<sup>4</sup> have observed that the coagulating action of fatty acids increases with the increasing number of carbon atoms in the acids, *i.e.*, in the decreasing order of the dissociation constants. The less coagulating action of the lower members of the series is due to the fact that comparatively larger amounts of hydrogen ions are given out and the medium becomes acidic, whereby the charge on the plasma is increased and the system is stabilised.

<sup>1</sup> Ann. Physiol. Physicochim. Biol., 3, 94 (1927).

<sup>2</sup> Biochem. Zeitsch., 71, 391 (1915).

<sup>3</sup> Loc. cit.

<sup>4</sup> Biochem. Zeitsch., 77, 333 (1916).

## SUMMARY

1. The influence of different concentrations of potassium chloride, calcium chloride, ammonium sulphate, potassium fluoride, potassium oxalate, sodium acetate, tartrate, citrate and hydroxide on the extent of syneresis of blood-clot has been studied.

2. It has been observed that in all the cases, the amount of syneresis decreases as the concentration of the electrolytes is increased. In some cases, the syneresis is totally stopped and in a few cases the electrolytes prevent the clotting of blood.

3. The influence of electrolytes is explained on the view that blood has a high tendency of adsorbing similarly charged ions from the salts, and thus the electric charge on blood is increased and it is stabilised. The stabilising influence of the salts is in the following order :

Sodium citrate > potassium oxalate > NaOH >  $K_2F_2$  >  $CaCl_2$  > KCl >  $Am_2SO_4$ .

4. It has been shown that the stabilising influence of fluoride, citrate or oxalate is not due to the removal of calcium ions from the blood, but is due to the stabilising influence of anions which are largely adsorbed by blood.

5. The syneresis and clotting of blood are guided by the same forces which give rise to the syneresis and formation of inorganic and organic jellies.

# INVESTIGATION ON THE PRODUCTS OBTAINED BY EXPOSING OILS AND CARBOHYDRATES TO SUNLIGHT IN PRESENCE OF AIR

BY

SACHINDRA NATH CHAKRABARTI, M.Sc.,

*Research Scholar, Chemistry Department.*

In a recent publication from this laboratory (Palit and Dhar, J. Phys. Chem., 1928, 32, 1663) it has been shown that the edible products like carbohydrates, fats and nitrogenous substances can be oxidised by passing air through their solutions in presence of sunlight. These results are interesting in view of the observations made by different workers who are of opinion that inert substances on being irradiated with quartz-mercury vapour lamp are endowed with antirachitic properties. These investigators are of opinion that vitamins are synthesised by the ultra violet radiations when edible substances are irradiated. The present work was undertaken in order to investigate whether actually vitamins are synthesised or some other type of activation takes place. In a recent paper from this laboratory the view had been advanced that when substances like cholesterol, olive oil, etc., are exposed to light in presence of air, peroxides are formed and these induce the oxidation of food materials mixed with them. Hence the antirachitic and beneficial properties of substances not containing the necessary vitamins are due to the presence of peroxides which help the oxidation of the food materials in the body. Substances can acquire antirachitic properties when exposed to light only in presence of air or oxygen. It will be observed that this view is supported by the following observations.



## EXPERIMENTAL

Equal quantities of different oils were taken in small beakers containing 25 c.c. of water and they were exposed to sunlight for 5 hours. A current of dry air free from carbon dioxide was constantly being passed through the oils. After the exposure, an excess of potassium iodide solution was added to the mixture and the mixture was acidified. The liberated iodine was titrated against N/100 sodium-thiosulphate solution with starch as an indicator. The results are shown in Table I.

TABLE I

Oils	Botanical name	Amount taken	Amount of Iodine liberated in term of N/100 thiosulphate
Olive oil ...	Olea Europea ...	3 c.c.	3.20 c.c.
Mustard oil ...	Brassica competris ...	"	1.4 c.c.
Coconut oil ...	Oocos nucifera ...	"	1.00 c.c.
Mahua oil ...	Bassia Latifolia ...	"	1.20 c.c.
Castor oil ...	Ricinus communis ...	"	0.95 c.c.
Til oil ...	Sesamum Indicum ...	"	1.2 c.c.
Linseed oil ...	Linum Usitissimum ...	"	0.90 c.c.

These experiments were repeated and almost the same results were obtained showing that the results are reproducible.

Not only these oils but also butter and some carbohydrates behaved in the same manner after being exposed to sunlight. The amount of iodine liberated by them from an acid solution of potassium iodide is given in the Table II.

TABLE II

Substance	Amount taken	Amount of Iodine liberated in term of N/100 thiosulphate
Butter ... ..	0.92 grm.	2.25 c.c.
Starch ... ..	0.10 "	0.20 c.c.
Glycogen ... ..	0.10 "	0.05 c.c.
Dextrin ... ..	0.10 "	0.45 c.c.
Glucose ... ..	0.10 "	0.05 c.c.

The irradiated substances had the property of oxidising other substances when mixed with them. The extent to which they oxidised glucose was determined in the following way. 10 c.c. of 1 per cent glucose solution was mixed with the oils after irradiation in presence of air and the mixture was kept at 40°C in a thermostat for 18 hours. The mixture was filtered when the oil remained in the filter paper. The oil was washed well with warm water. In each case a blank experiment was also done by keeping 10 c.c. of the same glucose solution in contact with the same quantity of unexposed oils, the temperature and time being the same. This brought the possible experimental error to a minimum. The solution containing glucose was precipitated with Fehling's solution and the cupric oxide was weighed. The oil which remained on the filter paper was taken out and again an acid solution of potassium iodide was added to it and the liberated iodine titrated against N/100 sodium thiosulphate. The results are given in Table III.

The experiments on oxidation was repeated for several times and fairly reproduceable results were obtained as shown in Table IV. On exposing these oils to sunlight without passing air similar results were obtained though to a much less degree as shown in Table V.

TABLE III

Substance	Amount of oil	Amount of N/100 iodine liberated before the oxidation of glucose	Amount of CuO in grams (Blank)	Amount of CuO in grams, (after oxidation)	Percentage oxidised	Amount of N/100 iodine liberated after oxidation of glucose.
Mustard oil ...	3 c.c.	1.50 c.c.	0.2183	0.2071	5.1%	0.20 c.c.
Coconut oil ...	3 c.c.	1.05 c.c.	0.2169	0.2108	2.9%	0.35 c.c.
Mahua oil ...	3 c.c.	1.20 c.c.	0.2222	0.2181	3.9%	0.15 c.c.
Castor oil ...	3 c.c.	0.95 c.c.	0.2166	0.2084	3.8%	...
Til oil ...	3 c.c.	1.25 c.c.	0.2217	0.2178	1.7%	0.85 c.c.
Linseed oil ...	3 c.c.	1.00 c.c.	0.2177	0.2140	1.2%	0.70 c.c.

TABLE IV

Mustard oil ...	3 c.c.	1.5 c.c.	0.2331	0.2202	5.5%	0.10 c.c.
Coconut oil ...	3 c.c.	1.05 c.c.	0.2309	0.2224	3.7%	0.15 c.c.
Mahua oil ...	3 c.c.	1.45 c.c.	0.2312	0.2235	3.3%	0.65 c.c.
Castor oil ...	3 c.c.	0.80 c.c.	0.2365	0.2209	4.1%	...
Til oil ...	3 c.c.	1.25 c.c.	0.2352	0.2238	2.3%	0.70 c.c.
Linseed oil ...	3 c.c.	1.00 c.c.	0.2313	0.2234	0.8%	0.80 c.c.

TABLE V

Mustard oil ...	3 c.c.	0.90 c.c.	0.2232	0.2168	2.9%	0.2 c.c.
Coconut oil ...	3 c.c.	0.65 c.c.	0.2208	0.2171	1.7%	0.25 c.c.
Mahua oil ...	3 c.c.	0.85 c.c.	0.2216	0.2176	1.8%	0.40 c.c.
Castor oil ...	3 c.c.	0.50 c.c.	0.2260	0.2229	1.4%	0.15 c.c.
Til oil ...	3 c.c.	0.75 c.c.	0.2251	0.2229	1.0%	0.50 c.c.
Linseed oil ...	3 c.c.	0.65 c.c.	0.2224	0.2211	0.6%	0.80 c.c.

In the light of the observations made we can safely say that when the food materials are exposed to sunlight in presence of air, they take up oxygen probably forming some

peroxide type of compound which can oxidise other food materials when mixed with them. Consequently, the addition of the exposed substances to ordinary food-stuff facilitates the proper assimilation of food materials and produce efficacious results. From the above tables we find that mustard oil (*Brassica competris*) when exposed to light and air, is capable of oxidising glucose when mixed with it to the extent of 5 per cent. It is interesting to note that Til oil (oil of *sesamum indicum*) has the least power of giving up oxygen from its peroxide and even after oxidising glucose more than half of the peroxide remains unchanged as can very well be seen from the amount of iodine liberated by the oil after the oxidation of glucose. Thus we see that the amount of oxidation of glucose is proportional to the amount of peroxide used up as shown in Table VI.

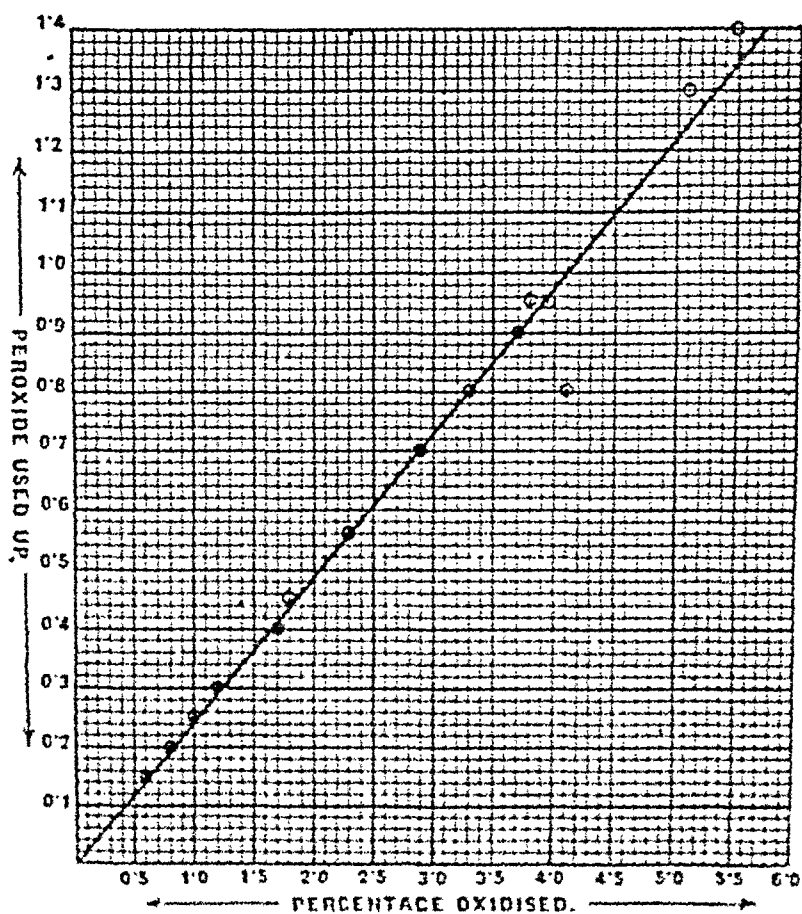
TABLE VI

Oils	Amount of peroxide in term of N/100 iodine before oxidation of glucose	Amount of peroxide in term of N/100 iodine after oxidation of glucose	Peroxide used up during oxidation in term of N/100 iodine	Percentage oxidised	Peroxide used up K = $\frac{\text{Percentage oxidised}}{\text{Peroxide used up}}$
Mustard oil ...	1.50 c.c.	0.20 c.c.	1.30 c.c.	5.1%	0.255
Coconut oil ...	1.15 c.c.	0.35 c.c.	0.70 c.c.	2.9%	0.241
Mahua oil ...	1.20 c.c.	0.15 c.c.	0.95 c.c.	3.9%	0.244
Castor oil ...	0.95 c.c.	...	0.95 c.c.	3.8%	0.250
Til oil ...	1.25 c.c.	0.85 c.c.	0.40 c.c.	1.7%	0.235
Linseed oil ...	1.0 c.c.	0.7 c.c.	0.30 c.c.	1.2%	0.250
Mustard oil ...	1.5 c.c.	0.1 c.c.	1.4 c.c.	5.5%	0.255
Coconut oil ...	1.05 c.c.	0.15 c.c.	0.9 c.c.	3.7%	0.243
Mahua oil ...	1.45 c.c.	0.65 c.c.	0.8 c.c.	3.3%	0.242
Castor oil ...	0.8 c.c.	...	0.8 c.c.	4.1%	0.195
Til oil ...	1.25 c.c.	0.70 c.c.	0.55 c.c.	2.3%	0.239
Linseed oil ...	1.0 c.c.	0.8 c.c.	0.2 c.c.	0.8%	0.250
Mustard oil ...	0.9 c.c.	0.2 c.c.	0.7 c.c.	2.9%	0.241
Coconut oil ...	0.65 c.c.	0.25 c.c.	0.4 c.c.	1.7%	0.235
Mahua oil ...	0.85 c.c.	0.40 c.c.	0.45 c.c.	1.8%	0.250
Castor oil ...	0.5 c.c.	0.15 c.c.	0.35 c.c.	1.4%	0.250
Til oil ...	0.75 c.c.	0.5 c.c.	0.25 c.c.	1.0%	0.250
Linseed oil ...	0.65 c.c.	0.5 c.c.	0.15 c.c.	0.6%	0.250
				Average	0.243

A glance at the Table VI will show that except in a few cases, the ratio between the available oxygen from the peroxides of the oils for the oxidation of glucose and the percentage of glucose oxidised is fairly constant. It can also be seen from Fig. 1 that the graph showing the relation between the percentage of glucose oxidised and the amount of peroxide used up is a straight line. The average of the constants in Table VI is calculated to be 0.243. The constant as read from the graph comes out to be 0.241, *i.e.*, quite concurrent. The percentage of glucose oxidised by the peroxide of the oil is proportional to the availability of oxygen from the peroxide. It is not dependent upon the actual amount of peroxide formed. Mustard oil has thus the greatest efficiency in producing this type of oxidation.

Having investigated these experiments on the efficiency of exposed oils in oxidising other food materials, we carried on experiments on metabolism of pigeons using these exposed and unexposed oils. Incidentally we have also investigated the influence of sunlight and small quantities of ferric chloride in the metabolism of pigeons.

Pigeons were divided amongst six compartments each containing four pigeons. The first set had sufficient amount of sunlight, the second set had sunlight to a much less extent whereas all other sets were kept in darkness. The main diet was Rangoon rice which is believed to be entirely devoid of vitamins. Each of the pigeons got 25 grams of Rangoon rice. In addition to that those in the second set got 5 grams of Bajra (*Pennisetum Typhoideum*) for each pigeon. Those in the third set got 3 c.c. of olive oil exposed to sunlight for 5 hours, for four pigeons. The oil was well mixed with rice. The fifth set got 20 c.c. of 0.1 per cent ferric-chloride solution for four pigeons. The sixth set got 3 c.c. of unexposed olive oil for four pigeons. The first and the fourth sets got only rice. This diet was continued for a month. All the pigeons were steadily decreasing in weight except those in the second



set which got Bajra and some sunlight. These pigeons were more or less normal in condition throughout the experiment. After two weeks the pigeons of the fourth set, *i.e.*, those receiving Rangoon rice in darkness showed stomachic trouble and one of the pigeons showed signs of polyneurites. It could not move and had lost its appetite. It also lost its eye-sight and was paralytic. The particular pigeon was separated from the lot and kept in sunlight for  $2\frac{1}{2}$  hours. It improved a little and could walk slowly. The eye-sight became normal but the appetite did not come back. It was then artificially fed with a little tomato juice and milk. In about 18 hours it became quite normal. The diet was changed to Rangoon rice mixed with a little Bajra and the pigeon was kept in light. Gradually it became quite normal in condition.

After three weeks the fifth and at about the same time but a little later, the sixth sets became affected with stomachic trouble. All the pigeons in these sets lost their appetite and the major portion of the food given was left untouched. The pigeons of the fourth set also had the same trouble, but all other pigeons in the first, second and third sets did not show any such trouble, though the pigeons in the first and third sets were steadily decreasing in weight. In the fourth week one of the pigeons in the fifth set got affected with polyneurites. It was kept in sunlight and was artificially fed with Bajra when it considerably improved but still was very weak. But it regained its appetite and could take a little rice mixed with tomato juice and milk, of itself. It gradually improved and became quite normal in 36 hours.

At the end of the fourth week, the eyes of the pigeons of the fourth set were greatly affected and majority of the pigeons in the fifth and sixth sets were seriously ill. In one night one pigeon of the fifth set and two of the sixth set became so much affected with the disease that they were beyond the power of treatment, and all of them died before any food could be administered. In about five hours another

pigeon of the fifth set became affected and in about an hour the case became very serious. It was then artificially fed with tomato juice and milk. When it improved, the diet was changed to Bajra. But after two days it had a relapse and died. After four weeks of experiment, the normal diet was resumed and all the pigeons were kept in well-lighted compartments. But on the same day one of the pigeons in the fourth set showed slight signs of paralysis. In the night the case became serious and in the morning it was dead.

During the experiment all the pigeons were weighed on alternate days. In order to compare the fall in weight and the general condition of the pigeons, the average weight of each set every day was calculated, taking 300 as the original weight of each set and a graph was plotted. The curve in the Fig. 2 clearly shows that the set No. 2 which received Bajra were more or less in normal condition. The first set which received sunlight and the third set which received olive oil exposed to sunlight were almost similar in condition. The fifth and sixth sets were almost equally affected but the fourth set was the most affected.

Our results show that animals receiving normal diet and sunlight keep very good health. Even if the animals do not get any vitaminous food but only sunlight they keep good health as the pigeons in the first set. Of course the pigeons which got olive oil exposed to sunlight were much better than those getting iron and unexposed olive oil though they were kept in darkness, still they were inferior in general health to those which obtained sunlight but no vitaminous food. We thus find that olive oil exposed to sunlight is not as efficacious as the vitaminous food or even as sunlight. In a previous paper it has been shown that iron in small doses as are present in leafy vegetables, are beneficial for health. Our results show that iron in larger doses are rather harmful to the pigeons and cannot prevent the attack of polynurites.



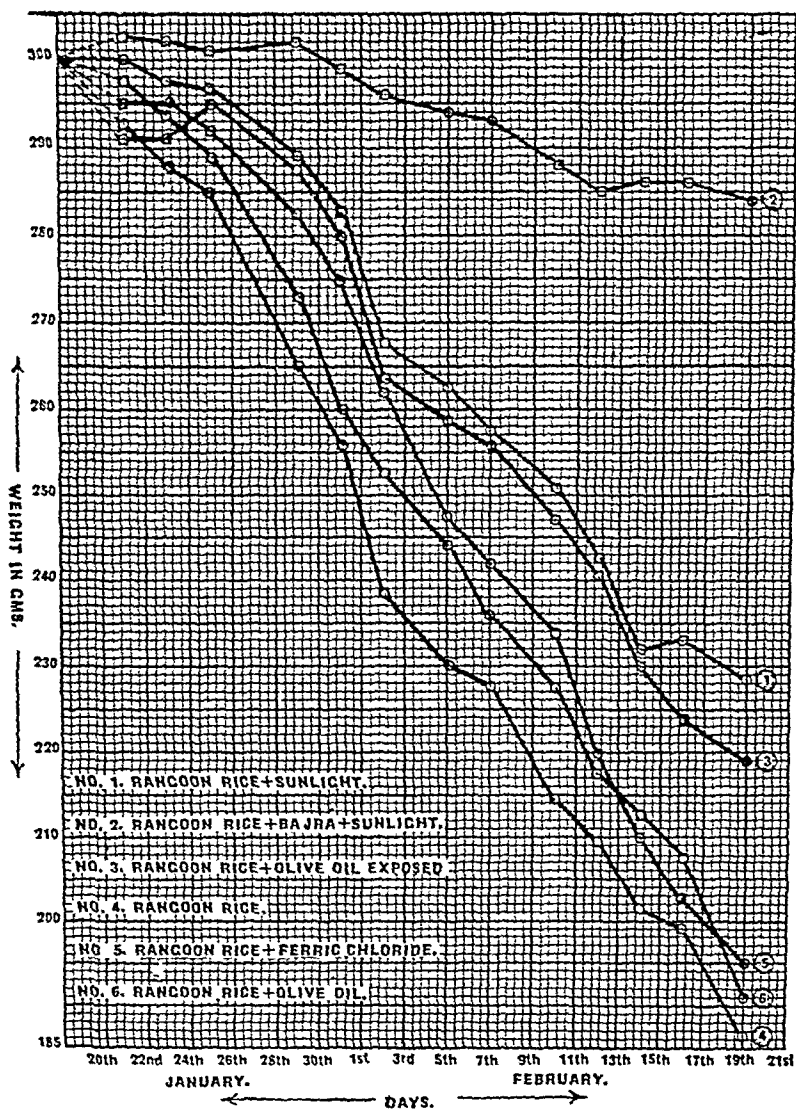


Fig. II.

Ordinary olive oil also is not a nutritive diet for pigeons and its presence does not help them in preventing the disease. These experiments confirm the view that sunlight acts as a promoter of oxidation of the food materials in the body and normal food with plenty of sunlight is the best kind of diet.

---

## SUMMARY

1. It has been shown that if olive, mustard, coconut, mahua, castor, til, and linseed oils, butter and some carbohydrates are exposed to sunlight, and air is passed through them, peroxides are formed. These peroxides have been estimated by the amount of iodine liberated by them from an acid solution of potassium iodide.

2. If the oils are only exposed to sunlight and air is not passed through them, the amount of peroxides is decreased to a great extent. The amount of peroxide formed is probably due to the layer of air which comes in contact with the oil surface.

3. All these oil-peroxides have the property of oxidising a solution of glucose, when mixed with them and kept at 40° for 18 hours. The amount of this oxidation is dependent upon the availability of oxygen from the peroxide.

4. From the experiments on metabolism of pigeons using exposed and unexposed oils, iron and sunlight, we have proved that sunlight is the best preventive for diseases like polyneurites and beri-beri. Olive oil exposed to sunlight and air comes a close second, whereas iron and unexposed oils are harmful to these pigeons.

5. The natural food with plenty of sunlight seems to be the best kind of diet for the maintenance of health.

---

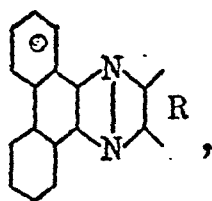
# DYES DERIVED FROM PHENANTHRAQUINONE THE PHENANTHRA-PHENANTHAZINES

BY

NARENDRANATH GHATAK, M.Sc.,  
*Research Scholar, Chemistry Department,  
Allahabad University.*

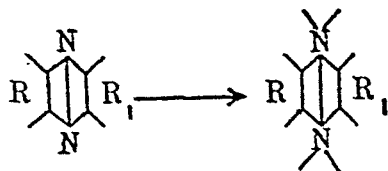
Phenanthraquinone as a source of azine-dyestuff, was first investigated by Watson and Dutt (J., 1921, 199, 1211) in which substituted phenanthraquinones were condensed with ortho-phenylene-diamine. Later on Sircar and Dutt (J., 1922, 121, 1944) continued the investigation and prepared another series of dyestuffs by condensing substituted phenanthraquinones with 1:2-naphthalene-diamine and its various derivatives. Finally 2:3-diamido-phenazine has also been condensed with substituted phenanthraquinones (Sircar and Dutt, J.I.C.S., 1924-25, 1, 201—206) with formation of another series of dyestuffs which have been termed the phenanthra-phenazine-azines.

In all these series of dyestuffs the complexity of structure of the phenanthraquinone nucleus and the ease with which it undergoes condensation with ortho-diamines have been utilised in the preparation of intensely coloured substances of which the general configuration is as follows:



in which R is the aromatic or heterocyclic complex. The most remarkable thing in connection with these dyestuffs is that though all of them are quite soluble in water, yet when in a fine state of division they are rapidly absorbed from aqueous suspensions into the body of fibres (whether

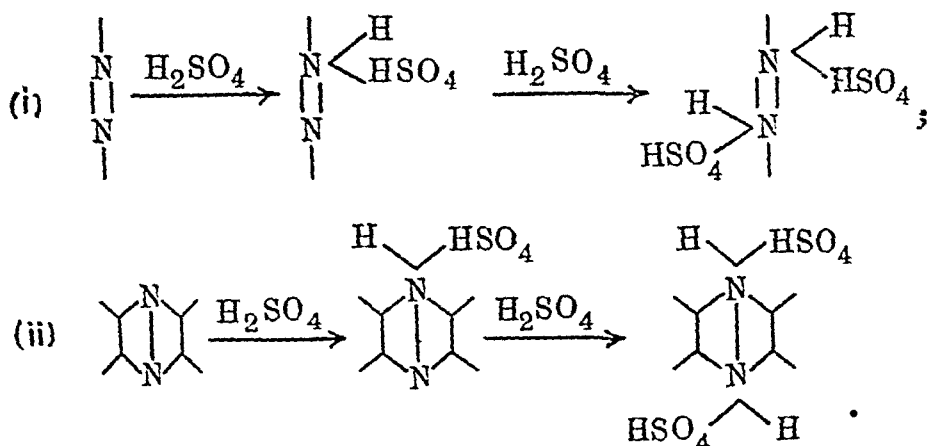
previously mordanted or not) with formation of uniform and bright shades of colour. This phenomenon must have something to do with the residual valencies of the two azine nitrogen atoms which though existing in the trivalent condition in the azine are nevertheless potentially capable of passing to the pentavalent state under suitable conditions. Thus :



It is quite probable that the dyestuffs exist in such pentavalent condition in combination with silk or wool which are quite well known to have acidic principles in them. Otherwise such bright and uniform shades, as are given by these azine dyestuffs on the fibre, would not have been possible from mere aqueous suspensions of these dyestuffs. Another point of interest in this connection pointing to the same conclusion is that in the majority of the cases the dyeings on wool and silk by these dyestuffs are brighter and in fact more intense than the dyestuffs themselves. In a series of papers by Dutt on "A Theory of Colour on the Basis of Molecular Strain" (J., 1926, 129, 1171; J.I.C.S., 1927, 4, 99) it has been shown that whenever the trivalent nitrogen in a dye molecule passes into the pentavalent state, there is invariably produced an increase of colour. Thus :

Names.	Absorption maxima.
Diamido-phenazine ...	... 5150
Pheno-safranine ...	... 5250
Phenanthraphenazine ...	... 4300
Flavinduline ...	... 4520
Crystal violet ...	... 5990
Methyl green ...	... 6260

The strong colour developed when azine and azo compounds are dissolved in concentrated sulphuric acid may be regarded as due to the same phenomenon, i.e., due to the loading effect produced by the addition of sulphuric acid radicle to one or both of the nitrogen atoms, thereby converting them to the pentavalent state.



Thus :

Name.	Absorption maxima.	
Benzene-azo-phenol (in alcohol) ...	...	4330
do. (in strong sulphuric acid) ...	...	4560
Benzene-azo-4-naphthol (in alcohol) ...	...	4350
do. (in strong sulphuric acid) ...	...	4720
Benzene-azo-2-naphthol (in alcohol) ...	...	4970
do. (in strong sulphuric acid) ...	...	5630
Phenazine (in alcohol) ...	...	4290
do. (in strong sulphuric acid) ...	...	4730
Phenanthra-naphthazine (in alcohol) ...	...	4320
do. (in strong sulphuric acid) ...	...	5630

But these pentavalent conditions of nitrogen being unstable in dilute solutions, they pass back into the original states by diluting the sulphuric acid solutions.

preparations of different substituted phenanthraquinones. Finally, under group (C) are given the preparations of the dyestuffs obtained by condensing different derivatives of phenanthraquinone with phenanthrene diamine.

#### (A) 9:10-DIAMINO-PHENANTHRENE-DIHYDROCHLORIDE

This substance was obtained by two reactions.

(i) *Phenanthraquinone dioxime*.—10 gms. (1 mol.) of phenanthraquinone and 7 gms. (2 mols.) of hydroxylamine hydrochloride was mixed and boiled in pyridine solution for an hour. It was poured into water and acidified with HCl. The oxime was precipitated and separated. It was dissolved in NaOH, filtered and re-precipitated with hydrochloric acid. The oxime was yellow. Melting Point—202°C. Yield—10 gms.

(ii) *Phenanthrene-diamino-dihydrochloride*.—10 gms. of finely divided phenanthraquinone dioxime, 35 gms. of stannous chloride and 45 c.c. of concentrated hydrochloric acid were mixed and refluxed for an hour. It was filtered and thoroughly washed with dilute HCl and finally with water. Yellowish green substance. Yield—7 gms.

#### (B) DERIVATIVES OF PHENANTHRAQUINONE

(i) *2 : 7-dinitro-phenanthraquinone*.—(Schmidt and Kämpf, *B.*, 35, 3119). 20 gms. of phenanthraquinone was boiled for thirty minutes with a mixture of 250 c.c. fuming nitric acid and 35 c.c. of strong  $H_2SO_4$ , the joint between the flask and the condenser being made up of plaster of paris. The cooled mixture was poured into eight times the quantity of water. Voluminous yellow precipitate separated after several hours of standing. It was recrystallised from boiling acetic acid. On cooling bright yellow needles separated. Melting point—300—303°C. Yield—11 gms.

(ii) *2 : 7-diamino-phenanthraquinone*.—(Auschutz and Meyer, *B.*, 18, 1944). A mixture of one part of 2:7-dinitro-phenanthraquinone, two parts of granulated zinc,

15 parts of fuming HCl was heated on a water bath until all the tin dissolved. The yellow colour of the nitro-quinone became red, then violet and finally a voluminous white precipitate (double salt with tin). The precipitate was washed with HCl and dissolved in water. The tin was precipitated by  $H_2S$ . The clear filtrate was rendered alkaline with  $K_2CO_3$ . Air was passed into it for a long time. The diamino derivative precipitated as violet crystals. It was recrystallised from pyridine. Melting point— $304^\circ C$ .

(iii) *2:7-dihydroxy-phenanthraquinone*.—3 gms. of the diamino derivative was treated with 300 c.c. of strong HCl. The violet compound turned yellow owing to the formation of the dihydrochloride. It was treated with 2.5 gms. of sodium nitrite in cold, and then the mixture diluted with 400 c.c. of cold water. Almost everything went into solution. The red solution was filtered and the diazotised compound hydrolysed by boiling for some time. A dark blue compound separated. It was crystallised from glacial acetic acid. The substance precipitated in the form of fine blueblack prismatic needles. Yield—2.0 gms. Melting point— $293^\circ C$ .

(iv) *2:7-dibromo-phenanthraquinone*.—12 gms. of phenanthraquinone, 20 gms. of bromine, 80 c.c. of water were heated in a sealed tube at about  $160^\circ C$  for 5 hours. The reaction product dissolved in excess of acetic acid and cooled. A pure sample of the bromo derivative was obtained. It was recrystallised from acetic acid. Yield—2.8 gms. Melting point— $295^\circ C$ .

(v) *2-nitro-phenanthraquinone*.—10 gms. of phenanthraquinone and 70 c.c. of concentrated nitric acid (1.45) were heated in a flask quickly to boiling and kept at boil for 3 minutes and poured into 700 c.c. of cold water. The precipitate quickly settled to the bottom and was washed by decantation. This crude product was boiled with excess of acetic acid for about half an hour. It was filtered and from the hot acetic-acid solution separated 4 gms. of pure



2-nitro-phenanthraquinone in golden yellow crystals. Melting point—257-258°C.

(vi) 4:5-dinitro-phenanthraquinone.—The filtrate after the precipitation of 2:7-dinitro-phenanthraquinone, (i), was concentrated to 1/8 the volume. On cooling not quite pure 4:5-dinitro-compound was deposited. It was dissolved in hot acetic acid, filtered and crystallised. The product was again treated with fuming nitric acid (1.5) and the substance recrystallised from hot acetic acid. Yield—8.7 gms. Melting point—227°C.

(vii) 4:5-diamino-phenanthraquinone.—(Schmidt and Kämpf, *B.*, 36, 3750). 6 gms. of the dinitro compound was mixed with 13 gms. of granulated tin and heated with 100 c.c. of fuming hydrochloric acid on water bath. When all the tin dissolved, the solution was cooled and the tin chloride double salt was crystallised out. It was filtered and washed with hydrochloric acid. It was then dissolved in water and the tin precipitated by  $H_2S$ . The filtrate was concentrated and treated with  $K_2CO_3$ . Air was passed in it for a long time. The base was precipitated in black flocks. It was filtered and crystallised from alcohol. Yield—2.3 gms. Melting point—287°C.

### (C) PHENANTHRA-PHENANTHRAZINES

(i) *Phenanthra-phenanthrazine*.—2 gms. (1 mol. 10% excess) of phenanthrene-diamine-dihydrochloride, 1.4 gms. (1 mol.) of phenanthraquinone were separately dissolved in concentrated sulphuric acid and mixed. It was kept for 24 hours. It was then poured into water. The precipitate filtered and dried. It was then dissolved in pyridine and filtered. Next it was boiled and a slow stream of boiling water was added to it until slight turbidity was noticed. It was kept apart. On cooling brilliant yellow needles separated. It was filtered and washed. Yield—1.3 gms. Melting point—211-212°C. Found  $N=7.21\%$ .  $C_{18}H_{16}N_2$  requires  $N=7.37\%$ .

(ii) 2 : 7-dinitro-phenanthra-phenanthrazine.—It was obtained by condensing 1.3 gms. of 2 : 7-dinitro-phenanthraquinone with 3 gms. of phenanthrene-diamine-dihydrochloride in concentrated sulphuric acid as in the previous case. The dyestuff was obtained as yellowish brown crystals after crystallisation. Yield—1.6 gms. Melting point—231-32°C. Shrinks at 210°. Found N=11.65%.  $C_{28}H_{14}O_4N_4$  requires N=11.90%.

(iii) 2 : 7-diamino-phenanthra-phenanthrazine.—1.5 gms. of the amino derivative previously prepared was condensed with 3 gms. of phenanthrene-diamine-dihydrochloride in concentrated  $H_2SO_4$ . The crystals were deep green. Yield—1.3 gms. Melting point—177°C. Found N=13.24%.  $C_{28}H_{18}N_4$  requires N=13.66%.

(iv) 2 : 7-dihydroxy-phenanthra-phenanthrazine.—1.5 gms. of 2 : 7-dihydroxy-phenanthraquinone was condensed with 2.6 gms. of the phenanthrene-diamine in concentrated  $H_2SO_4$ . The crystals were deep grey. Yield—1.4 gms. Melting point—205°C. Found N=6.43%.  $C_{28}H_{16}O_2N_2$  requires N=6.76%.

(v) 2 : 7-dibromo-phenanthra-phenanthrazine.—2 gms. of 2 : 7-dibromo-phenanthraquinone was condensed with 3 gms. of phenanthrene-diamine in concentrated  $H_2SO_4$ . The crystals were bright yellow. Yield—1.8 gms. Melting point—239-40°C. Found N=5.03%.  $C_{28}H_{14}N_2Br_2$  requires N=5.20%.

(vi) 2-nitro-phenanthra-phenanthrazine.—It was obtained in the form of yellowish green crystals by condensing 1.5 gms. of 2-nitro-phenanthraquinone with 2.8 gms. of phenanthrene-diamine in concentrated  $H_2SO_4$ . Yield—1.2 gms. Found N=9.61%.  $C_{28}H_{15}O_2N_3$  requires N=9.88%.

(vii) 4 : 5-dinitro-phenanthra-phenanthrazine.—It was obtained in the form of golden yellow crystals by condensing 1.8 gms. of 4 : 5-dinitro-phenanthraquinone with 2.5 gms. of phenanthrene-diamine in concentrated  $H_2SO_4$ .

Yield—1·4 gms. Melting point—197°C. Found N = 11·71%.  $C_{28}H_{14}O_4N_4$  requires N = 11·90%.

(viii) 4 : 5-diamino-phenanthra-phenanthrazine.— The product was obtained in the form of brilliant greyish brown crystals by condensing 1·3 gms. of 4 : 5-diamino-phenanthraquinone with 2·4 gms. of diamino-phenanthrene in concentrated sulphuric acid. Yield—0·9 gm. Melting point—182°C. Found N = 13·41%.  $C_{28}H_{14}N_4$  requires N = 13·66%.

---

# CHEMICAL EXAMINATION OF THE ROOTS OF HYGROPHILA SPINOSA

BY

NARENDRANATH GHATAK, M.Sc.,

*Kanta Prasad Research Scholar, Chemistry Department.*

The plant *Hygrophila Spinosa* of the natural order Acanthaceae is an annual marshy herb, with an ascending rhizome. It is found in abundance throughout India in ditches; from the Himalayas to Ceylon. Kirtikar and Basu (Indian Medicinal Plants, 1918, 2, 955) describe the stems to be numerous, stout, erect, hispid, 2—5 ft., usually fascicled and undivided or unbranched, somewhat compressed, thickened at nodes with long hair below each node.

*Alleged properties.*—As a medicine the Hindus consider *Hygrophila Spinosa* to be cooling, diuretic and strengthening; the roots, seeds and ashes of the plant are in general use, and are prescribed in hepatic obstructions, with dropsy, rheumatism, and urinary affections.

The Mohamedan writers mention the use of the plant for the same purposes, and also its external application in rheumatism, but they notice more especially the use of the seeds as an aphrodisiac given either with sugar, milk or wine in doses of from one to three dirhems.

On the Malabar coast a decoction of the root is considered as diuretic and given in dropsical cases and gravelish affections. The dose is about half a teaspoonful thrice daily.

*Chemistry.*—The chemical analyses of the roots of *Hygrophila Spinosa* have resulted in the identification of a new phytosterol,  $C_{29}H_{46}O$ , belonging to the phytosterol family having the general formula  $C_nH_{2n-10}O$ . Also quite a

good quantity of maltose has been obtained from it. A very small quantity of an essential oil, and a yellowish green waxy substance have also been obtained from it. An acetyl, a bromo, a digitonide and a chloro derivatives have been obtained from the phytosterol.

## EXPERIMENTAL

The material employed for this investigation consisted of 4 kilograms of sun-dried roots of *Hygrophila Spinosa*. It was cut into small pieces with the help of a chopping machine.

10 gms. of the roots were tested for the presence of an alkaloid, but with negative result.

In order to ascertain whether an enzyme were present, 50 gms. of the roots were kept soaked in water for few days at room temperature. It was then filtered through a filter pump and ethyl alcohol was added to the filtrate. No precipitate was formed and thus proving the absence of enzyme in the roots.

The root was next separately extracted with different solvents, taking 20 gms. of the substance every time. The root on estimation was found to contain 10.5% water.

### Extraction with Different Solvents

Solvent.	Wt. of extract.	Remarks.
1. Petroleum ether. (B.P. 60-80)	0.2007 gm.	The product was white needle-shaped crystals contaminated with a trace of yellow oil. The white substance gave all the characteristic colour reactions of phytosterol. Did not reduce Feling's solution.

Solvent.	Wt. of extract.	Remarks.
2. Carbon tetra-chloride.	0.2398 gm.	Greenish white substance having a waxy touch. The product on crystallisation gave reactions of phytosterol.
3. Benzene	0.2718 gm.	The waxy content was a little more in this case than in the previous one. The phytosterol was also present.
4. Chloroform	0.3270 gm.	The colour of the substance was green. A little chlorophyll was also present along with the phytosterol.
5. Carbon disulphide.	0.3338 gm.	This substance had properties like that of the previous one.
6. Acetone	0.4315 gm.	The dark-coloured substance obtained in this case had a strong aromatic odour.
7. Alcohol	0.9417 gm.	Some sugar and chlorophyll also came down along with the phytosterol.

The last alcoholic extract (7) was next extracted with hot water and the reducing sugars estimated. The amount of cuprous oxide obtained was 0.3389 gm.

The total reducing content was next estimated in terms of cuprous oxide by repeatedly extracting 20 gms. of the roots with hot water. The filtrate was boiled with a little animal charcoal. The filtrate was treated with basic lead acetate solution and filtered. The amount of lead salt obtained was 3.0536 gms. The excess of lead in the filtrate was removed by precipitating it as carbonate by adding 5% sodium carbonate solution. Lead carbonate was filtered off and the filtrate estimated for total reducing substances. The amount of cuprous oxide obtained was 0.7030 gm.

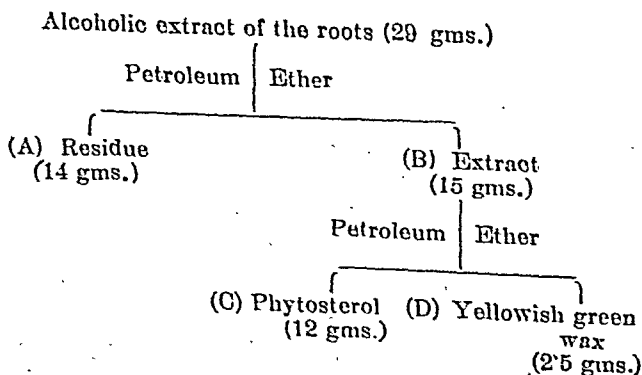
For the purpose of complete chemical analyses 3 kilograms of the dried roots were extracted several times with 90% ethyl alcohol. The extract on cooling gave out a dirty

white precipitate which collected at the bottom. The next day it was filtered. It was a sticky mass. It was first dried in a steam oven and then in a vacuum desiccator. It weighed 38 gms. On purification and examination it was found to be maltose.

The alcoholic filtrate was concentrated when a thick greenish liquid containing needle-shaped crystals was obtained. It was then steam distilled till the distillate came to about two-and-a-half litres. The distillate had peculiar aromatic odour. On extracting the distillate with ether few drops of an yellow essential oil was obtained. The quantity of the oil being so little its systematic analysis could not be done.

The residue after steam distillation was then filtered and washed with water several times. The filtrate was yellowish green in colour. Its reaction was slightly acidic towards litmus and contained sufficient quantity of sugar.

The substance on the filter paper was then dried and kept in a porous plate for few days to get rid of the oily substance mixed with it, but it could not be done. Then it was extracted in a shoxlet with light petroleum ether. The petroleum ether extract then on fractional crystallisation gave two products—(1) phytosterol, and (2) a yellowish green wax. The phytosterol first separated out. Thus :



Of these three products (A), (C), and (D) some work has been done on (C), which has been identified to be a new phytosterol, while the (A) and (D) are still under investigation.

(C) on several crystallisation with ethyl alcohol and animal charcoal gave beautiful needle-shaped white crystals. Its melting point was  $193^{\circ}\text{C}$ . This product gave all the characteristic phytosterol colour reactions with concentrated sulphuric acid in the presence of iodine, chloroform and acetic anhydride. On combusting the substance carbon and hydrogen were obtained in 83.91% and 11.60% respectively, giving the empirical formula  $\text{C}_{28}\text{H}_{46}\text{O}$ . The molecular weight by freezing-point method in benzene was found to be 396 ( $\text{C}_{28}\text{H}_{46}\text{O}$  gives a molecular weight of 398). This substance then evidently is a member of the phytosterol family having the general formula  $\text{C}_n\text{H}_{2n-10}\text{O}$ . The name spinosol may be given to this compound as it has been obtained from *Hygrophila Spinosa*.

A determination of the optical rotatory power of the substance gave the following result :

0.4318 gm. of spinosol dissolved in 100 c.c. chloroform, gave  $[\alpha]_D^{30} = +12^{\circ}$  in a 1-dm. tube, whence  $[\alpha]_D^{30} = +27^{\circ}8$ .

#### DERIVATIVES OF SPINOSOL

(1) *Acetyl spinosol*.—1.5 gms. of spinosol was refluxed for one-and-a-half hours with excess of acetic anhydride and fused sodium acetate. It was cooled and water added. A heavy brown liquid separated at the bottom which gradually solidified. It was filtered, washed free of acetic acid and dried. Next it was crystallised from dilute alcohol. Small needle-shaped white crystals separated. Its melting point was  $208^{\circ}\text{C}$ .



(2) *Bromo spinosol*.—Spinosol decolourised bromine in alcohol and chloroform solutions. The bromo derivative was prepared in cold chloroform solution. 1.4 gms. of spinosol was dissolved in 20 c.c. chloroform in a conical flask. Bromine dissolved in chloroform was added drop by drop till it was found to be in sufficient excess, and was kept over night. 150 c.c. of distilled water was put in the flask next morning and a current of air was passed through it by means of a suction pump. The current of air slowly evaporated the chloroform. On complete evaporation of chloroform and excess of bromine a semi-solid pasty yellow substance got separated and collected at the bottom of the flask. It was dried in a vacuum desiccator. The melting point of the crude product was  $100^{\circ}\text{C}$ . It was next purified and crystallised by dissolving the substance in chloroform in a beaker and then carefully diluting the chloroform by adding alcohol and heating. On cooling the bromo derivative slowly settled at the bottom as a yellow micro-crystalline powder. It was filtered and washed several times with dilute alcohol and dried. Bromo spinosol melted at  $138\text{--}139^{\circ}\text{C}$ .

(3) *Action of thionyl chloride on spinosol*.—0.8 gm. of spinosol was put in a dry test tube and about 2 c.c. of thionyl chloride was added to it. The reaction started immediately with the evolution of gas. When it slowed down a little the tube was dipped in boiling water which made the reaction go with a rapid speed. The colour of the liquid slowly darkened and ultimately it became deep green. It was kept over night. Next morning it was found completely solidified. It was then carefully crystallised several times from alcohol-chloroform (8 : 1) medium, when it was obtained as brown micro-crystalline powder. Melting point— $101\text{--}103^{\circ}\text{C}$ . It dissolved in solvents with a yellowish brown solution. The substance contained sulphur.

(4) *Carbanilate*.—An attempt was made to prepare the carbanilate by refluxing 1 gm. of spinosol and 0·8 gm. of phenyl-isocyanate in dry benzene solution for an hour. It was then poured in a dish and water was added to decompose the isocyanate. The product on crystallisation and purification was found to be a mixture of carbanilide and spinosol. Hence no carbanilate could be prepared.

---

# A STUDY ON VISCOSITY

BY

K. P. CHATTERJEE,

*Chemistry Laboratory.*

Though much work has been done on viscosity, little progress seems to have been made in elucidating the inner mechanism that causes it. In the following, an attempt has been made to explain it. As it appears, the subject is probably more amenable to study from the point of view of fluidity, which is reverse of viscosity. This notion is suggestive of the ease with which molecules can go past one another. It is therefore apparent that it depends on the resultant of at least three things, namely, the inherent nature of the molecular surface, the empty space in which they move and the cohesive force tending to keep them together. That there is a connection between volume and viscosity has often been felt, but the exact connection does not seem to have been formulated as yet. Fluidity, however, cannot be proportional to gross volume alone, for when there is little fluidity there is still almost the whole volume present. It will be more rational to suppose that fluidity depends on the empty space in the volume concerned and is affected by cohesive force which opposes shearing which empty space tends to bring.

Very little can be said of the nature of molecular surfaces, but the other two expressions have been evaluated in the following way.

According to van der Waal, the limiting volume  $b$  is 0.3 times the critical volume. Now, for water, the critical

density is 0.4. Hence the critical volume of 100 grams is 250 c.c. and hence the limiting volume would be 75 c.c. The empty space in 100 grams of water at any temperature would therefore be volume of it at that temperature less 75 c.c. as deduced. For cohesive force, surface tension may be taken as an approximate measure of it. Hence fluidity, surface tension and empty space might be formulated as related in the following way :

$$x \times \text{fluidity} + y \times \text{surface tension} = \text{empty space}$$

To illustrate applicability of the above idea, the following two cases are discussed, one a normal liquid and the other a typically associated one.

*Benzene*

Critical density = 0.3045

Critical volume of 100 grams = 328 c.c.

Limiting volume of the above = 98.5 c.c.

Temperature	0.0732 × fluidity	0.1392 × surface tension	Total	Actual empty space
10°	9.66	4.09	13.75	13.86
20°	11.21	3.92	15.13	15.29
30°	12.78	3.73	16.51	16.64
40°	14.64	3.49	18.13	18.12
50°	16.41	3.36	19.77	19.65
60°	18.07	3.20	21.27	21.14

*Water*

Critical density = 0.4

Critical volume of 100 grams = 250 c.c.

Limiting volume of the above = 75 c.c.

Temperature	0.032 × fluidity	0.305 × surface tension	Total	Actual empty space
0°	1.80	23.03	24.83	25.01
10°	2.45	23.57	25.02	25.03
20°	3.18	23.12	25.30	25.18
30°	3.99	21.66	25.65	25.43
40°	4.86	21.21	26.07	25.78
50°	5.78	20.68	26.46	26.21
60°	6.73	20.13	26.86	26.70
70°	7.72	19.58	27.20	27.27
80°	8.76	19.00	27.76	27.89
90°	9.79	18.42	28.26	28.50
100°	10.90	17.67	28.8	29.3

Considering that perfectly correct values of viscosity have not as yet been fully established, the agreement seems to be satisfactory.

It follows from the above hypothesis that if the surface tension be high, but the empty space be not large, fluidity naturally would be small. Many liquids are known which show this phenomenon. Again, if surface tension be moderate, high fluidity will be associated with much empty space, that is, will be causative of high volatility. All these are matters of common experience; they are now explainable with the help of the above idea.

This hypothesis, which serves pure liquid so well, is expected to throw light on solutions too. But as in these, definite valuation of certain data, notably limiting volume, is required, experiments are being carried on to elucidate them. Only general remarks with reference to sodium-chloride and potassium-chloride solutions need be made.

Concentration effect—Viscosity rises rapidly.

Temperature effect—For the same concentration, the increment of viscosity over zero concentration becomes less and less, as the temperature is increased.

Relative fluidity—With rise of temperature it decreases at lower concentrations only. It rises when the concentrations are high.

The viscosity lines—Potassium-chloride lines are flatter than the sodium-chloride lines.

Potassium-chloride solution shows negative viscosity at low concentrations, from 30°C downwards.

As regards relative fluidity, Ranken and Taylor, who think that non-electrolytes show a rise, and electrolytes the reverse, must have dealt with only dilute solutions. Taking, for example, solutions of sodium chloride, the fluidity factors are :

	0·1 conc.	0·2 conc.	0·3 conc.	0·4 conc.
at 40°	·919	·825	·724	·656
at 50°	·914	·826	·743	·666

It may, however, be said that concentrated solutions are more like non-electrolytes and hence the behaviour characteristic of non-electrolytes would be perceived here. Ions, evidently, are more viscous than molecules.

Incidentally, investigating water and benzene, a curious relation was observed. The change of absolute temperatures in benzene corresponds, in terms of rule of three, to the change of absolute temperatures of water, to produce a certain variation of viscosity from one value to another. Thus—

Viscosity for water	Absolute temperature	Viscosity for benzene	Absolute temperature
·008	303° A	·008	280·1° A
·007	309·5°	·007	288·3°
·006	317·8°	·006	299·2°
·005	329·5°	·005	313°
·004	345·3°	·004	334·3°

Now, for a variation of viscosity from 0·008 to 0·007, 6·5° for water corresponds to 8·2° for benzene ; hence for the variation of viscosity from '008° to '004, 42·3° for water, would need by rule of three, 53·3° for benzene. The actual temperature needed for benzene is 54·2°. The agreement is fair, considering the interpolated values used and the inherent uncertainties in them.

As has been mentioned, the above idea is being worked up to explain the behaviour of solutions, and with that end in view, more data are being secured.

# SOME VISCOSITY FORMULAE

BY

K. P. CHATTERJEE

A large number of empirical formulæ exists, which claim to yield correct values of viscosity, if used with properly chosen constants in them. The author has found out these constants and has in many cases improved and extended them. Although they are empirical, the author has given a rational meaning to some of them :

The following would be a classified scheme.

A. (a) Slotte's formula :  $\eta = \frac{c}{(a+t)^n}$

where, for water,  $c=5.9849$ ,  $a=43.252$  and  $n=1.5423$ .

A meaning can be given to it, namely, fluidity must vary as some power of the temperature counted from what may be called the 'critical melting point' below which point the particular substance cannot be made to remain in the molten state.

Tested for  $50^\circ$ , computed value is .00534  
experimental value is .00553

(b) Dorsey's  $\eta = \frac{k}{(t-a)^n}$ , and

(c) Batschiniki's  $\eta = \frac{-273}{(t-a)^3}$

may be passed over as only special cases of the Slotte type. Some of the more common formulæ, like the following, are also simplified forms of the Slotte type:—

(1)  $\eta = \frac{\eta_0}{1+at+bt^2}$

(2)  $\eta = \frac{c}{1+at+bt^2}$



$$(3) \frac{\eta_t}{\eta_0} = \frac{1}{1+at+bt^2}$$

$$(4) \frac{\eta_0}{\eta_t} = 1+at+bt^2$$

$$(5) \frac{1}{\eta} = a+bt$$

$$(6) \frac{1}{\eta} = A+BT$$

$$(7) \frac{1}{\eta} = a+bt+ct^2$$

$$(8) \frac{1}{\eta} = A+bT+cT^2$$

$$(9) \frac{1}{\eta_t} = \frac{1}{\eta_0} \{1+at+bt^2\}$$

$$(10) \phi_t = \phi_0 \{1+at+bt^2\}, \text{ etc.}$$

With constants calculated, some of them would be like the following:—

$$(a) \frac{1}{\eta} = -648.21 + 2.552 T \text{ (results, not satisfactory)}$$

$$(b) \frac{1}{\eta} = 82.38 - 2.3174 T + .00814 T^2 \text{ (results, not satisfactory)}$$

$$(c) \frac{1}{\eta} = 54.92 + 2.1t + .0077t^2$$

#### Results

Temperature	Computed values	Experimental values
20°	.01000	.01005
30°	.008003	.008005
100°	.002925	.002945

$$(d) 0.01780 = \eta_t \{1 + .034148t + .0002328t^2 - .000000762t^3\}$$

#### Results

Temperature	Computed values	Experimental values
10°	.01302	.01305
20°	.01005	.01005
40°	.00661	.00659
100°	.00297	.00295

B. Graetz formula:  $\eta_t = A \cdot \frac{t_c - t}{t - t_1}$

A meaning can be given to it, namely, viscosity is the ratio of the distances of its temperature from the two critical temperatures, the critical boiling temperature and the critical melting temperature.

Computing the constants, it would stand:—

$$\eta = 001408 \cdot \frac{t_c - t}{t + 29.58}$$

### Results

Temperature	Computed values	Experimental values
10°	01294	01305
20°	01005	01005
30°	008125	008020
40°	006754	006588
50°	005730	005537
70°	004296	004145

As at the critical temperature, there would be some viscosity still, a more rational formula would be of the type,

$$\eta = A \cdot \frac{t_c - t}{t - t_1} + \theta$$

namely,  $\eta = 00134 \cdot \frac{t_c - t}{t + 29} + 00016$

C. Bingham's formulæ:

$$(1) \quad \phi = \frac{c}{\phi - at - b}$$

$$(2) \quad t = A\phi - \frac{B}{\phi} + c$$

$$(3) \quad t = A\phi + \frac{B}{\phi + D} + c$$

$$(4) \quad T = a\phi - \beta + \frac{\gamma}{\phi} - \frac{\delta}{\phi}$$

where  $\phi$  is fluidity.

With constants, to suit the case of water, a formula of the above type may be put down as

$$\phi = 56.7 + 1.9292t + 0.1245t^2 - 0.00033t^3.$$

D. Arrhenius' formulæ:—

$$(1) \log \eta = a + bt$$

$$(2) \log \eta = \log n_0 + ct$$

$$(3) \log \eta = a + bt + ct^2$$

Thus, for water, the following is got

$$\log \eta = \bar{2} \cdot 184 - \cdot 01055t + \cdot 0000325t^2$$

### Results

Temperature	Computed values	Experimental
40°	·00652	·006588
50°	·00547	·005537
60°	·00466	·004752
70°	·00402	·004144
80°	·00354	·003655
90°	·00315	·003260

Extending it to the fourth power of temperature the following formula is devised:

$$\log \eta = \bar{2} \cdot 2500 - \cdot 0145313t + \cdot 00012064t^2 \\ - \cdot 0000007642t^3 + \cdot 0000000023t^4$$

### Results

Temperature	Computed values of viscosity	Experimental values of viscosity
0°	·01778	·01780
10°	·01306	·01305
20°	·01004	·01005
30°	·008013	·008020
40°	·006593	·006588
50°	·005545	·005537
60°	·004757	·004752
70°	·004137	·004144
80°	·003264	·003260
90°	·002949	·002945

E. Arrhenius' formulæ for solutions:

$$(1) \log \eta = \theta c + \phi$$

$$(2) \log \eta = \phi + \theta c + 4c^2$$

where  $c$  is concentration,

To devise a general formula embodying both concentration and temperature, has not been an easy affair. For the two solutions, namely, of sodium chloride and potassium chloride, the two following formulæ have at last been worked out.

(a) For sodium chloride solutions:

$$\log \eta = 2.184 - .01055t + .0000325t^2 \\ + c\{.35844 + .0069t - .00001t^2\} \\ + c^2\{.157 - .0013t\}$$

(b) For potassium chloride solutions:

$$\log \eta = 2.184 - .01055t + .0000325t^2 \\ + c\{.216 + .00825t - .000025t^2\} \\ + c^2\{.308 - .0042t\}$$

where  $c$  is concentration and  $t$  is temperature.

*Results for potassium chloride solutions.*

Temperature	Concentration (gm. mol. with 100 gms. water)	Computed values of viscosity	Experimental values of viscosity
40°	.1	.00671	.00674
	.2	.00689	.00689
	.4	.00741	.00743
50°	.1	.00573	.00578
	.2	.00595	.00594
	.4	.00651	.00650
60°	.2	.00521	.00522
	.4	.00577	.00576
	.6	.00636	.00638
70°	.2	.00462	.00460
	.4	.00518	.00512
	.6	.00582	.00572
80°	.2	.00416	.00410
	.4	.00471	.00462
	.6	.00530	.00512
90°	.2	.00380	.00371
	.4	.00430	.00422
	.6	.00487	.00476

The above work was done in order to provide ready-made suitable constants to those who might like to use them and in order to give some of the empirical formulæ a rational look and arouse interest to find a way in them.

---

*SECTION III*

PHYSICS

# THE SECONDARY SPECTRUM OF HYDROGEN

BY

D. S. JOG, M.Sc.,

*Empress Victoria Reader.*

It is really very remarkable that hydrogen, the simplest of all known substances should be capable of emitting spectra constituting thousands of lines. Hydrogen is known for a long time to emit the following spectra :

- (1) Spectrum due to atomic hydrogen consisting of—
  - (a) the well-known Balmer series in the visible and near ultra-violet,
  - (b) the Lyman series in the extreme ultra-violet,
  - (c) the Paschen series in the near infra-red,
  - (d) the Brackett series in the farther infra-red.

Out of these all, but the Balmer series, were discovered at a comparatively later date, after the development of spectroscopy on experimental and theoretical sides.

- (2) Spectrum due to molecular hydrogen.

Besides the spectral series of lines due to atomic hydrogen there are thousands of other lines constituting the spectrum of hydrogen. These lines are obtained under suitable conditions of excitation, and have been attributed to hydrogen in the molecular state. The spectrum is generally known as the Secondary—or sometimes also as the Many-lined—spectrum of hydrogen. Of course, only the portion of the spectrum lying in the visible and the near ultra-violet was subject of early investigation. Later works of Lyman, Wigner, Werner, Dieke and

Hopfield, Hori, Witmer, and others have explored the spectrum far into the extreme ultra-violet up to about  $\lambda$  840. On the infra-red side Gale, Monk, and Lee's data exist up to  $\lambda$  8900 and Poetekar's data extend up to  $\lambda$  11065. A further extension of the spectrum in this region is expected to be of great value in the analysis of the spectrum.

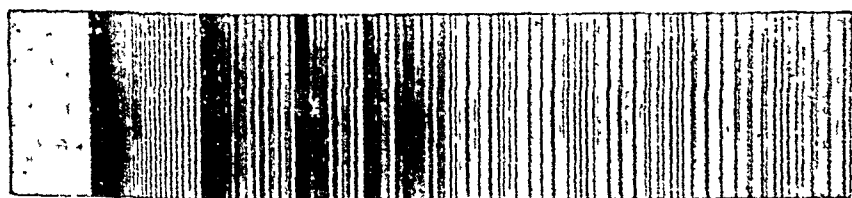
Besides the above two types of spectra hydrogen is also known to emit a continuous spectrum under proper excitation, in the region  $\lambda$  3300 to  $\lambda$  1600. In fact Dicke and Hopfield and several other investigators also have very successfully used this as a source of continuous spectrum in their investigations in the ultra-violet and Schumann region (upto  $\lambda$  1600).

### THEORETICAL IMPORTANCE

This molecular or secondary spectrum of hydrogen is very important from the theoretical point of view. For, as hydrogen is the simplest molecule we can conceive of, a theory giving satisfactory explanation of its spectrum may form a proper starting point for understanding and explaining spectra of other molecules (molecular spectra in general). It is, however, interesting to note that this spectrum defied attempts at explanation for a long time; and even now, it has only been possible to make very little progress in this direction. The chief difficulty confronted by early investigators in attempts to classify the spectrum arose from the fact that, whereas all other molecular spectra were known to possess a band structure with systems of bands possessing band-heads (very close grouping of lines sometimes giving appearance of a continuous spectrum), this secondary spectrum of hydrogen showed no such characteristics. As an example of characteristic banded structure with systems of bands possessing



band-heads picture of the spectrum of cyanogen molecule will serve excellent purpose. The following picture shows part of the spectrum of CN-molecule. The banded structure and band heads referred to above are clearly evident in the picture.



CN-Molecule Pictures of the spectrum of CN-molecule.

As stated above, the spectrum of hydrogen on the other hand instead of showing any such characteristic structure of band spectra seemed to consist of fairly widely spaced lines, and therefore greatest difficulty was found in attacking its analysis, as in early investigations of all molecular band spectra the band heads had always served as the best clues for classification. Fulcher was the first to give the clue that in the secondary spectrum also there are nearly constant frequency (vibration frequency) differences as is characteristic of other molecular spectra. The reason why spectrum shows no band heads is that the frequency intervals (rotation frequency intervals which are approximately equal to  $2B$ ) in the lines are large as the rotation term  $B$  for hydrogen is large.

$$B = \frac{h}{8\pi^2 I_0}$$

$$I_0 = \frac{M_h r^2}{4}$$

where,

$h$  = Planck's universal constant.

$I_0$  = moment of inertia of  $H_2$  mol.

$M_h$  = mass of hydrogen atom.

$r$  = the distance between the H-atoms in the molecule.

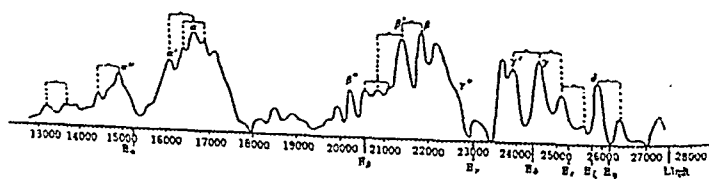
As in the case of hydrogen  $I_0$  is very small on account of  $M_n$ ,  $B$  which is inversely proportional to  $I_0$  is, therefore, large and consequently the frequency intervals (approximately  $=2B$ ) are large. This may be better realised after we shall have dealt (in brief) with the theory of bands.

Glitscher at the instigation of Sommerfeld plotted the intensities of the lines of the secondary spectrum (in the visible) and got marked maxima near about the  $H_\alpha, H_\beta, H_\gamma, H_\delta$ , Balmer lines of hydrogen atom. The following table is constructed to show how the intensity maxima in the molecular spectrum of hydrogen are situated relatively to the Balmer lines of hydrogen atom.

	$\alpha(A^\circ)$	$\beta(A^\circ)$	$\gamma(A^\circ)$	$\delta(A^\circ)$
H	6563	4861	4340	4102
$H_2$	6018	4490	4025	3812

TABLE I

The following figure illustrates the intensity curves obtained by Glitscher. It needs no additional explanation.



Intensity Curves by Glitscher.

In 1926 Richardson undertook an extensive investigation of the secondary spectrum. He showed that the four above groups obtained from Glitscher's analysis really

formed four band systems of similar structure. He also found that their electronic terms formed Rydberg sequences like the  $H_\alpha$ ,  $H_\beta$ ,  $H_\gamma$ ,  $H_\delta$ , Balmer lines and therefore denoted them by analogy as  $\alpha$ ,  $\beta$ ,  $\gamma$ ,  $\delta$ .

### ULTRA-VIOLET SPECTRUM

Lyman was the first to discover a number of bands in the extreme ultra-violet (in the Schumann region) these were further extended by Wigner. Witmer showed that they consist of a long progression of the same initial levels. Werner, in 1926, found a number of bands extending into farther extreme ultra-violet region (Lyman region). The bands discovered by Lyman and Werner are known after their discoverers as Lyman and Werner bands respectively. Dieke and Hopfield, in 1927, obtained absorption spectra of cold hydrogen gas and found that both Lyman as well as Werner bands were present in absorption. It was thus evident that both these systems of bands had the same initial level (in absorption, or the same final level in emission)—the ground state 'A' of hydrogen molecule. The transitions were represented as

Lyman bands       $A \longleftarrow B$ ,

Werner bands     $A \longleftarrow C$ ,

The level 'B' is about 90000  $\text{cms.}^{-1}$  above 'A' and the level 'C' is about 99000  $\text{cms.}^{-1}$  above 'A.' All these points will be detailed in the discussion to follow later on. Hori has made a more or less complete analysis of Werner bands. According to him these bands consist of P, Q, and R branches. He has also partly analysed the Lyman bands and concludes that these bands contain an R and identical P and Q' branches. Dieke and Hopfield from their absorption spectra had also given part analyses of both these bands. Later Schaafsma and Dieke gave an almost complete analysis of the Lyman bands as regards their vibrational and rotational structures. They obtain only P and R branches.

There are reasons (as will be seen later) to suppose that  $Q'$  branch is altogether absent. Now as the Werner, as well as, Lyman bands end on the ground state (and consequently obtained in absorption also) are, therefore, by analogy in the same relation to the  $\alpha, \beta, \gamma, \delta$ -bands, as the Lyman series to the Balmer series of lines.

## EXPERIMENTAL

The secondary spectrum of hydrogen is probably the most complicated of molecular spectra and as referred to above has defied attempts at complete analysis. Several investigators therefore performed qualitative experiments to find the effect of different kinds of excitation on the type of spectrum, so as to obtain clues for analysis. Till very recently, however, no accurate experimental data were available except those of Merton and Barratt. In recent years, however, many other investigators (Tanaka, Sandemann, Allibone, Deodhar, and others) have made accurate measurements in different regions of the secondary spectrum, observed under different conditions of excitation. The most comprehensive investigations were taken up only within the last couple of years in America conjointly by Gale, Monk and Lee and in Germany by Finkelburg, and today very accurate data are available from  $\lambda$  3314 to  $\lambda$  8902. Gale, Mank and Lee, have given measurements of 3064 lines between  $\lambda$  3394 and  $\lambda$  8902 which are accurate up to three places of decimals with the exception of a few lines in the red and infra-red part of the spectrum. Finkelburg obtained a very much larger number of lines and his list contains results of his measurements of 3667 lines between  $\lambda$  3314 and  $\lambda$  4860 measured accurately up to three places of decimals. Thus very excellent data for investigation into the structure and analysis of the spectrum exist from the near ultra-violet to the near infra-red. Though

almost all lines in the extreme ultra-violet seem to have been explained, there still remain some which have not yet been classified. The data in this region are those due to Lyman, Wigner, and Werner. It may be expected that additional data in this region may not only be helpful but is necessary for a more complete elucidation of the spectrum. The same may be said about the infra-red part of the spectrum where comparatively very little of good data are available, at present.

## THEORETICAL

### THEORY OF THE ELECTRONIC BAND SPECTRA

Before taking up a theoretical discussion of the spectrum it may not be out of place to give a brief survey of the theory of band spectra and the mechanism of their emission. It is quite well-known that in the case of atoms the atomic energy in the normal or any excited state is directly dependent upon and, therefore, determined from the configurations of the electrons in the atom. In the case of molecules, however, the matters are not so simple. The total energy 'W' possessed by a molecule is due to, and governed by, three factors :

- (1) Its electronic state; that is, the configuration of the electrons in the molecule. These as in atoms are a system of quantised states.
- (2) Its vibrational state; that is, the amplitude of vibrations of the nuclei of the molecule along the line joining the nuclei in the simple case of diatomic molecules. The amplitudes of the nuclear vibrations and therefore the vibrational energy can have only a set of values quantised by the vibrational quantum number ' $v$ '.
- (3) Its rotational state; that is, the angular velocity with which the nuclei rotate about an axis perpendicular to the nuclear axis (in diatomic

molecules). This angular velocity and therefore the rotational energy can possess only a set of values quantised by the rotational quantum number ' $m$ '.

The energies possessed by the molecule on account of these factors are respectively termed as—(a) electronic energy ( $W_e$ ), (b) vibrational energy ( $W_v$ ), and (c) rotational energy ( $W_r$ ). The total energy ' $W$ ' of the molecule therefore is given by,

$$W = W_e + W_v + W_r$$

It has been definitely established that the vibrational energy  $W_v$  of a molecule is given by the simple relation

$$W_v = v h \nu_0 (1 - x_v \dots \dots \dots)$$

where,  $v$  is the vibration quantum number (with half integral values of magnitude depending upon the state of vibration of the nuclei)

$$x = \frac{h}{4\pi^2 I_0 \nu_0} \left( \frac{3}{2} + \frac{15}{2}b + \frac{3}{2}c + \frac{15}{4}b^2 \right)$$

$\nu_0$ —the natural frequency for very small amplitudes of vibration of the molecule

Also  $W_r$  the rotational energy is given by the simple relation

$$W_r = \frac{h^2 m(m+1)}{8\pi^2 I} \text{ or } B h m(m+1); B = \frac{h}{8\pi^2 I}$$

where,  $h$  = Planck's universal constant.

$I$  = Moment of Inertia of the molecules.

$m$  = Rotational quantum number (having all integral values 0, 1, 2, . . .)

Now the total energy ' $W$ ' of the molecule can change corresponding to changes in any of the energies  $W_e$ ,  $W_v$ ,  $W_r$ . It may be mentioned here that generally in molecular spectra the magnitudes of these energies are in the order,

$$W_e \gg W_v \gg W_r$$

and also the magnitudes of the changes in these energies are in the order,

$$\Delta W_e \gg \Delta W_v \gg \Delta W_r.$$

Let us for the time being restrict ourselves to the changes  $\Delta W_v$  and  $\Delta W_r$ . It is known that the change  $\Delta W_v$ , in the vibrational energy, can take place only by transitions of the molecule from one vibrational state corresponding to a particular integral (or strictly, half integral) value of the vibration quantum number  $v$  to another state with another value  $v'$  so that  $\Delta V = v' - v$  is an integer which may have any integral value  $\pm 0, 1, 2, \dots$ . On the other hand the change  $\Delta W_r$ , in the rotational energy is restricted by the selection rule that  $\Delta m$  (the change in the rotational quantum number) must be,

$$\Delta m = 0, \text{ or } \pm 1.$$

Now, the total change of energy at any instant produced by the above three effects will be given out as a monochromatic radiation (forming one of the lines of the bands) of frequency  $\nu$  such that

$$\nu = \frac{\Delta W_e + \Delta W_v + \Delta W_r}{h}$$

$$\nu = \nu_e + \nu_v + \nu_r$$

where  $\nu_e$  etc. are the corresponding frequencies,  
or substituting for  $\nu_r$

$$\nu = \nu_e + \nu_v + \left( \frac{hm(m+1)}{8\pi^2 I} - \frac{h(m+1)(m+2)}{8\pi^2 I'} \right)$$

$$= \nu_e + \nu_v + Bm(m+1) - B'(m+1)(m+2)$$

$$B = \frac{h}{8\pi^2 I} \text{ and } B' = \frac{h}{8\pi^2 I'}$$

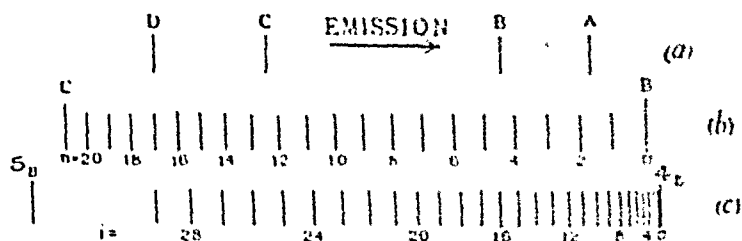
$I$  and  $I'$  are the moments of inertia of the molecule in the two different states of rotation.

Now as has been mentioned above the magnitudes of the frequency-values are generally

$$\nu_e \gg \nu_r \gg \nu_v$$

The above equation thus signifies that corresponding to every electron configuration of the molecule there is a set of vibrational states defined by the vibrational quantum numbers  $v=0, 1, 2, 3, \dots$ , and that corresponding to each of these vibrational states there is a set of rotational states

defined by the rotational quantum numbers  $m=0, 1, 2, \dots$ . This has been very beautifully illustrated by a diagram (due to Birge) reproduced below. It is a schematic representation of a part of the energy levels for the second positive group of Nitrogen.



- (a) Set of electronic levels, drawn to scale for the neutral nitrogen molecule.  $A-D=55,110 \text{ cm}^{-1}$ .  
 (b) Set of vibrational levels attached to electronic level  $B$ , and constituting initial states of the first positive group of nitrogen.  $20_v-0_v=29,477 \text{ cm}^{-1}$ .  
 (c) Partial set of rotational levels attached to vibrational level  $4_v$ , and constituting final states of the  $\lambda 3710$  band of the second positive group of nitrogen. In the  $\lambda 3371$  band, this set has been followed to  $j=96$ .

Picture of Energy levels of Second Positive Group of Nitrogen (Report on Molecular Spectra, p. 102, Birge.)

The set of vibrational states given correspond to a particular electronic configuration (say B). Again taking a particular vibrational state (say  $v=4_v$ ) of this set there is a number of rotational states corresponding to it as represented in the diagram. Thus when an electron transition takes place, say, from C to B, there are possible several transitions between the various vibrational states corresponding to C and B. Again restricting ourselves to a particular vibrational transition out of these (say,  $4_v \leftarrow 6_v$ ) there are possible several different transitions between the different rotational states corresponding to each of the two vibrational states ( $4_v \leftarrow 6_v$ ). Thus for each transition between two vibrational states there is a band (corresponding to the different transitions in the rotational states) with positive, negative, and zero branches corresponding to the change



$\Delta m = +1, -1$  or  $0$ , respectively, of the rotational quantum numbers. The above equation can be put in the form

$$\nu = A \pm Bm + Cm^2 \text{ for } \Delta m = \pm 1$$

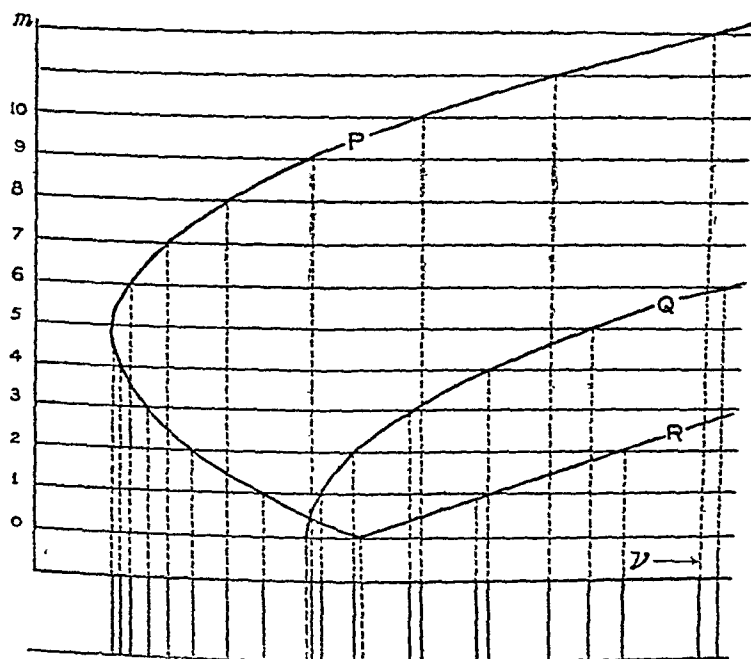
$$\text{where, } A = \nu_e + \nu_r + \frac{h}{8\pi^2 I}$$

$$B = \frac{h}{8\pi^2 I}$$

$$C = -\frac{h}{8\pi^2} \left( \frac{1}{I} - \frac{1}{I'} \right)$$

$$\text{or } = A' + Cm^2 \text{ for } \Delta m = 0, A' = \nu_e + \nu_r$$

$W_e$  and  $W_r$  being fixed the Change in  $W_r$  gives the above equation. Plotting the  $\nu, m$  curve two parabolas are obtained for  $\Delta m = +1$  and  $-1$ . These branches are known as positive (or R), and negative (or P) branches respectively. The picture below clearly explains this. Mark how the negative branch turns upon itself for higher values of  $m$ . There is a crowding of lines near this turning point, which gives to the band the appearance of a head at this place. These diagrams are known as Fortrat's diagram of bands,



Fortrat's Diagram—(Report on Molecular Spectra, Birge, —p. 50).

For  $\Delta m = 0$ , we get  $r = A' + Qm^2$  which also gives a parabola, and this system of lines is known as the zero or Q branch of the band.

In general each band is characterised with a head which, as referred to above corresponds to an apex in the negative branch. Bands with the same value of  $\Delta r$ , (say 2) but different values of  $r'$  and  $r''$  (e.g. 0' and 2'', 1' and 3'', 2' and 4'', . . . .) form a group of bands with a series of subheads under a chief head which is the strongest and generally corresponds to transitions,

$$\begin{aligned} r' = 0 &\longrightarrow r'' = 0 \\ \text{or } r' = p &\longrightarrow r'' = 0 \\ \text{or } r' = 0 &\longrightarrow r'' = p \end{aligned}$$

For other values of  $\Delta v$  (say 1, 3, 4 etc..) there are other similar groups of bands and so on. All these above are band systems for a particular electron transition, say, C to B. For other electron transitions (say, from D  $\longleftarrow$  B) there will be such other systems of bands, but they will lie in other region at a comparatively greater distance. With this information about the theory and mechanism of the emission of band spectra, we shall proceed with the theoretical discussion of the secondary spectrum of hydrogen.

## THEORETICAL DISCUSSION

It has been emphasised by several investigators that the secondary spectrum of hydrogen resembles that of He-atom on the one hand, and of He<sub>2</sub>-molecule on the other. The points of resemblance may be summarised as follows:

(a) Like the He-atom or the He<sub>2</sub>-molecule the electronic terms of H<sub>2</sub> are divisible into two distinct sets of non-intercombining states, triplets and singlets (ortho- and par- of He, and He<sub>2</sub>).

(b) As in the case of  $\text{He}_2$ -molecule the spacings of lines in the  $\text{H}_2$ -bands are wide and there are no heads.

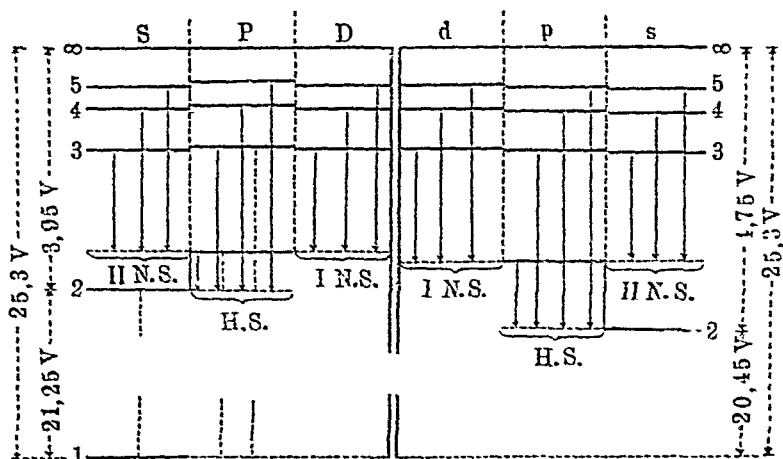


Diagram for showing par- and ortho-helium terms (Atomic Structure and Spectral Lines, Sommerfeld, Third Edition, English Translation, p 323). The two thick vertical lines in the central part of the diagram indicate that direct transitions between the par-helium and ortho-helium terms are not admissible.

(c) In the case of  $\text{He}_2$ -bands the alternate rotation levels are altogether absent thus causing absence, in the spectrum, of alternate lines in the rotational structure of the bands. In  $\text{H}_2$ -bands all the levels are present but are alternately weak and strong thus giving rise to alternation of strong and weak intensities of lines in the rotational structure.

(d) In hydrogen as in the case of helium ( $\text{He}_2$ ) the electronic ( $W_e$ ), vibrational ( $W_v$ ), and rotational ( $W_r$ ) energies of the molecule do not differ widely in magnitude as otherwise is commonly the case in molecular spectra in general. It has been already remarked before that for molecular spectra generally,  $W_e \gg W_v \gg W_r$ . But in the case of  $\text{He}_2$ ,

$W_e$  may be as small as  $1000 \text{ cm}^{-1}$

$W_v$  may be as great as  $1700 \text{ ,,}$

and  $W_r$  may be as great as  $3000 \text{ ,,}$

So also in the case of  $\text{H}_2$ , though this is less exaggerated than in  $\text{He}_2$ , they do not differ so widely as in other spectra. In hydrogen,

$W_r$  is as small as  $3107 \text{ cms.}^{-1}$  (for  $\delta$  bands)

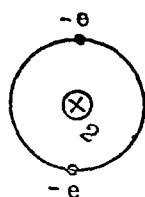
$W_r$  is as great as  $4159$  „ (A<sub>0</sub>—A<sub>1</sub>)

$W_r$  is as great as  $110$  „

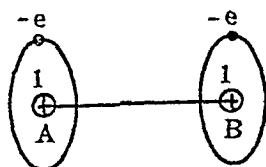
Let us now consider the electronic terms in the  $\text{H}_2$  molecule leaving aside for the present the vibrational and rotational terms. It is a well-known fact that before the development of modern atomic theories and even till the time the celebrated Heisenberg-Hund theory entered upon the field of spectroscopy the classification of the atomic spectral lines was carried out with arbitrary nomenclature assigned to the terms corresponding to different electronic states; the nomenclature being created at the free will of the individual investigator. With the advent of Hund's theory the whole jumble of arbitrary notations has been cleared up and a thorough and systematic elucidation of spectrum due to any atom can be given on a uniform and well established system of notation. A coordination between the electronic configurations of any atom and the types and number of possible terms arising from them can be conveniently worked out without much difficulty; and the identification of lines and their assignments can be made with definiteness as due to transitions between particular terms belonging to the particular electron configurations of the atom. Similar was (and still to a great extent is) the case with molecular spectra. The electronic transitions had been denoted by early investigators on arbitrary nomenclature as between electronic states  $A \leftarrow B$  or  $A \leftarrow C$  and so on (as is done in the case of Lyman and Werner bands of hydrogen). Such nomenclature, however, does not give any definite picture of the real process as is now obtainable in the case of atoms. In recent years, however, after the Heisenberg-Hund theory was fully recognised to have achieved

almost unquestioned success in the complete elucidation of atomic spectra, the same authors made attempts to extend the theory so as to be applicable to the case of molecules also; and they have pointed out that the same theory as was applied in calculating terms from electron configurations in the atom can be applied with some modifications for calculating the electronic energy levels from the electron configurations in molecules. This extension of the theory, however, has found success to a certain extent in the simple case of diatomic molecules. An explanation of the  $\text{He}_2$ -spectrum on this new electronic level scheme has been given to a certain extent by Curtis and Harvey (Proc. Roy. Soc., 125), while Richardson and coworkers as well as Finkelburg and Mecke have been only partly successful in doing so in the case of hydrogen. Very few assignments have been made with certainty. The details of this will follow in later discussion; for the present we shall consider in what manner has the Heisenberg-Hund theory been modified by its authors so as to fit in the case of molecular spectra.

The main features of this theory for the case of molecules may be briefly summarised as follows: We shall take the case of diatomic molecules only, and in particular that of hydrogen. Below are given pictures of the He-atom and hydrogen molecule for comparison, as one ( $\text{He}$ ) is an *atom* containing two electrons and the other ( $\text{H}_2$ ) is a *molecule* containing two electrons. A comparison of the two cases will be very interesting.



He-atom

 $\text{H}_2$ -molecule

A and B are the nuclei of the H-atoms in the  $\text{H}_2$ -molecules

## THE HEISENBERG-NEED THEORY FOR DIATOMIC MOLECULES.

(1) As on the central nuclear field is superposed a strong electric field (due to the two nucleii) along the nuclear axis, there should arise term sequences additional to the usual S, P, D, . . . in atoms.

(2) In atoms each electron has orbital angular momentum corresponding to azimuthal quantum number  $k$ , (for an individual electron) and a half quantum number  $s_e = \frac{1}{2}$  of the spin angular momentum. The result of all the  $k$ 's and  $s$ 's is denoted by ' $l$ ' and ' $s$ ' respectively. In molecular case this ' $l$ ' (the resultant of all electronic  $k$ 's) may be expected in the ordinary case to execute an essentially uniform precessional motion about the inter-nuclear axis because of the strong axial field due to the nucleii being superposed on the central field. The ' $l$ ' of the electrons being electrically coupled to the nuclear axis gets, therefore, quantised about it and gets resolved into two components one  $\lambda$  along this axis and the other perpendicular to it. The latter component may not concern us here for the present. The  $\lambda$  may have any integral values between ' $l$ ' and 0. Thus for,

$$\begin{array}{ll} 'l' = 0 & \lambda_1 = 0 \\ 'l' = 1 & \lambda_1 = 0 \quad \lambda_2 = 1 \\ 'l' = 2 & \lambda_1 = 0 \quad \lambda_2 = 1 \quad \lambda_3 = 2 \end{array}$$

and so on.

(3) As in atomic spectra ' $s$ ' is not affected directly by the electric field of the nucleii, but it tends to interact magnetically with ' $l$ '. Here  $\lambda$  (the component of ' $l$ ' along the nuclear axis) is effective in orienting ' $s$ ' (as ' $l$ ' precesses rapidly about this axis). There may arise two cases in this interaction between  $\lambda$  and ' $s$ '.

- (i) *The interaction between  $\lambda$  and ' $s$ ' sufficiently intense.*—(In this case ' $s$ ' is quantised with respect to the internuclear axis about which it precesses. The corresponding quantum number is ' $s$ '. This always happens when the molecule does not rotate as a whole and when  $\lambda > 0$  (for  $\lambda = 0$  means no

component of 'l' along the axis). With given values of  $\lambda$  and 's' the same terms as in the case of atom arise, but unlike the atoms the components will be equally spaced though the separation is of the same order of magnitude as in atoms.

- (ii) *The interaction between  $\lambda$  and 's' small.*—In this case the torque causing 's' to follow the rotation of the nuclear axis may become inadequate as the rate of the nuclear rotation increases. A gradual transition would then occur with increasing 'm' (rotation quantum number). from a condition in which 's' was quantised along the nuclear axis to a condition in which 's' is oriented and quantised with respect to K, the total rotation moment of the molecule (this is known as uncoupling phenomenon).

With this introduction let us now proceed to calculate and compare the electronic terms of the  $H_2$ -molecule and  $H_2$ -atom. We shall first calculate the terms of the  $H_2$ -atom. The normal  $H_2$ -atom has both the electrons in the  $K_1$ -level. The excited states are obtained (supposing one of the two electrons to be always fixed in the  $K_1$ -level) by the combinations:—

$K_1 X_1, K_1 X_2, K_1 X_3, \dots$   
 where  $X_1$  represents the  $L_1, M_1, N_1, \dots$  levels  
 $X_2$      "     "      $L_2, M_2, N_2, \dots$      "  
 $X_3$      "     "      $M_3, N_3, O_3, \dots$

Then for the different electron configurations we get the corresponding terms in Helium as follows:—

TABLE II

Electron Config.		Terms
Normal atom $2K_1$	$l_{e1} = 0, l_{e2} = 0; L=0$ $s_{e1} = \pm \frac{1}{2}, s_{e2} = \mp \frac{1}{2}; S=0$ (Pauli's principle)	$\therefore {}^1S_0.$
Excited atom $K_1 X_1$	$l_{e1} = 0, l_{e2} = 0; L=0$ $s_{e1} = \pm \frac{1}{2}, s_{e2} = \pm \frac{1}{2}; S=0,1$	$\therefore {}^1S_0, {}^3S_1.$

TABLE II (Continued).

Electron Config.		Terms
$K_1 X_2$	$l_{11}=0, l_{12}=1; L=1$ $l_{e1}=\frac{1}{2} s_{e2}=\frac{1}{2}; S=0,1$	$^1P_1, ^3P_{0,1,2}$
$K_1 X_3$	$l_{11}=0, l_{12}=2; L=2$ $s_{e1}=\frac{1}{2} s_{e2}=\frac{1}{2}; S=0,1$	$^1D_2, ^3D_{1,2,3}$

In this way we get the electronic terms of He-atom. In the case of the  $H_2$ -molecule though the number of electrons is the same as in He-atom (*viz.*, two) the matters are more complicated as mentioned above on account of the presence of two nuclei and a consequent axial field between them. The same procedure is to be adopted in calculation of terms for  $H_2$  as in the He-atom, with the only difference that instead of the  $l$ 's (the angular momenta for the different electrons) we have now to use  $\lambda$ 's (the components of  $l$ 's along the nuclear axis). Here also we make the assumption that whereas in the normal  $H_2$ -molecule the electron in both the atoms is in the  $K_1$ -level of the corresponding atom, not more than one electron is displaced in the excited state of the molecule; that is, one of the two electrons always remains fixed in the normal ( $K_1$ )-level of its atom, and that the other electron runs up to the higher levels. Richardson justified this assumption on the ground that as yet no such evidence has been found from the energy values that in any of the known levels more than one electron is excited. Thus we have got in  $H_2$ ,

one atom	other atom
$K_1$	$K_1$
(1)	(1)
$L_1, L_2$	$L_1, L_2$
	(1) (1)
$M_1, M_2, M_3$	$M_1, M_2, M_3$
	(1) (1) (1)
Normal	Excited



(It may be remarked here that even in this simplest case of hydrogen molecule it is not possible to give a physical picture of the actual state of the molecule in excitation.)

In the normal state of the molecule both the atoms will have electrons in the  $K_1$ -levels (that  $1s$ -states). The corresponding spectral terms are, therefore,

Electrons Config.	Terms
$K_1K_1$	$l_1=0, l_2=0$ $\lambda_1=0 \lambda_2=0 \therefore$ the resultant $\Lambda=0 \therefore$ a $\Sigma$ state

(Extending Pauli's principle to molecular case also, we suppose that the spins  $s_1 = +\frac{1}{2}$  and  $s_2 = +\frac{1}{2}$ , the resultant spin 'S'=0. The  $\Sigma$  term is therefore a singlet. The normal state of hydrogen molecule is therefore a  $^1\Sigma$  state corresponding to the  $^1S_0$  in the case of atoms (He-atom). This is consistent with the fact that hydrogen molecule is diamagnetic. Let us now calculate the terms for excited states  $K_1X_1, K_1X_2, K_1X_3 \dots$  of the hydrogen molecule.

Electrons Config.	Terms
$K_1X_1$	$\begin{array}{l} 1s \quad ns \\ l_1=0, \quad l_2=0; \\ \lambda_1=0, \quad \lambda_2=0; \\ \therefore \Lambda=0 \end{array} \left. \begin{array}{l} s_1=\frac{1}{2}, \quad s_2=\frac{1}{2}; \\ S=0, 1. \end{array} \right\} \begin{array}{l} {}^1\Sigma, {}^3\Sigma \end{array}$
$K_1X_2$	$\begin{array}{l} 1s \quad np \\ l_1=0, \quad l_2=1; \\ \lambda_1=0, \quad \lambda_2=0, 1 \\ \Lambda=0, 1. \end{array} \left. \begin{array}{l} s_1=\frac{1}{2}, \quad s_2=\frac{1}{2}; \\ S=0, 1. \end{array} \right\} \begin{array}{l} {}^1\Sigma, {}^3\Sigma \\ {}^1\pi, {}^3\pi \end{array}$
$K_1X_3$	$\begin{array}{l} 1s \quad nd \\ l_1=0, \quad l_2=2; \\ \lambda_1=0 \quad \lambda_2=0, 1, 2. \\ \Lambda=0, 1, 2. \end{array} \left. \begin{array}{l} s_1=\frac{1}{2}, \quad s_2=\frac{1}{2}. \\ S=0, 1. \end{array} \right\} \begin{array}{l} {}^1\Sigma, {}^3\Sigma \\ {}^1\pi, {}^3\pi \\ {}^1\Delta, {}^3\Delta \end{array}$

Comparing all these terms due to the  $H_2$ -molecule with those of the He-atom (as is done in the following

table) it will be quite evident that the corresponding terms in  $H_2$  are much larger in number.

TABLE III

Configuration.	He-Terms.	$H_2$ -Terms.
$K_1 K_1$	$^1S_0$	$^1\Sigma$
$K_1 X_1$	$^1S_0, ^3S_1$	$^1\Sigma, ^3\Sigma$
$K_1 X_2$	$^1P_1, ^3P_{0, 1, 2}$	$^1\Sigma, ^3\Sigma, ^1\pi, ^3\pi$
$K_1 X_3$	$^1D_2, ^3D_{1, 2, 3}$	$^1\Sigma, ^3\Sigma, ^1\pi, ^3\pi, ^1\Delta, ^3\Delta$

Comparison of the terms of  $H_2$ -molecule with those of He-atom.

It is necessary to mention here that the terms,  $\Sigma, \pi, \Delta$ , etc., correspond to values of  $\Lambda = 0, 1, 2, \dots$  respectively (as is evident from the calculation of the terms made above), and are so denoted by the Greek symbols merely to distinguish them from the atomic terms S, P, D, . . . for ' $l=0, 1, 2, \dots$ '. The selection rules for the molecular case are like the atomic case,

$$\Delta\Lambda = \pm 1$$

$\Delta S = 0$ , That is, no inter-combination of the triplet and singlet system is supposed to be allowed.

After thus calculating the electronic terms for different electron configurations of the excited molecule, attempts have been made by some investigators (Richardson and his co-workers, Finkelburg and Mecke, and others) at assigning definite electronic level terms on this new scheme to the arbitrarily denoted terms (A, B, C, L, M, N, . . .) used in the earlier analyses by different investigators. And though it has not

been possible to make these identifications of levels completely and with perfect definiteness, it seems so far quite certain that the steps are being taken in the right direction.

### CLASSIFICATION

The following table is drawn to represent the structure of electronic terms of  $H_2$  and gives the terms that are either definitely or provisionally identified and evaluated. A reference to this table will be helpful in following the details of classification of the bands identified up till now, as regards their electronic displacement according to the extended Hund's theory to molecular cases.

## EXPLANATION OF THE TABLE

Each horizontal row in the table corresponds to the same total quantum number,  $n=1, 2, 3, 4, \dots$  (written at the beginning of each row) according as the excited electron is in the  $L, M, N, \dots$  level ( $n=1$  being the normal state,  $K_1$  of the running electron and therefore of the molecule also). Each row is divided into columns as represented at the top by the ' $l$ ' values  $0, 1, 2, \dots$  (or the letters  $s, p, d, \dots$ ) of the excited electron, according as it occupies the  $X_1, X_2, X_3, \dots$  sublevels. The electronic terms corresponding to any excited state of the molecule (with given  $n$  and ' $l$ ' values) are written in the corresponding columns by dividing the columns into requisite number of parts (equal to the number of electronic terms for the given  $n$  and ' $l$ '). The numbers  $1, 3$ , written alternately in the sections along each row represent the multiplicity (singlet or triplet) of a term. Thus for the normal state of  $H_2$  ( $K_1 K_1$ ) corresponding to  $n=1$  and ' $l$ '= $0$  we have as calculated before, only a  $^1\Sigma$  term. It has been written in the corresponding position in the table as  $1s^1\Sigma$ , denoting by the prefix ( $1s$ ) the  $K_1$ -state of the running electron. The absence of  $1s^3\Sigma$  state (according to Pauli's principle) is supported as referred to before, by the fact that  $H_2$ -molecule is diamagnetic. For  $n=2$  there are two levels ( $L_1$  and  $L_2$ ) corresponding to the two ' $l$ ' values, ' $l$ '= $0$  and ' $l$ '= $1$ . The corresponding electronic terms due to each of these configurations ( $L_1$  and  $L_2$ ) of the running electron as calculated above are written at the head of each section in the respective columns,  $2s^1\Sigma$  and  $2s^3\Sigma$  for  $L_1$  and  $2p^1\Sigma, 2p^3\Sigma, 2p^1\pi, 2p^3\pi$ , for  $L_2$ . For  $n=3$  there are three levels  $M_1, M_2, M_3$  for the ' $l$ ' values  $0, 1, 2$ , respectively. The same procedure as above is adopted in this case also in writing the electronic terms in the table. The numbers in each section written below the term designation

signify the frequency values of the electronic terms, and those of the first vibration and rotation levels respectively. Where these latter (the term values for the first vibration and rotation levels) values are not known the respective places are left blank. Values not known definitely are marked (?). The abbreviations (*ab.* and *ca.*) represent 'about' and 'calculated' respectively.

### ULTRA-VIOLET BANDS

Band systems in this region were, as referred to on the beginning, discovered by Lyman and later extended by Wigner. Werner discovered another system of bands on the still shorter wavelength side of Lyman bands. As in Dieke and Hopfield's investigation of absorption spectrum of cold  $H_2$  gas both Lyman as well as Werner bands were obtained, it is quite definite that they both end on the ground state A (in the case of emission bands) of the  $H_2$ -molecule. On the new system of identification this ground state A and the electronic states B and C involved in the Lyman and Werner bands respectively ( $A \leftarrow B$  Lyman bands;  $A \leftarrow C$  Werner bands) are identified with electronic levels as follows,

$$A=1s^1\Sigma, B=2p^1\Sigma, C=2p^1\pi.$$

The identification of A (the ground state) with  $1s^1\Sigma$  (the ground state of the molecule as calculated by the new theory) is quite evident from the above explanation. As regards the identification of B and C, out of the possible levels in total quantum number two, only  $2p^1\Sigma$  and  $2p^1\pi$  (which is double  $2p^1\pi_a$  and  $2p^1\pi_b$ ) are capable of combining with  $1s^1\Sigma$  giving strong band systems in this region. The level B, of Lyman bands (which contain P and R branches only and in which the Q branch is altogether missing) has no rotational level missing and gives P and R branches only in combining with  $1s^1\Sigma$  and is therefore

identified with  $2p^1\Sigma$  as these above properties of the bands are exactly those to be expected of a  $\Sigma$ -level. The level C of the Werner bands (which shows the properties of a  $\pi$ -level, *e.g.*, the initial rotation levels are altogether missing, and gives P, Q, R, branches in combining with  $1s^1\Sigma$ ) is therefore identified with  $2p^1\pi$ -level. These bands give P, Q, and R branches; and all known facts are in agreement with the classification.

Besides these bands lying in the extreme ultra-violet, there have been discovered by Richardson, band systems in the near ultra-violet (and some part of violet also) ending on Dicke's B-level (the  $2p^1\Sigma$ -level). The initial levels giving rise to this system of bands are arbitrarily termed as  $4^1A$ ,  $4^1B$ ,  $4^1C$ ,  $4^1E$ ,  $4^1x$ . Their effective quantum numbers lie between 3.9 and 4.1. They have very low term values and therefore for four of them only  $0' \leftarrow n''$  progression is known and only for one the  $1' \leftarrow n''$  progression also is obtained. Out of these systems

$$2p^1\Sigma \leftarrow 4^1B, 2p^1\Sigma \leftarrow 4^1C, \text{ and } 2p^1\Sigma \leftarrow 4^1E$$

are the strongest. The others  $2p^1\Sigma \leftarrow 4^1A$ ,  $4^1x$  are quite weak. As is shown by Richardson in his diagram of electronic levels all these five levels lie very close to one another and their band systems are very much mixed up together, strong parts of one system overlapping the weaker parts of the other. It is, therefore, very difficult to obtain a detailed classification and explanation of these systems. Richardson from a consideration of their properties assigns these levels provisionally as follows:—

$$4^1A=4d^1\pi_a, 4^1B=4d^1\pi_b, 4^1C=4d^1\Sigma, \left. \begin{matrix} 4^1C \\ 4^1E \end{matrix} \right\} = 4d^1\Sigma \left. \begin{matrix} \\ 4s^1\Sigma \end{matrix} \right\} ?$$

$$\text{and } 4^1x=4d^1\Delta^a \text{ or } b.$$

He remarks in this connection that for effective quantum number 4, there are no more known levels than the current theories can account for; of course, this may only mean that

there are others which are weak and have not yet been detected.

### VISIBLE BANDS

There is a very large number of bands in the visible. Let us first consider the  $\alpha, \beta, \gamma, \delta$ -bands which were the first band systems to be discovered in the secondary spectrum of hydrogen. As referred to in the beginning Glitscher was the first to obtain evidence of the existence of these band systems. Richardson later found that the null frequencies of these bands formed a Rydberg sequence, having a common final level. He and Das give a detailed classification, as regards the vibration and rotation structures of the Q-branches of the  $\alpha$  and  $\beta$  bands. Later on Finkelburg and Mecke gave a detailed vibration and rotation analysis of the Q-branches of the  $\alpha, \beta, \gamma$  and,  $\delta$ -band systems. Recently Richardson and Das have given further analysis of the  $\alpha$  and  $\beta$  bands as regards their vibration and rotation structures of the P' and R' branches also.

Richardson finds that for the initial levels of the  $\alpha, \beta, \gamma$ , and  $\delta$ -bands the effective total quantum numbers are,

$$\begin{aligned} \text{for } \alpha &= 2.937 \\ \beta &= 3.942 \\ \gamma &= 4.95 \\ \delta &= 5.95 \end{aligned}$$

and that for the final level it is 1.933.

The properties of the initial terms are identical with the initial terms of the principal series of ortho-Helium. It is interesting to compare the term values of these levels.

TABLE V

Ortho-Helium.		Hydrogen Molecule.	
Terms	Term Values	Term Values	Terms
3P	12746	12719	$3p\pi$
4P	7093.6	7067	$4p\pi$
5P	4510	4493	$5p\pi$
6P	3117	3107	$6p\pi$

All these bands have  $P'$ ,  $Q$  and  $R'$  branches, with  $Q$  strongest and  $P'$  weakest. This is found to be so on analysis on account of the double nature of the initial ( $=_a, =_b$ ) levels. No uncoupling has been found in these levels. The first rotation levels are missing. All these considerations lead to the conclusion that these initial levels must be  $mp \pi$ -levels ( $m = 2, 3, 4$ , and  $5$ ). Richardson is in favour of calling these levels as triplet  $\pi$ -levels ( $mp^3 \pi$ ) whereas Finkelburg assigns to them a singlet multiplicity ( $mp^1 \pi$ ). Richardson's justification for attributing triplet multiplicity to them is based on two facts. Firstly, as shown above the term-values have very close equality to ortho-helium (triplet) atomic P-terms, and secondly,  $2s^1 \Sigma$  which would otherwise be the final level for these bands has been already identified and explained as combining with  $2p^1 \Sigma$  to give strong band systems in the infra-red. Both these, however, are not quite decisive justifications. One point should be further noted that the triplet character assigned to these levels has not yet been found to exist actually; the lines are all single. This may perhaps be due to extremely small separations of component lines which may be further masked by the broadening of the spectral lines, which is so prominent in the case of hydrogen on account of its very small mass. The difficulties in accepting either Richardson's or Finkelburg's views as final will be stated later on at a more appropriate place, when we shall have discussed a few more bands. It may be mentioned here in brief about the vibration and rotation structure analysis of these bands, that the classification is extremely accurate, being correct to  $0.1 \text{ cm}^{-1}$ . The data used by Richardson and Das are that supplied by Gale, Monk and Lee. Several strong lines have been explained by this analysis. The unambiguity of the classification is evident from the extreme accuracy (of  $0.1 \text{ cm}^{-1}$ .) attained, in accounting for many of the strongest lines in the secondary spectrum of hydrogen.



A very large number of band systems in the visible is found to have a common final level, going down to the level  $2p^1\Sigma$  (or Dicke's B) level. These initial levels are all discovered by Richardson and arbitrarily denoted by him as  $3^1A$ ,  $3^1B$ ,  $3^1C$ ,  $3^1K$ ,  $3^1L$ ,  $3^1M$ ,  $3^1N$ ,  $3^1O$ ,  $3^1Q$ ,  $\lambda 4097$  (upper),  $\lambda 4143$  (upper), and the levels  $4^1A$ ,  $4^1B$ ,  $4^1C$ ,  $4^1X$ , and  $4^1E$ . These latter ( $4^1A$ , etc.) have been already considered above in the treatment of the ultra-violet bands. The others are to be considered hereafter. Richardson has recently made an attempt, with some success, at assigning to these arbitrarily denoted levels definite states on the new electronic term scheme. In some cases it has been possible to make definite identifications, some are only provisionally identified, while a few have not yet been identified at all. All these levels go down to  $2p^1\Sigma$ -level to give rise to bands in the visible. These levels, however, differ very greatly in their properties and the characteristics of the band systems obtained from the transitions to  $2p^1\Sigma$ . These levels will be taken up one by one, or in groups as may be found convenient, and the justifications put forward by Richardson for identifying them with particular electronic terms on the new scheme, will be considered in each case.

*The band systems from  $3^1A$ ,  $3^1B$ ,  $3^1C$ , to  $2p^1\Sigma$  :—* These band systems are very extensive. They contain four initial and eight or nine final vibrational levels. The systems include some of the strongest lines in the visible spectrum of  $H_2$ . All these bands show uncoupling effect of the type noted in the spectrum of  $He_2$  (this point may be taken up later). The system  $2p^1\Sigma \leftarrow 3^1A$  has only  $P^1$  and  $R^1$  branches whereas  $2p^1\Sigma \leftarrow 3^1B$  has only  $Q$ -branches. Both these ( $3^1A$ ,  $3^1B$ ) have initial rotational levels missing. They are, therefore, evidently  $\pi$ -levels. They also show some uncoupling. Their effective quantum number is approximately 3, and being  $\pi$ -levels they cannot be of  $3s$  origin but must naturally be of  $3d$ -origin. They lie very

close to each other and also to  $3^1C$  which as will be seen below is of  $3d$ -origin; so that they must be,

$$3^1A = 3d^1\pi_a \text{ giving P and R branches}$$

$$\text{and } 3^1B = 3d^1\pi_b \text{ giving Q branch only.}$$

The system  $2p^1\Sigma \leftarrow 3^1C$  gives only  $P'$  and  $R'$  branches. Moreover the level  $3^1C$  has no missing rotational level and shows very pronounced uncoupling; and therefore it must be a  $3d^1\Sigma$ -level. Taking Richardson's views on this to be right, great difficulty arises in trying to explain the fact that whereas the singlet bands

$$3p^1\Sigma \leftarrow 3d^1\Sigma^1\pi$$

show a complicated and abnormal rotational structure the triplet (Fulcher bands)  $2s^3\Sigma \leftarrow mp^3\pi$  which should (on account of the multiplicity of the levels) be expected to show a much more complicated structure are very simple and normal. On the other hand if Finkelburg's view (which removes the difficulty) be adopted the B-level of Dieke must be identified as a triplet ( $2p^3\Sigma$ ) level. This would mean that the Lyman bands ( $A \leftarrow B$ ) which end on  $1s^1\Sigma$  we must expect are intercombination bands,  $1s^1\Sigma \leftarrow 2p^3\Sigma$ . If so, we must expect another very strong system of bands in the extreme ultra-violet, corresponding to the singlet combination,

$$1s^1\Sigma \leftarrow 2p^1\Sigma.$$

But as yet no trace of such band system has been obtained. How to explain this? It seems evident therefore that in absence of further convincing evidences regarding this point the present assignments of these levels is quite uncertain and indefinite.

Two other singlet levels of  $3d$ -origin (*viz.*,  $3d^1\Delta_a$ ,  $3d^1\Delta_b$ ) are capable of giving band systems with  $2p^1\Sigma$  in the visible, though they may be very faint. These levels may be giving the system of bands starting with  $\lambda 4097$ , and  $\lambda 4143$ . The characteristics of the band systems tend to show that the initial levels of the bands beginning with  $\lambda 4097$  and  $\lambda 4143$  as,

$$\lambda 4097 \text{ (upper level)} = 3d^1 \Delta_u$$

$$\lambda 4143 \text{ (upper level)} = 3d^1 \Delta_b$$

giving rise to the corresponding bands in going down to the same final level  $2p^1 \Sigma$ .

From Table I, a transition  $2p^1 \Sigma \leftarrow 3s^1 \Sigma$  may be expected to give a strong system of bands in the visible. None of the unidentified level going down to  $2p^1 \Sigma$  has been yet quite definitely assigned to this state. Richardson ambiguously assigns the levels  $3^1 K$ ,  $3^1 O$  or  $3^1 N$  to this state. The  $3^1 K$ -level though it is more properly in the expected place has got a peculiar rotational structure, and if the  $2'$  progression is placed correctly in this system it shows strong uncoupling which is not to be expected of an  $s\Sigma$ -state. As regards another probable identification of this  $3^1 K$  some suggestions will be made later on.

The  $3^1 O$ -level possesses a rather high energy-value though it shows the proper rotation structure. Moreover, the band system is rather weak whereas the transition,  $2p^1 \Sigma \leftarrow 3s^1 \Sigma$  should be expected to be very strong. Very recently Richardson has discovered bands in the visible green region going down to the level  $2p^1 \pi$  (or the initial level C of the Werner bands). The initial levels  $4^1 A$ ,  $4^1 B$ ,  $4^1 C$ ,  $4^1 E$ , and  $4^1 X$  are identically the same as have been mentioned previously to give bands in the extreme violet and near ultra-violet in going down to  $2p^1 \Sigma$ .

Richardson has identified another level  $3^1 Q$  which gives only one weak progression in going down to  $2p^1 \pi$ . The level has the initial rotational level missing. It may therefore be identified as  $3p^1 \pi$ . The extremely weak nature of the progression can then be explained as due to the fact that the  $3p^1 \pi$  cannot be ordinarily expected to combine with  $2p^1 \pi$  as  $\Delta K=0$  is forbidden by usual selection rules. By this identification Richardson seems to support the view (to be detailed later) of the possible existence of forbidden transitions in molecular spectra. A

more detailed discussion of this point will be taken up later.

### INFRA-RED BAND SYSTEMS

A strong infra-red system of bands has been discovered by Richardson ending on the  $2p^1\Sigma$ -level. The initial level which was originally denoted by Richardson as 'Infra-red' and has a term-value of 25300, has been found by him to definitely have an effective quantum number 2. It should, therefore, evidently be a  $2s^1\Sigma$ -level which alone can be expected to give strong band systems in this region (infra-red) in going down to  $2p^1\Sigma$ . There is, however, found an abnormality of rotation structure, similar to that caused by uncoupling, and this gives a point for doubt as no uncoupling can be expected for  $s\Sigma$ -levels. Richardson, however, assumes this abnormality to be of some other kind and fixes up this 'Infra-red' level as  $2s^1\Sigma$ . It will be shown later that this upper level of the infra-red bands is distinct from the  $2p^1\pi$  which lies very close to it. Other band systems in the infrared have been recently discovered by Richardson. The initial levels  $3^1A$ ,  $3^1C$ ,  $3^1K$  and  $3^1O$  are identically the same as those which give bands in the visible with  $2p^1\Sigma$ . They are comparatively weak systems and full progressions have not been traced for them. These bands have  $P'$ ,  $Q$ , and  $R'$  branches, with  $Q$  generally the strongest and  $R$  the weakest. The bands lie in the near infra-red about  $\lambda$  7000—8000 bands corresponding to  $0' \rightarrow 0''$ ,  $1' \rightarrow 1''$ ,  $2' \rightarrow 2''$  and  $3' \rightarrow 3''$  have been obtained. This final level of these infra-red bands was found to be identical with Hori's C-level (or the  $2p^1\pi$ -level) and is therefore quite distinct from the initial level (termed as 'Infra-red' or the  $2s^1\Sigma$ -level, of the strong infra-red system ending on  $2p^1\Sigma$  though the levels ( $2s^1\Sigma$  and  $2p^1\pi$ ) lie very close to each other, as will be quite evident from their term-values given in the Table I.

Two other band systems going down to the level  $2s^3\Sigma$  have been identified by Richardson. The characteristics of these band systems go to confirm that the final level is a  $2s\Sigma$ -level whether it be  $2s^1\Sigma$  or  $2s^3\Sigma$ . The bands give  $P'$  and  $R'$  branches only and no  $Q$  branch. The initial levels must therefore necessarily be  $\Sigma$  levels. Richardson calls them  $np^3\Sigma$  and  $(n+1)p^3\Sigma$ -respectively ( $n$ =either 2 or 3). The effective quantum numbers are respectively 2.485 and 3.53. The point whether  $n$  definitely possesses the value 2 or the value 3 has not been finally decided as yet. Some suggestions have, however, been made by the writer at the end of this discussion. In a recent paper (P. R. S., August 1930) Dr. Chalk has extended Richardson's analysis of the infra-red bands going down to the  $2p\pi$ -level. He also obtains some lines corresponding to  $1'-1''$  of  $2p^1\pi \leftarrow 3^1B$ .

Thus after trying to explain the different levels, there still remain some to be accounted for. There are the levels  $3^1M$ ,  $3^1L$  and two out of  $3^1O$ ,  $3^1N$ , and  $3^1K$  which are additional to those which can be explained on the  $s$  and  $d$  scheme for total quantum number 3. No definite assignment has been possible for any of these levels. Let us, however, consider their general properties. All these levels are very similar in their properties. They

- (1) give rise to  $P'$  and  $R'$  branches only, in combining with  $2p^1\Sigma$ .
- (2) have no missing rotational levels thus strongly exhibiting the properties of  $\Sigma$ -levels.
- (3) show the same abnormal type of rotational structure which suggests strong uncoupling.
- (4) give bands with  $2p^1\Sigma$  with more complicated intensity distribution than other levels.

Richardson suggests that perhaps by rearrangement of the initial vibrational levels this number may be reduced but not to less than 3; this point, therefore, still remains a puzzle.

So far we have seen how the different levels have been fitted into the new scheme. It will, however, be obvious from the table and the above discussion that there is yet much uncertainty regarding the identifications. A few suggestive remarks, regarding one or two points, are ventured in this communication. Richardson assigns the  $np^3\Sigma$  and  $(n+1)p^3\Sigma$  without definiteness to either  $n=2$  or 3. This is represented in the Table I by thick arrows with a mark of (?) at the end. From the following considerations, however, it seems that these levels correspond more suitably to the value of  $n=3$  than to  $n=2$ . Comparing the energy-values of the already identified  $2p$ - as well as  $2s$ -levels with that of the  $np^3\Sigma$  level, it seems more probable that this  $np^3\Sigma$ -level may be a  $3p^3\Sigma$ -level instead of a  $2p^3\Sigma$ -level. This leaves the  $2p^3\Sigma$ -level, with an approximate term-value of 48000, unidentified. The existence of this level is quite necessary, for otherwise it would be difficult to explain the secondary spectrum in the region  $\lambda 3400$ . This level  $2p^3\Sigma$  may also give intercombination bands with  $1s^1\Sigma$  ( $1s^1\Sigma \leftarrow 2p^3\Sigma$ ) in the extreme ultra-violet, in the region about  $\lambda 1300$  to 2000. It will overlap the part of the Lyman bands up to  $\lambda 1600$  and extend beyond to higher wavelengths up to  $\lambda 2000$ . The bands, however, may be expected to consist of very weak progressions, and might possibly on that account have escaped detection up to the present time.

Now as regards the  $3^1K$ -level, Richardson has classified it ambiguously as a  $3s^1\Sigma$ -level. He has, however, as referred to before, stated that it shows a peculiar rotation structure. Besides it does not form a proper Rydberg sequence to  $2s^1\Sigma$  (which has got a term-value of 25300). But for the uncoupling strongly shown by the bands (which cannot be expected of an  $s\Sigma$ -level) the level clearly shows all signs of an  $s\Sigma$ -level and, therefore, may possibly be identified with the  $3s^3\Sigma$ -level which has not been identified as yet. It forms a fairly proper Rydberg sequence to  $2s^3\Sigma$

(which has a term-value 29340) and would readily combine with the  $2p$ -terms. An objection that may be raised against this view is that it gives a strong system of bands in combining (intercombining) with  $2p^1\Sigma$ , whereas if it is triplet ( $2s^3\Sigma$ ) level this intercombination may not ordinarily be expected to give such a strong system of bands. As these points regarding the intensities of intercombination systems, etc., have, however, not yet been quite definitely established in molecular spectra, this objection need not be too seriously considered.

#### DETERMINATION OF TERM VALUES.

The electronic term-values for hydrogen molecule have been obtained by Richardson by adopting the following procedure. He assumed that the band systems

$$2p^1\Sigma \leftarrow 3^1B \text{ and } 2p^1\Sigma \leftarrow 4^1B$$

form a Rydberg sequence. Then using the Rydberg formula,

$$\nu = A - \frac{109678.3}{(m-x)^2}$$

where the symbols have their usual significance, namely,

$A$  = the term-value of the final level (here of  $2p^1\Sigma$ )

$m$  = order number (always an integer)

$x$  = a fractional constant characteristic of the initial term

he obtained the values of  $A$  (i.e., of  $2p^1\Sigma$ ) and  $x$  by substituting the values of the null frequencies of the above bands ( $2p^1\Sigma \leftarrow 3^1B$  and  $2p^1\Sigma \leftarrow 4^1B$ ) for  $\nu_1$  and  $\nu_2$  in the above formula. He obtained the following values :

$$\begin{aligned} A(2p^1\Sigma) &= 34365 \\ x &= 0.0395 \end{aligned}$$

From Dieke's analysis of the extreme ultra-violet Lyman bands it was known that,

$$1s^1\Sigma - 2p^1\Sigma = 90204.$$

From this knowing the term-value of  $2p^1\Sigma$  as given above  $1s^1\Sigma$  becomes easily known.

$$1s^1\Sigma - 2p^1\Sigma = 90204$$

$$1s^1\Sigma - 34365 = 90204$$

$$1s^1\Sigma = 90204 + 34365 \\ = 124569$$

From Hori's analysis of the Werner bands in the Lyman region it was known that

$$1s^1\Sigma - 2p^1\pi = 99205$$

From this we can get the value of  $2p^1\pi$ .

$$2p^1\pi = 1s^1\Sigma - 99205 = 124569 - 99205 \\ = 25364.$$

Thus knowing  $2p^1\Sigma$  and  $2p^1\pi$  the term-values of other numerous levels combining with them to give the known systems of bands can easily be obtained. Richardson has obtained all his values by this method. The justification put forward by Richardson in support of the correctness of these values is as follows: From the term-value of the ground state  $1s^1\Sigma$  of the hydrogen molecule the (spectroscopic) ionization potential comes to be 15.381 volts, in comparison to the electrically determined value 15.9 which is sure to be higher than the proper value as it includes the vibrational energy of the molecule. Also from the ionization potential 15.381 calculated spectroscopically the heat of dissociation of the hydrogen molecule comes out to be 4.465 (taking Burrau's value of the negative energy of  $H_2^+$ ). From Witmer's extrapolation of the frequency intervals of  $1s^1\Sigma$  (using Birge's method for determining the heats of dissociation of diatomic molecules) the value for the heat of dissociation of the hydrogen molecule is obtained equal to 4.34 volts, while direct experimental determination by Copeland and Bichowsky gives a value  $4.55 \pm 0.16$ . These values are fairly in agreement with the values 4.465 volts



as derived from Richardson's term-values. It, therefore, seems quite certain from these considerations that Richardson's term-values have been correctly assigned.

### HEAT OF DISSOCIATION OF HYDROGEN MOLECULE

It may not be out of place to briefly describe here the method by which the heat of dissociation of diatomic molecules ( $H_2$  in particular) is determined from spectroscopic data. Birge has given a theory of the method employed in these cases. The following is a brief sketch of his theory, and its application in the case of hydrogen molecule. Supposing we have a molecule consisting of two atoms A and B in their fundamental states. The vibrational energy  $W_v$  in the fundamental states varies with the progress of ' $v$ .' As for example, Witmer finds the following values for  $\Delta W_v$  from the analysis of band spectra for  $H_2$ .

$$\begin{aligned} A_0 & 4159 \text{ A}, 2923 \text{ A}, 3694 \text{ A}, 3470 \text{ A}, 3243 \text{ A}, \\ A_1 & 3017 \text{ A}, 2784 \text{ A}, 2547 \text{ A}, 2290 \text{ A}, \dots \end{aligned}$$

(Hori represents the progression of these values of  $\Delta W_v$  by

$$\Delta W_v = 4415.2v - 130.22v^2 - 2.694v^3 - 0.1483v^4)$$

Birge states that one of the most striking facts concerning the sets of energy levels is that they are often observed to approach a point of confluence, that is, the separation of successive levels approaches zero. It has been experimentally proved in case of atoms that an electron is separated from the atom at the critical energy corresponding to the atom, that is, the energy at which separation of the successive electronic levels just becomes zero. This will of course only happen when the central force of attraction (to which the separation between any two electronic levels is directly proportional) has just become zero, so that the electron is just beyond the influence of the atomic nucleus (or core as the case may be). Similar set of electronic levels have been observed for a few molecules notably  $H_2$  and  $He_2$

A much more prevalent case, however, is that of vibrational energy levels. It can be said in these cases that dissociation occurs at the point of confluence (where the separation of successive levels just becomes zero) of such molecular energy levels. If we find the energy of the molecule corresponding to this point of confluence (that is, the energy of the molecule for the value of ' $v$ ' at which  $\Delta W_v = 0$ ) this energy will give us the heat of dissociation of the molecule.

It is well known that molecules in the most excited states and sometimes in normal state dissociate into parts containing at least one excited atom. We have, however, to calculate the heat of dissociation as defined by the chemist, that is, the heat of dissociation of the molecule corresponding to its separation into two atoms in the normal state; and this can be achieved from the above method due to Birge. The matters are quite simple so long as we know sufficient number of vibrational levels so that we can directly determine the energy of the molecule at the point where  $\Delta W_v = 0$ . But when only a few vibrational states of a molecule can be followed so that the point of confluence cannot be directly reached, what course is to be taken for the determination of the heat of dissociation of a molecule? Birge has suggested that a proper extrapolation of such incomplete sets is to be made either mathematically or graphically and the limiting energy (that is, the energy corresponding to  $\Delta W_v = 0$ ) must be determined. This is to be done as follows:—

The vibrational energy  $W_v$  in  $\text{cm}^{-1}$  is given by the formula

$$W_v = \frac{W_0 v - W_0 x v^2}{h c}$$

The separation  $\Delta W_v$  of successive energy levels is given by

$$\Delta W_v = \frac{\partial W_v}{\partial v} = W_0 - 2W_0 x v$$

$\frac{\partial W_v}{\partial v}$  = average frequency for two adjacent levels, on Bohr's original principle of Correspondence. Numerically however it represents separation of two adjacent levels, and is therefore put here equal to  $\Delta W_r$ .

The curves of  $\Delta W_r$  against  $f(v)$  shows it to be often linear. In such cases (where this relation was found to be linear) Birge and Sponer made a simple extrapolation to  $\Delta W_r = 0$ .

If  $v_0$  be the corresponding value of 'v' for which  $W_r = 0$ , then the heat of dissociation 'D' of a molecule will be given by

$$D = h \int_0^{v_0} \Delta W_r \, dv$$

In the case of hydrogen molecule if sufficient vibrational terms were known then for some value of 'v'  $\Delta W_r = 0$ . It is clear as remarked above that this corresponds to a state when the constituting atoms are completely separated from each other without any electron displacement taking place in the atoms.  $\Delta W_r$ , the separation between two consecutive states, shows the magnitude of the central force. When  $\Delta W_r$  just becomes zero it means the force vanishes at this point, that is, the atoms have just gone out of the sphere of the mutual force of attraction. The total amount of energy required for this purpose can easily be calculated from the above formula,

$$D = h \int_0^{v_0} \Delta W_r \, dv$$

Substituting for  $\Delta W_r$  in this, from the expression due to Hori given above, we get,

$$D = h \int_0^{v_0} (av - bv^2 + cv^3 - dv^4) \, dv$$

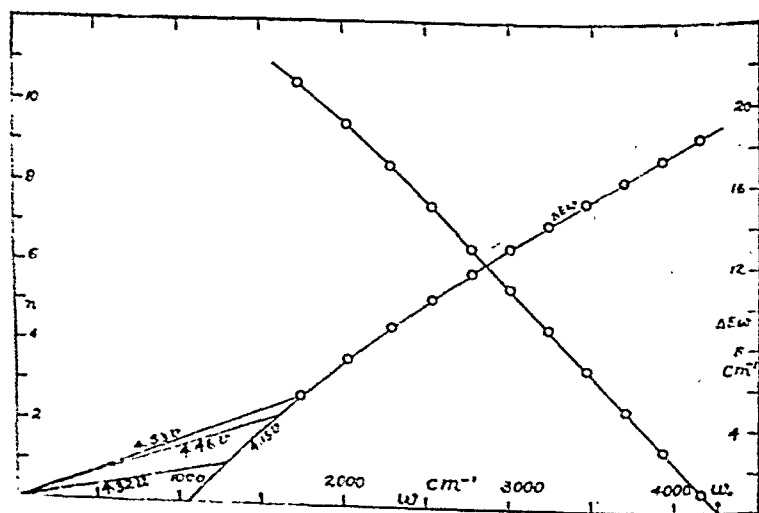
(writing  $\alpha, \beta, \gamma, \delta$  for the numerical constants given by Hori)

$$=h\left[\frac{\alpha v^2}{2}-\frac{\beta v^3}{3}+\frac{\gamma v^4}{4}-\frac{\delta v^5}{5}\right]_0^{v_0}$$

The value  $v_0$  of ' $v$ ' for which  $\Delta W_r$  becomes zero can be obtained either graphically, by extrapolation of the curves (shown in the figure) or mathematically from Hori's empirical formula giving  $\Delta W_r$  by the expression,

$$\Delta W_r = 4415.2 v - 130.22 v^2 + 2.694 v^3 - 0.1483 v^4.$$

(equating this expression to zero and finding the corresponding value  $v_0$  of ' $v$ ').



(Extrapolation of graphs for determining heats of dissociation of  $H_2$ -molecule.)

By this method D was found to have a value equal to 4.34 volts. This value is in fairly good agreement with the experimentally determined value of Copeland and Bichowsky, which as stated above in the last section is equal to  $4.55 \pm 0.16$  volt.

### ALTERNATION OF INTENSITIES IN THE SECONDARY SPECTRUM OF HYDROGEN

In the foregoing discussion reference has been made to the fact that in the molecular spectrum of hydrogen the intensities of the lines constituting different band systems are found to be alternately strong and weak. An explanation of this phenomenon will be contained in what follows. This phenomenon of alternation of intensities in band systems of a molecular spectrum is not uniquely observed in the case of the molecule of hydrogen only, but is found to occur in several other cases. In general for molecules (diatomic molecules) with (two) nuclei of equal mass and nuclear charge, every alternate line in every series of bands is either weak or missing. The explanation of this phenomenon has been given by Heisenberg and Hund on the spin of the nucleus. The full explanation is based on a very complicated mathematical treatment of Schrödinger's wave function and the conditions of symmetry and anti-symmetry of this function. The full treatment cannot form part of this article and, therefore, only the results of their theory will be described here.

It has been pointed out that the nucleus like the electron possesses a spin quantum number  $s_n = \frac{1}{2}$  (in the case of hydrogen the nucleus is the proton and, therefore, this spin quantum number  $s_n$  will be denoted for it by  $s_p = \frac{1}{2}$ ). It has also been proved that two electron spins  $s_e$ 's in a magnetic field three symmetrical terms (for  $S_e = 1$ ) giving rise to triplet characteristic, and one anti-symmetrical electron term (for  $S_e = 0$ ) giving a para- or singlet term. In the same manner the behaviour of  $S_p$ 's (the proton spins) and their functions in a magnetic field should be exactly analogous to that of the electron spin  $S_e$ 's. Thus the resultant of the two proton spins ( $S_p$ ) will have three magnetic sub-levels for  $S_p = 1$ , corresponding to the components

1, 0, -1 of  $S_r$  along the rotation axis around which it is space quantised. Corresponding to  $S_r=0$  there will be only one magnetic sub-level. The  $S_r=1$  states will thus have thrice the statistical weight of  $S_r=0$ . After some discussion, it has been concluded that the rotational levels of any electronic state of  $H_2$  can be divided into two distinct sets, one having  $S_r=1$  and the other  $S_r=0$ . Transitions involving  $S_r=1 \leftarrow S_r=0$  are forbidden or may be expected to occur exceedingly slowly, even under influence of collisions (this is true both, when we are considering transitions between different electronic states or in the same electronic state). The selection rules for combination are

$$\Delta K = 0, \pm 1 (S_r = 1 \longleftrightarrow S_r = 0 \text{ prohibited}).$$

Thus for any given electronic state there are two distinct sets of non-intercombining rotational levels with odd and even  $K$ -values corresponding to  $S_r=1$  or  $S_r=0$  depending upon the level under consideration. Accordingly the rotational levels of normal hydrogen molecule can be divided into two distinct classes,

(a) Even  $K$ -values, 0, 2, 4, . . . .

$$S_r = 0 \quad \text{statistical weight :—} 2K + 1.$$

(b) Odd  $K$ -values, 1, 3, 5, . . . .

$$S_r = 1 \quad \text{statistical weight :—} 3 (2K + 1)$$

That there actually exist such two distinct sets of levels which do not, or if at all, do very slowly, intercombine has been very beautifully established experimentally (at least in the case of normal hydrogen molecule), the evidence being quite conclusive. This point will be taken up later, after showing how this theoretical deduction of the existence of two distinct sets of non-intercombining rotational levels is helpful in explaining the alternation of intensities. For illustration we shall consider the case of Lyman and Werner bands

only. The diagram below will be very helpful for this purpose.

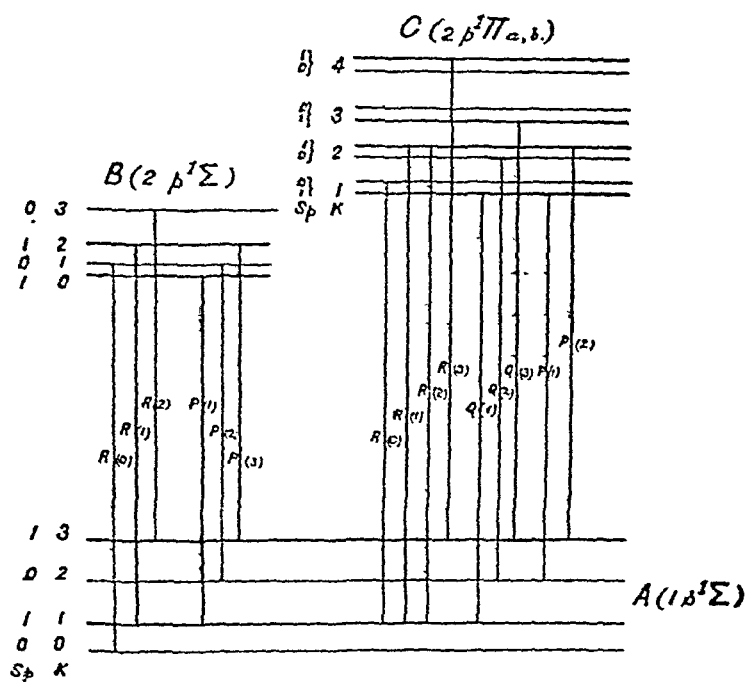


Diagram explaining the alternation of intensities of lines in hydrogen for Lyman and Werner bands

Horizontal lines in the diagram represent the rotational levels of the electronic states  $A(1s^1\Sigma)$ ,  $B(2p^1\Sigma)$ , and  $C(2p^1\Pi)$ . The respective  $S_p$ - and  $K$ -values for these have been denoted on the left side of each level. The levels with greater statistical weights (*i. e.*,  $S_p=1$  levels) are represented by dark lines. The vertical lines represent the different transitions giving rise to corresponding spectral lines in the bands. It should be marked that whereas  $A$  and  $B$  are both  $\Sigma$ -levels, even values of  $K$  correspond to  $S_p=0$  for  $A$  and  $S_p=1$  for  $B$  and *vice versa*. In the case of  $C$  which is a  $\pi$ -level (a double level) corresponding to each  $K$ -value there are both values of  $S_p$  (0 and 1) possible according as levels  $\pi_a$  or  $\pi_b$  are under consideration. In all the above cases,

however, the statistical weights of the levels depend upon the values of  $S_p$  (and not upon the odd or even natures of the K-values), that for  $S_p = 1$  being thrice that for  $S_p = 0$ , in each case.

Applying the selection rules given above ( $S_p = 1 \rightarrow S_p = 0$  forbidden and  $\Delta K = 0$  or  $\pm 1$ ) we see that the stronger lines are those arising from the combinations,

$K = 1, 3, 5, \dots$  of A

$\leftarrow 0, 2, 4, \dots$  of B (P' and R' branches)  
or  $\leftarrow 1, 3, 5, \dots$  of C (Q branch)  
or  $\leftarrow 2, 4, 6, \dots$  of C (P' and R' branches)

and the weaker lines are those arising from the combinations,

$K = 0, 2, 4, \dots$  of A

$\leftarrow 1, 3, 5, \dots$  of B (P' and R' branches)  
or  $\leftarrow 2, 4, 6, \dots$  of C (Q branch)  
or  $\leftarrow 1, 3, 5, \dots$  of C (P' and R' branches).

In short the transitions between  $S_p = 1 \leftarrow S_p = 1$  give rise to stronger lines and the transitions between  $S_p = 0 \leftarrow S_p = 0$  give rise to weaker lines. Thus taking for example the R-branch of the Lyman bands the lines  $R_0, R_2$  (transition  $S_p = 0 \leftarrow S_p = 0$ ) are weak whereas the lines  $R_1, R_3$  (transition  $S_p = 1 \rightarrow S_p = 1$ ) are strong. In the above diagram the stronger lines are represented by thick vertical lines. Similarly for the P-branch. The same explanation holds for the Werner bands and therefore need not be repeated here. One point of interest may be noted here that the above theory of Heisenberg and Hund while supplying the explanation of the alternation of intensities, also explains the facts why the transitions between some electronic levels give P- and R-branches only whereas others give all the branches (P', Q, and R'). Thus referring to the diagram above, it will be clear that in the Lyman bands ( $A \leftarrow B$ ) there is no possibility of obtaining a Q-branch as this involves transitions  $S_p = 1 \leftarrow S_p = 0$ , which are forbidden according to the



selection rules given by the above theory. Similar explanation holds for the Werner bands ( $A \leftarrow C$ ) in which due to the double nature ( $\pi_a, \pi_b$ ) of the C-level which is a  $\pi$ -level we get only P- and R-branches from the transition  $A \leftarrow \pi_a$  and only the Q-branch from the transitions  $A \leftarrow \pi_b$ . For clarity it may also be mentioned here in the diagram the  $\pi_a$  levels are those for which the even K-values correspond to  $S_p=1$  and odd K-values to  $S_p=0$ ; and the  $\pi_b$  levels are those for which the even K-values correspond to  $S_p=0$  and odd K-values to  $S_p=1$ . The above statement can now be thoroughly followed without any difficulty.

Now to resume, let us consider the experimental evidences in support of the existence of two distinct sets of non-intercombining rotational levels in any electronic state of a molecule. As we have stated above this evidence is fairly conclusive (in the case of the normal hydrogen atom). The above result of the Heisenberg-Hund theory, that in the normal state, hydrogen consists of two distinct sets of non-intercombining systems of odd and even rotational levels, which is equivalent to saying that in the normal state hydrogen consists of two distinct kinds of hydrogen, one with only *odd* rotational states and the other with only *even* rotational states, the change from one type of the molecules into the other being very slow, was expected or rather prophesied by Hund from analogy of behaviour in the case of Helium atom. We have just seen above how satisfactorily it explains the alternation of intensities. The theory also requires that the number of hydrogen molecules possessing the odd rotation levels only ( $S_p=1$ ) must be three times the number of hydrogen molecules having only even rotational levels ( $S_p=0$ ). All these facts are strongly supported by a number of evidences. These are given below :—

(1) *Specific Heat of Hydrogen*.—If the theoretical and experimental curves of specific heat, against temperature are compared they are found to diverge very widely from each

other. Great difficulty was found in giving an explanation of this effect. Dennison however showed that if the following assumptions (which are equivalent to the above statement) are made the curves agree within the limits of experimental error. The assumptions suggested by Dennison are:

- (a) That, at ordinary temperature the hydrogen gas contains a mixture of two kinds of hydrogen molecules, those of one type ( $S_r = 1$ ) being three times as numerous as the other ( $S_r = 0$ ).
- (b) That, transition from one type to the other is very slow (negligible during the time of experiment).

This evidence thus supports the above results.

2. *Raman Effect in Liquid Hydrogen*.—McLennan measured Raman Effect in liquid hydrogen and found that the changes in frequencies in the spectrum of scattered light showed that hydrogen gas at that temperature contained a mixture of molecules having even and odd rotation levels, the number of the latter being three times that of the former. The details of how he arrived at this conclusion are very interesting and, therefore, although a full description cannot be given, a brief account of the method is given below: McLennan obtained the following observations:

Excited Radiation		Scattered Radiation		Observed	Calculated
$\lambda(A)$	$\nu(\text{vac})$	$\lambda(A)$	$\nu(\text{vac})$	$\text{cm}^{-1}$	$\text{cm}^{-1}$
4358.3	22938	4426.6	22584	354	347
4358.3	22938	4473.1	22350	588	578
4046.6	24705	4863.5	20556	4149	4159

By the use of suitable light screens it was found that the scattered radiations  $\lambda 4426.6$  and  $\lambda 4473.1$  were obtained from the exciting radiation  $\lambda 4358.3$  and  $\lambda 4863.5$  by the radiation  $\lambda 4046.6$ .

Out of these the change in frequency  $4149\text{ cm}^{-1}$  corresponds to the vibrational frequency difference between the first and the second vibrational levels  $A_0$  and  $A_1$  of the normal hydrogen atom (the actual value is  $4159\text{ cm}^{-1}$ ). The changes in frequency  $354$  and  $588\text{ cm}^{-1}$  must correspond to the difference in rotational energies. These are approximately in the ratio  $3 : 5$ . Now from the quantum theory of the band spectra the rotational energy of a diatomic molecule is given by the formula,

$$E = B.h.m(m+1), \quad \text{where } B = \frac{h}{8\pi^2 I}$$

$h$  = universal const. of  
Planck

$m$  = rotational quantum  
number

From this we obtain the rotation energy levels,

$$E = 0, 2Bh, 6Bh, 12Bh, 20Bh, 30Bh, \dots$$

It will be seen from this that the only changes in rotational energies having a ratio of  $3 : 5$  can be,

$$\begin{aligned} 6Bh - 0 &= 6Bh \\ 12Bh - 2Bh &= 10Bh \end{aligned}$$

giving the desired ratio  $3 : 5$  ( $6Bh : 10Bh$ ). It should be marked that he obtained no trace of any lines for which the ratio of the corresponding changes of frequency was  $2 : 3$ ;  $2 : 5$ ;  $3 : 4$ ;  $4 : 5$ ; etc. Now the above transitions supplying the frequency ratio of  $3 : 5$  are,

$$\begin{aligned} \text{from } m=2 \text{ to } m=0 &\text{ giving } 6Bh \text{ and} \\ \text{from } m=3 \text{ to } m=1 &\text{ giving } 10Bh. \end{aligned}$$

No transition from  $m=0 \leftarrow m=1$  or  $m=1 \leftarrow m=2$  seems to have occurred at all, as no trace of such lines giving the corresponding ratio of frequency required by these changes have been observed, as already stated above. It is concluded, therefore, that in liquid hydrogen there are two distinct sets of molecules, one in which the transitions

of rotation from  $m=2$  to  $m=0$  can occur and the other in which the rotational transitions  $m=3$  to  $m=1$  can occur. That is equivalent to saying, that in the normal state hydrogen consists of two types of molecules, one with only odd rotation levels and the other with only even rotational levels, and that there is no (or if at all, very slow) transition from one type of molecules to the other. The ratio of the intensities of the Raman Lines corresponding to the rotational transitions is found to be between 2 and 3, the one corresponding to change in frequency  $588 \text{ cm}^{-1}$  ( $10Bh$ ) being the stronger. It therefore clearly follows that in liquid hydrogen there must be between 2 and 3 times the number of molecules with odd rotational levels (as  $10Bh$  corresponds to the transition  $m=3$  to  $m=1$ ), as compared to the number of molecules having even rotational levels.

Now before taking the third and the most important evidence in this connection it is necessary to mention certain facts bearing on this point. Though at ordinary temperature  $\text{H}_2$  may be composed of a mixture of two kinds of molecules with odd and even rotational levels respectively, it should be expected that at absolute zero ( $T^\circ=0$ ) all molecules must be in the lowest energy state which would be  $K=0$  state ( $S_r=0$ ). So that on lowering the temperature below the ordinary all the molecules should tend to the  $S_r=0$  state. But as transitions  $S_r=1 \longrightarrow S_r=0$  is very slow true equilibrium is not obtained for a considerable time. In ordinary experiments only a partial equilibrium is obtained in which molecules with either  $S_r$ -values distribute themselves independently according to their weights

$$(2K+1) e^{-B K (K+1) / KT}$$

(the symbols having the usual significance)

After cooling in the ordinary manner it should be expected

that the gas near  $T=0$  would contain a mixture of three-fourths of molecules in  $K=1$  and one-fourth in the  $K=0$  state if no transition  $S_p=1 \longleftrightarrow S_p=0$  can take place ; but if this transition occurs even though slowly (or comparatively more quickly under favourable conditions) then as stated above we should expect all molecules in the  $K=0$  state at  $T=0$ . Bonhoeffer, Harteck and Eucken have recently shown that,  $S_p=1 \longrightarrow S_p=0$  from room temperature equilibrium ratio 3:1 to  $T=0$  equilibrium ratio 0:1 actually proceeds very slowly as expected, in cold hydrogen gas—(a) under very high pressure,<sup>3</sup> or (b) in presence of charcoal. (This change in ratio was followed by observing changes in the specific heats at different intervals, or measuring the heat conductivity which varies with the specific heat, by noting the resistance of a heated wire in presence of the gas.)

The third and the most important evidence is that obtained by Bonhoeffer and Harteck. They have shown that just as in cooling hydrogen below the ordinary temperature the ratio 3:1 of molecules with  $S_p=1$  to those with  $S_p=0$  is observed to be persisting, so also conversely the ratio 0:1 of molecules with  $S_p=1$  to  $S_p=0$  for hydrogen kept near absolute zero in charcoal, continues to persist on warming the gas from  $0^\circ$  to higher temperatures. They used hydrogen which had been in equilibrium at a very low temperature so that practically all the molecules were in the  $S_p=0$  state. On warming the gas if the  $S_p=0$  state persists it should be expected that the molecules will distribute themselves over the levels  $K=0, 2, 4, \dots$ . This has been found to be actually the case ; for on taking the spectrum of such gas, they observed that in the  $\alpha$  bands ( $2s^3\Sigma \longleftrightarrow 3p^3\pi$ ) of the secondary spectrum every alternate line was practically missing in each branch instead of being merely weak ; moreover it should be noted that the missing lines are just those ( $S_p=1 \longleftrightarrow S_p=1$ ) which in the ordinary hydrogen are stronger.

All these evidences thus quite strongly support the theoretical result that hydrogen consists of two distinct sets of molecules with odd and even rotation levels respectively and that the number of molecules with  $S_p=1$  is three times the number with  $S_p=0$ .

#### PRESENT ANALYSIS OF BANDS BY THE AUTHOR

It has already been stated that Richardson has been successful in classifying a number of bands and identifying some electronic levels in the secondary spectrum of hydrogen. In a recent discussion held under the auspices of the Faraday Society, Prof. Richardson has given a comprehensive account of the identification of electronic levels and classification of spectral lines in the secondary spectrum of hydrogen (a summary account of which has also been given in his latest paper in P. R. S. L., 126, 487), as regards their electronic transitions in the molecule. (This has been briefly given above in this article also.) From a study of the discussion and other papers (referred to therein) which give the detailed vibrational and rotational classification of the lines it appears that the origin of more than 80 per cent of the lines is still unknown. Even amongst bands whose vibration and rotation structures are known it has not been found possible to assign the exact electronic levels between which the particular transition has taken place. It is quite evident therefore that a large number of bands and electronic levels yet remain to be discovered. A careful study of the analysis hitherto effected shows clearly that band systems so far discovered all satisfy the usual rules of the selection principles for electronic transitions, namely, only the transitions

$\Delta K \pm 1, \Delta j = 0, \pm 1$  and  $\Delta S = 0$  are allowed

where  $S$  is the spin quantum number  $0, \frac{1}{2}, 1, \dots$

for singlets, doublets, triplets  $\dots$ ).

These selection rules initially discovered for and found applicable, almost without exception, in the case of atomic

spectra under normal conditions, have been found to be violated under certain abnormal conditions. It is well-known that in the case of atoms the selection rules  $\Delta K = \pm 1$  and  $\Delta S = 0$  are readily violated in presence of strong electrostatic fields. For example, Koch obtained in a strong electrostatic field the  $2p$ - $mp$  lines of helium and found that the intensity varies proportionally to the field strength. Recently Niels Ryde obtained the forbidden lines ( $p-f$ ,  $p-g$  combinations) of Neon by a similar arrangement. The violation of the other rule  $\Delta S = 0$  is very common, and is exhibited by the intercombination lines in atomic spectra. The intercombination lines are readily obtained in heavy current arcs, and Dr. Sur in this laboratory obtained these lines for  $P_L$  in a heavy current arc. The present author also got the fundamental intercombination lines of carbon in the heavy arc of carbon. Recently Paschen announces the discovery of the  $^1S$ - $^3P$ -lines of helium in a heavy current discharge through helium. In the case of molecules, therefore, it may quite reasonably be expected that these selection rules  $\Delta K = \pm 1$ ,  $\Delta S = 0$  may be very readily violated, for in the formation of molecules out of atoms the electrons are subjected to intense electrostatic fields; and therefore, it is expected that such usually forbidden transitions as  $K = 0, 2, \dots$  and  $\Delta S = 1$ , may possibly be more readily obtained in molecular spectra.

Proceeding on this idea I have tried to find if lines can be selected corresponding to the electronic transition  $\Delta K = 0$  between the hitherto discovered electron levels of hydrogen molecule. As a result of this attempt I have been successful in classifying about 80-90 lines. The particular transition that I have chosen is between the B-level of Dieke (or  $2p^1\Sigma$ -level) and the  $3^3p$ =(or  $3p^3\pi$ ) level of Richardson. The vibration and rotation structures of both these levels are more or less completely known from the analyses of other bands

of hydrogen by Richardson and his co-workers. As the point as to whether the  $3^3p$ -level of Richardson (the initial level of the  $\alpha$  bands) is a triplet  $^3\pi =$  level or a singlet  $^1\pi =$  level is not yet definitely decided, it cannot be said just now if in this present analysis the selection principle  $\Delta S=0$  is also simultaneously violated. As has been mentioned in the part dealing with the classification, Richardson seems to be in favour of this view, ( $\Delta K=0$  transition) as can be concluded from the fact that he assigns a level (which he had arbitrarily termed as  $3^1Q$ ) giving very weak progressions in combining with  $2p^1\Sigma$ , as  $3p^1\pi$ . This point, however, came to my notice after I had finished my classification. It is not possible to give the results of my analysis here in detail. Certain main points may, however, be mentioned. The data for classification are used from the wavelength measurements of Finkelberg and also those of Gale, Monk, and Lee. The classification is accurate up to  $0.5\text{ cm}^{-1}$ , which is the maximum deviation from the correct value. Almost all lines are very weak (as is to be expected) with intensity 0 or 00; scarcely any line with intensity 1 or 2 occurs. The progressions are also very weak. The  $0'0''$ ,  $1'0''$ ,  $0'1''$ ,  $0'2''$ , progressions come out fairly consistently; the others are too weak to follow completely and the indication of their existence is obtained from the presence of isolated members of the progressions. All these facts are quite consistent with what would be expected for such transitions which are ordinarily forbidden. It may be possible to explain the origin of a large number of lines by similar transitions. The results of analysis have been communicated for publication to the 'Philosophical Magazine.' I wish finally to take this opportunity of expressing my sincerest gratitude to Prof. M. N. Saha for the keen interest and valuable guidance during the course of the preparation of the paper.



# ON AN ATTEMPT TO DETECT COMBINATION SCATTERING BY ATOMS

BY

G. R. TOSHNIWAL, M.Sc.,  
*Lecturer, Allahabad University.*

Solids, liquids and gases have all been found to scatter light and give rise to Raman Lines by combination-scattering. The frequency difference between the unmodified and the modified line is generally found to correspond to a characteristic infra-red absorption line of the substance, notable exceptions being carbon disulphide<sup>1</sup> and a few other things which do not show infra-red absorption lines corresponding to the observed Raman Lines. This anomaly finds an easy explanation on the third level theory put forward by several investigators<sup>2</sup> from the original Kramers-Heissenberg theory the modified lines are all due to vibration frequency of the molecules of the substance. Gases such as ether,<sup>3</sup> hydrochloric acid gas,<sup>4</sup> carbon monoxide, carbon dioxide,<sup>5</sup> etc., give modified lines corresponding to their molecular spectra. No modified line has so far been discovered which is due to addition or subtraction of the frequency difference between two energy levels of an atomic spectrum. With this end in view the following investigation was undertaken.

<sup>1</sup> Ganeshan and Venkateswaran in Journ. of Phy., Vol. IV, 242 (1928).

<sup>2</sup> See for example, Langer, Nature, 123, p. 345 (1923), and Dieke, Nature, 123, 564 (1923); Majumdar and Kothari, Nature, 125, 165 (1930).

<sup>3</sup> Ramdas, Ind. Journ. of Phy., Vol. III, 131 (1928).

<sup>4</sup> Wood, Nature, 123, 166 (1929).

<sup>5</sup> Raseti, Nature, 123, 205 (1929).

According to the generally accepted ideas in order to obtain Raman Scattering, it is essential that atoms or molecules must be present in the two states  $k$  and  $l$  and transition must be possible to a common level  $n$  from both  $k$  and  $l$  states. The Boltzmann law gives the ratio of the number of atoms in the higher state  $k$  to that in the lower state  $l$  as  $e^{-v_{kl}/kT}$ , where  $v_{kl}$  is the frequency difference between  $k$  and  $l$  states and  $T$  is the temperature in Kelvin scale. This relation evidently shows that in order that quite a good number of atoms may be present in the higher state  $l$ , the value of  $v_{kl}$  must be small, the second necessary condition follows from the fact that the intensity of the Raman Scattering varies directly as the total number of scattering centres, which means that at the temperature under our command there must be a large number of atoms in a cubic centimeter of space. Thus the first condition that  $v_{kl}$  should be small, means that we can observe the effect easily with atoms which have metastable levels lying close together. The second shows that we must have quite a large vapour pressure of the element at the temperature in use.

The elements belonging to the I and II groups have no metastable states. The III group elements have two metastable states, namely,  $^2P_1$ ,  $^2P_2$ . Boron and Aluminium the first two members have small values of  $\Delta v$  (i.e.,  $v_{kl}$ ), but their boiling points are very high (see Table I). Gallium and Indium seem to be the two promising members of the group, but as they are too costly to work with (about £8 per gram) they could not be used. Out of the two Gallium seems to be the most promising one. There are five metastable states for elements of the IV group, viz.,  $^3P_{0,1,2}$ ,  $^1D_2$ ,  $^1S_0$ . But they are ruled out because of the second condition (Table II). The fifth group of elements have again five metastable states, viz.,  $^4S_2$ ,  $^2D_{3,3}$ ,  $^2P_{1,2}$ . The first two members, i.e., nitrogen and phosphorus are polyatomic at ordinary temperatures and

even at high temperatures the percentage dissociation is not much. Arsenic gives a copious amount of vapour and exists both in polyatomic and atomic state. Now according to the analysis of Ruark, Mohler, Foote and Chenault,<sup>6</sup>  $\Delta\nu$  for arsenic is  $1469.8 \text{ cm}^{-1}$ . Therefore this element was selected for the present investigation. But after a good deal of work no modified lines were found. This result was rather contrary to expectations as all the necessary conditions for the success of the experiment were apparently fulfilled. Almost when all hopes were given up, an analysis of the arc spectrum of Arsenic by Meggers and de Bruin<sup>7</sup> appeared in the 'Journal of Research of the Bureau of Standards.' Their paper definitely proves that the former analysis of Ruark, etc., on which we proceeded was quite wrong and that  $\Delta\nu$ , *i.e.*, the wave number difference between  $^4\text{S}_2$  and  $^2\text{D}_2$  is  $10,591 \text{ cm}^{-1}$  instead of  $1469 \text{ cm}^{-1}$ . This value of  $\Delta\nu$  greatly reduced the number of atoms in the  $^2\text{D}_2$  state.

$$\begin{aligned} n/n_0 &= e^{-2.1} \text{ nearly for } \Delta\nu = 1469 \text{ cm}^{-1}, \\ \text{and } n/n_0 &= e^{-15.4} \text{ nearly for } \Delta\nu = 10,591 \text{ cm}^{-1}. \end{aligned}$$

This means that the combination-scattering becomes extremely feeble and it is not possible to observe it with the present methods.

The members of the VI and the VII groups are also molecular and hence cannot be used.

The tables in the following pages give us at a glance the various constants for elements that are of importance for the experiment.

<sup>6</sup> Ch. Ruark, Mohler, Foote and Chenault, Bur. of Stand., So. Papers, 19, 463 (1924).

<sup>7</sup> Meggers and de Bruin, Bur. of Stand., Jour. of Research, 3, 765 (1929).

TABLE I  
*Elements of the III Group\**

Element	$^2P_1 - ^2P_2$ $\text{cm}^{-1}$	Melting Point $^{\circ}\text{C}$	Boiling Point $^{\circ}\text{C}$	Remarks
B	15.3	2300	...	...
Al	112.0	658	1800	...
Ga	826.0	30	...	Slightly evaporates at red-heat.
In	2212.0	154	...	Does not evaporate even at $1450^{\circ}\text{C}$ .
Tl	7793.0	303—227	1306	Gives dense vapour at lower temp.

TABLE II  
*Elements of the IV Group†*

Element	Metastable States in $\text{cm}^{-1}$				Melting Point $^{\circ}\text{C}$	Boiling Point $^{\circ}\text{C}$	Remarks
	$^3P_0 - ^3P_1$	$^3P_1 - ^3P_2$	$^3P_2 - ^1D_2$	$^1D_2 - ^1S_0$			
C	20	40	...	...	3917	...	Sublimes
Si	77	146	...	...	1404	...	Volatilizes in Argon between 1200-1300
Ge	557	853	...	...	958	...	
Sn	1692	1736	...	...	231	2218	
Pb	7817	2831	...	...	327	1525	

\* Data for Metastable states, Fowler's Report on Series Spectra.

† VI-Group Elements :

C—Flower, P.R.S. (Lond.), A 118, 34 (1929).

Si—Flower, P.R.S. (Lond.), A 123, 422 (1929).

Ge—Gartlein, Phy. Rev., 31, 782 (1928).

Sn—Sur. Zs. f. Phy., 41, 791 (1927).

Pb—Sur. Phil. Mag., 3, 736 (1927).

TABLE III  
Elements of the V Group \*

Element	Metastable States in $\text{cm}^{-1}$				Melting Point $^{\circ}\text{C}$	Boiling Point $^{\circ}\text{C}$	Remarks.
	$^4\text{S}_2-^3\text{D}_2$	$^2\text{D}_3-^3\text{D}_3$	$^3\text{D}_3-^3\text{P}_1$	$^3\text{P}_1-^3\text{P}_2$			
N.	17362	...	...	...	-210.5	-195.7	Polymorphous
P	...	...	...	...	44	287	"
As	10591	...	...	...	Under pressure 817	633	Sublimes Polymorphous
Sb	8511	...	...	...	630	1440	
Bi	11417	...	...	...	271	1420	

TABLE IV  
Elements of the VI Group †

Element	Metastable States $\text{cm}^{-1}$				Melting Point $^{\circ}\text{C}$	Boiling Point $^{\circ}\text{C}$	Remarks
	$^3\text{P}_2-^3\text{P}_1$	$^3\text{P}_1-^3\text{P}_0$	$^3\text{P}_0-^1\text{D}_2$	$^1\text{D}_2-^1\text{S}_0$			
O	67	225	10490	17925	-258.9	-252.5	Polymorphous.
S	398	572	9200	16200	112.8	444.5	"
Se	1991	2535	8067	13794	217	688.0	"
Te	4707	4751	7406	12640	446	1390.0	
Po	...	...	...	...	...	...	

\* V-Group Elements :—

N—Compton and Boyce, *Phy. Rev.*, 33, 145 (1929).

P—

As—Meggers and de Bruin, *Loc. Cit.*

Sb—Ruark and others, *Loc. Cit.*

Bi—Toshniwal, *Phil. Mag.*, 4, 774 (1927).

† VI-Group elements :—

McLennan and Crawford, *Nature*, (Dec. 1929).

TABLE V  
*Elements of the VII Group \**

Element	Metastable State $\text{cm}^{-1}$ $^2P_{1/2} - ^2P_{1/2}$	Melting Point $^{\circ}\text{C}$	Boiling Point $^{\circ}\text{C}$	Remarks
Fl	407	-223	-187	Diatomic
Cl	881	-102	-33.6	"
Br	3688	-7.3	63	"
I	7609	113	184	"

The melting and boiling points of the transitional-group elements are too high and need not be considered in detail. The same remark applies to the rare-earth group.

### EXPERIMENTAL

Trial experiments were begun in the end of 1928, using high temperature furnace devised by Prof. Saha, Sur, and Majumdar.<sup>5</sup> The carbon tube was provided with a rectangular opening through which light could pass for illuminating the vapour. In these experiments antimony was used, which was placed in a small carbon boat, in the middle of the heater tube. The furnace was evacuated and then filled with nitrogen at atmospheric pressure. But in spite of all these precautions, it was found that antimony vapour did not stay in the furnace for more than half an

\* VII-Group Elements :

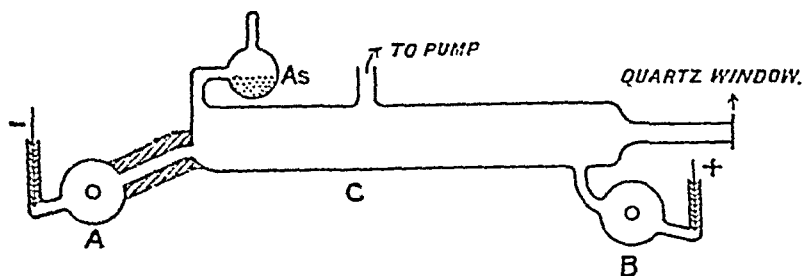
Fl—Bowen, *Phy. Rev.*, Vol. 29, p. 246.

Cl—Kiess and de Bruin, *Bur. of Stand. J. of Research*, 2, 1117 (1929).

Br } —Turner, *Phy. Review*, Vol. 27, 597 (1926).

<sup>5</sup> Saha, Sur, and Majumdar, *Zs. f. Phys.*, 40 648 (1926).

hour. Moreover, it was very difficult to manipulate the furnace for long exposures as needed for the success of the experiment. Therefore, this had to be given up. It was then decided to put arsenic vapour directly in a mercury arc, as has been done by Venkatesachar and Sibaiya.<sup>9</sup>



The mercury arc which was used was of the horizontal type, and consisted of two mercury reservoirs A and B. A was connected with the arcing-chamber C by means of a thick-walled capillary tube. A small bulb containing arsenic powder communicated with the arcing-chamber near the end of this capillary tube. The other end of the arcing-chamber was provided with a quartz window for end on observations. The whole of the apparatus was made of pyrex glass in this laboratory.

The arc was struck in the usual way, and after some time, the bulb containing arsenic was heated slowly, and a continuous stream of arsenic vapour was introduced in the arcing-chamber C. In the presence of a large amount of arsenic vapour, the arc was reduced to a narrow beam, and was rather unstable. End on photographs were taken in the usual way, which on examination revealed no new lines due to combination scattering, although many lines due to arsenic particularly, the 'raies ultimes' occurred in the plate very strongly.

<sup>9</sup> Venkatesachar and Sibaiya, *Nature*, 124, 838 (1929).

The attempt, therefore, had to be given up for the present, but it seems that probably the experiment would be successful if it is tried with Gallium. From Table I, we see that it melts at  $30^{\circ}\text{C}$  and that the boiling point is unknown. There is no data on the vapour pressure of Gallium, but Dr. Sur and Majumdar, in course of their work on the absorption spectrum of Aluminium, observed that even at  $1000^{\circ}\text{C}$ , when the fundamental Aluminium lines did not appear, the corresponding Gallium lines were observable, though the latter occurred merely as an impurity in Aluminium.

The transitional elements as well as the rare earths have also been carefully surveyed, but as far as the present data go, there seems to be no suitable elements with which atomic Scattering may be observable.



# ON THE DISTRIBUTION OF INTENSITY AMONGST THE FINE STRUCTURE COMPONENTS OF SERIES LINES OF HYDROGEN AND IONISED HELIUM ACCORDING TO DIRAC'S THEORY OF THE ELECTRON

BY

M. N. SAHA AND A. C. BANERJEE

## INTRODUCTION

The fine structure of the series lines of hydrogen and of ionised helium, and the distribution of intensity amongst the fine structure components have formed the subject of study by many eminent investigators during past and recent years. The interest in the subject has not yet abated, as in a recent paper published in the *Journal de Physique* (Dec., 1929), L. Goldstein studies the distribution of intensity, amongst the fine structure components of  $H_\alpha$  and  $\lambda 4686$  of  $He^+$  from the relativistic wave-mechanical theory of Dirac, and finds rather glaring disagreement with experimental data. The result seemed to be rather surprising for two reasons:—(1) Dirac theory of the electron has been so successful in accounting for the duplicity phenomena, and the fine structure of  $H_\alpha$ -lines, that it is difficult to believe that it would give wrong values of intensity in case of  $He^+$ ; (2) Sommerfeld and Unsöld, in the paper above referred to, worked out a theory of intensity distribution on the basis of Schrödinger-mechanics and statistical considerations with the aid of which they were able to explain in a very satisfactory way all the discrepant results in the intensity distribution amongst the fine-structure components of the series lines of H and of  $He^+$ . The authors of the present paper have been engaged in the same problem prior to the publication of Goldstein's paper, but their results are in excellent

agreement with experimental data, and with the results of Sommerfeld and Unsöld. We have used the Dirac theory as presented by Darwin and Weyl. Before we give our calculations, we give a short history of this time-honoured problem.

### FINE STRUCTURE OF HYDROGEN LINES

According to Sommerfeld, the energy in an orbit is distinguished by the quantum numbers  $n$ ,  $k$  and in case of H is given by:—

$$\nu_{nk} = -R\alpha^2 \left[ \frac{1}{n^2} + \frac{\alpha^2 z^2}{n^4} \left( \frac{n}{k} - \frac{3}{4} \right) + \dots \right]$$

$$\text{Energy} = h\nu_{nk},$$

$$\alpha = \text{Sommerfeld fine-structure constant } \frac{2\pi e^2}{ch}.$$

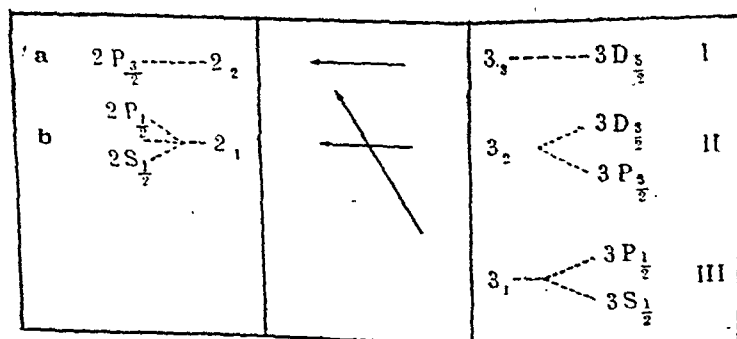
The frequency of an emission line is given by:—

$$\nu = -R\alpha^2 \left[ \frac{1}{n^2} - \frac{1}{n'^2} \right] + R\alpha^4 z^4 \left[ \frac{1}{n^4} \left( \frac{n}{k} - \frac{3}{4} \right) - \frac{1}{n'^4} \left( \frac{n'}{k'} - \frac{3}{4} \right) \right] + \dots$$

$$= \nu_0 + \Delta\nu,$$

$$\text{where } \Delta\nu = R\alpha^4 z^4 \left[ \frac{1}{n^4} \left( \frac{n}{k} - \frac{3}{4} \right) - \frac{1}{n'^4} \left( \frac{n'}{k'} - \frac{3}{4} \right) \right]$$

The fine-structure components are obtained by giving all possible values to  $k$  and  $k'$ , and calculating  $\Delta\nu$  for each combination. The components of  $H_\alpha$  are:—



According to Sommerfeld,  $H_\alpha$  should consist of three lines ( $2_2 \leftarrow 3_2$ ), ( $2_1 \leftarrow 3_2$ ), ( $2_2 \leftarrow 3_1$ ).

## THE DUPLICITY PHENOMENON

Lande however showed that Sommerfeld's theory was insufficient to account for the fine-structure, in all its details, particularly as regards intensity. He showed that a better agreement is established if we suppose the fine-structure to be of magnetic origin, as in alkalis. As a matter of fact, Lande showed that the structure of the spectrum of hydrogen is just like that of alkali elements. This theory was put on a more picturesque basis by Goudsmit and Uhlenbeck's hypothesis of the rotating electron; they showed that this hypothesis leads to the same expression for the doublet-separation as the Sommerfeld formula, only  $k$  has to be substituted by the inner-quantum number ' $j$ .' Heisenberg and Jordan showed from matrix-mechanics that such terms as  $3_{3,2}$  and  $3_{3,1}$  which possess identical inner quantum number (in this case 2), but differ in the value of the azimuthal quantum number by unity, have the same energy value as Sommerfeld's  $3_2$ -term. The structure of the  $H_\alpha$ -line, according to these views, is shown in the following diagram:—

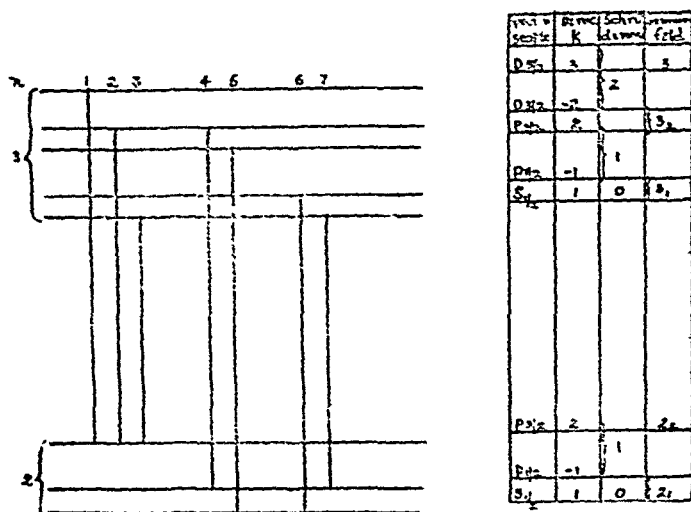


Fig. 1

[In the first column, the level is specified on the Russell-Saunders' scheme with their half-valued inner quantum numbers. The second column

contains Dirac's  $k$ -values for each term. The third column gives Schrödinger's  $l$ -values. The fourth column gives Sommerfeld's original classification  $D_{\frac{3}{2}}, P_{\frac{3}{2}}$  have the same energy-value as Sommerfeld's  $3_2$ , similarly  $P_{\frac{1}{2}}, S_{\frac{1}{2}}$  have the same value as  $3_1$ .]

As contrasted with Sommerfeld's original scheme, the  $H_\alpha$ -line is now seen to consist of 7-components instead of Sommerfeld's 3-components, but since the energy-values of some coincide, all these components are not different from each other.

Thus we have

I $a$	coinciding with	...	(1)
II $a$ (forbidden)	„ „	...	(2)
III $a$	„ „	...	(3)
II $b$	„ „	...	(4, 5)
III $b$ (forbidden)	„ „	...	(6, 7).

Of these  $IIa, IIIb$ , are forbidden according to Sommerfeld's older theory.

The position and observed intensity of these lines on a wave-length scale is shown in the following diagram:—

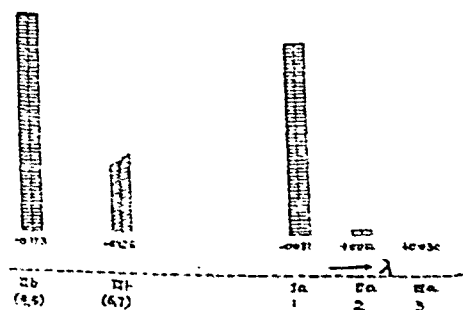


Fig. 2

[Actually in experimental work, only the red and violet components can be distinguished from each other.]

The  $H_{\alpha}$ -line thus consists of three multiplets as shown below 2P-3D, 2S-3P, 2P-3S. The lines forming a multiplet, say the 3-lines forming the 2P-3D-multiplet, should obey the Ornstein-Burger-Dorgelo formula; in 2P-3D, the intensities are as 9 : 5 : 1.

		-1	2	-2	3
3	$S_{1/2}$	$P_{1/2}$	$P_{3/2}$	$D_{5/2}$	$D_{3/2}$
1	$S_{1/2}$	1 <small>0.05</small>	2 <small>0.25</small>		
-1	$P_{1/2}$	1 <small>0.05</small>		5 <small>0.25</small>	
2	$P_{3/2}$	2 <small>0.25</small>		1 <small>0.25</small>	9 <small>0.45</small>

Fig. 3

[The broken lines enclose a multiplet. The central figures show the relative intensities of lines of a multiplet according to Ornstein-Burger-Dorgelo formula; the small figures '005, etc., represent the intensities as calculated by Goldstein in the paper abovementioned. The figures in the corners of squares represent the number of the component according to the scheme in Fig. 3.]

It is clear that it is not possible to test any theory with experimental results unless we know *the ratio of units of intensities in the three multiplets*. Let us denote these ratios by :—

$$I_{pd} : I_{sp} : I_{ps}.$$

Then the intensity of the red component =  $9I_{pd}$

and " violet " =  $5I_{pd} + 2I_{sp}$ .

It is now well-known that wave-mechanics have now opened the way for the calculation of absolute values of intensities. Taking advantage of a suggestion by

Wentzel who applied such theories for calculating the intensities of characteristic X-ray spectra of elements, Sommerfeld and Unsöld applied the Schrödinger-mechanics to calculate  $I_{rd} : I_{rp} : I_{pv}$ . In Schrödinger's calculus, no account is taken of duplicity phenomenon. Hence the multiplets 2P-3D, 2S-3P, 2P-3S . . . are regarded as single lines, and the calculated intensity represents the value for each one of the whole multiplet. Thus Sommerfeld and Unsöld found that

$$\begin{array}{l} 2P-3D : 2S-3P : 2P-3S \\ \text{as} \quad 1 : \frac{5}{2^3 \cdot 3} : \frac{5}{2^{10}} \end{array}$$

Now the statistical weight of the lines composing 2P-3D is  $15 = (9 + 5 + 1)$ , of 2S-3P is  $(2 + 1)$ , and of 2P-3S is  $(2 + 1)$ . Hence to get the units, we must divide these ratios by 15, 3, 3 respectively. We thus get

$$\begin{array}{l} I_{pd} : I_{rp} : I_{pv} \\ = 1 : 1.04 : .096 \end{array}$$

With these values, we have that the intensities of the red component and the violet components are to each other as  $9 : 5 + 2(1.0) = 7.06$ .

Actually Hansen finds, as Figure 2 indicates that the violet component is slightly more intense than the red component, but the violet component is slightly asymmetrical towards the red. The asymmetry is probably caused by the presence of component (6) having an intensity of 1.04. Components (3) and (7) have very slight intensity, and are neglected.

Sommerfeld and Unsöld extended their investigations to an examination of the fine-structure of  $\lambda 4686$  of  $\text{He}^+$ . Their results were later found by Paschen to be in full agreement with his new experiments on the intensity of the fine-structure components of  $\text{H}_\alpha$ .

## APPLICATION OF DIRAC'S THEORY

We have applied the Dirac theory of the electron to calculate the intensities of the fine-structure components of  $H_{\alpha}$  and  $\lambda 4686$  of  $\text{He}^+$ . As observed in the Introduction, the results are in perfect accord with the works of Sommerfeld and Unsöld, and hence with experimental facts. This suggests that Goldstein's work is vitiated by some grave mathematical error.

We have besides been able to obtain rigorous mathematical expressions for the magnetic components of each one of the fine-structure lines. The Ornstein-Burger-Dorgelo rule comes out as a deduction from calculations of transition-probabilities. Sommerfeld-Unsöld's procedure gives correct results, because the Schrödinger-mechanics is a limiting form of the Dirac-mechanics when  $c \rightarrow \infty$ , which is equivalent to putting  $W = 0$  (*vide supra*).

## OUTLINES OF THE MATHEMATICAL THEORY

We have all along followed the method given by Darwin and Weyl. The solutions in the case of a central field is given by :

$$\left. \begin{aligned} \psi_1 &= \frac{V}{r} (l+m+1) P_l^m \\ \psi_2 &= -\frac{V}{r} (l-m) P_l^{m+1} \\ \psi_3 &= -\frac{iW}{r} P_{l+1}^m \\ \psi_4 &= -i\frac{W}{r} P_{l+1}^{m+1} \end{aligned} \right\} \begin{array}{l} \text{for the term} \\ X_l, l+\frac{1}{2} \end{array} \quad (1)$$

and

$$\left. \begin{aligned} \psi_1 &= \frac{V}{r} P_l^m \\ \psi_2 &= \frac{V}{r} P_l^{m+1} \\ \psi_3 &= -\frac{iW}{r} (l+m) P_{l-1}^m \\ \psi_4 &= -\frac{iW}{r} (l-m-1) P_{l-1}^{m+1} \end{aligned} \right\} \begin{array}{l} \text{for the term} \\ X_l, l-\frac{1}{2} \end{array} \quad (2)$$

' $l$ ' now denotes the Schrödinger-value of the azimuthal quantum number. The second set corresponds to Dirac's negative  $k$ -values.

$$\text{Where } P_l^m = \frac{l-m!}{2^l l!} (\sin \theta)^m D^{l+m} (\mu^2 - 1)^l \quad (3)$$

$$P_l^{-m} = (-1)^m P_l^m, \quad D = \frac{d}{d\mu}, \quad \mu = \cos \theta.$$

We have further

$$V = e^{-\beta r} F \dots W = e^{-\beta r} G \dots \quad (4)$$

where  $F$  and  $G$  are polynomials of the form

$$F = r^{\mu_0} \sum_{s=0}^{s=n_r} a_{\mu_0+s} r^s \quad G = r^{\mu_0} \sum_{s=0}^{s=n_r} b_{\mu_0+s} r^s$$

$$\mu_0 = \sqrt{(l+1)^2 - a^2} \quad \alpha = \frac{2\pi e^2}{ch} \cdot z.$$

$$\left. \begin{aligned} v_0 &= \frac{m_0 c^2}{h} \cdot \frac{v}{\sqrt{v_0^2 - v^2}} = \frac{1}{\alpha} \left[ n_r + \sqrt{(l+1)^2 - a^2 z^2} \right] \\ \text{and } \beta &= \sqrt{v_0^2 - v^2} \\ &= \frac{z}{a(n_r + k)} = \frac{z}{an} \text{ (approximately)} \end{aligned} \right\} \quad (5)$$

$n_r$  = radial quantum number

$n$  = total quantum number

$a$  = normal hydrogen orbit.

We have the following recursion-formula for  $a_{\mu_0+s}$  when  $a$  can be neglected.

$$a_{\mu_0+s+1} = -a_{\mu_0+s} \cdot \left( \frac{2}{an} \right) \cdot \frac{n_r - s}{(s+1)(2k+s)} \quad (6)$$

$G$  and consequently  $W$  is a small quantity. In fact  $|W| = \alpha |V|$

With the aid of the recursion-formula for the coefficient  $a$ 's, we can write out  $V$  in a form more suitable for calculation:—

$$V = a_0 \rho^{\mu_0} e^{-\frac{\rho}{2}} L_{n+2l+1}^{2l+1}(\rho) \quad (7)$$

$$\text{where } \rho = 2\beta r = \frac{2r}{a} \cdot \frac{1}{n}$$



$L(\rho)$  is the Laguerre Polynom, introduced by Schrödinger.

The only unknown constant is  $\alpha_0$  which is eliminated by normalisation.

Let

$$\lambda_{lm} = \psi_1 \overline{\psi_1} + \psi_2 \overline{\psi_2} + \psi_3 \overline{\psi_3} + \psi_4 \overline{\psi_4} \quad (8)$$

Then we have to put

$$\int \lambda_{km} d\Omega = 1.$$

We have for the term  $X_{l, l+\frac{1}{2}}$

$$\int \rho_{lm} d\Omega = 4\pi \frac{l-m}{l+1} \int (V^2 + W^2) dr = 1 \quad (9)$$

for  $X_{l, l-\frac{1}{2}}$

$$\int \rho_{lm} d\Omega = 4\pi \frac{l+m}{l-1} \int (V^2 + W^2) dr = 1 \quad (10)$$

#### TRANSITION-PROBABILITIES

Let the initial and final states be denoted by the numbers  $(l, m)$ ,  $(l', m')$ , and let  $\psi, \psi'$  denote the corresponding  $\psi$ -functions. Let  $\chi$  denote the expression:—

$$\chi = \psi_1 \overline{\psi'_1} + \psi_2 \overline{\psi'_2} + \psi_3 \overline{\psi'_3} + \psi_4 \overline{\psi'_4} \quad (11)$$

We shall now find out the mean values of the displacements.

$$Z = r \cos \theta, \quad x + iy = r \sin \theta e^{i\phi}, \quad x - iy = r \sin \theta e^{-i\phi}.$$

Corresponding to the transition  $(lm) \rightarrow (l' m')$  we have

$$\left. \begin{aligned} \overline{Z} &= \int r \cos \theta \chi d\Omega \\ \overline{x+iy} &= \int r \sin \theta e^{i\phi} \cdot \chi d\Omega \\ \overline{x-iy} &= \int r \sin \theta e^{-i\phi} \cdot \chi d\Omega \end{aligned} \right\} \quad \dots \quad \dots \quad (12)$$

Every one of these integrals can be written in the form—  $R\theta\phi$ , where  $R, \phi$ , and  $\theta$  are integral involving  $r, \theta, \phi$  alone respectively.

It is unnecessary to reproduce the steps by which it has been proved that

$$\begin{aligned} \bar{Z} &\neq 0 \quad \text{only when } m=m', m'=m+1, m'=m-1 \\ \overline{x+iy} &\neq 0 \\ \overline{x-iy} &\neq 0 \quad \dots \quad \dots \end{aligned} \quad (13)$$

as they are to be found in many books.

The above is the Selection Principle for the magnetic quantum number. A consideration of the  $\theta$ -integrals shows that  $\theta \neq 0$  only when

$$l'=l-1, l+1, (l-3), (l+3), (l-5) (l+5), \text{ etc.}$$

We now find out the value of  $\bar{Z}$  for the transition  $l \rightarrow l-1$ .

We have

$$\bar{Z} = \frac{\int \chi \bar{Z} d\Omega}{\left[ \int \rho_{l,m} d\Omega \int \rho_{l-1,m} d\Omega \right]^{\frac{1}{2}}} \quad \dots \quad (14)$$

and we obtain, after some reduction that

$$\bar{Z} = \frac{1}{2l+1} \sqrt{(l+m+1)(l-m)} [r], \quad \dots \quad (14')$$

$$\text{where } [r] = \frac{\int (VV' + WW') r dr}{\sqrt{\int (V^2 + W^2) dr} \cdot \int (V'^2 + W'^2) dr} \quad (15)$$

When we neglect the  $W$ -functions in comparison to  $V$ 's, we get

$$[r] = \left\{ \frac{\ln r}{((n+l)^2)} \cdot \frac{\ln r'}{((n'+l')^2)} \right\}^{\frac{1}{2}} \frac{a_n 2^{l+r+2}}{n^{l+2} n'^{l'+2}} S. \quad \dots \quad (16)$$

and  $S$  is the integral introduced by Sommerfeld

$$S = \int e^{-\left(\frac{1}{n} + \frac{1}{n'}\right)s} L_{n_r+2l+1}^{2l+1} \left(\frac{2s}{n}\right) L_{n_r+2l'+1}^{2l'+1} \left(\frac{2s}{n'}\right) S^{l+r+2} ds. \quad (17)$$

We can now calculate the other transition probabilities, in a similar way. Their values are shown in the following table:—

Transition . . .  $\bar{Z}$   $\overline{x+iy}$   $\overline{x-iy}$  . . .

$$l \rightarrow l-1 \quad \sqrt{(l+m+1)(l-m)} \cdot \frac{\sqrt{(l-m)(l-m-1)}}{\sqrt{(l+m+1)(l+m)}}.$$

$$l \rightarrow l+1 \quad \sqrt{(l-m+1)(l+m+2)} \cdot \frac{\sqrt{(l+m+2)(l+m+3)}}{\sqrt{(l-m+1)(l-m+2)}}.$$

$$F_l^{l-1} = \left\{ \frac{|n_r|}{(|n_r+2l+1|)^3} \frac{|n_r'|}{(|n_r'+2l'+1|)} \right\}^{\frac{1}{2}} \frac{2^{2l+1} S}{n^{l+2} n'^{l+1}} \cdot \frac{\alpha}{2l+1}$$

$$F_l^{l+1} = \left\{ \frac{|n_r|}{(|n_r+2l+1|)^3} \frac{|n_r'|}{(|n_r'+2l'+1|)^3} \right\}^{\frac{1}{2}} \frac{2^{2l+3}}{n^{l+2} n'^{l+3}} \cdot \frac{\alpha}{2l+1}$$

and four other expressions.

The factors  $\sqrt{(l+m+1)(l-m)}$ , etc. . . . are in essence identical with the corresponding expressions involving  $l$  and  $m$ , which have been obtained by Heisenberg and Jordan for transition-probabilities on matrix-mechanics (Cf. Birtwhistle, New Quantum Theory, Chap. XV, p. 122).

In the work of Heisenberg and Jordan, the values of the multiplying functions  $F_l^{l'}$  are left indeterminate in the form of  $B, C, A$ . Here the  $F$ 's are calculated in terms of known quantities.

#### CALCULATION OF INTENSITIES\*

The possible values of  $m$ , the magnetic quantum number are:—

$$l, l-1, l-2 \dots \dots - (l+1)$$

The expressions for  $\bar{Z}$ ,  $\overline{x+iy}$ ,  $\overline{x-iy}$  enable us to calculate the intensities of the magnetic components into which any particular line is decomposed when excited in a magnetic field;  $\bar{Z}$  corresponding to the component vibrating parallel to the field,  $\overline{x+iy}$ ,  $\overline{x-iy}$  referring to the circularly polarised components. The transitions corresponding to these components are shown below for  $l=2$ ,  $l=1$ .

---

\* These calculations were given by Hönl., Ann. der Physik, Vol. 79.

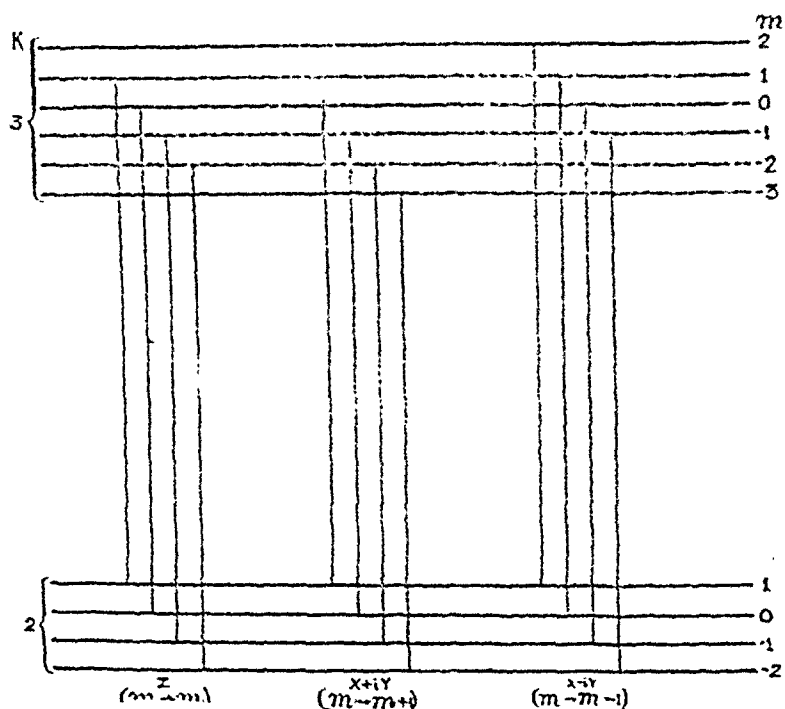


Fig. 4

The above diagram represents the magnetic splitting of the line  $P_{\frac{3}{2}} D_{\frac{5}{2}}$ .

When there is no magnetic field, all these components unite to give a single line. In this case, we have to calculate the sum of the intensities of all the components. It can be shown that:

$$\sum (x+iy)^2 = \sum (\overline{x+iy})^2 = 2 \sum Z^2$$

the summation extending over all the possible values of  $m$ .

After working out the summation, we find that the intensities are given by expressions of the form:

$$\{ F_k^{k'} \}^2 f(l)$$

where  $f(k) = 3 \sum (l+m+1)(l-m)$ , etc.

The values of  $f(l)$  are given for the different transitions:—

$$l \rightarrow l-1 \dots 2(l+1). l.(2l+1)$$

$$l \rightarrow l+1 \dots 2(l+1)(l+2)(2l+3)$$

and for

$$2(l+1)(2l+1)(2l+3).$$

Thus the intensity of the line due to the  $l$ -transition  $1 \leftarrow 2$ , is given by the expression :

$$I = \left\{ \left[ \frac{|n_r|}{(n+2l+1)^3} \left( \frac{|n_r'|}{|n'+2l'+1|} \right)^3 \right]^{\frac{1}{2}} \frac{2^{2l+1}}{n^{l+2} n'^{l+1}} \frac{a^2}{(2l+1)^2} \right\} \times 2(l+1)(2l+1)l.$$

We can now easily calculate the intensities of the lines forming a multiplet, *viz.*—(1, 4, 2), constituting the 2P-3D multiplet. It can be easily seen that the expression within the curly brackets is the same for all these lines. Hence their intensities will be proportional to expression outside these brackets. We have, therefore,

$$I_1 : I_4 : I_2 \\ = \left[ \frac{2(l+1)l}{2l+1} \right] : \left[ \frac{2l}{(2l-1)(2l+1)} \right] : \left[ \frac{2l(l-1)}{2l-1} \right]$$

where  $l=2$

$$= \frac{6 \cdot 2}{5} : \frac{4}{3 \cdot 5} : \frac{4 \cdot 1}{3} \\ = .9 : 1 : 5.$$

The result is in perfect agreement with the Ornstein-Burger-Dorgelo rule for the distribution of intensities amongst the components of a 2P-3D multiplet.

It can be shown in a similar way that the other multiplets obey the O-B-D rule perfectly.

Let us now obtain the ratios of units of intensities.

We get, after some calculation :—

$$I_{pd} : I_{ep} : I_{ps} \\ = \frac{I_1}{9} : \frac{I_1}{2} : \frac{I_1}{2} \\ = 1 : 1 \cdot 04 : \cdot 025.$$

These are in perfect agreement with the result obtained by Sommerfeld and Unsöld.

The  $\text{H}\alpha^+$ -line,  $\lambda 4686$ .

According to Lande's theory, this line is composed of a number of multiplets as shown in the following diagram :

	1	-1	2	-2	3	-3	4
3 $\begin{smallmatrix} 4 \\ 3 \end{smallmatrix}$	$S_{1/2}$	$P_{1/2}$	$P_{3/2}$	$D_{3/2}$	$D_{5/2}$	$F_{3/2}$	$F_{5/2}$
1	$S_{1/2}$	$\begin{smallmatrix} 12 \\ 1 \end{smallmatrix}$	$\begin{smallmatrix} 11 \\ 2 \end{smallmatrix}$				
-1	$P_{1/2}$	$\begin{smallmatrix} 13 \\ 1 \end{smallmatrix}$		$\begin{smallmatrix} 10 \\ 5 \end{smallmatrix}$			
2	$P_{3/2}$	$\begin{smallmatrix} 9 \\ 2 \end{smallmatrix}$		$\begin{smallmatrix} 6 \\ 1 \end{smallmatrix}$	$\begin{smallmatrix} 5 \\ 9 \end{smallmatrix}$		
-2	$D_{3/2}$	$\begin{smallmatrix} 8 \\ 5 \end{smallmatrix}$	$\begin{smallmatrix} 7 \\ 1 \end{smallmatrix}$			$\begin{smallmatrix} 4 \\ 14 \end{smallmatrix}$	
3	$D_{5/2}$		$\begin{smallmatrix} 3 \\ 9 \end{smallmatrix}$			$\begin{smallmatrix} 2 \\ 1 \end{smallmatrix}$	$\begin{smallmatrix} 1 \\ 20 \end{smallmatrix}$

Fig. 5

We have 3D-4F multiplet consisting of [1, 2, 4]  
 3P-4D " " [5, 6, 10]  
 3S-4P " " [11, 12]  
 3D-4P " " [3, 7, 9]  
 3P-4S " " [9, 13]

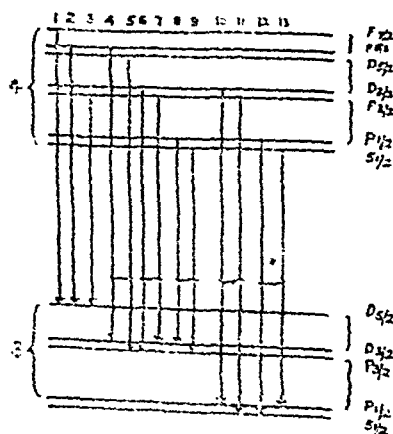


Fig. 6

The intensity-ratios in any particular multiplet according to the Ornstein-Burger-Dorgelo rule are indicated by the central figures. Thus [1, 2, 4] constitute the 3D-4F-multiplet, their theoretical intensities ought to be as 20 : 1 : 14. Goldstein's figures have not been reproduced as they are evidently wrong.

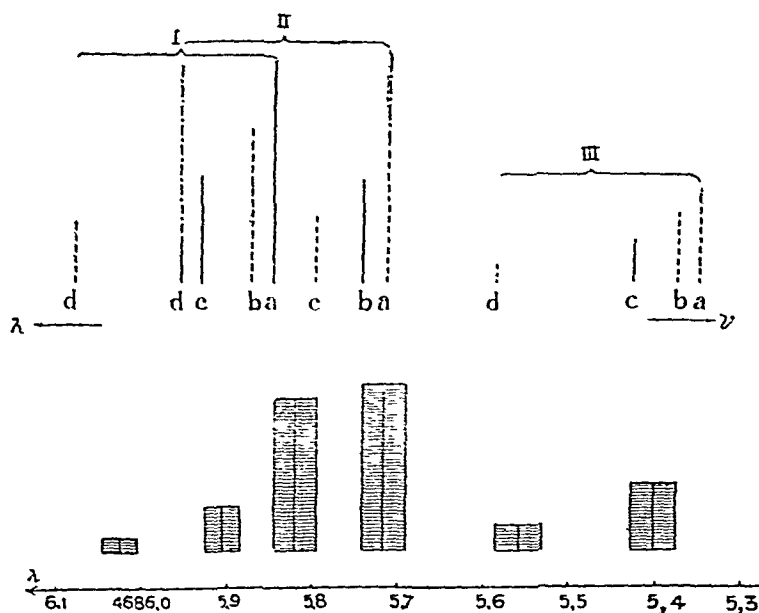


Fig. 7

The position of the components on a wavelength scale is reproduced from a recent paper by Paschen [Ann. d Physik, Vol. 82].

It is easy to see that Paschen's results are in very good agreement with theoretical calculation :

Firstly, as regards the O-B-D-rule we have :

$$\begin{aligned}
 I_1 : I_2 : I_3 &= \left[ \frac{2l(l+1)}{2l+1} \right]_{l=3} : \left[ \frac{2l}{(2l-1)(2l+1)} \right] : \left[ \frac{2l(l-1)}{2l+1} \right] \\
 &= \frac{8 \cdot 3}{7} : \frac{6}{5 \cdot 7} : \frac{6 \cdot 2}{5} \\
 &= 20 : 1 : 14
 \end{aligned}$$

We obtain, after some calculation, the ratios of units of intensity in the five multiplets as follows :

$$\begin{array}{ccccccccc} 3D-4F & : & 3P-4D & : & 3S-4P & : & 3D-4P & : & 3P-4S \\ 1 & : & '85 & : & & : & & : & \end{array}$$

We quote from Paschen, regarding the accordance of these results, which are the same as those given by Sommerfeld and Unösld on the Schrödinger theory, with his experimental data.



# RAMAN EFFECT

BY

YUDHISHTHIR BHARGAVA

AND

R. C. MAJUMDAR

*Physics Department, Allahabad University.*

## PART I

The discovery of what is known as Raman Effect by Prof. Sir C. V. Raman<sup>1</sup> on February 28, 1928, caused a flutter in the scientific world. A discovery of the first magnitude, it came at a moment when a new field of research was badly needed by the physicists. The spectra of molecules had been studied with great labour and perseverance and Raman Effect was the very thing required for a more intimate study and ordering.

The phenomenon of the blue colour of the sky besides being a source of poetic inspiration, has been noticed by philosophers since very ancient times. As is well known the explanation on rigorous scientific lines was given by Lord Rayleigh<sup>2</sup> in 1873. He based his explanation on an experiment of Tyndall who passed white light through a tube containing fine particles formed by bringing butyl nitrite vapour and hydrochloric acid gas together at a low pressure. When the particles had developed a correct size they scattered the blue light strongly and the tube on being looked at sideways showed an azure colour. This experiment showed that particles of a particular size scattered light in such a manner that the blue light preponderated over the red and further the scattered beam was polarised.

<sup>1</sup> Raman, Ind. J. Phys., Vol., II, p. 387 (1928).

<sup>2</sup> Rayleigh, Collected Papers.

Lord Rayleigh showed that the scattering should vary inversely as the fourth power of the wavelength and that the scattered light should be polarised. He found theoretically that the amount of light scattered at an angle  $\theta$  is given by:—

$$S = \frac{\pi^2 (1 + \cos^2 \theta)}{\gamma^2} \frac{(E - E_0)^2}{E^2} \left( \frac{3E_0}{E + 2E_0} \right)^2 \frac{NV^2}{\lambda^2} J_0$$

where  $\gamma$  = Distance of the point of observation.

$V$  = Total volume of scattering space.

$N$  = Number of particles per unit volume.

$E_0$  = Dielectric constant of surrounding atmosphere.

$E$  = Dielectric constant of the medium.

$\lambda$  = The wavelength of scattered light.

Tyndall's experiment, in fact, showed the scattering by comparatively large particles. There was some doubt whether particles of atomic size would show the effect. Lord Rayleigh (junior) and Cabannes independently carried out experiments to show that the scattering was shown even by molecules.

The above theory is only phenomenological as it does not take into account the constitution of the scattering particles. The first step in this direction was taken by Cotton and Mouton who introduced the idea of molecular anisotropy for explaining electric and magnetic birefringence. After the experimental discovery of the depolarisation of scattered light by Rayleigh (junior), Rayleigh (senior) utilised the idea of molecular anisotropy for calculating the amount of depolarisation. Later on L. Vessot King, Rocard, and Ramanathan perfected a theory of scattering for a perfect gas.

The investigation of light scattering was taken up in Prof. Raman's laboratory at Calcutta to investigate in detail this phenomenon of molecular scattering. According to workers of that laboratory the presence of the effect was felt since the beginning of the work. As Prof. Raman writes.

"From the very first, however, evidence was encountered of the presence of a disturbing effect." It was labelled as a 'Special type of feeble fluorescence.' The idea that it was a new phenomenon gained ground in 1927 when Prof. Raman was engaged in working out a theory of Compton Effect and after a series of brilliant investigations this effect was brought to light, having been already predicted by Smekal in 1923, from the Kramers-Heisenberg theory of dispersion.

It is strange that nobody had up to this time conceived the idea of studying the scattering of monochromatic light. Raman<sup>1</sup> did this and discovered that benzol on being illuminated by monochromatic light from a mercury arc scattered in addition to the original wavelength of frequency  $\nu$  rays of frequency  $\nu \pm \nu_k$  where  $\nu_k$  was a characteristic infra-red frequency of the benzol molecule as measured by Coblentz and V. Henri. These modified lines as they are called had several points characteristic to themselves; their intensities as compared to the unmodified lines were very small and in most cases they were accompanied by a faint continuous spectrum. The line of enhanced frequency was very weak as compared to that of degraded frequency, and increased in intensity as the temperature of the scattering substance was raised. Strong polarisation of the lines was in evidence and the radiations appeared to be incoherent.

As the study of the phenomenon progressed it was found that the change in frequency did not always correspond to the infra-red absorption line or band of a substance, *e.g.*, in HCl the Raman Line corresponded to the 'missing line' in the absorption spectrum of HCl and in some cases it corresponded to the inactive frequencies.

A month later Landsberg and Mendelstam<sup>2</sup> in Russia discovered the same phenomenon of combination scattering in Quartz.

<sup>1</sup> Raman and Kirshnan, *Loo. cit.*, and *Ind. J. Phys.*, 2, 399 (1928).

<sup>2</sup> Landsberg and Mendelstam, *Naturwiss.*, 28, 557 (1928).

Shortly after the publication of Raman's results Pringshiem<sup>1</sup> gave a thorough description of the effect. He recognised that the Raman Effect was entirely different from other types of secondary radiations such as Tyndall Scattering, Compton Effect, fluorescence and the resonance scattering.

A fact of great importance which distinguishes the Raman Effect is that the shift in frequency of the incident beam is dependent only on the nature of the substance.

The difference between fluorescence and Raman Effect is:

- (a) The frequencies of fluorescence spectrum are independent of those of the exciting radiation provided they can excite fluorescence at all. On the other hand, the frequencies of radiation modified by Raman Scattering are directly related to  $\nu$  being  $\nu \pm \nu_k$  where  $\nu_k$  is either an actual infra-red frequency in the absorption spectrum of the scattering material or the difference in such frequencies.
- (b) The intensity of the Raman Lines is of an entirely different order from that of fluorescence lines.
- (c) Most of the lines obtained in the Raman Spectrum are strongly polarised.

The relation between Wood's Resonance Scattering with sodium and iodine vapour and Raman Effect needs a more critical examination. Wood discovered that when iodine and sodium vapours are illuminated by certain monochromatic radiations which have not the same wavelength as the known absorption lines, there are found to be present close double lines on each side of the primary line separated by multiples of frequency  $\nu_0$  where  $\nu_0$  is the fundamental

<sup>1</sup> Pringshiem, Naturwiss, 16, 597 (1928).

frequency of the sodium molecule (sodium forms temporary molecules of  $\text{Na}_2$ ) or iodine molecules. There are Stokes lines  $\nu - n\nu_0$  and anti-Stokes lines  $\nu + n\nu_0$ . Each line is a narrow doublet and the separation is found to be  $2 \times \frac{h}{8\pi^2 I}$ , i.e., the rotational interval of the  $\text{Na}_2$  molecule.

The process is usually explained as a fluorescence phenomenon. The sodium molecule absorbs the whole quantum of light and is raised to a higher excited state, and after a short time returns to some lower allowed state of excitation. We may visualise the process by the following diagram.

Let A denote the state of the molecule absorbing the incident light ( $e$ =electronic state,  $n$ =vibration quantum number,  $m$ =rotational quantum number), B is the state to which it is raised by absorption, and A' is the state to which it returns on re-emission.

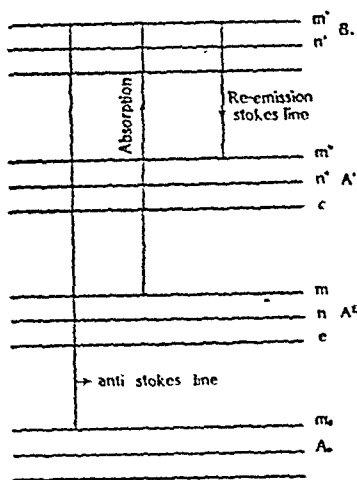


Fig. 1

Production of Raman Lines in a Molecule.

Here the electronic state may be supposed to be the same though they may be generally different; the re-emitted radiation has the frequency  $\nu - (\nu_A - \nu_{A'})$ . The production of the anti-Stokes line is also illustrated.

Now in choosing the values of  $n'$ ,  $m'$ ,  $n''$ ,  $m''$ , we must be guided by the selection principle. There is no selection principle for the vibration quantum number. Hence  $n' - n''$  may have any value 0, 1, 2, . . . . But we are not so free in our choice of  $m' - m''$ . According to the selection principle for absorption lines

$$\Delta m = \pm 1, \text{ are allowed.}$$

Taking  $\Delta m = \pm 1$ , we have,

$$m' = m + 1 \text{ or } m - 1$$

Again in re-emission,  $\Delta m = \pm 1$

$$\therefore m'' = m \text{ or } m + 2$$

$$m \text{ or } m - 2$$

Hence  $m'' - m = 0$

or  $\Delta m_R = 0 \text{ or } \pm 2.$

This explains the occurrence of close doublets with double the frequency interval. This argument was first adduced by Lenz in accounting for the occurrence of doublets in Wood's Resonance Spectrum, as an illustration of the selection principle for the rotational quantum number, and has been rediscovered in trying to account for the occurrence of a similar phenomenon in Raman Scattering by Schrödinger, Rassetti, Dieke and Langer, Majumdar and Kothari.

Wood's Resonance Spectrum shows a number of anti-Stokes lines. We can account for them if we suppose that the initial state A is not the absolutely lowest state, but a slightly excited state. This slightly excited state is produced by the influence of thermal agitation. If now in the process of re-emission, the molecule returns to a still lower state  $A_0$  the re-emitted energy has the frequency

$$\nu + (\nu_{A_0} - \nu_A)$$

We thus get the anti-Stokes lines. The anti-Stokes lines are naturally weaker than the Stokes lines.

The vibrational frequencies are equivalent to  $(n-n') \nu_0$  approximately, where  $\nu_0$  = fundamental vibrational frequency. They are quite small for  $\text{Na}_2$  and  $\text{I}_2$ ; hence the proportion of excited states under even not very high temperatures is quite great, and we sometimes get quite a large number of anti-Stokes lines.

The question is: What is the difference between Raman Effect and Wood's Resonance radiation? In explaining Raman Effect, we substitute 'Scattering' in place of absorption. But we think the mechanism of Raman Effect is rather widely different from that of ordinary scattering. Light which is pictured as a progressive sine wave excites the harmonic oscillator and sets it into forced vibration. The accelerated electron sends out coherent radiation in the classically allowed directions. The radiation pulse causes no internal change. But in Raman Scattering, an internal change is induced (change from State A to B and back to A'), hence it cannot be denied that the light is partly absorbed.

But this absorption is of a different type altogether from those to which we are accustomed in atomic absorption.

In the case of absorption by atoms we have two types:—

(1) Absorption of characteristic lines, *i.e.*, of  $D_1$ ,  $D_2$  and other lines of the principal series by sodium vapour.

(2) Absorption of all frequencies lying beyond the series limit, resulting in the ionization of the element.

In type (1) only characteristic frequencies are absorbed.

Other frequencies are inoperative.

Molecular absorptions are also of two types—(1) Absorption of band lines; (2) Continuous absorption resulting in the dissociation of the molecule into a normal atom and excited atom (Franck's Theory).

It is clear that the absorption of the quantum for producing Raman Scattering belongs to neither of these two types and is an essentially new type and intermediate

between orthodox scattering and orthodox absorption. The nature of radiation finally emitted depends upon the period of interaction between matter and the quantum, the constitution of the molecule and the nature of its surroundings.

Pringsheim thinks that Raman Effect is different from Fluorescent radiation ; because

- (1) the intensity is of a different order ;
- (2) the polarization is very strong ;
- (3) the displaced spectrum can be produced by all spectral lines.

As regards (1) the intensity of fluorescent radiation depends on the amount of absorption and this is generally varied within wide limits. As regards (3) Wood showed that  $\lambda$  5461 contains six absorption band lines of iodine, but this may be quite fortuitous because it has been found that some strong lines of Li (?) all produce resonance spectra. The iodine molecule may possess absorption lines in all parts of the spectrum. It is not quite improbable. As regards (2) it has been shown that Wood Lines are partially polarized. We are of opinion that Wood's Resonance Spectrum is a particular case of Raman effect which is a much more general phenomenon and is shown by matter in all states of aggregation. Wood's Resonance Spectrum is merely Raman Effect by diatomic molecules the exciting line being near the absorption bands.<sup>1</sup> Cotton thinks that it is different because in Raman Effect there are a few combination lines whereas there are a large number of lines in Wood's Resonance Radiation. But this is easily explained. In  $\text{Na}_2$ , for example, the vibration frequency corresponding to  $(0 \leftarrow 1)$  is only 146. Hence a large number of excited states are present even when the temperatures of the illuminated vapour is moderate for according to Maxwell's law  $n =$

<sup>1</sup> This aspect is discussed in the appendix.



$n_{0c} \sim \frac{nh\nu_k}{kT}$ . In the substances in which Raman Effect has been studied,  $\nu_k$  is too large, and under the conditions (temperature as well as due to the state of aggregation) not more than one or two modified lines can be produced.

Another very important difference which may be pointed out is that Wood's Resonance Spectrum is excited by certain lines only, *e.g.*, the red and orange lines of lithium are the only lines which excite the resonance spectrum in the red region. The greenish blue resonance is excited only by certain lines of certain metallic arcs. (For data see Baly's Spectroscopy, Vol. II, p. 239.) No such restriction is imposed in Raman Effect; neither is it confined to a particular region nor does it favour certain lines. This however might be due to the presence of absorption bands in this region. In iodine there are bands with small separation.

A very interesting type of Scattering has been observed by Gross<sup>1</sup> of the Optical Institute, Leningrad. Several liquids, *e.g.*, aniline, toluene, benzene, water, etc., were illuminated by the mercury line  $\lambda$  4358 Å. U. The scattered radiation was examined by an echelon grating (30 steps). Besides the unmodified several other lines—differing in wavelength by about 0.5 Å. U.—were observed. The intensities of the 'red' and the 'blue' components were nearly equal. The sharpness of the displaced as well as the undisplaced component varies with the scatterer, and between the components a continuous spectrum is present. Some components do exhibit polarisation. The displacement from the central line varies with the direction of observation.

It seems fairly clear that these are not due to Raman Effect (rotational). The explanation suggested by Gross is that the splitting may be due to the acoustic oscillations like those used by Debye<sup>2</sup> to explain the specific heat

<sup>1</sup> Nature, Vol. 126, 201 (1930).

<sup>2</sup> Ann. de Phys., 39, 789 (1912).

phenomenon. These elastic waves travelling with the speed of sound produce as it were 'modulations' in the optical wave train. Two new frequencies given by  $\nu = \nu_0 \pm 2\nu_0 v/c \sin \theta/2$  are produced,  $\nu_0$  being the incident frequency,  $v$  the velocity of sound,  $c$  that of light in the medium, and  $\theta$  the angle between the incident and the scattered ray.<sup>1</sup> The multiple components can be given by  $\nu = \nu_0 (1 \pm 2n v/c \sin \theta/2)$ ,  $n = 0, 1, 2, 3$ , etc. It should be noted that the length of the acoustic waves involved is of the order of that of light waves. Gross has observed  $n \leq 3$ . In the first report agreement with the calculated values was found to be fairly good, but later it was observed<sup>2</sup> that the displaced components did not strictly follow the above equation—the observed values in all the cases except aniline being greater than the calculated values.

These observations are of great interest, theoretical as well as practical and further work in this direction may reveal its connection, if any, with Raman Effect.

## EXPERIMENTAL METHODS

*Raman's Method.*<sup>3</sup>—In the original experiment the apparatus was arranged as shown below:—

Light from the source Hg which is a 3000 c.p. mercury vapour lamp is concentrated by an 8-inch condenser into a flask of clear non-fluorescent glass containing the liquid under study. The scattered light was viewed at right angles to the direction of the original beam by focussing the light on the slit of a spectrograph of large light-gathering power. Wavelengths greater than  $\lambda 4358 \text{ \AA. U.}$  were excluded by suitable filters. A few hours' exposure is reported to be sufficient for a good spectrogram, but exposures of as much as 24 hours are necessary to bring out faint Raman lines.

<sup>1</sup> Brillouin, *Ann. de Phys.*, 17, p. 88 (1922).

<sup>2</sup> *Nature*, Vol. 126, p. 400 (1930).

<sup>3</sup> Raman, *Loc. cit.*

The above method has been characterised by Wood as 'wasteful and inefficient,' and he<sup>1</sup> has perfected a method of

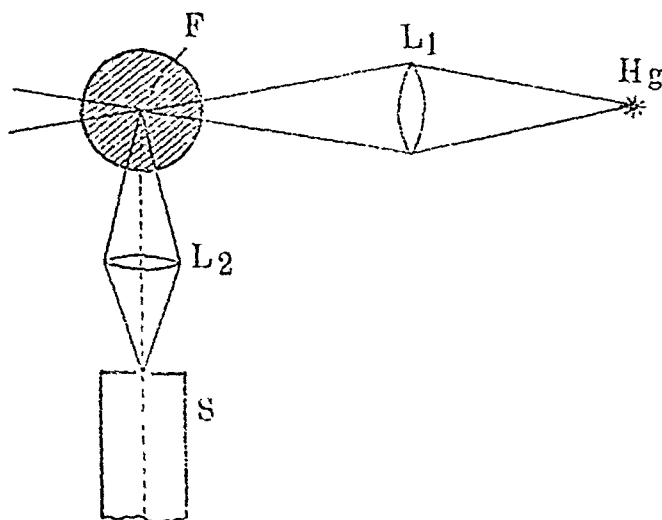


Fig. 2

## Raman's Arrangement.

(Hg—Mercury vapour arc; F—Flask containing benzene;  $L_1 L_2$ —Lenses; S—Spectroscope)

working which can record Raman lines in a few minutes. The arrangement of his apparatus is seen in the following diagram.

The mercury arc is placed almost in contact with the tube containing the liquid. One end of the tube is drawn

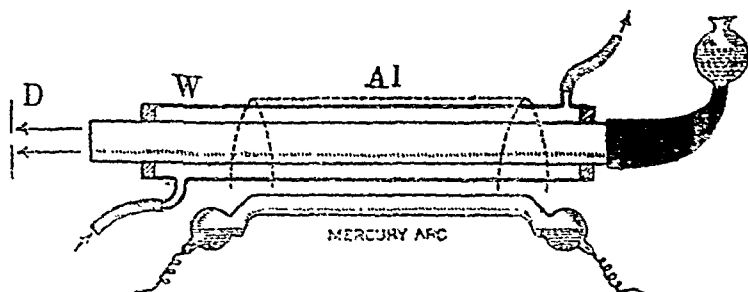


Fig. 3

## Wood's Arrangement

(W—Water Jacket; Al—Aluminium reflector; D—Slit of the spectroscope)

<sup>1</sup> Wood, Phil. Mag., 6, 729 (1928).

out into a cone of the shape shown in the diagram with a funnel at the top to facilitate the filling of the liquid. A head is also blown on the horn in line with the axis of the tube to enable accurate collimation to be made. The other end is either covered with a piece of optically good glass or the tube itself is drawn out and ground plane, a piece of cover glass being fixed with Canada balsam if necessary. The tube is surrounded with a glass jacket through which water can be circulated for cooling the tube. If it be necessary to use a filter it can be circulated through the glass jacket, in solution or otherwise. The whole apparatus is surrounded more or less completely with cylindrical reflectors made of polished sheet aluminium. Thus not only is the entire radiation from the lamp utilised but rays of light being reflected to and fro traverse the scattering liquid a number of times. The spectrometer which must necessarily be of large light-gathering power to avoid long exposures is placed along the axis of the tube. A number of diaphragms are used to cut out the light reflected from the sides of the container or otherwise.

For further details the original paper of Wood<sup>1</sup> should be consulted.

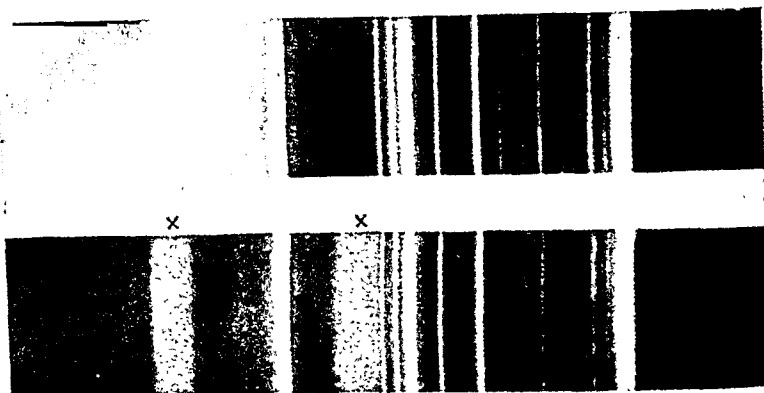
The next improvement by Wood<sup>2</sup> consists in substituting helium for mercury arc excitation. As a source a helium discharge tube about 9 ft. in length wound in the form of a helix over a nickel glass tube is used. This ultra-violet glass has the peculiar property of transmitting  $\lambda$  3888 Å. U. and very little else. The helix is filled with helium at 8 mm. pressure and is excited at 20000 volts.

More recently a new type of hot cathode low voltage helium tube has been constructed by the General Electric

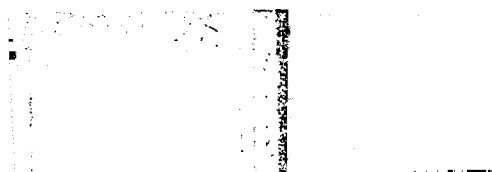
<sup>1</sup> Wood, *Loc. cit.*

<sup>2</sup> Wood, *Phil. Mag.*, 7, 858 (1929).

# PLATE 1



(i) Incident Spectrum Hg arc.  
(ii) Raman Spectrum of Water.



(a) Incident Spectrum.



(b) Benzene Scattering.



(c) Raman Spectra of Toulene.

Company, which is specially suited for studies on Raman Effect.

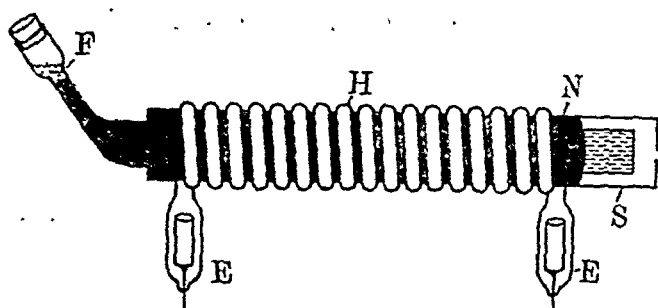


Fig. 4

Wood's Helium tube excitation.

(F—funnel; H— discharge tube with He; E—Electrode;  
N—Nickel glass tube.)

The advantages of helium excitation are :—

- (i) The Raman Spectrum is excited by a single line and lines spread out without any contamination from other lines.
- (ii) Continuous background gives no trouble.
- (iii) The short wavelength exciting is a favourable factor.
- (iv) No water cooling is required; the heat generated in the discharge tube being very small.

Section (iii) requires comment. As a consequence of Rayleigh's law of classical scattering the intensity of the scattered beam is inversely proportional to  $\lambda^4$ . So light of shorter wavelength is expected to be scattered more. At the first sight therefore it would appear that it would be best to use light of as short wavelength as possible. But this only holds for substances which do not show any appreciable absorption, fluorescence or chemical change under the ultra-violet radiation.

Since Raman Scattering is incoherent the intensity of the lines will depend on the aggregation of the molecules. It is clear, therefore, that the scattering will be very feeble with gases and special technique is required for their study.

Wood, Rassetti<sup>1</sup> and others have successfully carried out experiments on Raman Effect with gases.

Rassetti illuminates a column of gas at about 10—15 atmospheres pressure by a quartz mercury arc placed close to it. The gas is enclosed in a quartz tube about 20 cms. long and fastened to a large steel tube by means of sealing-wax. Another quartz tube encloses the first and the space between them can be used to put filters. The following diagram shows the apparatus.

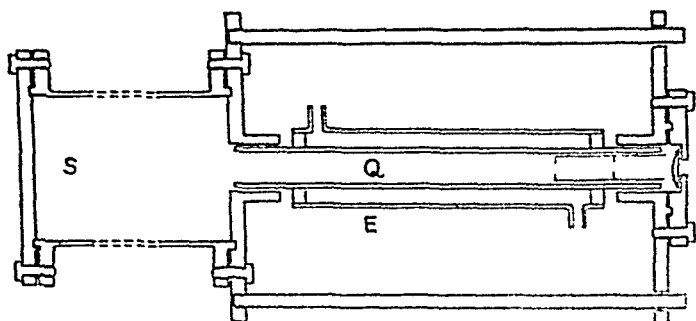


Fig. 5

Rassetti's apparatus for gases.

(Q—Thick-walled Quartz tube; S—Steel tube; E—External Quartz tube for filters.)

Wood<sup>2</sup> studied the Raman Effect for HCl gas by means of what he calls a 'light furnace.' He enclosed the gas in a glass tube 150 cms. long and 5 cms. in diameter at atmospheric pressure. The tube towards the ends was drawn out into special shape in order to eliminate scattered light from the front window and to ensure a perfectly black background. In contact with this was placed a Cooper-Hewitt mercury arc in glass about 4ft. long. The whole apparatus is surrounded by an aluminium reflector which merely clamps the two tubes. An exposure of only 5 hours suffices to record the Raman lines.

<sup>1</sup> Rassetti, *Nature*, 123, 205 (1928); and *Proc. Nat. Ac. Sc.* 15, 234 and 515.

<sup>2</sup> Wood, *Phys. Rev.*, 35, 1355 (1930).

The method used by Venkatesachar and Sibaiya is a very ingenious one. They run the mercury arc in an atmosphere of the gas to be studied and instead of studying the transverse beam they observe in the direction of the primary beam. Using  $\text{CO}_2$  atmosphere they recorded two lines which agree with Rassetti's values. That they are Raman lines is supported by the fact that they disappear when  $\text{CO}_2$  is pumped out of the arc. However Wood has criticised this experiment unfavourably.<sup>1</sup>

McLenan and McLeod<sup>2</sup> have studied the Raman Effect with liquid oxygen, nitrogen and hydrogen, the latter yielding some very important and interesting results which serve to verify a speculation by Dennison regarding the existence of two kinds of hydrogen molecules (Para and Ortho hydrogen).

Their apparatus is shown below.

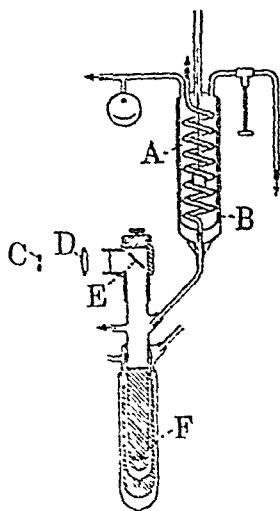


Fig. 6

McLenan's apparatus for study of liquefied gases.

(A—Tube conveying liquefied gas; B—Cooling Jacket; E,F—Mirrors;  
D—Lens)

<sup>1</sup> See also Venkatesachar and Sibaiya, *Ind. J. Phys.*, Vol. V, p. 747.

<sup>2</sup> McLenan and McLeod, *Nature*, 123, 160 (1929); *Trans. Far. Soc.*, Sep. 1929.



The liquefied gas is enclosed in the inner tube shown in the lower part of the diagram. It is surrounded by a tube containing liquid air or liquid hydrogen to prevent visible ebullition of the gas under examination. E and F are two platinum mirrors made by cathodic spluttering. For purposes of illumination four or five mercury arc lamps surround the thermos flask containing the liquefied gas. The scattered light is focussed on the slit C of the spectroscope.

Menzies<sup>1</sup> and Bär,<sup>2</sup> independently have developed a method of studying the Raman Effect of substances in the form of coarsely powdered crystals or crystal aggregates. Studies of solid substances had been carried out by previous workers including Raman himself by illuminating a small piece of the solid. This required the crystal to be large and optically good. This method (Menzies') besides giving a greater convenience in experimenting with crystals reduces considerably the time of exposure. Menzies filled a flask with coarsely powdered crystals and directed light from a quartz lamp to the flask. The light which diffused out from the sides was observed. Faint Raman Lines were recorded after an exposure of 23 hours.

Later Krishnamurti<sup>3</sup> has improved on this method and reports that the continuous background that gave trouble to the previous workers might be reduced considerably in intensity by running the arc on low current and directing a gentle blast of air by means of a table fan. The powder is placed in a triangular glass container with mirrored sides. The arc is placed near one of the prism faces while the scattered light is observed in a transverse direction. Strong lines can be obtained in as short an exposure as  $\frac{1}{2}$ -1 hour.

<sup>1</sup> Menzies, *Nature*, 124, 511 (1929).

<sup>2</sup> Bär, *Nature*, 124, 692 (1929).

<sup>3</sup> Krishnamurti, *Ind. J. Phys.*, (5) part I, 1 (1930).

Among the methods outlined above Raman's method is only of historical importance though still conveniently used for solids. For liquids if a helium tube is available the helium excitation method described by Wood appears to be the best, though nothing can equal the mercury arc for speed.

As regards the gases, for workers who have not the means of American laboratories at their disposal, Rasetti's method appears to be the most practicable. Other methods have their own uses.

## PART II

### RAMAN EFFECT IN SOLIDS, LIQUIDS AND GASES

(i) *Raman Effect in Solids.*—Raman during his very first investigations used a block of ice. Subsequently ice has been studied in detail and apart from it quartz, calcite, gypsum, rock salt, glass, etc., have been investigated. Ice is specially interesting because of the fact that direct comparison in the solid and the liquid state is possible.

Speculations have been rife since long regarding the constitution of water. Attempts have been made and evidence brought forth from various quarters to show that water consists of mono-, di and tri- hydrols [ $\text{H}_2\text{O}$ ,  $(\text{H}_2\text{O})_2$ ,  $(\text{H}_2\text{O})_3$ ]. The former is supposed to be prominent at high temperatures and the latter at low.

As is well known water when freezing slowly forms hexagonal crystals of ice. The structure has been investigated by means of X-rays by various workers. This is clearly brought out in the Raman Effect of ice and water. Water gives broad Raman Bands while ice gives sharp lines. Daure, Venkateswaran, etc., got the  $2.9 \mu$ -band, while Kimura and Uchida got the  $6.1 \mu$ -band also. These bands

are markedly influenced by temperature and support the assumption of the various hydrols. The band corresponding to  $2.9 \mu$  in water shifts to  $3 \mu$  for ice, and further the interesting fact is revealed that the band becomes doubled for the latter, the shifts corresponding to  $3.2 \mu$  and  $3.0 \mu$ . It is doubtful whether the water band at  $2.93 \mu$  is double.

A large number of workers have studied quartz, prominent among them being Pringshiem and Rosen,<sup>1</sup> Wood,<sup>2</sup> Landsberg and Mendalstam,<sup>3</sup> Krishnan,<sup>4</sup> etc. With quartz, lines are obtained corresponding to  $8.64$ ,  $21.5$ ,  $37.4$ ,  $48.5$ ,  $79 \mu$  etc. Owing to the important optical properties of quartz it is expected that the complete data when collected and ordered will yield some important information.

Gypsum yields some important data. Krishnan found that in addition to frequency shifts that could be attributed to  $\text{SO}_4$  radical three sharp lines at  $2.8$ ,  $2.9$ , and  $3.0 \mu$  were also present. They can be attributed to the water of crystallization. It is remarkable that they are sharper than in the case of ice. Related with this is the fact that in the spectra of concentrated acids also water lines are sharp. It appears therefore that in such states water approaches the states of solid crystals. Another remarkable fact is the sharpness of the lines due to the crystal. With the rise of temperature they become diffuse which indicates that the crystal state is undergoing a change. In amorphous quartz, for example, the lines are very diffuse.

Rock salt, sylvine, etc., do not give any Raman lines<sup>5</sup> corresponding to the *Rest-Strahlen* or the residual rays.

<sup>1</sup> Pringshiem and Rosen, Zeit. f. Phys., 50, 741 (1928).

<sup>2</sup> Wood, Phil. Mag., 6, 729 (1928).

<sup>3</sup> Landsberg and Mendalstam, Loc. cit.

<sup>4</sup> Krishnan, Ind. J. Phys., Vol. IV, Part I, p. 131.

<sup>5</sup> Wood, Phil. Mag., 6, 729 (1928); Schaefer, Trans. Farad Soc., 25, 841 (1929), etc.

Schaefer<sup>1</sup> says that Raman Effect implies an assymetrical vibration while in NaCl the vibrations are symmetrical.

Diamond is very convenient to work with. Ramaswamy<sup>2</sup> first studied the substance and found a shift of  $1322\text{ cm}^{-1}$ . E. Schrödinger has worked out the *Rest-Strahlen* frequency to be  $38.9 \times 10^{12}$  per sec. applying Dobye's theory while Raman Effect data give  $40.0 \times 10^{12}$ . Calculations on Nernst-Lindeman empirical formula however gives exactly  $40 \times 10^{12}$ .

This was studied in greater detail by Bhagwantam.<sup>3</sup> He studied nine different samples of diamond. All show one well-defined shift corresponding to  $1331.93\text{ cm}^{-1}$  regardless of the nature of the sample though the intensity varies from a maximum in colourless and well-defined samples to a minimum in the blue diamond. The line obtained corresponds to an optically active frequency represented as the edge of the infra-red absorption band at  $8.02\mu$ . This case is interesting because a broad band in absorption corresponds to a very sharp line in the Raman spectrum.

The study of diamond clearly indicates that it is not necessary for a crystal to contain molecules to give Raman Effect. The "lattice vibrations" in diamond appear to be sufficient to exhibit the effect.

Krishnamurti<sup>4</sup> has studied a large number of solid crystalline inorganic nitrates, chlorides and sulphates, by the powder method described before.

He divides the chlorides into three groups:—

(1) Those which give strong Raman Lines, viz., chlorides of Hg(ous), Hg(ic), P, As, Sb, C, Si, Ti, Sn, and H. [Hg(ous), and Hg(ic) chlorides give very intense Raman Lines.]

<sup>1</sup> Schaefer, Zeit. f. Phys., 54, 153 (1929).

<sup>2</sup> Ramaswamy, Ind. J. Phys., Vol. V, Part I, 97 (1930).

<sup>3</sup> Bhagwantam, Ind. J. Phys., Vol. V, 169 (1930).

<sup>4</sup> Krishnamurti, Ind. J. Phys., V, pp. 1, 183 (1930).

(2) Those which give faint lines.— $\text{BiCl}_3$ ,  $\text{ZnCl}_2$ ,  $\text{CdI}_2$ ,  $\text{AuCl}_3$ .

(3) Those which give no lines at all—Chlorides of Na, K,  $\text{NH}_4$ , Ba, Ag, Cu(ic), Cd, Mg, Sn(ous),  $\text{CdBr}_2$ ,  $\text{PbI}_2$ , KI, LiF, NaF,  $\text{CaF}_2$ .

It is seen from the above classification that chlorides of electro-positive elements do not show the effect, while those of non-metals and metalloids do show it. Two groups can be made, based on the consideration whether union between any atom and the chlorine atom is of the electro-valent type (ionic binding, electron transfer complete) or covalent type (electron sharing). The former are completely ionised in solution. It is also observed that the non-conductors and feeble conductors show the Raman Effect well, while good conductors do not.

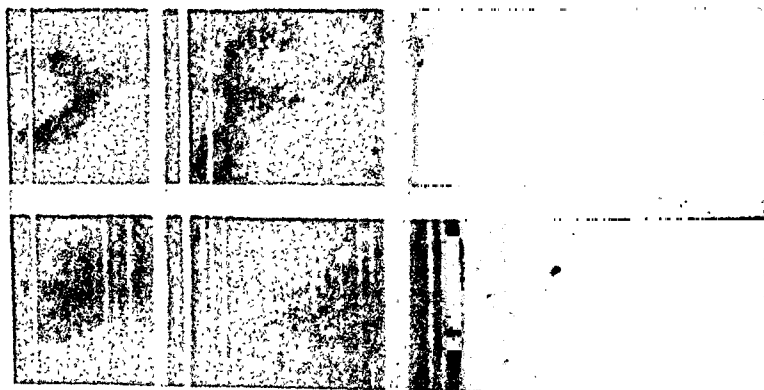
The structure of the crystal—whether it is formed into ionic or molecular lattice—is also very important. Ionic crystals like NaCl and KCl do not show any effect while those arranged in molecular lattices do so. Krishnamurti<sup>1</sup> publishes some interesting results on the study of Raman Effect in crystalline rhombic sulphur. It is found from the Raman Lines that the corresponding infra-red frequencies lie in the region  $20\mu$  to  $120\mu$ . Lines are found corresponding to 118, 66, 46, 41, 23 and  $21\mu$  in the infra-red. Now Coblentz, Schubert and Taylor and Rideal observed absorption maxima in the infra-red at 7.76, 10.73, and 11.90,  $\mu$ . These then must be due to combinations of the fundamental frequencies. Other substances such as carbon tetrachloride show this effect.

Mention also should be made of the observation of Krishnamurti<sup>2</sup> on ferrous and nickel sulphate which it will be noted are paramagnetic crystals. No lines appeared in these crystals while lines from copper and manganese

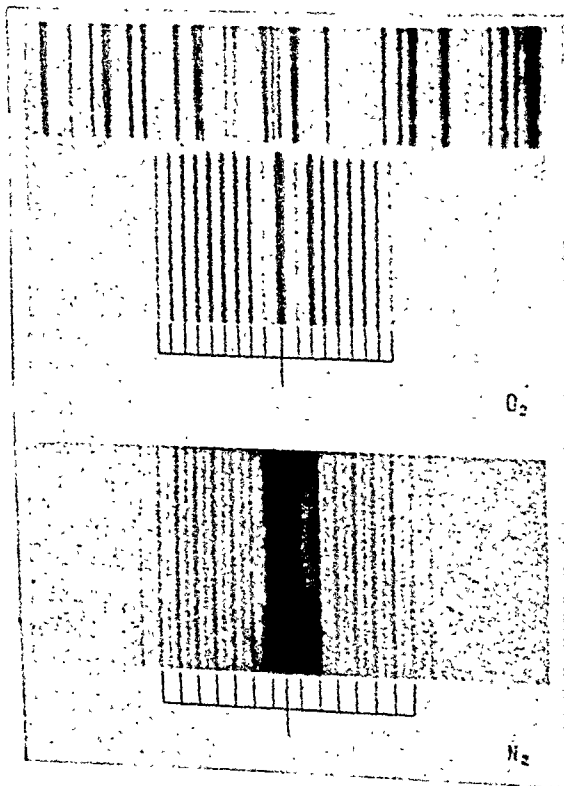
<sup>1</sup> Krishnamurti, Ind. J. Phys., 5, 105 (1930).

<sup>2</sup> Krishnamurti, Ind. J. Phys., 5, 182 (1930).

# PLATE 2

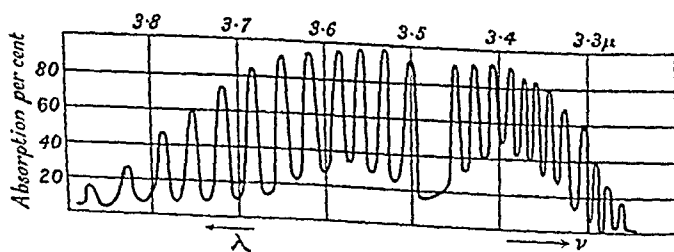


(x) Incident Spectrum (y) Raman Spectrum of Carbon Tetrachloride.



(a) Raman-Spectrum of  $O_2$  showing absence of alternate rotational levels.

(b) Raman-Spectrum of  $N_2$ . Alternate rotational levels are weak.



Rotation-vibration Spectrum of HCl in near infra-red. Note the missing line in the centre.

sulphates were weak. This shows that the paramagnetic cations tend to weaken the lines due to the radical  $\text{SO}_4$ . In an aqueous solution of ferrous sulphate the line appears. Paramagnetic nitrate of copper and manganese also show a weakening of the inactive  $\text{NO}_2$  frequency.

## LIQUIDS

The liquids have been most extensively studied for the Raman Effect. Easiest to work with they are expected to yield valuable information regarding the nature of chemical bonds and the ionic states. The liquids studied may be broadly divided into three classes :

- (1) Organic liquids.
- (2) Liquefied gases.
- (3) Mixtures and solutions.

The organic liquids have received the greatest attention because of their variety and the ordered arrangement in them. They have been studied from various points of view.

(a) The frequency of vibrations of such bonds as  $\text{C—H}$ ,  $\text{C=C}$ ,  $\text{C=O}$ , etc., may be investigated and the modification introduced in the presence of other bonds found.<sup>1</sup>

(b) The effect of substitution of chemical groups may be studied.

(c) The effect of substitution of a heavier atom for a lighter one of the same family, *e.g.*, halogens can be found.

(d) The structure of the molecule may be determined or verified and fundamental difference between different types of compounds such as Aliphatics and Aromatics can be investigated.

The greatest time has been devoted to the study of Benzene and its derivatives, the nitro compounds, paraffins, halogen derivatives, alcohols, etc. We shall consider some typical examples of such studies.

<sup>1</sup> See Appendix II.

In the case of C—H-bond in tetrachlor-ethane the shift corresponds to  $3.35\mu$  but in trichlorethylene where the carbon atom has a double bond the C—H line shifts to  $3.25\mu$ .

Daure<sup>1</sup> has shown that for hydrogen compounds with single bonds the shift is  $2780\text{--}3400\text{cm}^{-1}$ , while the double bond C=O gives  $1660\text{--}1740\text{cm}^{-1}$ . Bhagwantam and Venkateswaran<sup>2</sup> find that the C—H bonds show  $\Delta\nu = 2950\text{cm}^{-1}$ . The lines are equally spaced, the spacing being about  $40\text{cm}^{-1}$ . In compounds with a single hydrogen atom the multiple structure disappears and a line at  $3020\text{cm}^{-1}$  appears. In  $\text{CH}_2\text{Cl}_2$  the lines are (2930, 2985), in methane in the gaseous states they are 2915, 3022,  $3072\text{cm}^{-1}$ . The shift  $1440\text{cm}^{-1}$  seems to be connected with H atoms in the aliphatics.

The compounds  $\text{CH}_2\text{Cl}_2$ ,  $\text{CHCl}_3$ ,  $\text{CHBr}_3$ , and  $\text{CCl}_4$  give several Raman Lines close to the exciting lines, the difference being of the order of  $400\text{cm}^{-1}$ . The opinion is expressed that these are differential frequencies, i.e., differences between certain observed infra-red absorptions. But Marvin "explains them as due to fundamentals. The infra-red absorption in fact may be explained as due to certain combinations."<sup>3</sup> The evidence seems fairly clear that the vibrational frequencies observed in light scattering are really fundamental frequencies and not due to intercombination between the fundamental vibration frequencies of the molecules. "This would seem to be fairly clear from the comparative data for substances with similar chemical constitution, but with atoms of different weight in the molecule. Daure's results with a series of chlorides and Ganesan and Venkateswaran's results on Bromoform, as compared with chloroform, show a remarkable and parallel shifting of the frequencies observed in light scattering

<sup>1</sup> Daure, *Compt. Rend.* 186, 1833 (1928).

<sup>2</sup> Bhagwantam and Venkateswaran, *Proc. Roy. Soc.*

<sup>3</sup> Raman, *Transactions of the Faraday Society*, September, 1928.



towards longer wavelengths with increasing weight of the substituent atoms." Corresponding frequency shifts attributed to the chlorine and bromine atoms are well illustrated in the following table:—

*Cl.* . .  $\Delta\nu = 750, 660, 320, 250 \text{ cm}^{-1}$ .

*Br.* . .  $\Delta\nu = 660, 550, 230, 160 \text{ cm}^{-1}$ .

$\Delta\nu = 750\text{cm}^{-1}$  for chlorine, and  $660\text{cm}^{-1}$  for bromine are diffuse. They might be two close lines or the diffusivity might be due to the isotopes of chlorine and bromine.

In benzene  $\Delta\nu = 1000 \text{ cm}^{-1}$  is very prominent while in chloro- and bromo-benzenes  $\Delta\nu = 1025$  appears. This illustrates the effect of substitution.

Solutions have been studied to observe the frequency due to radicals and ions. Carreli, Daure, Venkateswaran, Ganesan and others have studied this aspect. Daure found sharp lines for the M-Cl bond. Mukherji and Sengupta<sup>1</sup> have studied the sulphates and found frequencies characteristic of the  $\text{SO}_4$  group. Taylor<sup>2</sup> has studied the Raman Spectra of  $\text{H}_2\text{SO}_4$ ,  $\text{HClO}_4$  and the alkali sulphates and compared the shifts with infra-red data. An energy diagram of the  $\text{AX}_4$  group is suggested.

The spectra of several nitrates and carbonates have been studied in solution as well as in the solid state. In some cases for certain ions the inactive frequencies have been detected. The frequency for the  $\text{NO}_3$  group found in the nitrates agrees for the measurement of the  $\text{NO}_3$  ion in nitric acid.

The liquefied gases form an interesting study. McLenan and McLeod<sup>3</sup> have studied oxygen, hydrogen, and nitrogen in the liquid state. For oxygen and nitrogen, a

<sup>1</sup> Mukerji and Sengupta, *Ind. J. Phys.*, 3, 503 (1929).

<sup>2</sup> Taylor, *Trans. Farad. Soc.*, p. 830 (1929).

<sup>3</sup> McLenan and McLeod, *Loc. cit.*

frequency of  $1551.5 \text{ cm}^{-1}$ ,  $2328.5 \text{ cm}^{-1}$  has been found. The results obtained from liquid  $\text{H}_2$  are very interesting and serve to verify some earlier speculations regarding the existence of ortho and para-hydrogens.

In this case a frequency difference of  $354 \text{ cm}^{-1}$  and  $588 \text{ cm}^{-1}$  are found which are in the ratio 3 : 5, while a line shifted by  $4159 \text{ cm}^{-1}$  is also observed.

From the theory of band spectra the energy of rotation of a diatomic molecule is given by :—

$$E = \frac{m^2 h^2}{8\pi^2 I} = B h m^2; \quad B = \frac{h}{8\pi^2 I}$$

$m$  = Rotational quantum number.

$h$  = Planck's constant.

$I$  = The moment of inertia of a molecule.

For  $m = 0, 1, 2, 3$ , etc., we get

$E = 0, Bh, 4Bh, 9Bh$ , etc., This as we see does not give any  $h\nu = E_1 - E_2$  such that the frequency ratio is 3 : 5. If we however substitute the half quantum numbers we get for  $m = \frac{1}{2}, \frac{3}{2}, \frac{5}{2}$ , etc.,  $E = Bh/4, 9Bh/4, 25Bh/4, 49Bh/4$ , etc. If we now consider a transition  $25/4 Bh \rightarrow Bh/4$  and another  $49/4 Bh \rightarrow 9/4 Bh$  two frequencies are obtained whose ratios are as observed.

Also if we proceed according to wave-mechanics where the energy is represented by  $E = B h m(m+1)$  with  $m = 0, 1, 2, 3$ , etc., we get  $E = 0, 2Bh, 6Bh, 12Bh, 20Bh$ , etc. Now taking the transitions  $m=2$  to  $m=0$  and  $m=3$  to  $m=1$  into consideration we get the two frequencies in the ratio 3 : 5. It should be noted that no trace of such ratios as 2 : 3, 2 : 5, 3 : 4, etc., appears, and hence we conclude that these do not occur. The two facts now brought to light are :—

- (1) The wave-mechanical formula has a physical reality.

- (2) In liquid hydrogen there are two sorts of molecules—one in which transitions from  $m=2$  to  $m=0$  can occur and the other in which  $m=3$  to  $m=1$  can take place.

The intensity of  $\lambda 4473.1$  corresponding to a shift of  $588\text{ cm}^{-1}$  was between two to three times that of  $\lambda 4426.6$ —a shift of  $354\text{ cm}^{-1}$ . This shows therefore that the molecules of one kind are two to three times as numerous as the molecules of the other type.

These results fit in very well with the assumption of Dennison that there are two kinds of hydrogen molecules. In one group only odd rotation levels are present while in the other only even. It was found that the experimental curves for the specific heat of hydrogen did not agree with the theoretical calculations unless an assumption of this sort were made. The relative abundance of the types of molecules as required by the data is nearly the same as revealed by the Raman Effect. Line with the shift  $4149\text{ cm}^{-1}$  is found to be associated with the transition from the normal state to the first vibrational state of the  $\text{H}_2$  molecules. Subsequent work by McLennan, Wilhelm and Smith<sup>1</sup> has shown that the slow transformation from ortho hydrogen to para hydrogen at liquid hydrogen temperature can be studied by following the change in the intensity of Raman lines due to these molecules.

Salant and Sandow<sup>2</sup> find shifts for liquid  $\text{HCl}$  and  $\text{HBr}$   $\Delta$ , to be  $2781\text{ cm}^{-1}$  and  $2479\text{ cm}^{-1}$  while in the gaseous state Wood found  $2886\text{ cm}^{-1}$  for  $\text{HCl}$ . This shows that on liquefaction the shift is towards the lower frequency.<sup>3</sup> The Lorentz-Lorenz theory affords an explanation of this phenomenon.

<sup>1</sup> McLennan, Wilhelm, and Smith, Trans. Roy. Soc., Canada, 22, 413 (1928).

<sup>2</sup> Salant and Sandow, Phys. Rev., 35, 214 (1930).

<sup>3</sup> See Appendix II.

The study of other liquefied gases does not reveal anything very remarkable.

### GASES.

The gases so far studied are  $\text{HCl}$ ,  $\text{NH}_3$ ,  $\text{O}_2$ ,  $\text{N}_2$ ,  $\text{H}_2$ ,  $\text{CO}_2$ ,  $\text{CO}$ ,  $\text{NO}$ , and  $\text{SO}_2$ .

$\text{CO}$  and  $\text{CO}_2$  were first studied by Rasetti.<sup>1</sup> In carbon monoxide a shift of  $2154 \text{ cm}^{-1}$  is obtained which coincides with the infra-red absorption band at  $4.66 \mu$ . In carbon dioxide there are three infra-red absorption bands at  $2.7$ ,  $4.25$ , and  $14.7 \mu$  but none of these is represented as Raman Lines. The frequency shifts are  $1284 \text{ cm}^{-1}$  and  $1392 \text{ cm}^{-1}$ , which it should be noted corresponds to the difference in frequency between the two components of the double band at  $2.7$  and  $4.25$ .

Wood<sup>2</sup> has studied the effect for  $\text{HCl}$  gas in great detail. A Raman line at  $\lambda 4581.8 \text{ \AA.U.}$  is photographed and is found to correspond to the infra-red wavelength of  $3.466 \mu$ . Now this corresponds exactly to the missing line or the centre of the gap between the two branches of the absorption band of  $\text{HCl}$  in the infra-red as measured by Imes.<sup>3</sup> Close to the exciting mercury line  $4358 \text{ \AA.U.}$  there are nearly equidistant bands. These correspond to the pure rotation levels of  $\text{HCl}$  as found by Czerny.<sup>4</sup> It is remarkable that only alternate bands appear in the Raman Spectrum. The tables given below show the results.

Czerny	Wood
44.1	43.6
48.5	...
53.8	53.9
60.4	...
68.9	67.1
80.4	...
96	90 (uncertain)

<sup>1</sup> Rasetti, *Nature*, 123, 205 (1928).

<sup>2</sup> Wood and Dieke, *Phys. Rev.*, 35, 1355 (1930).

<sup>3</sup> See plate II.

<sup>4</sup> Czerny, *Z. für. Phys.*

$\lambda$ in Å.U	$\Delta\nu$ in $\text{cm}^{-1}$	Transition	Infra-red $\mu$
.....	.....	$0 \rightarrow 2$	62.69
4377.60	101.1	$1 \rightarrow 3$	104.29
85.6	142.7	$2 \rightarrow 4$	146.03
94.2	187.5	$3 \rightarrow 5$	187.45
4402.4	229.4	$4 \rightarrow 6$	228.87
10.4	271.0	$5 \rightarrow 7$	270.03
18.6	312.9	$6 \rightarrow 8$	311.23
26.5	353.0	$7 \rightarrow 9$	352.23
4314.7	143.8	$4 \rightarrow 2$	146.03
23.8	183.3	$5 \rightarrow 3$	187.45
31.2	232.2	$6 \rightarrow 4$	228.87
4581.8	2886.0	$j \rightarrow j$	2885.4 <sup>1</sup>

The first column gives the observed wavelength of the Raman lines. The second column gives the frequency difference with the exciting line  $\lambda$  4358. In the third column we find the rotational transitions in the molecule to which the line corresponds and the fourth column gives a comparison with the infra-red data."

$\text{NH}_3$  studied by Wood gives a single line identified with an absorption band at  $6.5\mu$ . The other strong bands at  $6.8\mu$  and  $10\mu$  are not represented.

Oxygen gives a number of equally spaced lines (6 or 7) on both the sides of the exciting lines, they can be recognised as corresponding to changes in molecular rotational energy. It is found that alternate levels are missing, only odd levels being in evidence.

In hydrogen a Raman line corresponding to the transition  $1 \rightarrow 3$  giving a frequency difference of  $583 \text{ cm}^{-1}$ . While McLennan in addition has obtained the weaker  $0 \rightarrow 2$  transition for the liquid state. Thus the odd levels are found to have greater statistical weight.

In nitrogen the pattern<sup>2</sup> is the same but all rotational transitions are represented. Lines corresponding to transitions between even rotational states are strong and others are weak.

<sup>1</sup> This line is excited by  $\lambda$  4047.

<sup>2</sup> See Plate II.

Nitrogen monoxide gives a shift corresponding to a purely electronic transition. NO has  $^2P$ -state as normal, the separation being  $124\text{ cm}^{-1}$ . This frequency shift appears. This interpretation has however been questioned, and there is, as yet, no definite proof of combination scattering involving electronic transitions. For a negative experiment on this line, see a paper by Toshniwal in the present volume.

Sulphur dioxide has been experimented with by Dickinson and West.<sup>1</sup> It gives three shifts  $524.3$ ,  $1145.9$ ,  $1340.1$ ,  $\text{cm}^{-1}$ . Last two agree with the absorption bands as found by Coblentz. The first shift is outside the range of his measurements. The structure of  $\text{CO}_2$  molecule and the  $\text{SO}_2$  one is the same and it appears strange that such a fundamental difference should exist between the two as far as the Raman Effect is concerned.

The results obtained in the case of the gases have all been explained by Rassetti,<sup>2</sup> Hill and Kemble,<sup>3</sup> Langer,<sup>4</sup> Dieke,<sup>5</sup> etc. We shall deal with them in a separate section. Mention should however be made of the important fact that the selection rule for the Raman Effect in transitions come out to be  $\Delta m = 0$  or  $\pm 2$  while for absorption it is  $\Delta m = \pm 1$ .

## SOME ASPECTS AND APPLICATIONS OF RAMAN EFFECT

Some interesting applications of Raman Effect have been attempted by Kothari,<sup>6</sup> Deodhar<sup>7</sup> and Allan.<sup>8</sup> Kothari points out that some faint Fraunhofer lines in the solar spectrum may be supposed to be Raman lines arising from "a

<sup>1</sup> Dickinson and West, *Phys. Rev.*, 35, 1126 (1930).

<sup>2</sup> Rassetti, *Proc. Nat. Ac. Sc.*, 15, 234.

<sup>3</sup> Hill and Kemble, *Proc. Nat. Ac. Sc.*, 15, 387.

<sup>4</sup> Langer, *Nature*, 123, 345 (1929).

<sup>5</sup> Dieke, *Nature*, 123, p. 564 (1929).

<sup>6</sup> Kothari, *Nature*, 124, 90 (1929).

<sup>7</sup> Deodhar, *Z. f. Phys.*, 57, 570 (1929).

<sup>8</sup> Allan, *Nature*, 123, 127 (1929).

combined effect of Raman Scattering and ordinary absorption."

The molecules responsible for the production of the cyanogen and the swan bands may modify a beam of light from the photosphere to  $\nu - \nu'$ ,  $\nu'$  being a strong vibration-rotation frequency. If  $\nu - \nu'$  happens to coincide with H or K frequencies the modified light will be absorbed by the high level  $\text{Ca}^+$  atoms. Thus in place of  $\nu$ , we shall get a black absorption line.

Kothari finds that this view can explain the appearance of certain faint lines in the solar spectrum. "If this view be correct it will give us a method of calculating the total number of CN molecules in the solar atmosphere from a comparison of the intensities of the modified line with that of K line with the aid of known dispersion formula." For the coronal spectrum he does not find good agreement. (See also Macke and Wildt—Z. f. Phys., 59, 501, 1930.—The spectrum of Sun's corona.)

Allan suggested that some lines in the secondary spectrum of hydrogen might be due to the Raman Effect excited in the hydrogen molecules by the Balmer lines produced by the atoms during the electric discharge. Deodhar has identified some lines due to  $\text{H}_\alpha - \text{H}_\lambda$  in the secondary spectrum. Due to the great number of lines in the spectrum nothing very definite can be said in this connection unless a detailed and systematic investigation is undertaken. We have to leave a large margin for chance coincidences before we can attach any value to such identifications.

#### RAMAN EFFECT AND ELECTROLYTIC DISSOCIATION

Rao<sup>1</sup> has recently published results of his study of the Raman Spectra of Nitric acid at different dilutions. By

<sup>1</sup> Rao, Proc. Roy. Soc., A., 127, 279 (1929).

the study of the intensity of the Raman lines he was able to trace the progress of electrolytic dissociation in the acid.

A modified form of Wood's tube was used and in general his method was followed. To ensure uniform illumination for exposures at different concentrations the mercury arc and the reflectors were placed at the same distance and the voltage and the current were kept nearly constant. This method of procedure appears to be hardly satisfactory and for a quantitative problem like this more elaborate precautions seem to be necessary.

About ten lines are obtained in the scattered spectrum out of which four are identified as due to the undissociated  $\text{HNO}_3$  molecules, three to  $\text{NO}_3$  ion—are common to nitrates—and three to water. The decrease in the intensity of the  $\text{HNO}_3$  lines and increase in those due to the  $\text{NO}_3$  ion give an ocular demonstration of the dissociation theory.

From micro-photometric records of the plates the relative number of  $\text{NO}_3$  ions and the  $\text{HNO}_3$  molecules can be calculated and the progress of dissociation with increasing dilution be traced.

The two methods generally used for studying dissociation are—(1) by osmotic pressure measurement, (2) from electrical conductivity measurements. In the first method help is taken of Henry's law of solutions. The second utilises Kohlrausch's law which states that the mobility of ions is independent of the concentration. The curves reproduced below from Rao's paper illustrate the results. The uppermost curve is from Raman Effect data, the middle one from conductivity measurements and the lowest from viscosity-conductivity formula. The form of the curve is the same but the numerical agreement is far from good. The Raman Effect data, as the author suggests, are the most reliable because the intensity of Raman lines is accurately proportional to the total molecular aggregate while the general validity of the other laws is doubtful.



Results of various other workers on the same subject disagree with those of Rao in some details but there is

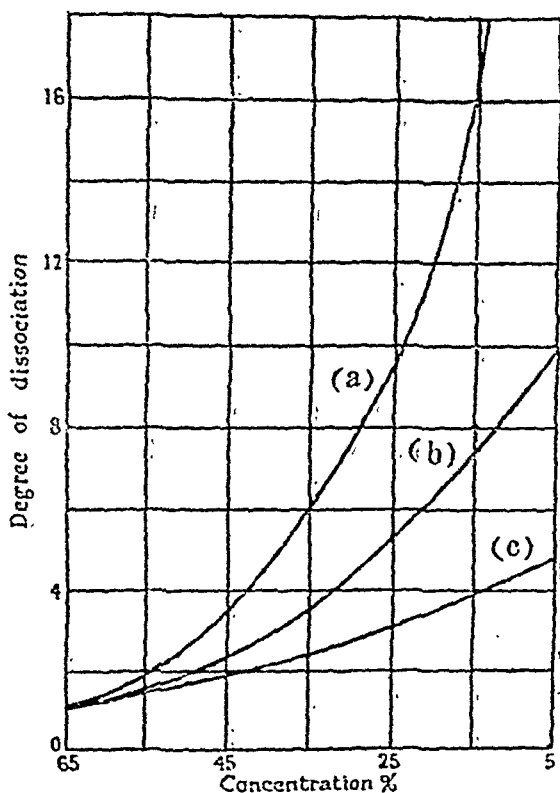


Fig. 8

#### Dissociation of $\text{HNO}_3$

(a)—Curve from Raman Effect; (b)—Conductivity measurements; (c)—Viscosity conductivity formula.)

absolutely no doubt about the value of the method as a means of making an accurate study of dissociation.

#### CALCULATION OF THE SPECIFIC HEAT OF SOLID ORGANIC SUBSTANCES

Some lines in the Raman Spectra can be definitely identified with fixed modes of vibrations in the molecule.

Taking the help of this Andrews and Southard<sup>1</sup> have succeeded in calculating the specific heat of some solid organic substances. A correct number of degrees of freedom can be assigned to each frequency. "If we then consider that the various modes of vibrations act as Einstein oscillators it is possible to employ the frequencies from the Raman Spectra and calculate the specific heat of molecules for any temperature." This has been done for methyl alcohol, ethyl alcohol, benzene, toluene, etc., from 15° to 260° K, the average deviation being about 5 per cent.

### RAMAN EFFECT IN THE X-RAY REGION

Experiments have been performed by Davis and Mitchell<sup>2</sup> and others on the scattering of X-rays by beryllium, aluminium and graphite as diffusing substances. They used the  $K_{\alpha_1, \alpha_2}$  of molybdenum with the double X-ray spectrometer developed by Davis and Purks.<sup>3</sup> In addition to the undisplaced  $K_{\alpha_1, \alpha_2}$  they observed lines displaced towards the longer wavelength side by an amount to be expected if it be assumed that part of the energy of the incident quantum is utilised in ionizing the K shell of the atoms and the remainder is scattered as a quantum of less energy. In case of graphite the line displaced agrees with  $h\nu' = h\nu - V_K$ , being the energy level (287 volts) of the carbon atom. They used an ionisation chamber for detection. All efforts to detect a displacement towards the shorter wavelength side proved fruitless.

These results do not however stand unchallenged. Ehrenburg<sup>4</sup> used photographic methods but failed to obtain any such shift. More recently Kast<sup>5</sup> used Al as the diffusing substance and 612 X.E. (Rh  $K_{\alpha}$ ) as the incident light.

<sup>1</sup> Andrews and Southard, *Phys. Rev.*, 35, 670 (1930).

<sup>2</sup> Davis and Mitchell, *Phys. Rev.*, 31, 119 (1928).

<sup>3</sup> Davis and Purks, *Proc. Nat. Ac. Sc.*, 13, 419, (1927).

<sup>4</sup> Ehrenburg, *Zeit. f. Phys.*, 53.

<sup>5</sup> Kast, *Zeit. f. Phys.*, 58, 519 (1929).

The exposure given was twenty times that required to obtain the Compton Effect. No trace of the Raman line reported by the previous workers was obtained.

Dr. B. B. Ray<sup>1</sup> has obtained new lines in a photograph got by passing X-rays through a film of soot and taken in the direction of the incident light. The frequency modification corresponds to the line of carbon, oxygen and hydrogen. This Dr. Ray attributes to a sort of Raman Effect but Bhargava<sup>2</sup> in his note to Nature points out that this is merely photoionisation.<sup>3</sup>

Due to the doubtful nature of the experiments nothing definite can be said at present as regards the existence or otherwise of Raman Effect in the X-ray region. It is interesting to note however that Carrelli<sup>4</sup> in a note to Nature published certain theoretical calculations and arrived at the conclusion that the conditions to be satisfied to observe the effect in the X-rays are

- (1) Substances giving semi-optical lines should be used.
- (2) The scattering substance should be of low atomic number.
- (3) The ratio  $\frac{E_v}{E_\mu}$  should be high  $E_v$  being the kinetic energy of the electron emitted in the Compton Effect in one direction with a particular exciting frequency.  $|E_\mu|$  is the energy of the K orbit.

### RAMAN EFFECT NEAR THE CRITICAL POINT

The fact that there is a close connection between Raman Effect and classical scattering cannot be disputed, for substances which show strong classical scattering also give strong Raman lines.

<sup>1</sup> Ray, Nature, Vol. 125, 746, 856 (1930).

<sup>2</sup> Bhargava, Nature, Sep. 13 (1930).

<sup>3</sup> See also Bhargava and Mukerji, Nature, Feb. 22, 1931, p. 273.

<sup>4</sup> Carelli, Nature, Vol. 125, 201 (1930).

At the critical point classical scattering increases a hundred or a thousand times giving rise to the phenomenon of critical opalescence. It is natural therefore that Raman Effect too will be intensified in this state.

Raman experimenting with  $\text{CO}_2$  and a mixture of  $\text{CS}_2$  and methyl alcohol found an increase in the intensity of the lines near the critical point and so did Ramdas<sup>1</sup> working with  $\text{CO}_2$ . Bogros and Rocard<sup>2</sup> studying a mixture of phenol and water did not even find the Raman Spectra. Ziemecki<sup>3</sup> made a careful study of iso-butyric acid which with water gives a mixture whose critical point is at  $24^\circ\text{C}$  and finds that the change in the intensity of the Raman lines is small. A possible increase of 30—40% is observed while the classical scattering increases by as much as 500 per cent. This change of 30—40 per cent might be due to the increase in the intensity of the overlapping continuous spectrum, and hence the increase in intensity of Raman lines can be regarded as practically nil.

This it will be observed leads us to conclude that Raman Scattering is non-coherent in nature. It is well-known that the critical point is a state of fluctuation and so the classical scattering—to express in loose terms—takes advantage of the confusion amongst the molecules and appears in its full intensity, while Raman Scattering being incoherent, *i.e.*, there being no phase relation between scattering by different molecules, is unaffected by the critical state and hence there is no increase in intensity.

We shall now refer to some special aspects of Raman Effect *e.g.*, the width, intensity, polarisation, etc., of the Raman lines.

*Width.*—It is found that Raman Lines vary greatly in width. We can generalise the results by saying that for

<sup>1</sup> Ramdas, Ind. J. Phys., II, part 3, 387 (1928).

<sup>2</sup> Bogros and Rocard, Jour. de. Phys., 10, 72 (1929).

<sup>3</sup> Ziemecki, Phil. Mag., p. 300, Feb., 1930.

any ordered arrangement like a crystal the lines are sharp while in liquids and amorphous solids they are diffuse.

The change in sharpness is well illustrated in the study of ice and water. The comparatively sharp lines in ice become diffuse as ice melts though no appreciable change of frequency occurs. This is interpreted by saying that the damped vibrations of the molecule in the liquid may be responsible for the broad lines. But clearly the question of broadening is intimately connected with different types of molecular bindings for there are liquids in which the lines are very sharp. In viscous liquids like glycerine it is observed that a continuous spectrum is prominently associated with the modified scattering, and is present in almost all liquids to a greater or less extent. In the alcohols the continuous background increases as we go up the series, being practically absent in the earlier members.

*Polarisation.*—It was noticed during the very first experiments of Prof. Raman that the modified lines were polarised. This aspect is very fundamental from the point of view of the investigation of the exact nature of the scattering and the scattering molecule.

The modified line in the liquid may be polarised in a direction parallel to the direction of the polarisation of the unmodified lines, partially polarised or unpolarised. In quartz it is found that depending on the direction of the optic axis with respect to the incident and the scattered beams the modified line may be polarised in a direction perpendicular to that in the unmodified line.

Bhagwantam<sup>1</sup> has made a detailed study of Raman Lines occurring in compounds like  $\text{SO}_2$ ,  $\text{CS}_2$ ,  $\text{SO}_3$ ,  $\text{NH}_3$ , etc. He finds that the polarisation characteristic of lines from compounds with similar structure are the same. "A high degree of polarisation for any Raman Line is generally

<sup>1</sup> Bhagwantam, Ind. J. Phys., 5, 59 (1930).

accompanied by relatively large intensities but the converse relation is not true."

We shall deal with the various explanations offered for the polarisation in the next section.

For details regarding this aspect of the phenomenon papers by Menzies,<sup>1</sup> Cabannes,<sup>2</sup> Daure,<sup>3</sup> and Bhagwantam should be consulted.

*Intensities.*—If lines having the same frequency shifts but due to different exciting lines be considered it was found even during the earlier investigations of Raman and Krishnan that the intensity increases as the wavelength of the exciting line decreases. The increase in the scattering is more rapid than indicated by the Rayleigh fourth-power law.

Daure<sup>4</sup> also made measurements on the light scattered by  $\text{AsCl}_3$ . He found that the increase in the intensity is less rapid than the Rayleigh law. In a subsequent experiment he studied the scattering of the mercury lines 4358 Å.U. and 5460 Å.U. He found that the ratio of the intensity of the lines showing the same shift is equal to the ratio of the exciting lines in the scattered spectrum. More recently Ornstein and Rekveld<sup>5</sup> from their study of the scattering by  $\text{CCl}_4$  conclude that the intensities of the modified lines obey the Rayleigh law accurately. Sircar has studied the Raman Effect of  $\text{CCl}_4$  from the point of view<sup>6</sup> of intensity measurements and finds that the scattering increases more rapidly as the exciting line approaches the ultraviolet absorption line of the liquid. It is suggested that the different results obtained by Ornstein and Rekveld are

<sup>1</sup> Menzies, *Phil. Mag.*, 8, 504 (1929).

<sup>2</sup> Cabannes, *Trans. Farad. Soc.*, 25, 813 (1929); *Compt. Rend.*, 187, 654 (1928).

<sup>3</sup> Daure, *Compt. Rend.*, 186, 1833 (1928).

<sup>4</sup> Daure, *Compt. Rend.*, 187, 826 (1928); *Compt. Rend.*, 188, 1605 (1929).

<sup>5</sup> Ornstein and Rekveld, *Zeit. f. Phys.*, 61, 593 (1930).

<sup>6</sup> Sircar, *Ind. J. Phys.*, 5, 159 (1930).

due to the fact that they have overlooked the slight absorbing power of the liquid in the region  $4046 \text{ Å.U.}$  Sircar has also found the ratio of the intensity of the strongest Raman Line to the exciting line to be  $1/410$  while for all the lines taken together (*i. e.*, lines due to same original line) it comes out to be  $1/150$ .

The ratio of the intensities of the Stokes and anti-Stokes line is very important as it forms a criterion for various theories of Raman Effect. According to the Maxwellian distribution the ratio should be  $1 : e^{\frac{-h\nu}{kT}}$  while from Schrödinger's original theory of dispersion it follows that the ratio ought to be one. Statistical mechanics yields a more or less correct ratio.

The unsymmetrical continuous spectrum accompanying the Raman lines may be interpreted as due to the unresolved rotational effect and varies in intensity from substance to substance. This was correlated with the optical anisotropy of the molecules by Raman and Krishnan and subsequent theoretical work by Manneback<sup>1</sup> has lent a theoretical justification for the explanation.

In this connection we can also consider the effect of temperature on Raman Effect. An increase produces a change in (i) the general character of all the lines, and (ii) a change in the relative intensities of the Stokes and anti-Stokes Lines.

According to the simple picture of the phenomenon given by Raman the modified line of enhanced frequency arises as follows. The incident quantum of energy  $h\nu$  coming in collision with the molecule extracts  $h\nu'$  from it if it happens to be in the excited state.

$h\nu + \text{excited molecule} \longrightarrow (h\nu + h\nu') + \text{normal molecule.}$  A modified line of enhanced frequency thus appears.

The intensity of the Raman line of enhanced frequency will clearly depend on the number of excited molecules

<sup>1</sup>Manneback, Nature, 125, 88 (1930).

present which is proportional to  $e^{\frac{-h\nu}{kT}}$ . As the temperature increases the number of excited molecules also increases and so does the intensity of the anti-Stokes line.

Krishnan<sup>1</sup> in a preliminary experiment found this to be the case in  $\text{CCl}_4$ , and subsequently this has been verified by various workers. Brickwedde and Peters<sup>2</sup> studied quartz between  $-180^\circ\text{C}$  and  $550^\circ\text{C}$ . The intensity of the anti-Stokes Line increases greatly with temperature. Quantitative experiments also confirm the theory which says that at high temperatures the intensity of the Stokes and anti-Stokes Lines should be equal. Experiments on the effect of temperature also confirm the assertion that the Raman Scattering is non-coherent.

## PART III

### THEORIES OF RAMAN EFFECT

The existence of Raman Effect had been predicted long before the experimental discovery of Prof. Raman by more than one theoretical worker. Smekal<sup>3</sup> in 1923 discussed the question of thermodynamic equilibrium between radiation and matter, on the lines laid down by Einstein and arrived at the conclusion that if molecules are capable of existing in several metastable and excited states then the principle of thermodynamic equilibrium requires that in addition to the original beam we should have scattering of the beam of frequency  $\nu \pm \nu_k$  where  $\nu_k$  is a characteristic frequency of the molecule. Later on Kramers and Heisenberg<sup>4</sup> came to the same conclusion to which we shall refer later on.

<sup>1</sup> Krishnan, *Nature*, 122, 650 (1928).

<sup>2</sup> Brickwedde and Peters *Bull. Am. Phys. Soc.*, Vol. 3.

<sup>3</sup> Smekal, *Naturwiss.*, 11, 873 (1923).

<sup>4</sup> Kramers and Heisenberg, *Zeit. f. Phys.*, 31, 681 (1929).



Raman simultaneously with the discovery of the effect gave a simple picture of the process. A quantum of energy  $h\nu$  was supposed to collide with an unexcited molecule, impart to it the energy  $h\nu_k$  and escape with  $h\nu - h\nu_k$ . In case the molecule was already in the excited state the quantum  $h\nu_k$  got added to the exciting quantum and a line of enhanced frequency was observed.

It is clear that with the discovery of the missing line in case of HCl, of the two lines of  $\text{CO}_2$  and other apparent anomalies such a simple picture could not account for all the observed facts. Further the previous explanation threw no light whatever on the mechanism of the interaction between the quantum and the molecule.

We shall now give a brief outline of the theory of Raman Effect as outlined by Langer, Dieke, Rasetti, Hill and Kemble, etc., from the original dispersion theory of Kramers and Heisenburg.

*Kramers' Dispersion Theory.*—In the dispersion theory of Kramers and Heisenburg<sup>1</sup> the problem of scattering and dispersion is attacked from the consideration of the atom as postulated by the quantum theory. The atom is supposed to react with the incident field like a virtual radiation field whose frequencies are those corresponding to the various transitions in the atom.

They consider the incidence of mono-chromatic light represented by the electric vector  $E_e^{2\pi i\nu t}$ . The change in the electric moment of the system is found to be

$$\sum_T \sum_{T'} \frac{1}{4} \left[ \frac{\partial c}{\partial J'} \cdot \frac{(Ec')}{\omega' + \nu} - c \frac{\partial}{\partial J} (Ec) \right] e^{2\pi i(\nu + \omega + \omega')t}$$

The occurrence of  $e^{2\pi i(\nu + \omega + \omega')t}$  shows that the radiation from the atom will consist of the frequency  $\nu + \omega + \omega'$  where  $\omega$  and  $\omega'$  correspond to the two periods of the disturbed atom.

The terms  $\nu + \omega + \omega'$  have been interpreted by Kramers and Heisenburg as incoherent radiation of frequency  $\nu \pm \nu'$

<sup>1</sup> Loc. cit.

where  $h\nu'$  is the energy difference between the considered and any other state. This dispersion theory of Kramers and Heisenberg contains the fundamental assumptions on the basis of which later on the matrix mechanics was developed, and hence the result is the same as given by wave-mechanics.

Let us consider the atom in a particular state. If a light wave of frequency  $\nu$  perturbs the system it gives rise to harmonic components of the frequency

$$\nu_{lk} = \nu - \nu_{lk} = \nu - \left[ \frac{E_l - E_k}{h} \right]$$

Consider a case in which the electric moment associated with the transition has the same direction as the electric vector of the light wave, then the amplitude of  $\nu_{lk}$  or the modified beam can be put as

$$\sum_s x_{ls} x_{sk} \left[ \frac{1}{\nu_{sl} + \nu} + \frac{1}{\nu_{sk} - \nu} \right]$$

when  $x_{lk} = \int \psi_l^* \psi_s d\tau$  give the transitions between the state  $l$  and the state  $s$  and so does  $x$  between  $k$  and  $s$ . This clearly brings out the fact that the condition that a Raman transition  $l \rightarrow k$  should occur is that there should be an "allowed" transition between  $l \rightarrow s$  and  $k \rightarrow s$ , i.e., both the states involved should be capable of combining with a third state. In case a transition is forbidden, i.e.,  $x_{lk} = 0$  the amplitude of  $\nu_{lk}$  will be 0 and hence if the third common state does not exist then no Raman line will be observed.

As has been shown earlier (see Part I) this implies a selection rule  $m = \pm 2$  or 0.

This theory leads us to expect some peculiarities in the Raman Spectrum of non-polar molecules like  $O_2$  and  $N_2$ . In the infra-red spectrum of these gases transitions between different vibrational states (without electronic changes) do not give rise to radiation for the molecules are non-polar. But in the Raman Effect since the condition for

the appearance of a line is that  $x_{ls} = \int x \psi_l \psi_s \partial \tau$  should not be 0 the corresponding shifts appear. This consequence is verified in Rasetti's<sup>1</sup> experiments.

The results of Wood with HCl can now be easily explained. Before going into the detailed explanation of the observations it would be better to go through a brief sketch of the HCl spectrum.

The rotation-vibration spectrum of HCl was studied by Imes and the following curve is obtained.<sup>2</sup>

The centre represents the "missing line." We shall now consider how this arises.

The frequency  $\nu$  is represented by

$$\nu = \nu_0 (n_2 - n_1) + c (m_2^2 - m_1^2)$$

where  $n_1$  and  $n_2$  denote two vibrational states and  $m_1$  and  $m_2$  two rotational states. The selection rule for  $m$  is  $\Delta m = \pm 1$ . Taking  $n_2 - n_1 = 1$ , we have,

$$\begin{aligned} \nu &= \nu_0 + c[(m_1 \pm 1)^2 - m_1^2] \\ &= \nu_0 \pm 2 m_1 c + c. \end{aligned}$$

The number of lines obtained can be represented diagrammatically as follows ( $m$  is the quantum number of the initial state):—

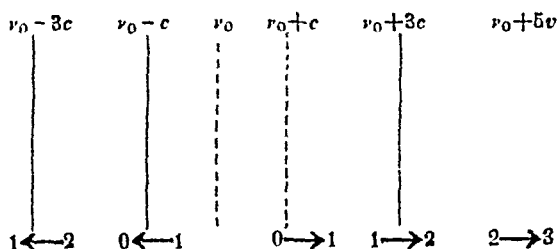


Fig. 9

We see that besides  $\nu_0$ ,  $\nu_0 + c$  also is not present or  $m=0$  is not possible as an initial state in absorption while it is possible in the reverse process. This is difficult to account for. The difficulty is removed if half-quantum

<sup>1</sup> Rasetti, Nature, 124, 792 (1929).

<sup>2</sup> See Plate II.

numbers are substituted or the wave-mechanical expression is employed. The expressions now become—

$$\begin{aligned} \nu &= \nu_0 + B[(m + \tfrac{1}{2} + \Delta m)^2 - (m + \tfrac{1}{2})^2] \\ &= \nu_0 + B\Delta m [2m + 1 + \Delta m] \quad \dots (a) \\ &= \nu_0 + 2Bm\Delta m + B\Delta m + B, \text{ since } \Delta m = \pm 1 \\ &= \nu_0 + B \pm 2B(m + \tfrac{1}{2}) \end{aligned}$$

This yields the following numbering:—

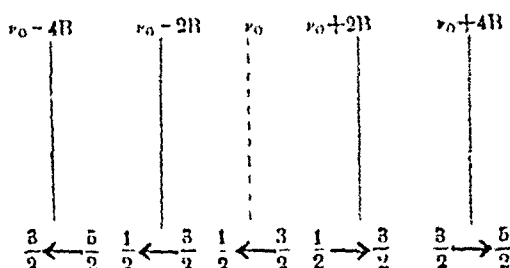


Fig. 10

$\Delta m = 0$  corresponds to  $\nu_0$  [see (a)] and hence being forbidden does not appear.  $\nu_0$  is unique and thus all anomalies are set right.

The energy in the wave-mechanical form is

$$E = Bm(m+1)$$

$$\text{now } m(m+1) = (m + \tfrac{1}{2})^2 - \tfrac{1}{4}$$

$$\text{and } m_2(m_2+1) - m_1(m_1+1) = (m_2 + \tfrac{1}{2})^2 - (m_1 + \tfrac{1}{2})^2$$

Thus the results from both the points of view are identical.

In Raman Effect the selection principle in consideration of the third common level theory is shown to be  $\Delta m_R = 0$  or  $\pm 2$ . Now

$$\begin{aligned} \nu &= \nu_0 + B[(m + \tfrac{1}{2} + \Delta m_R)^2 - (m + \tfrac{1}{2})^2] \\ &= \nu_0 + B\{\Delta m_R^2 + 2\Delta m_R(m + \tfrac{1}{2})\} \\ &= \nu_0 \text{ for } \Delta m_R = 0. \end{aligned}$$

Thus we see that the missing line  $-\nu_0$  appears as a Raman line whatever be the value of  $m$ . This also explains why it is

most prominent, for whatever be the value of  $m$  it is bound to appear, for  $\Delta m_R = 0$ .

For  $\Delta m_R \neq 0$  but  $\pm 2$  we have

$$\nu_i = \nu_0 + B [4 \pm 2(2m+1)]$$

we shall get a series of lines corresponding to various values of  $m$ . The following diagram shows the Raman Lines as contrasted with the absorption lines.

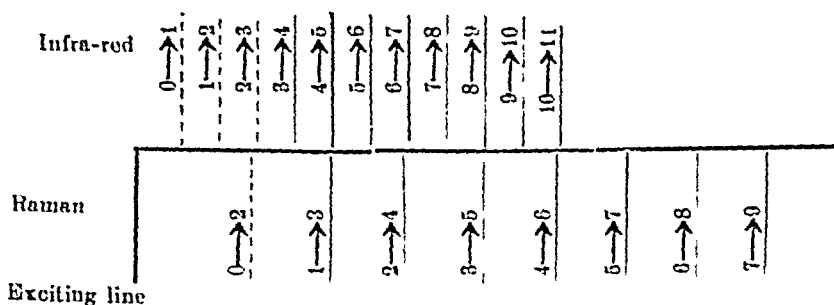


Fig. 11

It has been mentioned before that the lines accompanying the exciting line correspond to the alternate bands in the rotation spectrum of HCl as investigated by Czerny, but the correspondence is only accidental, for the transitions which give rise to the two are entirely different, as is clearly shown in the diagram. The absorption line involves the expression  $m(m+1)$  so that the Raman Transition  $j+1 \longrightarrow j-1$  corresponds with  $2j+1 \longrightarrow 2j$ . If higher terms in the expression for the absorption line are considered the correspondence will not be exact.

Now the most important question arises as to what is the physical significance of the third common level which plays such an important part in the occurrence of lines in the Raman Spectrum? In the works of Kramers and Heisenburg and also in the theory advanced by Schrödinger it occurs as a process of calculation; but the physical significance is not far to seek, when we consider the works of Pauli, Einstein and Ehrenfest on the problem of equilibrium between radiation and matter combined with the idea

underlying the correspondence principle. Scattering from the classical standpoint is (i) absorption of the incident light, and (ii) its simultaneous re-emission. The Hertzian oscillator to which the atom is likened in the classical theory as a result of the vibrations can be pictured as a simultaneous absorber and emitter of the light of the same frequency. But even in cases in which the incident and scattered light are different, that is, the scattering is not classical we should expect from the general idea of correspondence between the classical and quantum concepts, that the mechanism of the process should still be the same as it is known to be in the limiting classical case. When light of frequency  $\nu$  is incident, the molecule during the process (i) passes from the level  $E_n$  to the level  $E_l$ . (ii) reverts from the level  $E_l$  to the level  $E_n$  or  $E_k$  thus giving rise to light of frequency  $\nu$  and  $\nu - \nu_{kl}$ . The importance of the third common level in all cases of scattering is thus evident and the selection rule  $\Delta m = 0$  or  $\pm 2$  for Raman Effect is derived accordingly. The intensities of the Raman Lines can be derived from this point of view.

*Cabannes' Theory.*—Ordinary scattering is explained in terms of wave theory by supposing that the electric vector of the electromagnetic light wave excites an electric moment in the molecules forming an electric doublet. They vibrate with the frequency of one exciting light and scatter it, no change in the frequency being produced.

However if we suppose that the molecules are in motion whether it be rotation or vibration it can be shown that the re-emitted vibrations will not be sinusoidal but will be composed of  $\nu_1, \nu \pm \alpha_1, \nu \pm \alpha_2$  where  $\nu$  is the incident frequency and  $\alpha_1$  and  $\alpha_2$ , etc., are the frequency involved in the rotation-vibration. Thus a change in the wavelength of the scattered radiation occurs and on both sides of the primary scattered beam should be found the modified lines. In liquids free motions of the molecules cannot occur and the

incident light will react with the damped oscillations of the molecules and a representation of this by Fourier's series shows that a strong continuous spectrum is produced apparent as a symmetrical spreading of the primary line. Another result which can be deduced is that at the critical point no modified light will be present.

It can at once be said that the above theory is incapable of explaining facts observable in the Raman Effect. The most serious discrepancy occurs in the case of the intensity of the Stokes and anti-Stokes lines. Let us say they are given by  $N+n$  and  $N-n$ . On the above theory the ratio between the intensities will be  $\left(\frac{N+n}{N-n}\right)^2$ . The lines of enhanced frequency thus come out to be more intense. This is contrary to the observed facts. The appearance of sharp lines in some liquids finds no explanation on the theory while forbidden lines and the occurrence of inactive frequencies is also unaccounted for. At the most it can be made to explain stray facts such as the occurrence of lines corresponding to alternate rotation bands in the case of HCl.

It seems therefore that it is only the theory of light quanta which explains or seems to explain the exchanges of energies between radiation and matter and would be successful in coordinating the observed facts.

We shall not attempt to go into detail regarding the recent attempts to give a theory on lines indicated by wavemechanics. Recent attempts by Manneback and others give indications of going a long way to give a clear understanding of the processes involved in the effect.<sup>1</sup>

### CONCLUSION

We have reviewed briefly the immense amount of work done in so short a time on one of the most

<sup>1</sup> The authors regret that the very interesting work of Manneback could not be incorporated here for which his papers in *Z. f. Phys.* should be consulted.

important and epoch-making discoveries in Modern Physics. Though the phenomenon observed and data collected await ordering and coordination yet the relation of Raman Effect to other branches of Physics and Chemistry can be pointed out.

At the very first it was evident that it was going to prove a powerful probe for examining the interior of the molecule. A more detailed study is sure to lead to a complete understanding of the molecule and perhaps the atom. The other observed properties such as electric and magnetic birefringence, optical activity, specific heat, etc., on being connected with Raman Effect and infra-red data will describe the molecule in detail.

We might take as an example the dissociation theory. The variation in the intensity of the Raman Lines with dilution provides an ocular demonstration of the phenomenon in progress. Reference to the work of Rao on Nitric acid has already been made.

In some investigations it has revealed mysterious properties of crystals and their solutions. The frequency shift  $233\text{ cm}^{-1}$  has been found by Krishnamurti in lithium nitrate crystal but it disappears in solution. Another observation throwing light on the nature of crystalline binding is that the frequency shift to be attributed to the  $\text{NO}_3$  ion is the same in all solutions but it differs in crystals with different cations.<sup>1</sup> Experiments of Dadiou and Kohlrausch are valuable from the point of view of the modification produced in the molecule when two liquids are mixed.

The nature of chemical bonds is often revealed from the Raman Effect data. The covalent or the electro-valent type of bindings profoundly effect the Raman Spectra.

The organic molecules are expected to reveal the secret of their structure through Raman Lines and speculations are already rife regarding the modifications introduced in our ideas of the structure of the molecule by our new knowledge.

<sup>1</sup> See Appendix II.



The crystal structure stands in direct relationship with Raman Effect. The X-ray data as is well-known can give information about the constituent atoms and the electron distribution in them while Raman Effect reveals the nature of binding between the constituents of the crystal. As Bhagwantam observes : "The Raman Effect offers us a new method of studying crystals which in a sense is complementary to X-ray diffraction, for it furnishes just the kind of information X-rays do not give concerning the strength and nature of the forces which hold the crystals together."

It has further revealed the real nature of the speculations regarding the inactive frequencies which could not be studied by any other method.

The importance of the effect in the study of the infra-red spectrum of substances and the mode of their production cannot be overestimated. Practically whole of the infra-red spectrum has been shifted to the visible region to be studied with what we may term spectroscopic accuracy.

The subject is still in its infancy and it is too early to conjecture the new venues of research it may be expected to open. That its potentialities are many there is no occasion to doubt.

In the end we have to express our grateful thanks to Prof. M. N. Saha, F.R.S. for his kind interest and helpful suggestions and guidance during the course of the preparation of this essay.

# APPENDIX I

## THEORIES OF RAMAN-EFFECT

BY

R. C. MAJUMDAR.

The theoretical treatment of the Raman Phenomena has not progressed much. Smekal's as well as Kramers' and Heisenberg's treatments were rather general. They simply predicted the phenomenon. There is nothing new in the explanation given by Rasetti, Dieke, and Langer about the occurrence of combination lines  $\nu \pm \nu_k$  where  $\nu_k$  is a forbidden transition of the molecule, as such explanation has been already given by Lenz, and repeated by Schrödinger. The explanation can be deduced on very general grounds and throws no light on the mechanism. Cabannes and Rocard treat the phenomenon according to the electromagnetic theory of Maxwell and Lorentz, and find that the results are at variance with experimental data. Attempts have been made by Rossi, Hill and Kemble, Amaldi, Mannebeck, but without any appreciable advance being made. In all these attempts, the molecule has been likened to a *harmonic oscillator*.

It does not appear that all classes of Raman Effect can be treated according to the same procedure. We must take note of the actual constitution of the molecules producing Raman Effect, as well as of surroundings.

In the case of Raman Effect produced by gaseous molecules, it is well-known that the harmonic oscillator model does not correspond to facts. The actual model corresponds to the anharmonic oscillator (introduced by Kratzer). I have therefore treated the phenomenon of scattering by an anharmonic oscillator.

The present treatment is on lines somewhat similar to that pursued by Kramers and Heisenberg, their treatment being very general from the mathematical point of view, the physical points involved in the problem are a little obscure. Here, a particular case is treated. The anharmonic oscillator is supposed to be acted upon by:—

- (1) The field of the incident light of frequency  $\nu$ .

(2) "Virtual" field due to the oscillator itself of frequency  $2\pi n$ , this being the natural frequency of the oscillator.\*

It seems that if on the classical theory we are to take account of the excited states a procedure somewhat like this must be adopted.

The an-harmonic oscillator is represented by

$$m\ddot{x} + K\dot{x} + fx + gx^2 = eE \cos pt + eF \cos qt$$

$$\text{or } \ddot{x} + b\dot{x} + n^2x + ax^2 = \frac{e}{m} E \cos pt + \frac{e}{m} F \cos qt$$

Here  $e$  is not the charge of the electron, but the charge of the ions forming the anharmonic oscillator, and  $b$  is the damping coefficient.

When " $p$ " =  $n$ , we have

$$x = X \sin nt + Y \cos qt - a \frac{X^2 + Y^2}{2n^2} + \frac{aX^2 \cos 2nt}{6n^2} \\ - \frac{aY^2 \cos 2qt}{2(n^2 - 4q^2)} - \frac{aXY \sin (n+q)t}{n^2 - (n+q)^2} - \frac{aXY \sin (n-q)t}{n^2 - (n-q)^2}$$

$$\text{where } X = \frac{e}{m} \frac{E}{bn} \quad .$$

This classical result must be translated into quantum form; the correspondence principle helps us to identify  $2\pi n$  the frequency of the oscillator with  $\nu_k$

$$= \frac{W_n - W_m}{n}$$

(1) This expression immediately shows us that provided  $\frac{n}{q}$  is small as is always the case in all practical cases dealing with Raman Effect, the ratio of the intensities of the  $\nu - \nu_k$  and  $\nu + \nu_k$  lines will be unity and hence taking into account the fact that

\* That there be something like a virtual field surrounding an atom has been postulated by many authors and may be seen from the following argument. Let us consider sodium vapour. If this be bombarded by radiation quanta of frequency differing from one of the absorption frequency of sodium the quanta are allowed to pass through the mass of vapour without any appreciable loss; whereas if quanta of sodium D light be allowed to bombard the vapour they are almost completely stopped. It seems as if the small region surrounding an atom captures the quantum if its frequency coincides with one of the characteristic frequencies of the atom itself or in the small region surrounding the atom is present a virtual field of the frequency of the atom.

the atoms already in the excited state which gives rise to  $\nu + \nu_k$  line are to the atoms in the unexcited state as  $e^{-\frac{h\nu_k}{kT}}/1$

We have for the intensity of the

$$\frac{\text{anti-Stokes line}}{\text{Stokes line}} = e^{-\frac{h\nu_k}{kT}}$$

A result which agrees fairly well with experiment.

(2) We are also enabled to find the ratio of the intensities of the modified to the unmodified Raman Lines. On this point however the experimental material is very scanty.

$$\begin{aligned} \frac{\text{Primary line (unmodified)}}{\text{Secondary line (modified)}} &= \frac{P}{S} \\ &= \frac{X q^2}{a} \end{aligned}$$

We must evaluate (1)  $X$  and (2)  $a$ . The first we do from special application of the corresponding principle and the second from data on band spectra.

$$(1) \quad X = \frac{e}{m} \frac{E}{nb}$$

$b$  = coefficient of damping.

The virtual field of the oscillator must be supposed to be in equilibrium with the oscillator, i.e., we can calculate the energy density of the virtual field by exactly the method used by Planck in calculating the energy of an oscillator in terms of the energy density of the field

$$\therefore \frac{E^2}{4\pi} = \frac{8\pi\nu^2}{c^3} W$$

putting  $W = W_n - W_m = h\nu_k$

we have

$$E = \sqrt{\frac{32\pi^2\nu_k^2 h}{c^3}}$$

$$X = \frac{e}{mb} \sqrt{\frac{4}{\pi} \frac{hn}{c^3}}$$

Calculating  $a$  (see Report on Molecular Spectra by National Research Council)

If  $r_0$  be the normal distance between the two lines forming the diatomic anharmonic oscillator, we have

$$\text{Force} = \frac{a}{r_0} \left( -\frac{\xi}{\rho^3} + 3b\xi^2 \dots \dots \dots \right)$$

$$\rho = \frac{r}{r_0}, \xi = \frac{r-r_0}{r_0} = \frac{y}{r_0}, \quad a = n^2 m r_0^2$$

$$= \frac{a}{r_0} y + \frac{3ba}{r_0} y^2$$

$$= mn^2 y + a m y^2$$

$$\therefore a = 3bmr_0 n^2$$

$$\text{Again} \quad x = \frac{h}{4\pi^2 I_0 \omega_0} \left( \frac{3}{2} + \frac{5}{2} b + \dots \dots \dots \right)$$

where  $x$  is defined by

$$E_n = n' h \omega_0 (1 - x n')$$

$n'$  = the vibration quantum number and  $E_n$  = energy of the oscillator.

$$\therefore b = \frac{8}{15} \pi^2 \frac{(x \omega_0)}{h} I_0$$

$$\text{and} \quad a = \frac{8}{5} \pi^2 \frac{(x \omega_0) n^2 r_0}{h} I_0$$

$$\text{Hence} \quad \frac{P}{S} = \frac{P}{mb} \sqrt{\frac{hn}{c^3} \frac{4}{\pi}} \frac{5h}{8\pi^2 n^2 r_0 I_0} \frac{q^2}{(x \omega_0)}$$

$$= \frac{z}{b} \sqrt{\frac{4h^3}{c^3 n^3 \pi}} \frac{5}{8} \pi^2 \frac{q^2}{I_0^2 (x \omega_0)}$$

$Z$  = electric moment of the molecule.

As an illustration let us take the case of CO.

$$Z = 10^{-18} \text{ e.s.u. (See Polar Molecules, Debye) and putting } q = 2\pi \times 10^{15}$$

$$\text{and } n = 2\pi \times 10^{14}$$

$$\text{we get } P/S = \frac{10^2}{b}$$

Regarding the value of  $b$  it may be stated that it will be of the order of  $10^1$  to  $10^2$ , for the life of the metastable atoms  $= \frac{1}{b}$  is of the order  $10^{-1}$  to  $10^{-2}$  second.

Hence this shows that  $P/S$  is of the order of 10. The exact value cannot be calculated unless we estimate " $b$ " accurately.

*N.B.*—The above calculations are only approximate in some respects but an exact calculation can be readily made when the sufficient experimental data are available.

## RELATION BETWEEN WOOD'S PHENOMENA AND RAMAN EFFECT

In the next section the relation between the ordinary scattering and resonance scattering has been brought out. From the works of Schrödinger and more recently of Langer already mentioned, it is evident that the relation between Wood's phenomenon and Raman Effect is exactly the same as between the resonance and ordinary scattering. When the "common level  $n$ " of Dieke . . . coincides with the incident frequency, resonance occurs. The modified scattering is consequently very intense and the Wood's phenomenon is obtained. A quantitative theory is being developed.

## ORDINARY SCATTERING AND RESONANCE SCATTERING

Let us take a harmonic oscillator, represented by the equation

$$m\ddot{x} + fx = 0$$

Let  $P = ex$  be the electric moment.

when this is acted upon by an electromagnetic pulse  $eEe^{i\omega t}$  the equation of forced oscillation is given by

$$\ddot{p} + \omega_0^2 p = \frac{e^2 E}{m} e^{i\omega t} \quad \text{where } \omega_0 = \sqrt{f/m}$$

Let  $p = \xi e^{i\omega t}$

Then 
$$\xi = \frac{e^2 E}{m(\omega_0^2 - \omega^2)}$$

Therefore 
$$p = \frac{e^2 E}{m(\omega_0^2 - \omega^2)} e^{i\omega t}$$

and 
$$\ddot{p} = \frac{-e^2 E}{m(\omega_0^2 - \omega^2)} \omega^2 e^{i\omega t}$$

According to Hertz's theory of resonators, if a charge  $e$  moves with an acceleration  $\ddot{X}$  it creates an electromagnetic field about it. The intensity of the electrical and magnetic fields are given by:—

$$E = H = \frac{\ddot{p} \sin \theta}{c^2 r}$$

According to Poynting's theorem, the flow of energy is given by

$$\begin{aligned} S &= \frac{c}{4\pi} [E.H.] \\ &= \frac{e^2 \omega^4}{4\pi c^3 r^2} \xi^2 e^{2i\omega t} \sin^2 \theta \end{aligned}$$

$$\therefore |S| = \frac{w^4}{4\pi c^3 r^2} \frac{\sin^2 \theta}{2} (e\xi)^2$$

Hence scattering by a single electron is equivalent to

$$S = \frac{w^4}{4\pi c^3 r^2} \left( \frac{1 + \cos^2 \phi}{2} \right) (e\xi)^2$$

If there are N electrons in a cubic centimeter, independently effective in scattering, we have,

$$S_N = \frac{Nw^4}{4\pi c^3 r^2} \left( \frac{1 + \cos^2 \phi}{2} \right) (e\xi)^2$$

We now suppose that the electrons belonging to the same molecule vibrate coherently. Hence it is not their energy-radiation S, but their amplitudes  $\xi$  that are superposed. We write  $(Se\xi)$  instead of  $\xi$ . "S" denoting summation over all the electrons of the individual molecule. On the other hand, the radiation from the different molecules are all non-coherent hence summation of energy has to be taken over all the molecules.

The radiation scattered by unit volume:—

$$S_n = \frac{4N\pi^2 c}{\lambda^4 r^2} \frac{1 + \cos^2 \phi}{2} \sum (Se\xi)^2$$

The summation being taken over all the molecules.

$$w = \frac{2\pi c}{\lambda}$$

Now applying the ideas of the theory of dispersion  $\sum (Se\xi) =$  total moment of electric displacement in unit volume = P  
The total dielectric displacement

$$D = E + 4\pi P = \epsilon E = n^2 E$$

Hence

$$\sum (Se\xi) = \frac{n^2 - 1}{4\pi} E.$$

Hence we express the unknown quantity  $(Se\xi)$  in terms of known physical quantity. Now we have

$$S_N = \frac{N\pi c}{\lambda^4 r^2} E^2 \cdot \frac{1 + \cos^2 \phi}{2} \cdot \frac{(n^2 - 1)^2}{4}$$

Now we have the density of energy

$$= \frac{E^2}{4\pi} = \frac{I}{c}$$

where I = Intensity

$$\therefore E^2 = \frac{4\pi I}{c}$$

$$\therefore \frac{S_n}{1} = \frac{N\pi^2}{\lambda^2 r^2} \cdot \frac{1 + \cos^2 \phi}{2} \cdot (n^2 - 1)^2$$

or the coefficient of scattering, i.e., the fraction of the primary energy which is scattered per cm. path is

$$a = \frac{8\pi^3 N}{3\lambda^4} (n^2 - 1)^2$$

we have,

$$n^2 - 1 = \frac{\frac{4}{3}\pi e^2/m}{\omega_0^2 - \omega^2} = \frac{e^2/m}{\pi(\omega_0^2 - \omega^2)}$$

$\therefore \frac{a}{N} =$  scattering by one particle

$$\begin{aligned} &= \frac{8\pi e^4}{3m^2 c^4} \cdot \frac{\lambda_0^4}{(\lambda_0^2 - \lambda^2)^2} \\ &= 6.63 \times 10^{-25} \cdot \frac{\lambda_0^4}{(\lambda_0^2 - \lambda^2)^2} \end{aligned}$$

*Resonance Scattering or Fluorescence.*—The formula evidently fails when  $\omega = \omega_0$ , i.e., at place of absorption. We have then the phenomenon of resonance scattering. We must now introduce a damping coefficient. The equation of the harmonic oscillator is now:—

$$\begin{aligned} \ddot{p} + \gamma \dot{p} + \omega_0^2 p &= \frac{e^2 \epsilon e^{i\omega t}}{m} \\ p &= \frac{e^2 \epsilon e^{i\omega t}}{m[(\omega^2 - \omega_0^2) + i\omega\gamma]} \end{aligned}$$

The rate of absorption of energy

$$\begin{aligned} U_a &= (\dot{p}\epsilon) = i\omega(p\epsilon) \\ &= \frac{e^2/m i\omega}{(\omega^2 - \omega_0^2) + i\omega\gamma} \epsilon^2 \\ &= \frac{e^2/m \cdot \gamma\omega^2}{(\omega^2 - \omega_0^2)^2 + \gamma^2\omega^2} \epsilon^2 \end{aligned}$$

Let us also calculate the energy which is being radiated:

$$\begin{aligned} U_s &= \frac{2}{3c^3} \ddot{p}^2 \\ &= \frac{2}{3c^3} \frac{e^4/m^2 \epsilon^2 \omega^4}{[\omega^2 - \omega_0^2 + i\omega\gamma]^2} \end{aligned}$$

$$\text{Let } \gamma_0 = \frac{2\omega^2 e^2}{3m c^3}$$



$$U_s = \gamma_0 \frac{e^2}{m} \frac{w^2 \epsilon^2}{[(w^2 - w_0^2) + i w \gamma]^2}$$

We have now to find out the value of  $\gamma$ . At a distance from  $w = w_0$  we shall have  $U_s = U_a$

$$\text{Now } U_s = \gamma_0 \frac{e^2}{m} \frac{w^2 \epsilon^2}{(w_0^2 - w^2)^2 + \gamma^2 w^2}$$

Thus we got from the condition  $U_s = U_a$

$$\gamma = \gamma_0$$

This gives us the value of the damping coefficient. The energy radiated

$$\int U_s dv = \frac{\gamma e^2}{m} \frac{2\rho v}{3} \int \frac{w^2 dw}{(w_0^2 - w^2)^2 + w^2 \gamma^2}$$

$$\text{where } dv = \frac{dw}{2\pi} \text{ and } \epsilon^2 = \frac{4\pi\rho}{3}$$

$\rho$  = energy density.

Thus

$$U_s = \frac{\pi e^2}{3mc} I$$

where  $I$  = intensity of the light.

The formula shows that resonance scattering or intensity of fluorescence is of quite a different order from ordinary scattering. The scattering per particle is

$$\alpha = \frac{\pi e^2}{3mc} = 8.2 \times 10^{-3}$$

which is of quite a different order than the ordinary scattering already discussed.

## APPENDIX II

Some collected data are given below from an article by Smekal in "Zeitschrift für Electrochemie und Angewandte Physikalische Chemie," September, 1930. For a detailed discussion of these the reader is referred to the above article.

TABLE I.

*Raman Lines and the Infra-red Spectrum of Benzene.*

$\nu$ in $\text{cm}^{-1}$	Wavelength in $\mu$		Wavelength in $\mu$			
	Raman spectrum	Infra-red	Raman spectrum $\text{cm}^{-1}$		Infra-red	
3148.8	3.140 (2)				7.25 (0)	
3162.9	3.162 (1)				7.8 (0)	
3001.3	3.267 (4)	3.25 (4)	1170.0	8.48 (1)	8.67 (4)	
3046.9	3.284 (1)				9.78 (5)	
2946.8	3.394 (2)		991.3	10.09 (5)	10.3 (2)	
		4.4 (0)	(924)		(10.8)	
		4.9 (0)	848.1	11.78 (0)	11.8 (2)	
		5.5 (1)				
1604.1	6.234 (1)	6.2 (0)			12.45	
1583.6	6.315 (1)	6.75 (5)	604.6	16.54 (2)	12.95	

TABLE II.

*Influence of State on Raman-effect.*

HCl	Gas	2885					
	Liquid	2780					
NH <sub>3</sub>	Gas	3333.6	(1630)	(966)	(933)		
	Liquid	3298.4	1580	1070			
CH <sub>4</sub>	Gas	3071.5	3022.1	2914.8	(1700)	(1520)	(1320)
	Liquid	...	...	2908	...	...	...
C <sub>2</sub> H <sub>4</sub>	Gas	3272.3	3240.3	3019.3	2880.1	1623.3	1342.4
	Liquid	...	...	3080	3000	1620	1340

For the influence of dilution upon the Raman-shifts in  $H_2SO_4$  see the article quoted above p. 627 as also for the effect of mixing equal parts of benzene, ether, alcohol and water with acetic acid (Tabelle 4 und 5).

TABLE III

Raman frequencies of tri and tetra halides in liquid state or in solution.

PBr <sub>3</sub>	116	162	380	400
PCl <sub>3</sub>	190	257	480	510, 590
AsCl <sub>3</sub>	157	195	370	400
SbCl <sub>3</sub>	130	155	320	360
BiCl <sub>3</sub>	110	Band	240	290
CCl <sub>4</sub>	217	315	458	757, 793
SiCl <sub>4</sub>	152	220	427	600
TiCl <sub>4</sub>	120	140	390	500
SnCl <sub>4</sub>	103	137	365	410

TABLE IV

Molecule	Binding	Frequency in $cm^{-1}$	Average force in dynes ( $10^{-4}$ )
C <sub>6</sub> H <sub>6</sub>	C—C	990	2.08
H <sub>3</sub> COO.NH <sub>2</sub>	C—N	860	1.98
H <sub>3</sub> C. OH	C—O	1031	2.27
C <sub>2</sub> H <sub>4</sub>	C=C	1620	4.20
Ketone	C=O	1700	4.44
O <sub>2</sub>	O=O	1552	4.19
O <sub>2</sub> H <sub>2</sub>	C≡C	1960	5.43
CN	C≡N	2240	6.52
CO	C≡O	2155	6.35
N <sub>2</sub>	N≡N	2339	7.38

TABLE V

*Inactive Raman shifts in  $\text{cm}^{-1}$  of crystalline Nitrates.*

$\text{LiNO}_3$	1085.8	$\text{Ca}(\text{NO}_3)_2$	$1064.3 \pm 1.5$
$\text{NaNO}_3$	$1067.5 \pm 1.1$	$\text{Sr}(\text{NO}_3)_2$	$1054.4 \pm 1.5$
$\text{KNO}_3$	$1048.4 \pm 0.7$	$\text{Ba}(\text{NO}_3)_2$	$1046.5 \pm 1.0$
$\text{AgNO}_3$	$1045.0 \pm 1.0$	$\text{Pb}(\text{NO}_3)_2$	$1045.0 \pm 1.7$

$\text{Sr}(\text{NO}_3)_2 + \text{OH}_2\text{O}$	$1054.4 \pm 1.5$
$+ 4\text{H}_2\text{O}$	$1053.5 \pm 0.7$
$+ 6\text{H}_2\text{O}$	1052.9
$+ 8\text{H}_2\text{O}$	$1044.4 \pm 0.9$

$\text{NO}_3^-$  in solution . . . . 1045       $\text{NaNO}_3 + \text{KNO}_3$  in melted state . . . . . 1042.

The above table illustrates the effect on the "inactive" frequency of the  $\text{NO}_3$  group of different cations with single or double valency. The modification can be considered as a sort of deformation. A value with which comparisons can be made is obtained from the  $\text{NO}_3$  ion in solution. It is seen that smaller the atomic number of the cation greater is the deformation. The comparison of  $\text{KNO}_3$  and  $\text{Ca}(\text{NO}_3)_2$  is interesting. The mass and the electron arrangement of the cation is practically the same but the greater ion-charge gives a greater deformation. The effect of the water of crystallisation is illustrated by the Raman-effect of  $\text{Sr}(\text{NO}_3)_2$ .

the velocity of electrons towards one side is increased while on the other side it is retarded; thus, the electrons move with a drift velocity in a direction opposite to the applied electromotive force. This drift of electrons is responsible for the current through the conductor. The positively-charged particles take no part in conduction, as is evident from the fact that at the junction of two conductors atoms of one metal are not to be detected in another metal. The following facts also support the above view:—

1. An unlimited number of electrons are emitted when conductors are heated, proving that electrons are flowing from other portions of the system into the heated conductor.
2. According to the modern theories of atomic structure, elements having one or two electrons in their outermost shells are the best conductors, which has been experimentally verified.
3. For explaining the Hall effect and the change of resistance in a magnetic field, we must assume that the mass of the conducting particles is very small in proportion to its charge.

We shall now give Drude's mathematical treatment of conduction.

### ELECTRICAL CONDUCTIVITY

Let  $F$  be the applied electromotive force and  $u$  the velocity of the electrons at a temperature  $T^\circ \text{K}$ .

The acceleration due to the applied e. m. f. is

$$Fe/m \quad \dots \quad \dots \quad (1)$$

If the mean free path of the electron is  $l$  the time during which the electron is moving freely is  $l/u$  and hence the average drift velocity

$$v = \frac{Fe}{m} \frac{1}{2} \frac{l}{u} \quad \dots \quad \dots \quad (2)$$

The current is given by

$J = Ncv$ , where  $N$  is the number of electrons per unit volume.

Thus

$$J = Ne \cdot \frac{Fe}{m} \frac{1}{2} \frac{l}{u} \quad \dots \quad \dots \quad (3)$$

and

$$\begin{aligned} \sigma &= \frac{J}{E} = \frac{Ne^2 l}{2mu} \\ &= \frac{Ne^2 lu}{6kT} \quad \dots \quad \dots \quad (4) \end{aligned}$$

This expression alone does not enable us to explain anything regarding metallic conduction, as we have no independent means of knowing either  $N$ , the number of free electrons, or the mean free path of the electron. We must also remember the assumptions made in the above deduction, which are :—

Same value of both (a)  $l$ , the mean free path, and (b)  $u$ , the velocity of the electrons.

The third assumption is (c) that the motion of the electron is independent of its history previous to collision.

It is well known from experiments that  $\sigma \propto 1/T$ , except at very low temperature. Thus since  $u$  varies as  $T^{\frac{1}{2}}$ , we should have  $Nl$  varying inversely as  $T^{\frac{1}{2}}$  so that  $Nlu$  may become independent of  $T$ . But nothing definite can be said about the dependence of  $N$  or  $l$  upon  $T$ .

### THERMAL CONDUCTIVITY

Drude now supposes that the free electrons are also responsible for heat conduction in metals. The atoms are supposed to be at rest and the electrons are treated like a gas. Thus the problem of heat conduction of metals is just the same as heat conduction in the case of a gas, the free electrons taking the place of gas particles.

The thermal conductivity of a metal due to the electron gas is then

$$\kappa = \frac{1}{2} Nlu k \quad \dots \quad \dots \quad (5)$$

From equations (4) and (5), we get

$$\frac{\kappa}{\sigma} = 3 \left( \frac{h}{e} \right)^2 T \quad \dots \quad (6)$$

This is exactly the law of Wiedemann and Franz and of Lorentz. We have now to see how far the deduction agrees quantitatively with experimental facts.

Jaeger and Diesselhirst set out to verify equation (6) at 18°C. Their results are tabulated below.

TABLE I

Material	$\kappa/\sigma$ at 18°C	Temp. Coeff. of $\kappa/\sigma$
Copper, pure ...	6.71 $\times 10^{10}$	.39
Silver, pure ...	6.86	.37
Gold (1) ...	7.27	.36
Gold (2), pure ...	7.07	.37
Nickel ...	6.99	.39
Zinc (1) ...	7.05	.38
Zinc (2), pure ...	6.72	.38
Cadmium, pure ...	7.06	.37
Lead, pure ...	7.15	.40
Tin, pure ...	7.35	.34
Aluminium ...	6.36	.43
Platinum (1) ...	7.76	...
Platinum (2), pure ...	7.53	.46
Palladium ...	7.54	.46
Iron (1) ...	8.02	.43
Iron (2) ...	8.38	.44
Steel ...	9.03	.35
Bismuth ...	9.64	.15
Constantan (60 Cu, 40 Ni) ...	11.06	.23
Manganin (84 Cu, 4 Ni, 12 Mn)	9.14	.27

Theoretically we have from (6)

$$\begin{aligned} \kappa/\sigma &= 3 \times \left( \frac{1.37 \times 10^{-16}}{1.59 \times 10^{-20}} \right)^2 \times 291 \\ &= 6.5 \times 10^{10} \text{ o.m. units.} \end{aligned} \quad \dots \quad (7)$$

The temperature coefficient is theoretically proportional to the absolute temperature and is thus given by  $\frac{100}{273} = .366$ .

It is quite evident from the above table that  $\kappa/\sigma$  is very nearly equal to the theoretical value and so is the value of the temperature coefficient. For good conductors the experimental value is very close to the theoretical one but marked deviations are noticed in the case of poor conductors. But one peculiar fact emerges from the above table which shows that the deviations in all cases from the theoretical value are always in the direction of values greater than the theoretical.

Lorentz, Richardson and Thomson have all tried to improve the theory, and they have all arrived at the conclusion already arrived by Drude, although the numerical value for  $\kappa/\sigma$  is slightly different, but none agrees with the experimental value given in Table I. The discrepancy may partly be explained by assuming that the atoms contribute quite a considerable amount towards the conduction of heat especially in the case of bad conductors where there is a dearth of free electrons. The table also shows that the deviation is great from the theoretical value for bad conductors; thus supporting the above view. In 1921, Hall<sup>1</sup> put forward the dual theory of conduction, assuming that both the free as well as the bound electrons are responsible for conduction.

In the case of alloys the value of  $\kappa/\sigma$  is not nearly as constant as it is for pure metals. But, even, in the case of alloys any considerable variation in the electrical conductivity is usually accompanied by a similar variation in the thermal conductivity, which is very beautifully seen from a graph by Schulze (*Ann. der. Phys.*, IX, p. 584) (Fig. 1.)

Lord Rayleigh explains that the abnormal values in the case of alloys are also partly due to the Peltier heating effect at the junction of parts of material of varying composition. This introduces a spurious resistance in alloys which is absent in the case of pure metals.

<sup>1</sup> E. H. Hall, *Proc. Nat. Acad. Sci.*, 7, 98 (1921.)



Drude's treatment is rather elementary, but encouraged by its success Lorentz tried to work out a theory mathema-

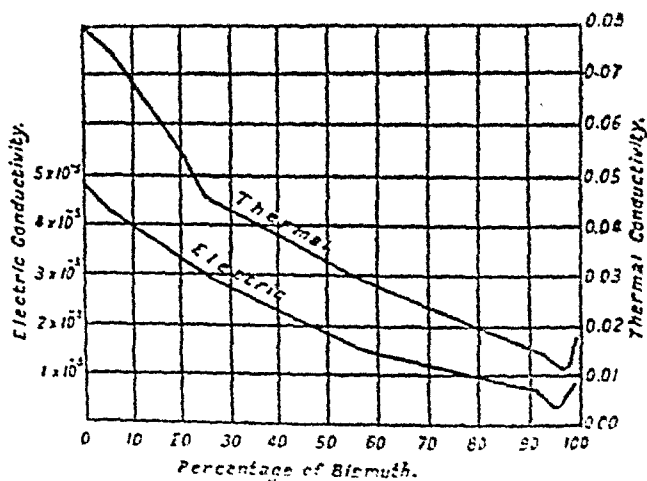


Fig. 1

tically more rigorous. His treatment differs from that of Drude in the assumption concerning the collisions between electrons and atoms. He takes for granted that the Maxwell's law of distribution of energy applies equally well to electrons and proves that

$$\kappa/\sigma = 2 \left( \frac{k}{e} \right)^2 T \quad \dots \quad \dots \quad \dots \quad (7)$$

The full treatment is given in the end in Appendix I.

Thus we see that Lorentz's value for  $\kappa/\sigma$  is only 66 per cent of the Drude-value. The rigorous treatment clearly points towards the view that atoms take quite a considerable part in the conduction phenomena.

*The Specific Heat Difficulty.*—Drude and following him Lorentz have assumed that the electrons are as numerous as the atoms or molecules in a metal, and also that they have the same energy as the material particles. This means that the presence of free electrons should considerably alter the specific heat of the metals, but experiments show that they have no influence over it. Hall and other investigators have pointed out that this difficulty can be

got over by assuming that the mean free path is much larger than  $10^{-8}$  cm. and thus the number of free electrons is only a small fraction of the total number of material particles and therefore the contribution to the specific heat is negligible.

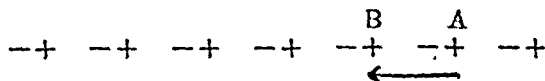
*Consideration of Intra-Atomic-Forces.*—In Lorentz's treatment, we made use of the idea of mean free path, considering the electrons to behave like perfect gases. This is hardly true, as electrons have to move in the interstices between the fixed positive residue, and also under the field of force of assemblage of other electrons. The motion of electrons is therefore least like that of particles in the perfect gas theory, and does not seem to be amenable to any mathematical treatment.

Richardson, however, assumes, that the electrons are subject to a force varying inversely as  $d^2$  when it approaches a positive particle, and deduces generalised expression for  $l$  under the action of such forces. He deduces for the Wiedemann-Franz's ratio

$$\kappa/\sigma = \frac{2s}{s-1} \left( \frac{k}{e} \right)^2 T \quad \dots \dots \dots (8)$$

which becomes Drude's expression for  $s=3$ .

*Thomson's Theory of Doublets.*—In this theory metals are supposed to consist of a large number of doublets, formed by the union of



a positively electrified atom with an electron. The electron from A is supposed to leave it and join B, the atom previous to it and thus the exchange of electrons takes place amongst the atoms. The doublets are supposed to arrange themselves along a line in the direction of the electric force as represented in the above figure.

Let us suppose that  $F$  is the electric force and  $\theta$  is the angle which the axis of the doublet makes with the direction of  $F$ . The potential energy of the doublet is given by  $-Fed \cos \theta$ ,  $d$  being the distance between the charges in the doublet.

Thomson assumes that the distribution is according to Maxwell's law and thus the number of doublets having the abovementioned potential energy is proportional to

$$e^{Fed \cos \theta / kT}$$

The number of doublets whose axis makes an angle between  $\theta$  and  $\theta + d\theta$  with the direction of  $F$  is proportional to  $e^{Fed \cos \theta / kT} \sin \theta d\theta$ . The average value of  $\cos \theta$  is given by

$$\overline{\cos \theta} = \frac{\int_0^\pi e^{Fed \cos \theta / kT} \cos \theta \sin \theta d\theta}{\int_0^\pi e^{Fed \cos \theta / kT} \sin \theta d\theta} \quad \dots (8)$$

Under the conditions in which the conductivity is determined we can easily see that  $Fed/kT$  is much smaller than unity for, if  $F=10$  volts and  $d=10^{-8}$  cm.

$$\frac{Fed}{kT} = \frac{1}{30} \cdot \frac{4.77 \times 10^{-10} \times 10^{-8}}{1.36 \times 10^{-16} \times 300} = 10^{-6} \times 4 \text{ approximately} \\ << 1 \quad \dots \quad \dots \quad \dots (9)$$

Thus the average value of  $\cos \theta$  is

$$\overline{\cos \theta} = \frac{2/3 \frac{Fed}{kT}}{2} = \frac{1}{3} \frac{Fed}{kT} \quad \dots \quad \dots \quad \dots (10)$$

Each doublet is supposed to discharge an electron  $p$  times a second in the direction opposite to that of  $F$ . Then the current through unit area is given by

$$J = \frac{1}{3} \frac{Fed}{kT} pb Nc \quad \dots \quad \dots \quad \dots (11)$$

Here  $N$  is the number of particles per unit volume, and  $b$  is the distance between the centres of the doublets.

The conductivity is given by

$$\sigma = \frac{1}{3} \frac{e^2 d p N b}{kT} \quad \dots \quad \dots \quad \dots \quad (12)$$

*Thermal Conductivity.*—It is supposed that the electrons are in thermal equilibrium with the doublet, then evidently on leaving one doublet at a temperature  $T + dT$  and joining the other at a temperature  $T$  carries an amount of energy from the first to the second, which is equal to  $\frac{3}{2} k\delta T$ . If the electrons are supposed to be moving equally in all directions, the number of electrons crossing a unit surface in unit time at right angles to the temperature gradient is given by

$$n = \frac{1}{3} N b p \quad \dots \quad \dots \quad \dots \quad (13)$$

Thus the total amount of energy taken by the electrons passing the unit cross section is

$$\frac{N b p}{3} \frac{3}{2} k\delta T$$

but

$$\delta T = \frac{dT}{dx} \cdot b$$

and the thermal conductivity is

$$\kappa = \frac{1}{3} N b^2 p \frac{3}{2} k = \frac{1}{2} k N b^2 p \quad \dots \quad \dots \quad (14)$$

$$\text{and } \frac{\kappa}{\sigma} = \frac{3}{2} \frac{k^2 T b}{e^2 d} \quad \dots \quad \dots \quad \dots \quad (15)$$

### VOLTA EFFECT

Volta discovered in 1795 that two plates of different metals placed parallel to each other when joined together by means of a wire or any conducting fluid, were found to be charged with a certain quantity of electricity when the connecting wire was removed. The voltage difference between the two plates depends entirely upon the materials composing the plates, and also upon the physical condition of the surfaces. This electromotive force was called by Volta--the Contact Electromotive Force.

Sir Oliver Lodge<sup>2</sup> expressed the view that when the two metals are in contact they are at the same potential but differently charged, thus forming an air battery. His view is that each metal is associated with an electromotive force proportional to the heat evolved on oxidation, and the volta e.m.f. is the difference between the two e.m.f.'s. On this hypothesis the contact e.m.f. for  $Zn - Cu$  will be about one volt. Pellat found it to be 0.71 volt, Ayrton 0.75 volt and Clifton 0.85 volt. Thus they are in very rough agreement with the theoretical value.

Bottomley<sup>3</sup> found that the contact e.m.f. of zinc-copper remained unchanged up to a pressure of  $2.5 \times 10^{-6}$  of an atmosphere, and also when air was replaced by hydrogen. Brown<sup>4</sup> found that in the presence of hydrogen sulphide the volta e.m.f. for iron-copper was reversed, which is evidently due to the surface films formed so easily.

Contact force has also been found to vary with the physical state of the materials.<sup>5</sup> Mairona<sup>6</sup> found that it is reduced by low temperatures, obtained by dropping liquid air on the junction.

Volta e.m.f. has been very carefully measured by de-Broglie<sup>7</sup> by the condenser method, by Shaw<sup>8</sup> and Greinacher<sup>9</sup> by the ionisation method. They found that if the layer of water was increasingly removed, the volta e.m.f. tended to disappear. But this may be attributed to the presence of a layer of phosphorus-pentaoxides deposited on each metal, and what was measured was the e.m.f. between the oxide coatings which must vanish. Perucca<sup>10</sup>

<sup>2</sup> Lodge, Brit. Assoc. Report, 1884, p. 464.

<sup>3</sup> Bottomley, Brit. Assoc. Report, 1885, p. 901.

<sup>4</sup> Brown, Phil. Mag., 5th Series, 1878, VI, 142.

<sup>5</sup> Erskine-Murray, Proc. Roy. Soc., 63, 113, 1898; Hoeschus, Journ. Russk. Chimicesk, 1902.

<sup>6</sup> Mairona, Nuovo Cimento, 1900, XII, 196.

<sup>7</sup> M. de-Broglie, C. R. 152, 698, (1911).

<sup>8</sup> Shaw, Phil. Mag., (25, 241,) 1913.

<sup>9</sup> Greinacher, Ann. d. Phys., 16, 723 (1905).

<sup>10</sup> Perucca, Cim., Vol. 23, 3 (1921).

measured the contact e.m.f. by the Kelvin method and found a residual effect which is however much smaller than the effect usually assigned. For zinc-mercury he found the e.m.f. to be 0.17 volt with mercury negative, but the e.m.f. was found to increase fourfold in the presence of oxygen.

*Method of Measurement of the Volta e.m.f.: Lord Kelvin's Method.*<sup>11</sup>—Two metallic plates, say zinc and copper, are put parallel to each other to form a parallel plate condenser.

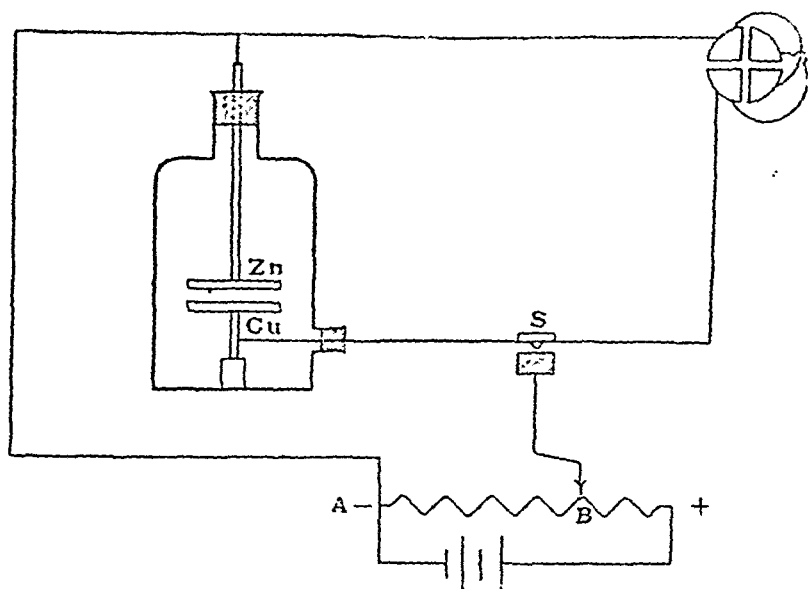


Fig. 2

They are connected to the two adjacent quadrants of a quadrant electrometer. The zinc plate is connected to the negative end A of a potentiometer, the other plate of copper through a switch S to the movable point B or the potentiometer.

The movable point B is brought to A and the switch S is closed, bringing the two plates in contact with each other. As soon as S is opened the quadrant electrometer shows a deflection which is a measure of the volta e.m.f. Then the movable arm B is brought in such a position that

<sup>11</sup> Lord Kelvin, *Phil. Mag.*, 46, 82 (1898).

the opening or the closing of S has no influence over the deflection in the quadrant electrometer. Then the potential drop between A and B is the measure of the volta e.m.f. for zinc-copper.

### THERMO-ELECTRICITY

In 1826 Seebeck discovered that when two junctions of different metals are kept at different temperatures a current flows in the circuit so formed.

In 1834, Peltier discovered the complementary effect that a passage of current through two dissimilar metals gives rise to heat one junction and produces cold at the other.

The heat given out in  $t$  seconds is equal to  $P \cdot q$  when  $q$  units of electricity is passed in  $t$  seconds. The constant  $P$  is known as the Peltier coefficient.

The Peltier effect is a reversible one, and a thermocouple is an arrangement which absorbs heat at one end and delivers a part of it at a lower temperature. This state of affairs is similar to a small Carnot's heat engine.

Thus, applying the second law of thermodynamics, we should have

$$\frac{P_2 q}{T_2} = \frac{P_1 q}{T_1}$$

where  $q$  is the quantity of electricity in absolute units passed in the circuits.

This gives,

$$P_2 - P_1 = E = P_1 \left( \frac{T_2 - T_1}{T_1} \right) \dots \dots \dots (1)$$

where  $E$  is the electromotive force in the circuit.

*Thomson Effect.*—The simple relation given in (1) does not hold good in practice. Lord Kelvin pointed out that in addition to the Peltier e. m. f. there is yet another e. m. f. developed due to difference of temperature between two

points of the same metal. If we have two different temperatures at two different places in the same metallic bar the e. m. f. due to the Thomson effect is given by

$$\int_{T_1}^{T_2} \sigma dT$$

where  $\sigma$  is the Thomson coefficient, which was called the specific heat of electricity by Lord Kelvin, reasons for which are apparent from the above expression.

Thus we have the total e.m.f. in a circuit

$$E = P_2 - P_1 + \int_{T_1}^{T_2} (\sigma_2 - \sigma_1) dT \quad \dots \quad \dots \quad \dots \quad (2)$$

Whence, the thermo-electric power for the two metals is given by

$$\frac{dE}{dT} = \frac{dP}{dT} + (\sigma_2 - \sigma_1) \quad \dots \quad \dots \quad \dots \quad (3)$$

It can be easily shown from thermodynamical considerations that

$$P = T \frac{dE}{dT} \quad \dots \quad \dots \quad \dots \quad (4)$$

$$\sigma_2 - \sigma_1 = -T \frac{d^2 E}{dT^2} \quad \dots \quad \dots \quad \dots \quad (5)$$

*Experimental Determination of Peltier Effect.*—There are several methods for determining the Peltier coefficient, but we shall describe only one of them due to Barker.<sup>12</sup>

He placed equal number of copper-nickel junctions in two Devar flasks, which were thermally equal in all respects. Equal amount of paraffin oil was used as heat absorbent which was kept stirred. Each Devar flask was provided with a sensitive thermometer so that any difference in temperature between the two flasks could be easily determined. A current was passed in one direction, so that one of the flasks was heated because of the Peltier effect while the

<sup>12</sup> Barker, Phys. Review, Vol. 31, p. 321 (1910).



other was cooled. There were two heater coils one in each flask, so that they could be kept at the same temperature.

The arrangement is shown in Fig. 3.

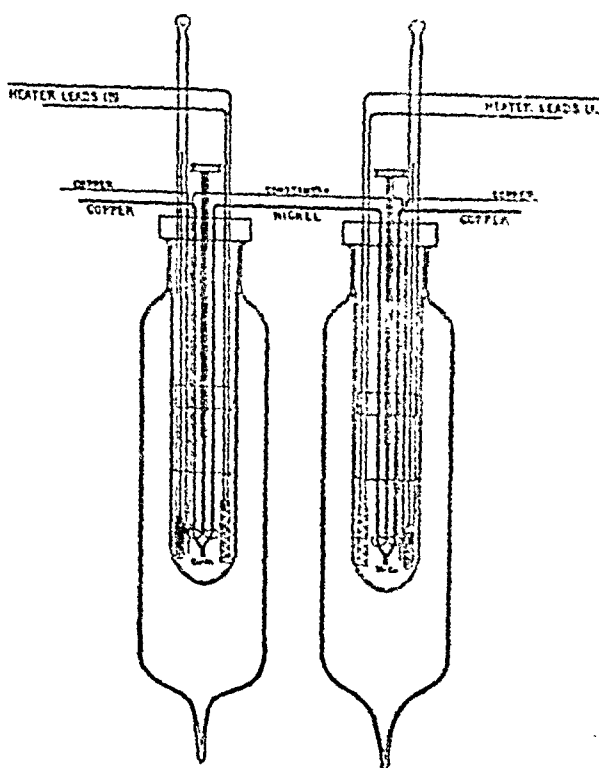


Fig. 3

In order to eliminate the resistance of the thermo-junctions current was reversed and the flasks again kept at the same temperature.

Then, we have,

$$R_a i^2 + nPi = R_b i^2 - nPi + bi_b^2$$

and on reversing the current

$$ai_a^2 + R_a i^2 - nPi = R_b i^2 + nPi$$

whence

$$P = \frac{ai_a^2 + bi_b^2}{4ni}$$

where

$i$  = current in the thermo-junctions whose resistances are  $R_a$  and  $R_b$ .

$a$  = resistance of the heater coil in one flask.

$b$  = resistance of the heater coil in the other flask.

$i_a$  = heating current in the first flask.

$i_b$  = heating current in the second flask.

$P$  = Peltier e.m.f.

For Cu-Ni, the value for  $P$  was found to be  $6.75 \times 10^{-3}$  volts at  $28.7^\circ\text{C}$ .

*Experimental Method of Determining Thomson Coefficient.*—There are several methods of determining the Thomson coefficient, the important ones are due to Worthing<sup>13</sup> and Nettleton.<sup>14</sup> Here we will describe the latter only.

The apparatus used by him is shown in the figures 4 (A) and 4 (B) below. The material to be experimented upon was

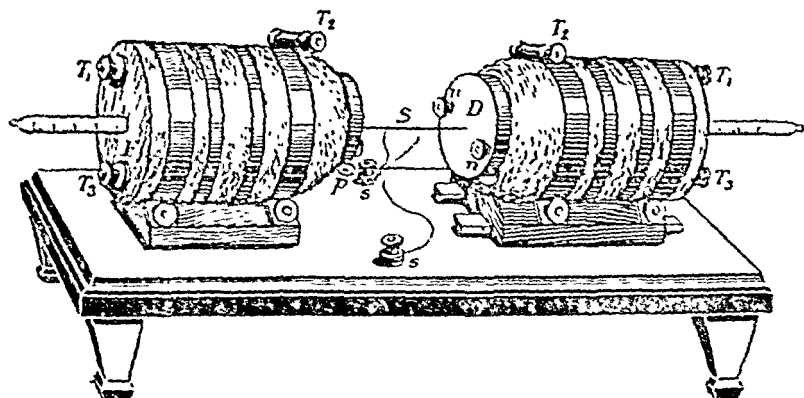


Fig. 4 (A)

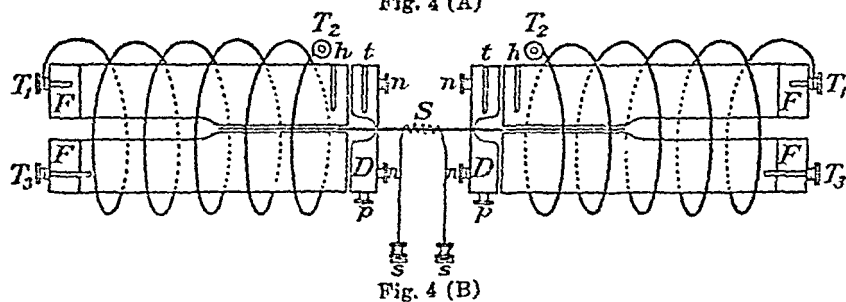


Fig. 4 (B)

used in the form of a wire, the two ends of which passed between two copper cylinders used as electrical heaters.

<sup>13</sup> Worthing, *Phy. Rev.*, 5, 446 (1915.)

<sup>14</sup> Nettleton, *Proc. Phy. Soc.*, (Lond.), 34, 78 (1921-22).

The wire was soldered to two copper discs DD, which were fitted on to the heaters. Thermocouples were placed in *tt* and the temperatures of the two discs DD could be easily determined.

A current could be easily passed through the operative portion of the wire between the discs DD by means of the binding screws *p, p*. A search coil S was used for determining the temperature of the middle portion of the wire.

A known current  $C_1$  was passed in one direction and the resistance of the coil S determined, then a current  $C_2$  was passed in the other direction, such that the resistance of the coil remained unchanged.

Let  $T_1$  and  $T_2$  be the temperatures of the two discs and  $R$  the resistance of the wire between D, D. Then,

$$RC_1^2 - \sigma (T_1 - T_2) C_1 = RC_2^2 + \sigma (T_1 - T_2) C_2$$

which gives

$$\sigma = \frac{R}{T_1 - T_2} (C_1 - C_2)$$

$$= \frac{R}{J(T_1 - T_2)} (C_1 - C_2) \text{ cal. per coulomb.}$$

His results for constantan and iron are given below :—

Constantan	
Mean Temp. °C	$\sigma \times 10^8$ cal/coul.
50.1	5.87
50.2	5.88
50.4	6.00
110.6	6.08
141.7	6.13
172.5	6.22
203.5	6.23

The results can be expressed by

$$\sigma_T \times 10^8 = 564 + 107T/100 - 12T^2/10^4.$$

*Iron*

Mean Temp. °C	$\sigma \times 10^6$ cal./coul.
48.2	2.56
49.9	2.62
79.5	3.30
110.1	3.97
140.5	4.59
172.6	5.18
204.9	5.69

The result can again be expressed by

$$\sigma_T \times 10^6 = 138 + 505T/200 - 12T^2/2 \times 10^4 - 5T^3/10^6$$

CLASSICAL THEORY OF VOLTA, PELTIER AND  
THOMSON EFFECTS.

*Volta and Peltier Effects.*—In the derivation of expressions for these effects, it is assumed that the pressure of electrons in different metals is not the same. Thus when two pieces of different metals are brought in contact with each other, the electrons from the piece A supposed to have larger pressure of electrons, flows into the piece B, till the positive charge left on A due to the deficit of electrons balances the difference in the pressure.

Let us suppose that the transition from A to B takes place in a thin layer at the point of contact. Let  $N$  be the number of electrons per c. c. at  $x$  cms. from one of the boundaries of this layer,  $p$  be the pressure of electrons and  $F$  the electric force, then the force on electrons in a unit volume must be equal to the force arising from the variation in pressure as we pass from one side of the layer to the other,

$$\frac{dp}{dx} = FeN \quad \dots \quad \dots \quad \dots \quad (1)$$

But  $p = NkT$  giving  $dp/dx = kT \frac{dN}{dx}$ , whence,

$$V = \int F dx = \frac{kT}{e} = \log_e \frac{N_1}{N_2} \quad \dots \quad \dots \quad (2)$$

From the method of derivation it is apparent that the expression (2) must hold good for both the Volta as well as the Peltier e.m.f. But the experimental results show that the Volta e.m.f. is of the order of a volt, while the Peltier e. m. f. is a few millivolts.

From the above expression  $N_1/N_2$ , the ratio of the number of electrons in the two substances can be calculated for one volt.

$$\log_e \frac{N_1}{N_2} = \frac{eV}{kT} = \frac{4.77 \times 10^{-10}}{1.36 \times 10^{-16} \times 300 \times 300} \\ = 36 \text{ nearly,}$$

Thus

$$\frac{N_1}{N_2} = 4.31 \times 10^{15} \quad \dots \quad \dots \quad \dots \quad (3)$$

which is quite inconsistent with the comparable values of the resistances of any two metals having one volt as contact potential difference.

For Antimony-Bismuth the Peltier e. m. f. is about 1/30th of a volt, which gives

$$N_1/N_2 = 3.8 \quad \dots \quad \dots \quad \dots \quad (4)$$

All other metals have smaller value for the Peltier e. m. f., and hence the theory shows that the number of free electrons does not vary much from one element to another.

There is a large change of resistance of some metals at fusion, e.g., the conductivities of solid zinc, tin, and lead at their melting point are about twice of what they are when the metals are in a liquid state at the same temperature. They contract on solidification, showing that  $l$  the mean free path of electrons is greater in the liquid than in the solid state. We have seen from the Drude theory that the conductivity is proportional to  $Nl$ . Hence  $N_1 l_1 = 2 N_2 l_2$ .

where  $N_1 l_1$  corresponds to the solid state and  $N_2 l_2$  to the liquid state, since  $l_2 > l_1$ ,  $N_1 > 2 N_2$ . But from the expression for the Peltier coefficient we see that we must get the Peltier e. m. f. between the solid and liquid state, but experiments so far conducted fail to show any such e. m. f. Thus we see one more shortcoming in the simple theory.

### THEORY OF THE THOMSON EFFECT

Let us take a bar the two ends of which are maintained at two temperatures. Now if the pressure of electrons depends upon temperature, there must be electric forces to keep the electrons from drifting.

Let  $p$  be the pressure at a point  $x$  cm. from one of the ends. Then the force acting on the electrons in a layer between  $x$  and  $x+dx$  per unit area of these planes is equal to  $\frac{\partial p}{\partial x} dx$ . If  $F$  is the e. m. f. to balance this drift, we have under conditions of equilibrium,

$$Fe N dx = \frac{\partial p}{\partial x} dx$$

$$\text{or } Fe = \frac{1}{N} \frac{\partial p}{\partial x} \quad \dots \quad \dots \quad \dots \quad (5)$$

where  $N$  is the number of particles in a unit volume.

The mechanical equivalent of heat abstracted by a single electron, in travelling from the layer at  $x$  at a temperature  $T$  to the layer at  $x+dx$  at a temperature  $T + \frac{\partial T}{\partial x} dx$  is given by

$$Fe dx = \frac{1}{N} \frac{\partial}{\partial x} (NkT) dx \dots \dots (6)$$

The difference in the kinetic energy of the electron in the two places is

$$\frac{3}{2} k \frac{\partial T}{\partial x} dx.$$

Thus the total amount of heat communicated by the electron to the metal is

$$\begin{aligned} dq &= \left\{ \frac{3}{2} k \frac{\partial T}{\partial x} - \frac{1}{N} \frac{\partial}{\partial x} (NkT) \right\} dx \\ &= \left\{ \frac{3}{2} k - \frac{1}{N} \frac{\partial}{\partial T} (NkT) \right\} dT \quad \dots (7) \end{aligned}$$

Let  $i$  be the current flowing in the bar in the direction in which  $x$  increases, then  $i/e$  is the number of electrons flowing through unit area in unit time. Then the total amount of heat carried by the electrons = the heat developed due to the Thomson effect, i.e.—

$$\frac{i}{e} \left\{ \frac{3}{2} k - \frac{1}{N} \frac{\partial}{\partial T} (NkT) \right\} dT = \mp i \sigma dT \quad \dots (8)$$

The minus sign is to be taken when the current is flowing from the cold to the hot part and positive sign when in the reverse direction.

Thus

$$\begin{aligned} \sigma &= \mp \frac{k}{e} \left\{ \frac{3}{2} - \frac{1}{N} \frac{\partial}{\partial T} (NT) \right\} \\ &= \mp \frac{k}{e} \left\{ \frac{1}{2} - T \frac{\partial}{\partial T} (\log N) \right\} \quad \dots (9) \end{aligned}$$

## EMISSION OF ELECTRONS FROM METALS

Under proper experimental conditions, electrons can be extracted from both hot as well as cold bodies. The former phenomenon, *i.e.*, the emission of electrons from hot bodies is generally classified under the heading thermionic phenomena, while the latter is a recent discovery and bound to play a very important part in the elucidation of the conduction of electricity. The two phenomena will be discussed under two headings.

## THERMIONIC PHENOMENA

Although many investigators announced the electrical conductivity of hot air, it was E. Becquerel,<sup>1</sup> who in 1853 described experiments showing that air heated to red-heat became conducting. Later Blondlot<sup>2</sup> in 1881 repeated Becquerel's experiments and proved in addition that the currents did not obey Ohm's law.

As a result of large number of experiments Elster and Geitel<sup>3</sup> established that at low temperatures current passed more readily between a hot wire and a cold electrode, when the former was positively charged; but when the wire was heated strongly negative charges could readily pass from the hot wire to the cold electrode. During the last decade of the nineteenth century, Edison discovered that a current could pass through a galvanometer one terminal of which was connected to one end of a filament heated by direct current and the other terminal to an auxiliary electrode placed in the same bulb as the filament. He found that there was a much stronger current when the filament negative end was connected to the galvanometer than when it was connected to the positive end. This phenomenon is known as the Edison Effect and was utilised

<sup>1</sup> E. Becquerel, *Ann. de. Chimie et Phys.*, 355, 39 (1853).

<sup>2</sup> Blondlot, *C. R.* 870, 92 (1881), 28 B, 104 (1887).

<sup>3</sup> Elster and Geitel. A series of papers in the *Annalen der Physik* from 1882.



by Fleming in the construction of the Fleming valve for detecting the Hertzian waves.

Sir J. J. Thomson's theory of conduction of electricity through gases gave an impetus to the experimenters, and it was MacClelland<sup>4</sup> who definitely proved that air passing over heated platinum wire became conducting due to ionisation. Thomson's<sup>5</sup> experiments threw a lot of light on the nature of the carriers of electricity in these experiments. He placed a hot filament in a cross electric and magnetic field and determined the value of  $e/m$  from the curve showing the relation between current and the magnetic field.  $e/m$  was found to be  $87 \times 10^7$  c.m. units, from which Thomson concluded that the carriers of electricity here are identical with the cathode particles. Wehnelt<sup>6</sup> in 1904 obtained  $e/m = 1.4 \times 10^7$  c.m. u., while more recently the value obtained is almost equal to  $1.77 \times 10^7$ , the present value for  $e/m$ .

Richardson,<sup>7</sup> in 1901, gave the first theory of electronic emission in vacua. He proved the saturation current  $i_s$  for a body heated to a temperature  $T^\circ$  absolute is given by

$$i_s = AT^{\frac{3}{2}} e^{-b/T} \dots \dots \dots (1)$$

In deriving this formula he assumed that, Drude's picture of a metal is correct according to which

- (1) Electrons are present in the glowing body in the form of monatomic gas.
- (2) The density of electrons is a constant independent of the temperature of the hot body, but depending on the nature of the body.
- (3) The potential energy of the electron inside the hot body is smaller than that when it is outside.
- (4) That the work done in the removal of an electron from the body depends only on the body.

<sup>4</sup> MacClelland, Phil. Mag., 29, 46 (1899).

<sup>5</sup> J. J. Thomson, Phil. Mag. 547, 48 (1899).

<sup>6</sup> Wehnelt, Ann. der Phys. 425, 14 (1904.)

<sup>7</sup> Richardson, Proc. Camb. Phil. Soc., 290, 11 (1901.)

- (5) Electrons coming out from the hot body exerts no force on the electrons outside.
- (6) The distribution of velocities for electrons obeys the Maxwell law.

Out of  $n$  electrons, present in a cubic centimeter of the hot body, the number having their velocity components lying between  $u, u+du; v, v+dv; w, w+dw$ ; is given by

$$dn = n \left( \frac{m}{2\pi kT} \right)^{3/2} e^{-m(u^2+v^2+w^2)/2kT} du dv dw.$$

Out of these the number coming out of a unit surface of the hot body in a second is given

$$dn' = nu \left( \frac{m}{2\pi kT} \right)^{3/2} e^{-\frac{m}{2kT}(u^2+v^2+w^2)} du dv dw \dots (2)$$

assuming  $x$ -axis to be perpendicular to the emitting surface  $ds$ .

Now if  $X$  is the component of the electric force along the  $x$ -axis, which attracts the electrons towards the hot body, we know from mechanics that the particle velocity is reduced from  $u$  to

$$u_0 = \sqrt{u^2 - \frac{2}{m} \int X dx} = \sqrt{u^2 - \frac{2W}{m}} \dots (3)$$

Thus only those electrons can escape which have a velocity such that

$$u^2 > \frac{2W}{m}, \text{ where } W \text{ is the work done by the electron}$$

in coming out of the hot surface.

The number escaping per unit time is given by

$$\begin{aligned} N &= \int_{\sqrt{\frac{2W}{m}}}^{\infty} \int_{-\infty}^{\infty} \int_{-\infty}^{\infty} nu \left( \frac{m}{2\pi kT} \right)^{3/2} e^{-\frac{m}{2kT}(u^2+v^2+w^2)} du dv dw \\ &= n \sqrt{\frac{kT}{2\pi m}} e^{-W/T} \\ &= A_0 T^{1/2} e^{-b/T} \dots \dots \dots (4) \end{aligned}$$

where,

$$A_0 = n \sqrt{\frac{k}{2\pi m}}$$

and  $b = \frac{W}{k}$

Now,

$$i_s = N e = A T^{\frac{5}{2}} e^{-b/T} \dots \dots \dots (5)$$

In 1918 van Laue \* treated the problem of emission of electron as one of evaporation of electrons from the condensed phase inside the solid to one of gaseous phase. On this assumption it can be shown that the vapour pressure  $p$  is given by the well-known equation (v. Laue *Loc. cit.* p. 707).

$$\log p = -\frac{\mu}{RT} + \frac{5}{2} \log T + \log C,$$

$$\text{where } C = \frac{(2\pi m)^{\frac{3}{2}} k^{\frac{5}{2}}}{h^3}.$$

$$\text{Thus } p = \frac{(2\pi m)^{\frac{3}{2}} k^{\frac{5}{2}}}{h^3} T^{\frac{5}{2}} e^{-\mu/RT} \dots (6)$$

The current is given by  $i_s = \frac{1}{4} n \bar{c} e$ , the analogy being taken from effusion phenomena in the kinetic theory of gases. The above equation gives

$$i_s = \frac{1}{4} n e \sqrt{\frac{8kT}{m\pi}}$$

$$= \sqrt{\frac{pe}{2m\pi kT}}$$

$$\text{since } \bar{c} = \sqrt{\frac{8kT}{m\pi}} \text{ and } p = n k T,$$

$$\text{which gives } i_s = \frac{2\pi k^{\frac{3}{2}} m e}{h^3} T^{\frac{5}{2}} e^{-\frac{\mu}{RT}},$$

$$A = \frac{2\pi k^{\frac{3}{2}} m e}{h^3} = 60.2 \text{ amp. / cm.}^2 \text{ deg.}^{\frac{5}{2}}$$

More recently Dushman<sup>o</sup> has called attention to the above theoretical fact which follows from van Laue's theory

\* van Laue, *Ann. d. Phys.*, 58, 695 (1919).

<sup>o</sup> Dushman, *Phy. Rev.*, Vol. 21, 624 (1923).

and shows experimentally that  $A = 60.24 \text{ amp. / cm}^2 \text{ deg}^2$  for tungsten.

From Lewis<sup>10</sup> Gibson and Latimer's theory

$$A = 51.2 \text{ amp./cm.}^2 \text{ deg}^2.$$

Various physicists have found a great discrepancy in the value of  $A$ , notable amongst them is Du Bridge<sup>11</sup> who finds that the Dushman's value for  $A$  is found only when  $\phi_0$ , the thermionic work function is 4.5 volts.

For different samples of pure platinum, he finds that as  $\phi_0$  is increased from 4.7 to 6.4 volts the value for  $A$  increased from 11.5 to 14,000 amp. / cm.<sup>2</sup> deg.<sup>2</sup> The abnormal value of  $A$  has been attributed to surface impurities by Bridgman<sup>12</sup> and others, but Du Bridge<sup>13</sup> finds for a clean piece of platinum  $A$  to be 17,000 amp. / cm.<sup>2</sup> deg.<sup>2</sup>

R. H. Fowler<sup>14</sup> has applied wave mechanics to the problem and shows that  $A$  should not be a constant quantity.

### EMISSION OF ELECTRONS FROM COLD METALS

In addition to the emission of electrons from hot bodies, it is well-known from the results of various experiments that even at much lower temperatures it is possible to pull out electrons by the mere application of intense electric field. Schottky has shown that although saturation is reached at ordinary electric field, the current goes on increasing with the increase in the field and is given by

$$i = i_0 e^{eV_0/kT} \quad \dots \quad \dots \quad \dots \quad \dots \quad (1)$$

where  $V_0$  is the potential at a distance  $x_0$ , where the image force is equal to the external force trying to pull the electron away from the metal.

<sup>10</sup> Lewis, Gibson and Latimer, J. Am. Chem. Soc., 44, 1008 (1922).

<sup>11</sup> Du Bridge, Phys. Rev., 31, 236 (1928).

<sup>12</sup> Bridgman, Phys. Rev., 31, 90 (1928).

<sup>13</sup> Du Bridge, Phys. Rev., 32, 961 (1928).

<sup>14</sup> R. H. Fowler, Proc. Roy. Soc., A. 122, 36 (1929).

The potential at a distance  $x$  in the neighbourhood of  $x_0$  is

$$V = \frac{e}{4x} + Fx \quad \dots \quad \dots \quad \dots \quad \dots \quad (2)$$

But at  $x_0$ ,  $\frac{dv}{dx} = 0$ , and hence

$$F = \frac{e}{4x_0^2}, \text{ i.e., } x_0 = \sqrt{\frac{e}{4F}} \quad \dots \quad \dots \quad \dots \quad (3)$$

From the equations (2) and (3), we get

$$V_0 = \sqrt{eF} \quad \dots \quad \dots \quad \dots \quad \dots \quad (4)$$

Substituting in (1), we have

$$i = i_0 e^{3/2 F^{1/2} / kT} \quad \dots \quad \dots \quad \dots \quad (5)$$

The above equation has been experimentally verified by several people and quite recently by Pforte<sup>15</sup> and De Bruyne.<sup>16</sup> The latter deduces a value for  $e$  to be  $4.84 \times 10^{-10}$  e.s. units from his observations.

Millikan and Eyring<sup>17</sup> and also Gossling<sup>18</sup> with his collaborators find that the equation (5) is not satisfied in the presence of very intense electric field. In addition to this Millikan and Eyring find that there is no change in the autoelectronic current when the temperature of the cathode is increased up to  $800^\circ\text{C}$  from ordinary room temperatures. The main part of this current came from submicroscopic peaks on the cathode surface, which is due to the presence of more intense field at the peaks than at the rest of the surface. From these facts it is quite clear that the Schottky equation does not hold good at such high intense fields of the order of  $10^6$  volts per cm. and that by the application of such high fields we can pull out electrons, the number coming out being independent of temperature.

<sup>15</sup> Pforte, Z. fur. Phy., 49, 46 (1928).

<sup>16</sup> De Bruyne, Proc. Roy. Soc., A, 120, 423 (1928).

<sup>17</sup> Millikan and Eyring, Phy. Rev., 27, 51 (1926).

<sup>18</sup> Gossling, Phil. Mag., 1, 609 (1926).

Millikan and Lauritsen<sup>19, 20</sup> have shown that  $\log i$  when plotted against inverse of the field strength gives a straight line, *i.e.*—

$$i = c \epsilon^{-b/F} \dots \dots \dots (6)$$

In addition to this relation they have also shown that the autoelectronic and thermionic currents are given by

$$i = A (T + cF)^2 \epsilon^{-b/(T+cF)} \dots \dots \dots (7)$$

Oppenheimer<sup>21</sup> has theoretically established the equation (6). Fowler and Nordheim<sup>22</sup> using Sommerfeld's picture of the metal have also obtained that  $i = cF^2 \epsilon^{-b/F}$ , a formula hardly differing from equation (6); but they fail to find any theoretical justification for equation (7). However, Houston<sup>23</sup> has obtained an equation very much similar to (7), but having no  $T$  in the exponential. The results of Houston have been found by Millikan to satisfy the experimental results very well.

It is generally believed that the electrons thus pulled out are the so-called free electrons responsible for the conduction of electricity by metals. Eyring, Mackeown, and Millikan<sup>24</sup> have found that for a current of  $2.3 \times 10^{-12}$  amp. the necessary field strength for tungsten is about  $10^6$  volts/cm.; for nickel it is  $2.4 \times 10^6$  volts/cm., and for platinum it is  $.46 \times 10^6$  volts/cm.

Thus it appears that if the view that the free electrons are responsible for the autoelectronic current be accepted then no emission must be expected from non-conductors, and in the light of above results the idea of free electrons has to be modified to a certain extent. It is just possible that the number of electrons pulled out depends to some

<sup>19</sup> Millikan and Lauritsen, Proc. Nat. Acad. Sci., 14, 45 (1928).

<sup>20</sup> Millikan and Lauritsen, Phys. Rev., 33, 598 (1929).

<sup>21</sup> Oppenheimer, Phys. Rev., 31, 914 A, 1928.

<sup>22</sup> Fowler and Nordheim, Proc. Roy. Soc., A 119, 173, 1928.

<sup>23</sup> W. V. Houston, Phys. Rev., 33, 361 (1929).

<sup>24</sup> Eyring, Mackeown and Millikan, Phys. Rev., 31, 900 (1928).

extent upon the ionisation potential, the thermionic work function and other properties of the individual metal, but nothing definite can be said until more data is available as to what extent it depends upon one or all of these factors.

#### EXPERIMENTAL ARRANGEMENT FOR PULLING OUT ELECTRONS FROM COLD METALS

As already pointed out Millikan and Eyring [Phys. Rev., 27, 51 (1926)] and various other workers used a

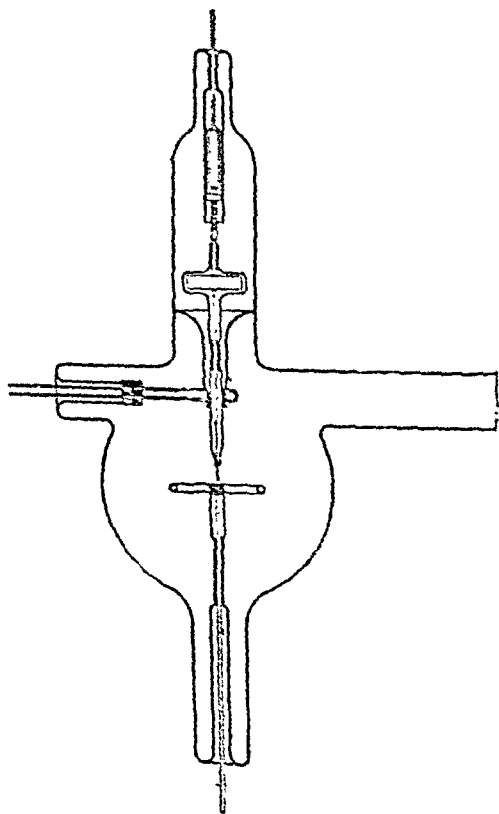


Fig. 5

very thin metallic wire in their experiments, but here it was rather impossible to get an exact idea of the field

strength existing at the submicroscopic peaks which emitted the auto-electronic current. The Research Staff of the G.E.C.<sup>25</sup> used fine edges of straight wires directed towards a spherical anode, but a much better arrangement has been used by Eyring, Mackeown and Millikan,<sup>26</sup> which will be described below Fig (5).

The anode consisted of a plane disc of steel and the cathode was a pointed metallic rod. By means of a nut and screw arrangement the distance between the anode and the cathode could be adjusted. The whole thing was put inside a glass bulb, which was thoroughly outgassed and exhausted, the pressure inside the bulb being about  $10^{-8}$  mm. of mercury. The distance between the anode and the cathode was determined by means of a travelling microscope, and the field strength at the point was calculated.

The results obtained by them have already been quoted (page 349) for platinum, nickel, and tungsten. The logarithm of the field current when plotted against the inverse of field strength or applied potential gave a perfect straight line.

<sup>25</sup> Gossling and others *Loc. cit.*

<sup>26</sup> Eyring, etc., *Phys. Rev.*, 31, 900, (1928).



## GALVANOMAGNETIC AND THERMO- MAGNETIC EFFECTS

When a conductor carrying an electric or heat current is placed in a magnetic field perpendicular to the lines of force the following phenomena are observed :—

### GALVANOMAGNETIC EFFECTS

Transversal effects.		Longitudinal effects.	
(a)	(b)	(c)	(d)
Hall effect ...	Ettingshausen effect.	Kelvin effect ...	Nernst effect
Trans. e.m.f.	Trans. temp. diff.	Long. poten. diff.	Long. temp. diff.
		or	
		Change in resis.	
R	P	A	L

### THERMOMAGNETIC EFFECTS.

Transversal effects.		Longitudinal effects.	
(e)	(f)	(g)	(h)
Nernst-Ettingshausen effect.	Rigghi-Leduc effect.	Ettingshausen-Nernst effect.	Maggi-Rigghi-Leduc effect. diff.
Trans. poten. diff.	Trans. temp. diff.	Long. poten. diff.	Long. temp. diff.
Q	S	N	M

(a) The Hall coefficient R is defined by

$$R = E \frac{d}{HI}$$

where E is the electromotive force developed, H is the magnetic field, I the electric current through the conductor,

and  $d$  the thickness of the conductor along the lines of magnetic field. Some metals show a positive while some a negative value for  $R$ .

(b) The Ettingshausen coefficient  $P$  is defined by

$$P = \Delta T \frac{d}{HI}$$

where  $\Delta T$  is the difference in temperature between the upper and lower faces of the conductor which is assumed to be lying horizontal.  $P$  has both positive and negative values.

(c) The Kelvin coefficient is given by

$$A = \frac{\Delta r}{rH^2}$$

$\Delta r$  being the change of resistance in  $r$ . This change is proportional to  $H^2$  for weak fields and is independent of the direction of  $H$ . But recently Kapitza [Proc. Roy. Soc., A, 123 (1929)] has shown that  $\Delta r$  is a linear function of  $H$  for stronger fields.

(d) The Nernst coefficient  $L$  is given by

$$L = \Delta T \frac{bd}{lHI}$$

where  $d$  = thickness of the bar

$b$  = breadth

and  $l$  = distance between the two points showing  $\Delta T$  difference in temperature.

(e) The Ettingshausen-Nernst coefficient  $Q$  is defined by

$$Q = E \frac{l}{bH(t_2 - t_1)}$$

or  $\frac{Q}{\kappa} = \frac{Ed}{WH}$ , a form similar to the expression for the

Hall coefficient  $R$

(f) The Rigghi-Leduc coefficient

$$S = \Delta T \frac{l}{bH(t_2 - t_1)}$$

(g) The Ettingshausen-Nernst coefficient

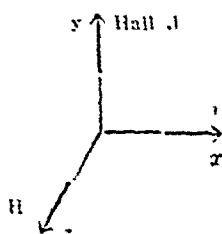
$$N = E \frac{l}{dH^2(t_2 - t_1)}$$

## (h) The Maggi-Rigghi-Leduc coefficient

$$M = \frac{\Delta_A}{H^2}$$

$\Delta_A$  being independent of the direction of  $H$ .

The values of these coefficients have been found to vary under varying physical conditions, but leaving these aside we shall confine ourselves to the attempts made for getting a theoretical expression for the Hall coefficient and for the change in resistance in magnetic field.

THEORY OF HALL EFFECT<sup>27</sup>

Let us suppose that the primary current flows along the  $x$ -axis and the magnetic field acts along the  $z$ -axis.

The components of the electric force at any point is  $X, Y, 0$ .

The equations of motion for an electron is

$$\left. \begin{aligned} m\ddot{x} &= eX - \frac{He}{c} \dot{y} \\ m\ddot{y} &= eY + \frac{He}{c} \dot{x} \\ m\ddot{z} &= 0 \end{aligned} \right\} \quad \dots \quad \dots \quad \dots \quad \dots \quad (1)$$

Solving these equations, we get,

$$\dot{y} = \frac{1}{2} \frac{e}{m} \tau \left[ Y + \frac{1}{3} \frac{H}{c} \frac{l}{m} X \tau \right] \quad \dots \quad \dots \quad (2)$$

where  $\tau$  is the time between two collisions. The Hall current density is  $ne\dot{y}$ , so that it becomes zero when we apply an external e.m.f. of the value,

$$Y = -\frac{1}{3} \frac{H}{c} \frac{e}{m} X \tau \quad \dots \quad \dots \quad (3)$$

From (1) we get

$$\ddot{z} = \frac{1}{2} \frac{e}{m} X \tau, \text{ since } \ddot{y} \text{ is negligible.}$$

$$i = ne \bar{z} = \frac{1}{2} n \frac{e^2}{m} X \tau.$$

<sup>27</sup> Richardson, Electron Theory of Matter, p. 437.

Thus,

$$Y = -\frac{2}{3} \frac{1}{c} \frac{H}{en} i.$$

The Hall coefficient

$$R = -\frac{Y}{Hi} = \frac{2}{3} \frac{1}{ne} \quad \dots \quad \dots \quad \dots (4)$$

where all the quantities are expressed in e. m. units.

But  $N = 10^{22}$  nearly,

Hence,  $R = -4 \times 10^{-1}$  approximately.

The value thus obtained for  $R$  is quite out of proportion for most metals. It also shows that  $R$  is always negative, but it is not so. Sir J. J. Thomson has suggested that the change in sign might be due to the fact that the conditions are effected by the orientations of the electron-orbits of the atoms in the presence of an external field.

### THEORY OF THE CHANGE OF RESISTANCE IN A MAGNETIC FIELD.

The equation of motion for an electron in this case is

$$\left. \begin{aligned} m\ddot{x} &= eX - \frac{He}{c} \dot{y} \\ m\ddot{y} &= \frac{He}{c} \dot{x} \\ m\ddot{z} &= 0 \end{aligned} \right\} \quad \dots \quad \dots \quad \dots (1)$$

$$\text{or } \ddot{x} = \frac{eX}{m} - \frac{H}{c} \frac{e}{m} \left[ \frac{H}{c} \frac{e}{m} \left( \frac{1}{2} \frac{e}{m} X t^2 + ut \right) + v \right]$$

Here  $He y/c$  has been neglected in comparison to  $\frac{1}{2} X t^2$  and  $u$  and  $v$  are supposed to be the initial velocities in the two directions just after collision.

$$i = ne\bar{x} = \frac{n}{2} \frac{e^2}{m} \left[ \tau - \frac{H^2}{12c^2} \frac{e^2}{m^2} \tau^3 \right] X$$

When  $H = 0$ ,

$$i = \frac{n}{2} \frac{e^2}{m} \tau_0 X = \sigma X \quad \dots \quad \dots \quad \dots (2)$$

In the presence of a magnetic field there is a possibility of alteration of the orientation of the systems with which the electron collides and a curvature may be introduced in the free paths and hence the free period will be  $(\tau_0 + \delta\tau)$

If  $\delta i$  is the change in the electric current, we get,

$$\delta i = \frac{n}{2} \frac{e^2}{m} \left[ \delta\tau \frac{1}{12} \frac{H^2}{c^2} \frac{e^2}{m^2} \tau^2 \right] \times \\ = \delta\sigma N.$$

$$\text{or } \frac{\delta\rho}{\rho} = - \frac{\delta\sigma}{\sigma} = - \frac{1}{\tau_0} \left[ \delta\tau - \frac{1}{12} \frac{H^2}{c^2} \frac{e^2}{m^2} \tau^2 \right] \quad \dots (3)$$

$$\text{i.e., } \frac{\delta\rho}{\rho} = - \frac{\delta\sigma}{\sigma} = - \frac{\delta\tau}{\tau_0} + \frac{1}{3} \frac{H^2}{c^2} \left( \frac{\sigma}{ne} \right)^2 \quad \dots (4)$$

Since  $\tau_0 \approx \tau$

Now  $\delta\tau/\tau_0$  can be neglected when compared to the last factor, and we get

$$\frac{\delta\rho}{\rho} = \frac{1}{3} \frac{H^2}{c^2} \left( \frac{\sigma}{ne} \right)^2 \quad \dots (5)$$

This equation has been utilised to get an idea about the number of free electrons in a cubic centimeter of a metal, which is found to be of the order of  $10^{22}$  for good conductors.

Kapitza<sup>2,3</sup> using a field of several hundred kilogauss has shown theoretically as well as practically that  $\frac{\delta\rho}{\rho}$  is a linear function of  $H$ , when is very much larger than  $H_k$ , the field due to the atoms inside the metal. His expression for the resistance change is

$$\frac{\Delta R}{R_i} = \beta_0 H^2 / 3H_k \text{ for } H \ll H_k$$

$$\text{and } \frac{\Delta R}{R_i} = \beta_0 (H + H_k^2 / 3H - H_k) \text{ for } H \gg H_k$$

where  $\beta_0$  is a constant for individual metals.

Almost all metals show that the above equation is accurately followed, except Germanium and Tellurium, which show a saturation value for  $\Delta R/R_i$  for higher values of  $H$ .

<sup>2,3</sup> Kapitza, Proc. Roy. Soc., A, 123, p. 346 (1929).

This shows that even Kapitza's theory cannot explain the phenomena fully. Recently Frank<sup>2,9</sup> has pointed out that the Sommerfeld's<sup>3,0</sup> equation for the change of resistance in a magnetic field is capable of explaining the experiments of Kapitza. According to Sommerfeld

$$\frac{\delta\rho}{\rho} = \frac{BH^2}{1 + CH^2}$$

which shows that at smaller fields the  $H^2$  law holds good, but at higher fields  $\delta\rho/\rho$  should reach a saturation value  $B/C$ .

Frank has also derived that

$$C = \left( \frac{e l \lambda}{h} \right)^2 \sigma^2 R^2 = S^2,$$

where  $l$  is the free path for the electron,  $\lambda$  is the de Broglie wavelength,  $h$  is the Planck constant,  $R$  is the Hall coefficient and  $S$  the Leduc-Rigghi coefficient.

Frank points out that Kapitza was using the fields corresponding to the transition period between the  $H^2$  law and the saturation value.

<sup>2,9</sup> N. H. Frank, *Naturwissen.* 34, 751 (1930).

<sup>3,0</sup> Sommerfeld, *Z. fur. Phys.*, 47, 1 (1927).

## APPENDIX I

As already pointed out Lorentz applied Maxwell's theory of equipartition of energy to the free electrons, but he neglected collision of electrons with electrons. His treatment is given in detail in his book on the Theory of Electrons, page 272. We give here a different and much simpler proof.

Consider a cylindrical bar, the electric force or the heat gradient acting along the axis of the cylinder, *i.e.*, along  $x$ -axis. The number of electrons in a unit volume, having velocity components  $\xi, \eta, \zeta$ , is given by the integral

$$\int f(\xi, \eta, \zeta) d\omega \quad \dots \quad (1)$$

extended over the whole space.

where,  $d\omega$  is the element of volumes  $= 4\pi v^2 dv$ ,  $v$  being the velocity  $= (\xi^2 + \eta^2 + \zeta^2)^{\frac{1}{2}}$ .

The stream of electrons passing through a unit plane perpendicular to the  $x$ -axis in unit time is evidently given by

$$\int \xi f(\xi, \eta, \zeta) d\omega \quad \dots \quad (2)$$

The electric current along the  $x$ -axis is then

$$J = e \int \xi f d\omega \quad \dots \quad (3)$$

and the heat current which is transport of energy by

$$W = \frac{1}{2} m \int \xi v^2 f d\omega \quad \dots \quad (4)$$

According to Maxwell

$$f_0(\xi, \eta, \zeta) = A e^{-h v^2}$$

denotes the distribution function, when there is no force acting. Here

$$A = N \sqrt{\frac{h^3}{\pi^3}} \quad \text{and} \quad h = \frac{m}{2kT} \quad \dots \quad (5)$$

In the presence of a force acting on the electrons, the above function is altered, which we may denote by  $f$ , while the undisturbed function is denoted by  $f_0$ . Then

$$f = f_0 + \frac{\partial f_0}{\partial \xi} d\xi + \frac{\partial f_0}{\partial x} dx = f_0 - \phi(-x, y, z) \quad \dots \quad (7)$$

The effect of the uniform force would be to impose a mass movement on the particles given by

$$d\xi = -\frac{\chi l}{v} \quad \dots \quad \dots \quad (8)$$

where  $\chi$  is the acceleration due to the force and  $l$  is the mean free path. The displacement of each particle is

$$dx = -\xi \frac{l}{v} \quad \dots \quad \dots \quad (9)$$

Thus we get from (7), (8) and (9),

$$f - f_0 = -\frac{l}{v} \left[ \chi \frac{\partial f_0}{\partial \xi} + \xi \frac{\partial f_0}{\partial x} \right] \quad \dots \quad (10)$$

$$\text{But } \frac{\partial f_0}{\partial \xi} = \frac{\xi}{v}, \quad \frac{\partial f}{\partial v} = -\xi \frac{2h}{\Lambda} e^{-hv^2} \text{ from (5)} \quad (10')$$

and

$$\frac{\partial f_0}{\partial x} = \left[ \frac{\partial A}{\partial x} - \Lambda v^2 \frac{\partial h}{\partial x} \right] e^{-hv^2}$$

Hence,

$$\begin{aligned} f - f_0 &= -\phi(\xi, \eta, \zeta) \\ &= +\frac{\xi l}{v} \left[ 2h \Lambda \chi - \frac{d\Lambda}{dx} + v^2 \Lambda \frac{dh}{dx} \right] e^{-hv^2} \quad \dots \quad (11) \end{aligned}$$

It is quite apparent that the value of  $f$  that we have to use in (3) and (4) is  $\phi(\xi, \eta, \zeta)$  given by (11)

$$J = -el \int \xi^2 \left[ 2h \Lambda \chi - \frac{d\Lambda}{dx} + v^2 \Lambda \frac{dh}{dx} \right] e^{-hv^2} dv$$

$$\text{and } W = -\frac{1}{2} ml \int \xi^2 v \left[ 2h \Lambda \chi - \frac{d\Lambda}{dx} + v^2 \Lambda \frac{dh}{dx} \right] e^{-hv^2} dv$$

Putting  $d\omega = 4\pi v^2 dv$  and  $\xi^2 = \eta^2 = \zeta^2 = \frac{1}{3} v^2$ , we have

$$\left. \begin{aligned} J &= -\frac{4\pi}{3} el \int_0^\infty v^3 \left[ 2h \Lambda \chi - \frac{d\Lambda}{dx} + v^2 \Lambda \frac{dh}{dx} \right] e^{-hv^2} dv \\ \text{and } W &= -\frac{2\pi}{3} ml \int_0^\infty v^4 \left[ 2h \Lambda \chi - \frac{d\Lambda}{dx} + v^2 \Lambda \frac{dh}{dx} \right] e^{-hv^2} dv \end{aligned} \right\} (12)$$



Putting  $v^2 = s$ ,  $2v^2 dv = ds$ , we have,

$$\int_0^\infty v^3 e^{-hv^2} dv = \frac{1}{2} \int_0^\infty s e^{-hs} ds = \frac{1}{2} \cdot \frac{1}{h^2}$$

$$\int_0^\infty v^5 e^{-hv^2} dv = \frac{1}{2} \int_0^\infty s^2 e^{-hs} ds = \frac{1}{2} \cdot \frac{2}{h^3}$$

and 
$$\int_0^\infty v^7 e^{-hv^2} dv = \frac{1}{2} \int_0^\infty s^3 e^{-hs} ds = \frac{1}{2} \cdot \frac{6}{h^4}$$

Thus

$$J = \frac{2}{3} \pi e l \left[ \frac{1}{h^2} \left( 2hAX - \frac{dA}{dx} \right) + \frac{2A}{h^3} \left( \frac{dh}{dx} \right) \right] \quad \dots (13)$$

and

$$W = \frac{2}{3} \pi m l \left[ \frac{1}{h^3} \left( 2hAX - \frac{dA}{dx} \right) + \frac{3A}{h^4} \left( \frac{dh}{dx} \right) \right] \quad \dots (14)$$

For electrical conduction the bar is at a constant temperature and an electromotive force  $F$  is applied along the  $x$ -axis.

Then

$$\frac{dh}{dx} = 0, \quad \frac{dA}{dx} = 0, \text{ and } X = \frac{eF}{m}$$

From (13), we get

$$J = \frac{4\pi l A e^2}{3hm} F$$

and hence

$$\sigma = \frac{4\pi l A e^2}{3hm} \quad \dots \quad \dots \quad \dots (15)$$

Putting the values of  $A$  and  $h$  from (6) and

$m = 3kT/u^2$ ,  $u^2 = \bar{v}^2$ , we get,

$$\sigma = \sqrt{\frac{2}{3\pi}} \cdot \frac{2}{3} \frac{e^2 l N u}{kT} \quad \dots \quad \dots (16)$$

For thermal conduction, we have to assume that a constant difference of temperature is maintained at the two ends of the bar, which are insulated.

Since there is no mass movement of the electrons in the thermal conduction problem, but only energy is transported because particles on one side have more energy than particles on the other side, we have,  $J=0$  and

$$2 h A X - \frac{dA}{dx} = - 2 \frac{A}{h} \frac{dh}{dx}$$

Thus

$$W = \frac{2}{3} \pi m l \frac{A}{h^2} \frac{dh}{dx}$$

$$\text{Now } h = m/2kT, \text{ hence } \frac{dh}{dx} = - \frac{h}{T} \frac{dT}{dx} = - \frac{2h^2 k}{m} \frac{dT}{dx}$$

and

$$W = \frac{4}{3} \frac{\pi A l k}{h^2} \frac{dT}{dx}$$

The coefficient of thermal conductivity

$$\begin{aligned} \kappa &= \frac{4 \pi A l k}{3 h^2} \\ &= \frac{4}{3} \sqrt{\frac{2}{3 \pi}} k l N u \quad \dots \quad \dots \quad (17) \end{aligned}$$

From the equations (16) and (17), we get,

$$\frac{\kappa}{\sigma} = 2 \left( \frac{k}{e} \right)^2 T \dots \dots \dots (18)$$

## APPENDIX II

## EXPRESSION FOR PELTIER EFFECT FROM LORENTZ THEORY

From equations (13), (14), (15), and (17) of Appendix I, we get

$$J = \frac{\sigma_0}{e} \left\{ mX - \frac{m}{2h} \frac{d \log A}{dx} + \frac{m}{h^2} \frac{dh}{dx} \right\}$$

$$= \frac{\sigma_0}{e} \left\{ mX - kT \frac{d \log A}{dx} - 2k \frac{dT}{dx} \right\} \quad \dots \quad (13)$$

and

$$W = \frac{1}{2} \pi e l \frac{m}{ch} \left\{ \frac{1}{h^2} \left( 2hAX - \frac{dA}{dx} \right) + \frac{2A}{h^2} \frac{dh}{dx} + \frac{A}{h^2} \frac{dh}{dx} \right\}$$

$$= \frac{mJ}{eh} + \frac{1}{2} \pi \frac{\lambda}{h^2} A \frac{dh}{dx} \frac{m}{h^2} \quad \dots \quad (14)$$

Thus

$$W = \frac{2kT}{e} J - \kappa \frac{dT}{dx} \quad \dots \quad (19)$$

If  $F$  is the electric intensity,

$$F = \frac{mX}{e}$$

The thermoelectric force  $E$  round any circuit is the value of  $\int F dx$  which is required to reduce the current  $J$  to zero, when there is no additional e. m. f. in the circuit. Then from (5) we get,

$$E = \int X_0 dx, \text{ when } J = 0.$$

$$= \frac{k}{e} \int \left\{ T \frac{d \log A}{dx} + 2 \frac{dT}{dx} \right\} dx$$

$$= \frac{k}{e} \left\{ \left| T \log A \right| - \int (\log A - 2) dt \right\} \quad \dots \quad (20)$$

When the integral is taken round a closed circuit of two metals with varying temperatures,  $T \log A$  vanishes in

the above expression. Since the integrand is not necessarily a perfect differential, the integrated part will not be zero, hence

$$E_{12} = \frac{k}{e} \int_{T_0}^{T_1} \left( \log \frac{A_2}{A_1} \right) dT \quad \dots \quad \dots (21)$$

The thermoelectric power is

$$P = T \frac{dE_{12}}{dT} = \frac{kT}{e} \log \frac{A_2}{A_1} \quad \dots \quad \dots (22)$$

Since  $A_1$  and  $A_2$  both vary as the number of free electrons inside the two metals, we have,

$$P = \frac{kT}{e} \log \frac{n_2}{n_1} \quad \dots \quad \dots (23)$$

## APPENDIX III

## EXPRESSION FOR THOMSON EFFECT FROM LORENTZ'S THEORY

The heat developed per unit area and thickness  $dx$  in the direction of the current = the total work done by the electric force inside the volume + the total energy retained due to the flow of electrons.

This is given by

$$\begin{aligned} & \left[ X_0 J - \frac{\partial W}{\partial x} \right] dx \\ &= \left[ J \left\{ \frac{J}{\sigma_0} + \frac{kT}{e} \frac{d \log A}{dx} + \frac{2k}{e} \frac{dT}{dx} \right\} \right. \\ & \quad \left. - \frac{2kJ}{e} \frac{dT}{dx} + \frac{\partial}{\partial x} \left( \kappa \frac{\partial T}{\partial x} \right) \right] dx \end{aligned}$$

From (13') and (19), we get

$$\begin{aligned} & \left[ X_0 J - \frac{\partial W}{\partial x} \right] dx \\ &= \left[ \frac{J^2}{\sigma_0} + \frac{JkT}{e} \frac{d \log A}{dx} + \frac{\partial}{\partial x} \left( \kappa \frac{\partial T}{\partial x} \right) \right] dx \quad (24) \end{aligned}$$

In the above equation  $J^2/\sigma$  is the Joulean heating effect, the last term is independent of  $J$  and the second term changes sign with the current and is hence the Thomson coefficient, i.e.,

$$\sigma = \frac{kT}{e} \frac{\partial}{\partial T} (\log A) = \frac{kT}{e} \frac{\partial}{\partial T} \log N \quad \dots \quad (25)$$

## APPENDIX IV

### SOMMERFELD'S THEORY OF CONDUCTION

In 1927, Sommerfeld applied Fermi-Dirac Statistics to the problem of conduction of electricity and other allied phenomena. His results are striking in some respects, but are unable to explain supraconductivity and contains many debatable points. We shall now give below the theory as given by Sommerfeld<sup>1</sup>

According to the Fermi-Dirac Statistics the distribution function is given by

$$f_0 = \frac{1}{\frac{1}{A} e^u + 1} \quad \dots \quad \therefore (1)$$

where  $u = \epsilon/kT$

The number of particles having energy lying between  $\epsilon$  and  $\epsilon + d\epsilon$  in a volume  $V$  is

$$N = \frac{\phi}{h^3} = \frac{2\pi V}{h^3} G (2m)^{\frac{3}{2}} \int \frac{\epsilon^{\frac{1}{2}} d\epsilon}{\frac{1}{A} e^{\epsilon/kT} + 1}$$

where  $\phi$  = total phase space described by the particles, (see Planck, *Wärmes, Trablung*, Fifth Edition)

$$\text{or } N = \frac{2\pi VG}{h^3} (2mkT)^{\frac{3}{2}} \int \frac{u^{\frac{1}{2}} du}{\frac{1}{A} e^u + 1}$$

where  $G$ , the electron moment is equal to 2 according to Pauli.<sup>2</sup>

The energy of these  $N$  particles is given by

$$E = \frac{2\pi VG}{h^3} (2mkT)^{\frac{3}{2}} kT \int \frac{u^{\frac{3}{2}} du}{\frac{1}{A} e^u + 1} \quad \dots \quad \dots (3)$$

<sup>1</sup> Sommerfeld, *Zs. f. Phys.*, 47, 1, 192.

<sup>2</sup> Pauli, *Zs. f. Phys.*, 41, 81 (1927).

$$\text{Let } U_p = \frac{1}{\Gamma(p+1)} \int \frac{u^p du}{\frac{1}{A} e^u + 1} \dots \dots \dots (4)$$

Sommerfeld and Fermi show that for  $A \ll 1$

$$U_p = A \left( 1 - \frac{A}{2^{p+1}} + \frac{A^2}{3^{p+1}} \right) \dots \dots \dots (5)$$

From (2) and (4), we get

$$\frac{N}{GV} = \frac{n}{G} = \frac{2\pi}{h^3} (2mkT)^{\frac{3}{2}} U_{\frac{3}{2}} = \frac{1}{2} \sqrt{\pi} \dots \dots \dots (6)$$

From (5),  $U_{\frac{3}{2}} = A$  approximately, from which

$$A = \frac{nh^3}{G} (2\pi mkT)^{-\frac{3}{2}} \dots \dots \dots (7)$$

Thus when  $A \ll 1$ , we get from (2), and (6) the Maxwellian function

$$f = \frac{dN}{n} = \left( \frac{m}{2\pi kT} \right)^{\frac{3}{2}} e^{-\frac{mv^2}{2kT}} v^2 dv \dots \dots \dots (8)$$

where  $\epsilon = \frac{1}{2} mv^2$ .

When

$$A = \frac{nh^3}{G} (2\pi mkT)^{-\frac{3}{2}} \gg 1, \text{ we have}$$

$$U_{\frac{3}{2}} = \frac{4}{3\sqrt{\pi}} (\log A)^{\frac{3}{2}} \left[ 1 + \frac{\pi^2}{8} \frac{1}{(\log A)^2} + \dots \right] \dots \dots \dots (9)$$

$$U_{\frac{5}{2}} = \frac{8}{15\sqrt{\pi}} (\log A)^{\frac{5}{2}} \left[ 1 + \frac{5\pi^2}{8} \frac{1}{(\log A)^2} + \dots \right] \dots \dots \dots (10)$$

Now from (6) we get

$$\frac{Nh^3}{VG} = \frac{nh^3}{G} = \frac{4\pi}{3} (2mkT \log A)^{\frac{3}{2}} \left[ 1 + \frac{\pi^2}{8} \frac{1}{(\log A)^2} + \dots \right] \dots \dots \dots (11)$$

From which we obtain

$$2mkT \log A = h^2 \left( \frac{3n}{4\pi G} \right)^{\frac{2}{3}} \dots \dots \dots (12)$$

—First Approximation,

and

$$2mkT \log A = h^2 \left( \frac{3n}{4\pi G} \right)^{\frac{2}{3}} \left[ 1 - \frac{(2\pi mkT)^2}{12h^4} \left( \frac{3n}{4\pi G} \right)^{-\frac{4}{3}} \right] \dots \dots \dots (13)$$

—Second Approximation.

For  $A \ll 1$ , i.e., in the case of non-degeneracy we have from equations 3, 4, 5 and 7,

$$\begin{aligned} E &= 2\pi V k T G \frac{(2\pi m k T)^{\frac{3}{2}}}{h^3} \cdot \frac{3\sqrt{\pi}}{4} \cdot A \\ \dots &\approx \frac{3}{2} n V k T \\ &\approx \frac{3}{2} N k T \\ \text{and } p &= \frac{2}{3} E = N k T = R T \end{aligned} \quad \left. \dots \dots \dots \right\} \dots \dots \dots (14)$$

Thus we get the classical values of both  $E$  and  $p$ .

For  $A \gg 1$ , we have from the equations 3, 4, 10 and 12,

$$E = \frac{2\pi}{5} \cdot \frac{G V h^2}{m} \left( \frac{3n}{4\pi G} \right)^{\frac{5}{3}} \left[ 1 + \frac{5}{12} \frac{(2\pi m k T)^2}{h^2} \left( \frac{3n}{4\pi G} \right)^{-\frac{4}{3}} \right] \quad (15)$$

Thus even at the absolute zero there is a null point energy given by

$$E_0 = \frac{2\pi}{5} \frac{G V h^2}{m} \left( \frac{3n}{4\pi G} \right)^{\frac{5}{3}} \quad \dots \dots (16)$$

$$\text{and } E = E_0 + \frac{1}{2} \gamma V T^2 \quad \dots \dots (17)$$

$$\text{where } \gamma = \frac{\pi}{3} \frac{m G}{h^2} (2\pi k)^2 \left( \frac{3n}{4\pi G} \right)^{\frac{1}{3}} \quad \dots \dots (18)$$

$$p = \frac{2}{3} E = p_0 + \frac{1}{2} \delta T^2 \quad \dots \dots (19)$$

where the null point pressure

$$p_0 = \frac{4}{15} \pi \frac{h^3 G}{m} \left( \frac{3n}{4\pi G} \right)^{\frac{5}{3}} = 2 \times 10^5 \text{ Atmos.} \quad \dots (20)$$

$$\text{and } \delta = \frac{2}{9} \pi \frac{m G}{h^2} (2\pi k)^2 \left( \frac{3n}{4\pi G} \right)^{\frac{1}{3}} \quad \dots \dots (21)$$

On the assumption that there is one free electron for each atom, we get the number of free electrons in a cubic centimeter of silver

$$n_{Ag} = \frac{10^5}{107.9} \times 6.06 \times 10^{23} = 5.9 \times 10^{22}$$



and from (6),  $\frac{E_0}{V} = 3 \times 10^{11}$  erg/cm<sup>3</sup>. Then for  $T = 300^\circ \text{K}$ .

$$\Lambda = \frac{nh^2}{G} (2\pi mkT)^{-\frac{3}{2}} = \frac{5.9 \times 10^{22} \times (6.55)^3 \times 10^{-61}}{2.(2\pi \times 9.02 \times 1.37 \times 300 \times 10^{-21})^{\frac{3}{2}}} \\ = 2.3 \times 10^3 \gg 1 \quad \dots \quad \dots \quad \dots \quad (22)$$

i.e., the electron gas inside the silver is a degenerate gas.

It may be noticed that  $\Lambda = \frac{n}{G} \lambda^3 \left(\frac{3}{2\pi}\right)^{\frac{3}{2}}$ , where  $\lambda$  = deBroglie wavelength. The specific heat per electron is

$$C_v = \frac{d}{dT} \left( \frac{E}{Vn} \right) = \gamma \frac{T}{n} = \frac{\pi}{3} \frac{mG(2\pi k)^{\frac{3}{2}}}{h^2} \left( \frac{3n}{4\pi G} \right)^{\frac{1}{2}} \frac{T}{n} \\ = \frac{\pi^2 mk^2}{h^2} \left( \frac{4\pi G}{3n} \right)^{\frac{3}{2}} T \quad \dots \quad \dots \quad \dots \quad \dots \quad (23)$$

The electron specific heat  $C_v$  for a mol of metal is given by

$$\frac{C_v}{R} = \frac{\pi^2 mk}{h^2} \left( \frac{4\pi G}{3n} \right)^{\frac{3}{2}} T = 2.4 \times 10^{-2} \quad \dots \quad \dots \quad \dots \quad (24)$$

when  $T = 300^\circ \text{K}$  and  $n = n_{\text{Ag}} = 5.9 \times 10^{22}$ .

Thus we see that at ordinary temperatures the electrons do not contribute much towards the specific heat of the metal. This meets the specific heat difficulty in the theory of conduction by electrons.

When the distribution function is equal to  $\frac{1}{2}$ , let the velocity be  $v$ . Then

$$f = \frac{1}{\frac{1}{A} e^{\frac{mv^2}{2kT}} + 1} = \frac{1}{2}$$

$$\text{i.e., } \frac{e}{kT} = \log A = \frac{1}{2} \frac{mv^2}{kT}$$

$$\text{or } v = \frac{1}{m} \sqrt{2mkT \log A}$$

From equation (12), we get,  $2mkT \log A$ , and then,

$$\bar{v} = \frac{h}{m} \left( \frac{3n}{4\pi G} \right)^{\frac{1}{3}} \quad \dots \quad \dots \quad \dots \quad \dots \quad (25)$$

$$\text{and } \lambda = \frac{h}{m\bar{v}} = \left( \frac{4\pi G}{3n} \right)^{\frac{1}{3}}$$

$$\text{or } \lambda^3 = \frac{4\pi}{3} a^3 G$$

as  $n = \frac{1}{a^3}$  and  $v_m$  = average velocity at absolute zero temperature, thus as  $N = nV$ , we get from (16)

$$\begin{aligned} \frac{E_0}{N} &= \frac{1}{2} m v_m^2 = \frac{2\pi}{5} \frac{G h^2}{m n} \left( \frac{3n}{4\pi G} \right)^{\frac{2}{3}} \\ &= \frac{3}{10} \frac{h^2}{m} \left( \frac{3n}{4\pi G} \right)^{\frac{2}{3}} \\ \text{i.e.,} \\ v_m &= \sqrt{\frac{3}{5}} \frac{h}{m} \left( \frac{3n}{4\pi G} \right)^{\frac{1}{3}} = 0.774 \bar{v} \quad \dots \quad \dots \quad (26) \end{aligned}$$

Thus we see that  $v_m$ , unlike the classical mean velocity, is independent of temperature and is determined by the density of the electrons.

#### APPLICATION OF THE FERMI STATISTICS TO THE PROBLEMS OF CONDUCTION AND ALLIED PHENOMENA

We get from equations (3), (10), (10') of Appendix I and from

$$d\omega = 4\pi G \left( \frac{m}{h} \right)^3 v^2 dv, \dots \dots \dots (27)$$

$$\begin{aligned} J = & - \frac{4\pi}{3} G e \left( \frac{m}{h} \right)^3 \left[ \frac{eF}{m} \int lv^2 \frac{\partial f_0}{\partial x} dv \right. \\ & \left. + \frac{\partial}{\partial x} \int lv^3 f_0 dv \right] \quad \dots \quad \dots \quad (28) \end{aligned}$$

$$\begin{aligned} \text{and } W = & - \frac{2\pi}{3} G m \left( \frac{m}{h} \right)^3 \left[ \frac{eF}{m} \int lv^4 \frac{\partial f_0}{\partial v} dv \right. \\ & \left. + \frac{\partial}{\partial x} \int lv^5 f_0 dv \right] \quad \dots \quad \dots \quad (29) \end{aligned}$$

$$\text{since } X = \frac{eF}{m}$$

The equation 28 and 29, can be written as

$$J = \frac{4\pi}{3} Ge \left(\frac{m}{h}\right)^3 \left[ \frac{eF}{m} \int \frac{\partial}{\partial v} lv^2 \cdot dv - \frac{\partial}{\partial x} \int lv^3 f \cdot dv \right] \dots \dots \dots (28')$$

$$\text{and } W = \frac{2\pi}{3} Gm \left(\frac{m}{h}\right)^3 \left[ \frac{eF}{m} \int \frac{\partial}{\partial v} lv^4 f \cdot dv - \frac{\partial}{\partial x} \int lv^5 f \cdot dv \right] \dots \dots \dots (29')$$

Let us introduce the new variable

$$u = \frac{m}{2kT} \cdot v^2 \text{ in place of } v.$$

Then let us put

$$\left. \begin{aligned} l(v) &= l \left( \sqrt{\frac{2kT}{m}} \cdot u \right) = L(u) \text{ or } L(uT) \\ \text{Then } l \cdot v^2 &= \frac{2kT}{m} u \cdot L(u) = \frac{2kT}{m} L_1(u), \\ &\quad \text{where } L_1(u) = u L(u) \\ l \cdot v^3 &= \left( \frac{2kT}{m} u \right)^{3/2} L(u) = \left( \frac{2kT}{m} \right)^{3/2} u^{1/2} L_1(u) \\ l \cdot v^4 &= \left( \frac{2kT}{m} u \right)^2 L(u) = \left( \frac{2kT}{m} \right)^2 u^2 L(u) \\ &\quad = \left( \frac{2kT}{m} \right)^2 L_2(u) \\ l \cdot v^5 &= \left( \frac{2kT}{m} u \right)^{5/2} L(u) = \left( \frac{2kT}{m} \right)^{5/2} u^{1/2} L_2(u) \end{aligned} \right\} \dots (30)$$

Let us put

$$\left. \begin{aligned} V_0 &= \int_0^\infty \frac{\partial L_1}{\partial u} \cdot f \cdot du, \quad V_1 = \frac{1}{2!} \int_0^\infty \frac{\partial L_2}{\partial u} \cdot f \cdot du \\ \text{and } V_2 &= \frac{1}{3!} \int_0^\infty \frac{\partial L_3}{\partial u} f \cdot du. \end{aligned} \right\} \dots (31)$$

where

$$L_1 = u L(u), \quad L_2 = u^2 L(u), \quad L_3 = u^3 L(u)$$

Then from (30), (31), (28'), and (29')

$$J = \frac{8\pi}{3} \frac{emG}{h^3} \left\{ eFkTV_0 - \frac{\partial}{\partial x} \left[ (kT)^2 \int L_1 f \cdot du \right] \right\} \dots (32)$$

$$\text{and } W = \frac{8\pi}{3} \frac{mG}{h^3} \left\{ 2eF(kT)^2 V_1 - \frac{\partial}{\partial x} \left[ (kT)^3 \int L_1 f_0 du \right] \right\} \dots \quad (33)$$

Performing the differential with respect to  $x$ , we get

$$J = \frac{8\pi emG}{3h^3} kT \left[ eFV_0 - 2k \frac{\partial T}{\partial x} \int L_1 f_0 du - kT \int \frac{\partial L_1}{\partial x} f_0 du - kT \int L_1 \frac{\partial f_0}{\partial x} du \right] \dots \quad (34)$$

$$\text{and } W = \frac{8\pi}{3} \frac{mG}{h^3} (kT)^2 \left[ 2eFV_1 - 3k \frac{\partial T}{\partial x} \int L_2 f_0 du - kT \int \frac{\partial L_2}{\partial x} f_0 du - kT \int L_2 \frac{\partial f_0}{\partial x} du \right] \dots \quad (35)$$

Now for  $a=1$  or  $2$  from (31), we get

$$\begin{aligned} \frac{\partial L_a}{\partial x} u^a \frac{dL(u, T)}{dT} &= u^a \frac{dL(u, T)}{dT} \frac{\partial T}{\partial x} \\ &= u^a \frac{U}{T} \frac{dL}{du} - \frac{\partial T}{\partial x} \dots \dots \quad (36) \end{aligned}$$

The second and third terms inside the brackets in the equations (34) and (35) along with the equation (31) gives us,

$$\begin{aligned} -k \frac{\partial T}{\partial x} \int \left( 2Lu + u^2 \frac{dL}{du} \right) f_0 du \\ = -k \frac{\partial T}{\partial x} \int \frac{d}{du} (u^2 L) f_0 du = -2k \frac{\partial T}{\partial x} V_1 \dots \quad (37) \end{aligned}$$

$$\begin{aligned} \text{and } -k \frac{\partial T}{\partial x} \int \left( 3Lu^2 + u^3 \frac{dL}{du} \right) f_0 du \\ = -k \frac{\partial T}{\partial x} \int \frac{d}{du} (u^3 L) f_0 du = -6k \frac{\partial T}{\partial x} V_2 \dots \quad (38) \end{aligned}$$

Now

$$\begin{aligned} \frac{\partial f_0}{\partial x} &= \frac{\partial f_0}{\partial A} \cdot \frac{\partial A}{\partial x} = \frac{1}{A^2} \cdot \frac{e^u}{\left( \frac{1}{A} e^u + 1 \right)^2} \cdot \frac{dA}{dx} \\ &= -\frac{\partial f_0}{\partial u} \cdot \frac{d \log A}{dx} \dots \dots \dots \quad (39) \end{aligned}$$

Then,

$$\begin{aligned}
 -kT \int L_1 \frac{\partial f_0}{\partial x} du &= -kT \frac{\partial \log A}{\partial x} \int L_1 \frac{\partial f_0}{\partial u} du \\
 &= -kT \frac{\partial \log A}{\partial x} \int \frac{dL_1}{du} f_0 du \\
 &= -kT \frac{\partial \log A}{\partial x} V_0 \quad \dots \quad \dots \quad (40)
 \end{aligned}$$

and also

$$-kT \int L_2 \frac{\partial f_0}{\partial u} du = -kT \frac{\partial \log A}{\partial x} V_1 \quad \dots \quad \dots \quad (41)$$

Then from (34), (35), (37), (38), (40), and (41), we get

$$J = \frac{8\pi e m G}{3h^3} kT V_0 \left\{ eF - 2k \frac{\partial T}{\partial x} \cdot \frac{V_1}{V_0} - kT \frac{\partial \log A}{\partial x} \right\} \quad (42)$$

$$\text{and } W = \frac{16}{3} \frac{mG}{h^3} V_1 (kT)^2 \left\{ eF - 3k \frac{\partial T}{\partial x} \cdot \frac{V_2}{V_1} - kT \frac{\partial \log A}{\partial x} \right\} \quad \dots \quad (43)$$

Thus from (42) when  $\frac{\partial T}{\partial x} = 0$  and  $\frac{\partial}{\partial x} \log A = 0$ , we have

$$\frac{J}{F} = \sigma = \frac{8\pi}{3} \frac{e^2 m G}{h^3} kT V_0 \quad \dots \quad \dots \quad (44)$$

which gives us

$$\sigma = \frac{4}{3} \frac{e^2 l n}{\sqrt{2\pi m k T}} \text{ for } A \ll 1 \quad \dots \quad \dots \quad (45)$$

and

$$\sigma = \frac{8\pi}{3} \frac{e^2 l(\tau)}{h} \left( \frac{3n}{8\pi} \right)^{2/3} \text{ for } A \gg 1 \quad \dots \quad \dots \quad (46)$$

For the thermal conductivity we get

$$\kappa = \frac{8}{3} \frac{l n k^2 T}{\sqrt{2\pi m k T}} \text{ for } A \ll 1 \quad \dots \quad \dots \quad (47)$$

and when  $A \gg 1$ , we get

$\kappa = 0$  as a first approximation,

$$\text{and } \kappa = \frac{8\pi}{9} \frac{l(\tau) k^2 T}{h} \left( \frac{3n}{4\pi} \right)^{2/3} \quad \dots \quad \dots \quad (48)$$

as a second approximation.

Thus from (45) and (47) we get the classical value of

$$\frac{\kappa}{\sigma} = 2 \left( \frac{k}{e} \right)^2 T \quad \dots \quad \dots \quad \dots \quad (49)$$

and from (46) and (48) we get

$$\frac{\kappa}{\sigma} = 3.3 \left( \frac{h}{e} \right)^2 T \quad \dots \quad \dots \quad \dots \quad (50)$$

Now we know that for silver

$$\sigma = \frac{1}{1600} \text{ C. G. S. units,}$$

$$\text{and } n = 5.9 \times 10^{22}$$

At  $T = 300^\circ \text{ K}$ , we get

$$l_{\text{class}} = 4.7 \times 10^{-7} \text{ cm. from (45),}$$

$$l = 5.2 \times 10^{-6} \text{ cm. from (46).}$$

i.e., the free path is about hundred times the atomic dimensions.

From (46) it is also clear that  $\sigma$  is independent of  $T$ , which is contrary to the known experimental facts. This is one of the weak points of the new theory.

Using the new statistics Sommerfeld has also deduced the Richardson's equation as follows.

The current is given by

$$J = e \int \xi f d\omega$$

$$\text{where } f = \frac{1}{\frac{1}{A} e^{\frac{\epsilon}{kT}} + 1}$$

$$\text{and } d\omega = \left( \frac{m}{h} \right)^3 G. d\xi d\eta d\zeta$$

Thus

$$J = e \left( \frac{m}{h} \right)^3 G \int_{\xi_0}^{\infty} \int_{-\infty}^{\infty} \int_{-\infty}^{\infty} \frac{e^{-\xi}}{\frac{1}{A} e^{\frac{\epsilon}{kT}} + 1} d\xi d\eta d\zeta \quad \dots \quad (51)$$

But using polar coordinates, we can put  $\eta^2 + \zeta^2 = \rho^2$  and thus  $d\eta d\zeta = 2\pi \rho d\rho$ .

Then (1) becomes

$$J = 2\pi G e \left( \frac{m}{h} \right)^3 \int_0^{\infty} \rho J_{\rho} d\rho, \quad \dots \quad \dots \quad (52)$$

where,

$$J_p = \int_{\xi_0}^{\infty} \frac{\xi d\xi}{\frac{1}{A} e^{\epsilon/kT} + 1} \quad \dots \quad \dots \quad (53)$$

$$\text{Put } \gamma = \frac{m}{2kT}, \quad B = A e^{-p^2 \gamma}$$

$$\text{Then } J_p = \int_{\xi_0}^{\infty} \frac{\xi d\xi}{\frac{1}{B} e^{r\xi^2} + 1}$$

By putting  $\gamma \xi^2 = u$ , we have,  $2\xi \gamma d\xi = du$ , and

$$J_p = \frac{1}{2\gamma} \int_{u_0}^{\infty} \frac{du}{\frac{1}{B} e^u + 1}$$

again put  $x = e^u$ ,  $dx = e^u du$

and  $x_0 = e^{u_0}$

$$\begin{aligned} J_p &= \frac{1}{2\gamma} \int_{x_0}^{\infty} \frac{dx}{x} \cdot \frac{B}{x+B} \\ &= \frac{1}{2\gamma} \int_{x_0}^{\infty} \left( \frac{1}{x} - \frac{1}{x+B} \right) dx \\ &= \frac{1}{2\gamma} \log \left( 1 + \frac{B}{x_0} \right) \\ &= \frac{1}{2\gamma} \log \left( 1 + A e^{-\gamma p^2} e^{-\gamma \xi_0^2} \right) \\ &= \frac{1}{2\gamma} \log \left( 1 + C e^{-\gamma p^2} \right) \dots \dots \dots (54) \end{aligned}$$

$$\text{where } C = A e^{-\gamma \xi_0^2} = A e^{-\frac{m \xi_0^2}{2kT}}$$

$$= A e^{-W a / kT}$$

Thus from (52) and (54) we obtain,

$$J = 2\pi e \left(\frac{m}{h}\right)^3 \frac{G}{2\gamma} \int_0^\infty \rho \, d\rho \log \left(1 + C e^{-\gamma \rho^2}\right)$$

which gives on partial integration

$$J = \pi e \left(\frac{m}{h}\right)^3 G \int_0^\infty \frac{C e^{-\gamma \rho^2} \rho^3 d\rho}{1 + C e^{-\gamma \rho^2}} = \pi e \left(\frac{m}{h}\right)^3 G \int_0^\infty \frac{\rho^3 d\rho}{\frac{1}{C} e^{\gamma \rho^2} + 1} \quad (55)$$

The integral in the last equation is of the form given in (4) of page 404.

Thus we get

$$J = \frac{2\pi emG}{h^3} (kT)^2 U_1 \left( A e^{-W_a/kT} \right)$$

where  $\gamma \rho^2$  is the integration variable in  $U_1$ .

Whence we get

$$J = \frac{2\pi emG}{h^3} (kT)^2 A e^{-W_a/kT} \quad \dots \quad (56)$$

Case (1) when  $A \ll 1$

$$A = nh^3 (2\pi m kT)^{-3/2}$$

and  $J = \sqrt{\frac{en}{2\pi m}} \left( kT \right)^{1/2} e^{-W_a/kT} \quad \dots \quad (57)$

Case (2) when  $A \gg 1$ ,

$$\log A = \frac{h^2}{\lambda^2} - \frac{1}{2mkT}$$

$$\text{i.e., } A = e^{W_i/kT}$$

where  $W_i$  is called the inner work function and is given by

$$W_i = \frac{h^2}{2m\lambda^2} = \frac{h^2}{2m} \left( \frac{3n}{4\pi G} \right)^{2/3}$$

Thus

$$J = \frac{2\pi em}{h^3} (kT)^2 e^{-(W_a - W_i)/kT} \quad \dots$$



# PELTIER AND THOMSON EFFECTS.

We have proved that [cf. equations (42) and (43)]

$$J = \frac{8\pi}{3} \frac{em}{h^2} kT V_0 \left[ eF - 2k \frac{\partial T}{\partial x} \frac{V_1}{V_0} - kT \frac{\partial \log A}{\partial x} \right] \quad (42)$$

$$\text{and } W = \frac{16\pi}{3} \frac{m}{h^2} (kT)^2 V_1 \left[ eF - 3k \frac{\partial T}{\partial x} \frac{V_2}{V_1} - kT \frac{\partial \log A}{\partial x} \right] \quad (43)$$

From (42) and the value of  $\sigma$  (equation 44), we get,

$$F = \frac{J}{\sigma} + \frac{2k}{\partial x} \frac{V_1}{V_0} + \frac{kT}{e} \frac{\partial \log A}{\partial x} \quad \dots \quad (59)$$

Putting (43) in (59), we obtain

$$W = \frac{16\pi}{3} \frac{mG}{h^2} (kT)^2 V_1 \left[ \frac{eJ}{\sigma} + k \frac{\partial T}{\partial x} \left( 2 \frac{V_1}{V_0} - 3 \frac{V_2}{V_1} \right) \right]$$

Again from the values of  $\kappa$  and  $\sigma$ , we get

$$W = \frac{2kT}{e} \cdot \frac{V_1}{V_0} J - \kappa \frac{\partial T}{\partial x} \quad \dots \quad (60)$$

But,

$$Q = JF - \frac{\partial W}{\partial x}$$

Whence from (59) and (60),

$$Q = \frac{J^2}{\sigma} + J \left[ \frac{kT}{e} \frac{\partial \log A}{\partial x} - \frac{2kT}{e} \frac{\partial}{\partial x} \frac{V_1}{V_0} \right] + \frac{\partial}{\partial x} \left( \kappa \frac{\partial T}{\partial x} \right) \quad \dots \quad (61)$$

*Thomson Effect.*—The first term on the right-hand side of equation (51) is the Joulean heat, the last term is for the conduction of heat, and the middle term is of the form

$$-\mu J \frac{\partial T}{\partial x},$$

$\mu$ , being the Thomson coefficient or the Specific Heat of Electricity.

From (61) we get,

$$\mu = \frac{2kT}{e} \frac{d}{dT} \cdot \frac{V_1}{V_0} - \frac{kT}{e} \frac{d \log A}{dT} \quad \dots \quad (62)$$

Case I.—When  $A < 1$ ,  $\frac{V_1}{V_0} = 1$ ,

and thus the first term in (62) disappears, then

$$\frac{d \log A}{dT} = -\frac{2}{3} \frac{1}{T} + \frac{d \log n}{dT},$$

and

$$\mu = \frac{2}{3} \frac{k}{e} \left( 1 - \frac{2}{3} T \frac{d \log n}{dT} \right) \quad \dots \quad \dots \quad \dots \quad (63)$$

which is the classical value of the Thomson effect as obtained by Lorentz.

Case II.—When  $A \gg 1$ ,

$$\frac{V_1}{V_0} = \frac{1}{2} u_0 = \frac{1}{2} \log A \quad \text{as a first approximation, and}$$

hence

$$\lambda = 0.$$

Thus, we have to use the second approximation, which gives

$$\frac{V_1}{V_0} = \frac{u_0}{2} \left[ 1 + \frac{\pi^2}{3} \left( \frac{1}{u_0^2} + \frac{1}{u_0} \frac{d \log L}{du_0} \right) \right]$$

$$\therefore \mu = \frac{\pi^2}{3} \frac{kT}{e} \frac{d}{dT} \left( \frac{1}{u_0} + \frac{d \log L}{du_0} \right)$$

But

$$u_0 = \frac{m \bar{v}^2}{2kT} = \frac{h^2}{2mkT\lambda^2}, \quad \text{and } L(u_0) = l(\bar{v}).$$

$$1 + u_0 \frac{d \log L}{du_0} = 1 + \frac{\bar{v}}{2} \frac{d \log l}{d\bar{v}} = 1 - \frac{\lambda}{2} \frac{d \log l}{d\lambda} = \Lambda, \quad \text{say.}$$

Then

$$\mu = \frac{2\pi^2}{3} \frac{mk^2T}{eh^2} \frac{d}{dT} \left[ T\lambda^2 \Lambda \right] \quad \dots \quad \dots \quad \dots \quad (64)$$

Now we know that,

$$\lambda^2 = \left( \frac{4\pi}{3n} \right)^{\frac{2}{3}}, \quad \text{hence } \frac{1}{\lambda^2} \frac{d\lambda^2}{dT} = -\frac{2}{3} \frac{d \log n}{dT} \quad \dots \quad \dots \quad (65)$$

But

$$\begin{aligned} \frac{d}{dT} \left[ T\lambda^2 \Lambda \right] &= \lambda^2 \Lambda + T \Lambda \frac{d(\lambda^2)}{dT} + T\lambda^2 \frac{d\Lambda}{dT} \\ &= \lambda^2 \Lambda \left[ 1 + \frac{T}{\lambda^2} \frac{d(\lambda^2)}{dT} + \frac{T}{\Lambda} \frac{d\Lambda}{dT} \right] \quad \dots \quad \dots \quad (66) \end{aligned}$$

Putting this value in the equation (64) we get,

$$\mu = \frac{2\pi^2}{3} \frac{mk^2T}{eh^2} \lambda^2 \Lambda \left[ 1 - \frac{2}{3} T \frac{d \log n}{dT} + T \frac{d \log \Lambda}{dT} \right] \dots (67)$$

The ratio of the above value of  $\mu$  and the  $\mu_{\text{classical}}$  is given by

$$\frac{\mu}{\mu_{cl}} = \frac{4\pi^2}{9} \frac{mkT}{h^2} \left( \frac{4\pi G}{3n} \right)^{2/3} \dots \dots (68)$$

when  $T = 300^\circ$ ,  $G = 2$ , and  $n_{Ag} = 5.9 \times 10^{22}$ , we get

$$\frac{\mu}{\mu_{cl}} \sim \frac{1}{100}$$

Thus we get a right order for  $\mu$  as found by Borelius and Gunneson<sup>3</sup> in the case of Cu, Ag, and Au.

*The Peltier effect.*—At constant temperature the last term in (61) disappears. The first term is the Joulean heat and the second term changes sign with  $J$ . At the junction of the two metals, we integrate the equation within the limits 1 and 2 and designate the integral by  $\Pi$ , we get the Peltier heat absorbed at the junction per unit current.

$$\Pi = \frac{kT}{e} \int_1^2 \left( 2 \frac{\partial}{\partial x} \frac{V_1}{V_0} - \frac{\partial \log \Lambda}{\partial x} \right) dx \dots \dots (69)$$

Case (1) when  $\Lambda \ll 1$  and  $l$  is constant,

$$\frac{V_1}{V_0} = 1 \text{ and } \Lambda = \frac{nh^3}{G} \left( 2\pi mkT \right)^{-3/2}$$

The first term in (69) disappears and when  $T$  is constant, we get

$$\Pi = \frac{kT}{e} \log \frac{n_1}{n_2} \dots \dots (70)$$

which gives the classical value of  $\Pi$ .

<sup>3</sup> Borelius and Gunneson, Ann. d. Phys., 65, 520 (1921).

Case (2), when  $A \gg 1$ ,

$$(a) \frac{2V_1}{V_0} = \log A \quad \text{First approximation.} \quad \dots (71)$$

Then  $\Pi = 0$

$$(b) \frac{2V_1}{V_0} = \log A + \frac{\pi^2}{3} \frac{\Lambda}{\log A} \quad \text{Second approximation.}$$

Then,

$$\begin{aligned} \Pi &= \frac{2\pi^2}{3} \frac{m(kT)^2}{eh^2} \int_1^2 \frac{\partial}{\partial x} (\lambda^2 \Lambda) dx. \\ &= \frac{2\pi^2}{3} \frac{m(kT)^2}{eh^2} \left[ \lambda_2^2 \Lambda_2 - \lambda_1^2 \Lambda_1 \right] \quad \dots (72) \end{aligned}$$

It we put  $\Lambda_2 = \Lambda_1 = 1$ , we get at  $T = 300^\circ \text{ K}$ ,

$\Pi = 100$  microvolt, a value found for many metals.

The main difference between the classical value of  $\Pi$  and the new value is that in the former case  $\Pi$  varies as  $T$ , while in the latter  $\Pi$  varies as  $T^2$ .

*SECTION IV*

MATHEMATICS

# A THEOREM ON INTEGRAL FUNCTIONS

BY

P. L. SRIVASTAVA, M.A., D. PHIL. (OXON),

*Reader, Allahabad University.*

1. The following is a particular case of a more comprehensive theorem established by Phragmén and Lindelöf in their classical memoir \* in Vol. 31 of the *Acta Mathematica*.

*If*

(1. 1)  $\phi(z)$  be an integral function of  $z$  of order of magnitude  $e^{\epsilon(r)r}$ , where  $|z|=r$ , and  $\epsilon$  is positive and tends to zero as  $r$  tends to infinity;

(1. 2)  $\phi(z) \longrightarrow 0$  as  $|z| \longrightarrow \infty$  along the real axis ;  
then  $\phi(z)$  is identically zero.

Now my main object in this paper is to show that the result of the above theorem remains true, when the condition (1. 2) is replaced by the following :—

(1. 3) 
$$\int_0^{\infty} \phi(\pm t) dt \text{ converges absolutely.}$$

I am not aware if this fact was ever noticed before. In appearance this theorem differs little from the Phragmén-Lindelöf's theorem, but essentially it is altogether distinct from it. The reason is obvious. None of the conditions (1. 2) and (1. 3) implies, by itself, the other, though, of course, each condition combined with (1. 1) leads to the other by virtue of this theorem.

---

\* Sur une extension d'un principe classique de l'analyse, etc., pp. 386-387.

In § 3 I show how our new theorem enables us to prove the Phragmén-Lindelöf's theorem in a manner that leaves hardly anything to be desired in the matter of simplicity. An ingenious and elegant proof of this theorem was given by Wigert\* in 1920, but I venture to say that the proof given here is much simpler and more elementary in character than Wigert's proof.

I am indebted to Prof. G. H. Hardy for expressing his opinion on certain points in the paper.

2. Let us begin by proving our main theorem which may be stated as follows :—

*Theorem I.—If  $\phi(z)$  satisfies the conditions (1.1) and (1.3), it is identically zero.*

The proof is extremely simple and rests on an application of the well-known Laplace-Abel integral.

Let  $\phi(z) = \sum_{n=0}^{\infty} \frac{a_n z^n}{n!}$ . Then, since  $\phi(z)$  satisfies (1.1),

we have, by Cauchy's theorem,

$$(2.1) \quad a_n = O(\delta^n), \text{ for every positive number } \delta.$$

Now supposing, in the first instance, that  $x$  is real, positive and  $< \frac{1}{\delta}$ , we have,

$$(2.2) \quad \begin{aligned} \int_0^{\infty} e^{-\frac{t}{x}} \phi(t) dt &= \int_0^{\infty} e^{-\frac{t}{x}} \sum_0^{\infty} \frac{a_n t^n}{n!} dt, \\ &= \sum_0^{\infty} \frac{a_n}{n!} \int_0^{\infty} e^{-\frac{t}{x}} t^n dt = \sum_0^{\infty} a_n x^{n+1} = f(x), \text{ say,} \end{aligned}$$

the inversion of order of summation and integration being

---

\* Un théorème sur les fonctions entières, *Arkiv för Matematik Astronomi och Fysik*, Bd. 15, No. 12.

easily justified by the fact that  $\int_0^{\infty} e^{-\frac{t}{x}} \sum_0^{\infty} \left| \frac{a_n t^n}{n!} \right| dt$  is convergent.

By virtue of (2.1)  $f(x)$  is an integral function of  $x$ , and vanishes at the origin.

Now, since  $\int_0^{\infty} |\phi(t)| dt$  is convergent, the integral

$$\int_0^{\infty} e^{-\frac{t}{x}} \phi(t) dt$$

is absolutely and uniformly convergent in the region  $|\theta| \leq \frac{\pi}{2}$ ,  $R \geq 1$ , where  $x = R e^{i\theta}$ . So that for all values of  $x$  lying in this region,

$$(2.3) \quad f(x) = \int_0^{\infty} e^{-\frac{t}{x}} \phi(t) dt,$$

since  $f(x)$  is an integral function of  $x$ .

It follows, therefore, that

$$(2.4) \quad |f(x)| \leq \int_0^{\infty} e^{-\frac{t \cos \theta}{R}} |\phi(t)| dt \leq \int_0^{\infty} |\phi(t)| dt = K_1,$$

say, uniformly in the region  $|\theta| \leq \frac{\pi}{2}$ ,  $R \geq 1$ .

Again, the integral function  $f(x)$  is also represented by means of the integral

$$- \int_0^{\infty} e^{-\frac{t}{x}} \phi(-t) dt$$

which is absolutely and uniformly convergent in the region

$|\theta| \geq \frac{\pi}{2}$ ,  $R \geq 1$ , since  $\int_0^{\infty} |\phi(-t)| dt$  is convergent. So that

$$(2.5) \quad |f(x)| \leq K_2,$$

uniformly in the region  $|\theta| \geq \frac{\pi}{2}$ ,  $R \geq 1$ .



Hence  $|f(x)| \leq K$  throughout the whole plane,  $K$  being the greater of the two constants  $K_1$  and  $K_2$ . So that  $f(x)$  reduces to a constant, which must be zero in this case, since  $f(0) = 0$ . This means that all the coefficients of the series  $\sum_0^{\infty} a_n x^{n+1}$  must vanish, so that  $\phi(z)$  is identically zero.

This completes the proof of our theorem.

The result of the theorem ceases to be true when  $\phi(z)$  is an integral function of order  $e^{kr}$ , where  $k$  is some positive number, as is seen by considering the function  $\left(\frac{\sin z}{z}\right)^2$ .

3. The main consequence of the preceding theorem is the following, of which the Phragmén-Lindelöf's theorem stated in §1 is only a particular case.

*Theorem II.*—If  $z = x + iy$ , and

(3.1)  $\phi(z)$  be an integral function of order  $e^{(r)r}$ ;

(3.2)  $\phi(x) = O(|x|^a)$ , as  $x \rightarrow \infty$ ;

(3.3)  $\phi(x) = O(|x|^b)$ , as  $x \rightarrow -\infty$ ;

then  $\phi(z)$  is a polynomial of degree not greater than the smaller of the numbers  $a$  and  $b$ , say  $a$ , if  $a$  is greater than or equal to 1. If  $a < 1$ ,  $\phi(z)$  reduces to a constant.

Let  $\phi_1(z) \equiv \phi(z) + \phi(-z)$ . Then  $\phi_1(z)$  is an even integral function of order  $e^{(r)r}$ , and  $\phi_1(x) = O(|x|^b)$ , as  $x \rightarrow \infty$ .

Now consider the function

$$(3.4) \quad g_1(z) \equiv \frac{\phi_1(z) - \sum_{n=0}^{\mu-1} \frac{\phi_1^{(n)}(0) z^n}{n!}}{z^{\mu+1}},$$

where  $\mu$  is an odd positive integer just greater than  $b$ . It is

evident that  $g_1(z)$  is an even integral function of order  $e^{(r)r}$ , and as  $x \rightarrow \infty$ ,  $g_1(x) = O\left(\frac{1}{|x|^\gamma}\right)$ , where  $\gamma > 1$ . So that  $g_1(z)$  satisfies all the conditions of Theorem I, and hence  $g_1(z) \equiv 0$ .

It follows, therefore, that  $\phi_1(z)$  is a polynomial of degree not greater than  $(\mu - 1)$ .

Next, let  $\phi_2(z) \equiv \phi(z) - \phi(-z)$ . Then  $\phi_2(z)$  is an odd integral function of order  $e^{(r)r}$ , and  $\phi_2(x) = O(|x|^\delta)$ , as  $x \rightarrow \infty$ .

Now consider the function

$$(3.5) \quad g_2(z) \equiv \frac{\phi_2(z) - \sum_{n=0}^{r-1} \frac{\phi_2^{(n)}(0)z^n}{n!}}{z^{r+1}},$$

where  $r$  is an even positive integer just greater than  $\delta$ .  $g_2(z)$  is an even integral function of order  $e^{(r)r}$ , and is of order  $\frac{1}{|x|^\delta}$ , where  $\delta > 1$ , as  $|x| \rightarrow \infty$ .

So that  $g_2(z) \equiv 0$ , by Theorem I. That is  $\phi_2(z)$  is a polynomial of degree not greater than  $(r - 1)$ .

It follows, therefore, that  $\phi(z) \equiv \frac{1}{2}[\phi_1(z) + \phi_2(z)]$  reduces to a polynomial, which, on account of (3.2), must be of a degree not greater than  $\alpha$ .

If  $\alpha < 1$ ,  $\phi(z)$  reduces to a constant. Further, if (i)  $\alpha < 0$ ; or (ii)  $0 \leq \alpha < 1$ , and  $\phi(z)$  has a zero anywhere in the plane; or (iii)  $\phi(x) \rightarrow 0$  as  $x \rightarrow \infty$ ; then  $\phi(z) \equiv 0$ .

4. An immediate consequence of Theorem II is the following:—

*An integral function of order  $e^{(r)\sqrt{r}}$  which vanishes when  $x \rightarrow \infty$  is identically zero.*

That this result ceases to be true when  $\phi(z)$  is an integral function of order  $e^{k\sqrt{r}}$ , where  $k$  is some positive number, is seen by considering the function  $\frac{\sin \sqrt{z}}{\sqrt{z}}$ . But what is

true of this class of functions in this direction is given by the following theorem :

*Theorem III.—If*

(4.1)  $\phi(z)$  be an integral function of order  $e^{k/\sqrt{r}}$ , where  $k > 0$ ;

(4.2)  $\phi(z) \rightarrow 0$  as  $z \rightarrow \infty$  along the positive real axis ;  
then on no other radius vector  $\phi(z)$  can satisfy the relation

$$(4.3) \quad \phi(z) = O(e^{\epsilon\sqrt{r}}),$$

for every positive  $\epsilon$ , however small, unless  $\phi(z)$  is identically zero.

Suppose, if possible, that  $\phi(z)$  is not identically zero, and there is a radius vector other than the positive real axis on which the relation (4.3) holds. Then  $\phi_1(z) \equiv \phi(z^2)$  is an even integral function of order  $e^{kr}$ , tends to zero as  $|z| \rightarrow \infty$  on the real axis, and  $\phi_1(z) = O(e^{\epsilon r})$  on two other opposite radii vectors. It follows, then, from the work of Phragmén and Lindelöf referred to in §1, that  $\phi_1(z)$  is an integral function of order  $e^{(\epsilon/r)r}$ . Hence, by Theorem II,  $\phi_1(z) \equiv 0$ , and so is  $\phi(z)$ . But this is a contradiction. Hence the theorem is proved.

While concluding it may be observed that in all the preceding theorems real axis can be replaced by any other radius vector.